The effects of the citrullinating enzyme, peptidylarginine deiminase, on the activation of T cells

Rita Barreto Duarte Carilho Torrão

Doctor of Philosophy

Aston University

September, 2016

Aston University

The effects of the citrullinating enzyme, peptidylarginine deiminase, on the activation of T cells

Rita Barreto Duarte Carilho Torrão

Doctor of Philosophy

2016

Rheumatoid arthritis (RA) and periodontitis (PID) are two chronic inflammatory diseases associated with the modification of self-proteins by citrullinating peptidyl arginine deiminase (PAD) enzymes, leading to a loss of tolerance by the immune system. The main goal of this study was to explore the action of PAD enzyme-mediated citrullination on T cell membrane proteins and gene expression in relation to the T cell phenotype in PID. Effects on cells of the adaptive immune system have been less well studied in PID and the data obtained here shows that citrullination of peripheral blood mononuclear cells (PBMC) by PAD enzymes impairs T cell activation. Microarray studies showed that PAD enzyme treatment led to the dysregulation of genes involved in glucose and amino acid metabolism in PBMC. Real time quantitative polymerase chain reaction (RT-QPCR) in CD4 and CD8 T cells from PID patients showed a trend towards down-regulation of hexokinase 3 and up-regulation of argininosuccinate synthase1. Also, proteomic and genomic studies in PBMC implicated the involvement of the complement system in the impairment of the T cell response by PAD enzymes. Taken together, the results obtained here support a potential link between T cell surface citrullination and metabolic asynchrony in T cells and may offer an explanation for the lack of immune suppression in PID.

Dedication

I would like to dedicate this thesis to my dear grandma “avó Tina”. Your smile, love and dedication to our family will always live in our hearts.

Acknowledgements

Firstly I would like to thank the MC-ITN-RAPID project for kindly funding my PhD, in particular to my supervisor Professor Helen Griffiths for all the guidance and support during my PhD.

I would also like to thank Professor Iain Chapple and Doctor Paul Weston from the Dental Hospital, University of Birmingham, for all the help in collecting samples. I would like to thank Doctor Andrew Creese and Lorraine Wallace from the Functional Genomics, Proteomics and Metabolomics Facility, University of Birmingham, for all the help and assistance with mass spectrometry and microarray. I would like to thank to my Aston family, present and former members of lab 358 and 360 and office 436, for all the help and support. In particular, I would like to thank Chris and Stuart for all the help in collecting blood, protein analysis and flow cytometry, and to Aisha for all the help and for being so adorable. Lastly, I would like to thank to RAPIDers, for making all the meetings and workshops so much more enjoyable and fun.

On a personal note, I would like to thank Shibu for being my person. I would also like to thank to Justin, Rachel, Sabah, Ali, Kiran, Chat, Iru, Aisha, Edyta and Charlie for making the last four years so fun and enjoyable and fulfilled with cake and chocolate. I would like to thank Ana for being such an amazing life mentor.

Finally, I would like to thank my lovely family, in special to my parents for all the guidance and love and to my brother for keeping up with me during all these years.

Last, but by no means least, I would like to thank to my wonderful husband, Flávio, who had to deal with my ups and downs and who always believed in me, and to my dearest son Manuel, for being the light of my days and for making every moment count.

Table of Contents

List of figures

List of tables

List of equations

Abbreviations

^{0} C	Degree Celsius
2D	Two-dimensional
2D BN/SDS-PAGE	Two-dimensional blue native/sodium dodecyl sulphate polyacrylamide gel electrophoresis
2D IEF/SDS-PAGE	Two-dimensional isoelectric focusing/sodium dodecyl sulphate polyacrylamide gel electrophoresis
3D	Three-dimensional
ABAP	Antibody based assay for peptidylarginine deiminase activity
ABC	Ammonium bicarbonate
ACA	Aminocaproic acid
ACN	Acetonitrile
ACPA	Anti-citrullinated protein antibodies
ADAP	Adhesion- and degranulation-promoting adaptor protein
AEBSF	4-benzenesulfonyl fluoride hydrochloride
AGC	Automatic gain control
AHR	Aryl hydrocarbon receptor
AICD	Activation-induced cell death
AKT	Protein kinase B
ANOVA	Analysis of variance
AP1	Activator protein 1
APC	Allophycocyanin
APC	Antigen presenting cell
APS	Ammonium persulfate
ASS1	Argininosuccinate synthase 1
ATCC	American type culture collection
ATP	Adenosine triphosphate
ATP5B	ATP synthase subunit beta, mitochondrial
Batf	B cell, activating transcription factor–like
BCA	Bicinchoninic acid
Bcl	B-cell lymphoma

Blimp1	B lymphocyte-induced maturation protein 1
BN	Blue native
BN-SB	Blue native sample buffer
BSA	Bovine serum albumin
c-Maf	Avian musculoaponeurotic fibrosarcoma
C1QBP	Complement component 1, Q subcomponent binding protein
Ca^{2+}	Calcium divalent cation
$CaCl_2$	Calcium chloride
CAM	Cell adhesion molecule
cAMP	Cyclic adenosine monophosphate
CBB	Coomassie brilliant blue
CCL4	Chemokine (C-C motif) ligand 4
CCP	Cyclic citrullinated peptide
CCR	C-C chemokine receptor
CCR	C-C Motif chemokine receptor
CD	Cluster of differentiation
cDNA	Complementary DNA
CHAPS	3-[(3-cholamidopropyl)dimethylammonio]-1-propanesulfonate
CID	Collision-induced dissociation
CO_2	Carbon dioxide
CP	Cytosolic protein
cps	Counts per second
CRT	Calreticulin
CT	Threshold cycle
CTH	Cystathionase / cystathionine gamma-lyase
Cu^{+}	Monovalent copper cation
Cu^{2+}	Divalent copper cation
$CuSO_4$	Copper sulphate
CXCL	C-X-C motif chemokine
CXCR	C-X-C chemokine receptor

Cy	Cyanine
Cys	Cysteine
DAG	Diacylglycerol
DC	Dendritic cell
DDM	n-dodecyl-beta-maltoside
DN	Double negative
DNA	Deoxyribonucleic acid
dNTP	Deoxynucleotide
DP	Double positive
DTNB	5,5'-dithiobis-(2-nitrobenzoic acid)
DTT	Dithiothreitol
E-cadherin	Endothelial cadherin
E-selectin	Endothelial selectin
EC	Extracellular
ECL	Enhanced chemiluminescence
EDTA	Ethylenediaminetetraacetic acid
EDTA-Na_2	Disodium ethylenediaminetetraacetate dihydrate
EGF	Epidermal growth factor
ELISA	Enzyme-linked immunosorbent assay
ENO	Enolase
Eomes	Eomesodermin
ER	Endoplasmic reticulum
ERK	Extracellular signal-related kinase
ESI	Electrospray ionisation
ETD	Electron transfer dissociation
$FADH_2$	Flavin adenine dinucleotide
FBS	Fetal bovine serum
FC	Flow cytometry
FITC	Fluorescein isothiocyanate
FL	Fluorescence

FNG	Human native fibrinogen
FOXP3	Forkhead box P3
FS	Functional studies
FSC	Forward-scattered light
FTMS	Fourier transform mass spectrometry
GADS	Grb2-related adaptor downstream of Shc
GATA3	GATA binding protein 3
GCF	Gingival crevicular fluid
GCL	Gamma-glutamylcysteine synthetase
gDNA	Genomic DNA
GFAP	Glial fibrillary acidic protein
Gfi-1	Growth factor independent 1 transcription repressor
GLUT1	Glucose transporter 1
GM-CSF	Granulocyte-macrophage colony-stimulating factor
GO	Gene ontology
GPCR	G-protein-coupled receptor
GR	Glutathione reductase
GRAIL	Gene related to anergy in lymphocytes
GRB2	Growth factor receptor-bound protein 2
Grx	Glutaredoxin
Grx-(SH)2	Reduced glutaredoxin
Grx-SS	Oxidised glutaredoxin
GSH	Glutathione
GSR	Glutathione reductase
GSSG	Oxidised glutathione
GST	Glutathione transferase
GWAS	Genome-wide association studies
H_2O	Water
H2O2	Hydrogen peroxide
H_2SO_4	Sulphuric acid

HC	Healthy control
HCl	Hydrochloric acid
HI	Heat inactivated
HIV	Human immunodeficiency virus
HK3	Hexokinase 3
HLA	Human leukocyte antigen
Hlx	H2.0-like homeobox
HPA	Health Protection Agency
HPLC	High performance liquid chromatography
HRP	Horseradish peroxidase
IAM	Iodoacetamide
IB	Immunoblotting
IC	Intracellular
ICAM	Intercellular adhesion molecule
ICOS	Inducible co-stimulator
ID	Inhibitor of DNA binding
IDA	Information-dependent acquisition
IEF	Isoelectric focusing
IFN	Interferon
IgG	Immunoglobulin
IL	Interleukin
IL-2R	IL-2 receptor
IP3	Inositol trisphosphate
IPG	Immobilized pH gradient
IRF	Interferon regulatory factor
ITK	Tyrosine-protein kinase
iTreg	Induced T regulatory cell
KOH	Potassium hydroxide
L-selectin	Leukocyte selectin
LAL	Limulus amebocyte lysate

LAT	Linker of activated T cells
LB	Loadding buffer
LC	Liquid chromatography
LC-CID-saETD-MS/MS	Liquid chromatography - collision induced dissociation – suplemental activation electron-transfer dissociation – tandem mass spectrometry
LCK	Lymphocyte-specific protein tyrosine kinase
LDH	Lactate dehydrogenase
LFA	Lymphocyte function-associated
LPS	Lipopolysaccharide
LTQ	Linear trap quadropole
LTα	Lymphotoxin α
M/F	Male/Female ratio
m/z	mass/charge ratio
MAC	Membrane attack complex
MAPK	Mitogen-activated protein kinases
MASP	Mannan-binding lectin serine protease
MBL	Mannose-binding lectin
MBP	Myelin basic protein
MFI	Median fluroresce intensity
Mg^{2+}	Magnesium ion
MHC	Major histocompatibility complex
MHC-I	Major histocompatibility complex class I
MHC-II	Major histocompatibility complex class II
miRNA	Micro RNA
MP	Membrane protein
MR1	Molecule-related 1
mRNA	Messenger RNA
MS	Mass spectrometry
MS	Multiple sclerosis
mTOR	mammalian target of rapamycin

MW	Molecular weight
MWCO	Molecular weight cutt-off
N	Number of samples
N-cadherin	Neural cadherin
Na_2CO_3	Sodium carbonate
Na_2HPO_4	Sodium hydrogen phosphate
NaCl	Sodium chloride
NAD^+	Nicotinamide adenine dinucleotide ion
NADH	Nicotinamide adenine dinucleotide
NADP+	Oxidised nicotinamide adenine dinucleotide phosphate
NADPH	Nicotinamide adenine dinucleotide phosphate
$NaHCO_3$	Sodium bicarbonate
NCAM	Neural cell adhesion molecule
NCK1	Non-catalytic region of tyrosine kinase adaptor protein 1
NET	Neutrophil extracellular traps
NF-κB	Nuclear factor-kappaB
NFAT	Nuclear factor of activated T cells
NH_3	Ammonia
NK	Natural killer cell
NKT	Natural killer T cell
Nrf2-KEAP	Nuclear factor erythroid 2-related factor-Kelch-like ECH-associated protein 1
nRTK	Non-receptor tyrosine kinase
OPD	*o*-phenylenediamine
OXPHOS	Oxidative phosphorylation
P-cadherin	Placental cadherin
P-selectin	Placental selectin
P. gingivalis	*Porphyromonas gingivalis*
PAD	Peptidylarginine deiminase
PAGE	Polyacrylamide gel electrophoresis
PAMP	Pathogen-associated molecular pattern

PBMC	Peripheral blood mononuclear cell
PBS	Phosphate buffered saline
PCA	Perchloric acid
PCR	Polymerase chain reaction
PDB	Protein data bank
PDI	Protein disulfide isomerase
PE	Phycoerithrin
PECAM-1	Platelet endothelial cell adhesion molecule
PHA-L	Leucoagglutinin *Phaseolus vulgaris* agglutinin
PI-3K	Phosphatidylinositol-4,5-bisphosphate 3-kinase
PID	Periodontitis
PLCG1	Phospholipase C, gamma 1
pNA	*p*-nitroaniline
PPAD	*Porphyromonas gingivalis* peptidylarginine deiminase
PPP	Pentose phosphate pathway
PRR	Pattern recognition receptor
Prx	Peroxiredoxin
Prx-(SH)2	Reduced peroxiredoxin
Prx-SO2H	Peroxiredoxin sulphinate
Prx-SOH	Peroxiredoxin sulphenate
Prx-SS	Oxidised peroxiredoxin
PTEN	Phosphatase and tensin homolog
PTK	Protein tyrosine kinase
PTM	Post-translational modification
PVDF	Polyvinylidene difluoride
QPCR	Quantitative polymerase chain reaction
RA	Rheumatoid arthritis
RAA	Arginine-Alanine-Alanine
RF	Rheumatoid factor
RhoGDI	Rho GDP-dissociation inhibitor

RNA	Ribonucleic acid
Rnase	Ribonuclease
RORγt	Retinoic acid receptor-related orphan receptor gamma-T
ROS	Reactive oxygen species
RP	Reversed-phase
RPMI	Roswell Park Memorial Institute
RSH	Protein
RSOH	Protein sulphenate
RSSG	Glutathionylated protein
RSSR	Protein disulphide
RT	Room temperature
RT-QPCR	Real time quantitative polymerase chain reaction
RTK	Receptor tyrosine kinase
Runx	Runt-related transcription factor
saETD	Supplemental activation electron-transfer dissociation
SD	Standard deviation
SDS	Sodium dodecyl sulphate
SDS-PAGE	Sodium dodecyl sulphate polyacrylamide gel electrophoresis
SE	Shared epitope
SEM	Standard error mean
SFK	Src-family kinases
SGMS2	Sphingomyelin synthase 2
SH	Thiol group
SH2	Src homology 2
SLE	Systemic lupus erythematosus
SLP-76	SH2 domain containing lymphocyte protein of 76 kDa molecule
SP	Single positive
SpA	Spondyloarthritis
SSA	Sulfosalicylic acid
SSC	Side-scattered light

STAT	Signal transducer and activator of transcription
T-bet	T-box transcription factor
TBS	Tris buffered saline
Tc	Citotoxic T cell
TCA	Tricarboxylic acid
TCR	T cell receptor
TEMED	Tetramethylethylenediamine
TF	Tissue factor
TFA	Trifluoroacetic acid
Tfh	Follicular helper T cells
TGF	Transforming growth factor
TGS	Tris-glycine-SDS buffer
Th	Helper T cell
TLR4	Toll-like receptor 4
TMB	3,3′,5,5′-Tetramethylbenzidine
TNB	Trinitrobenzene
TNF	Tumor necrosis factor
TOF	Time of flight
Treg	Natural regulatory T cell
Trx	Thioredoxin
TrxR	Thioredoxin reductase
TTBS	0.05% Tween-20 in Tris buffered saline
v/v	volume/volume
VAV1	Guanine nucleotide exchange factor
VCAM-1	Vascular cell adhesion protein 1
w/v	weight/volume
WHO	World Health Organisation
ZAP70	Zeta-chain-associated protein kinase 70
β-ME	β-mercaptoethanol

Chapter 1 General introduction

1.1. Inflammation and immunity

Inflammation is the biological response to internal or external harmful *stimuli*. As described by the four Latin words *calor, dolor, rubor* and *tumor*; inflammation is characterized by heat, pain, redness and swelling. These characteristics result from cytokines and other inflammatory mediators acting on specific receptors on circulating cells and endothelial cells in the local blood vessels in response to internal or external *stimuli* [1]. The immune system is responsible for this inflammatory response and can be separated into innate and adaptive immunity. The fine crosstalk between these two systems is crucial for the development of an effective immune response and cytokines have a key role in this modulation [1-3].

1.1.1. Innate immunity

When pathogens invade the human body, cells of the immune system initiate an innate immune response. The innate immune system comprises natural killer (NK) cells, macrophages, neutrophils, dendritic cells (DC), mast cells, eosinophils, basophils and complement factors, which account for the first, rapid and non-specific response to pathogens and damaged, injured or stressed cells [3]. The first cells to respond to an inflammatory stimulus are phagocytic macrophages and neutrophils. The activation of macrophages by bacteria and their component molecules in the site of inflammation triggers the release of cytokines and chemokines. Cytokines, such as tumour necrosis factor (TNF)-α, interferon (IFN)-γ, interleukins (IL)-1β, IL-4, IL-6, IL-10, IL-12, IL-18 and chemokine (C-C motif) ligand 4 (CCL4) are small soluble mediators, that mediate signalling processes and promote the extravasation of other immune cells to the inflammatory site [4]. Chemokines have a major role in the attraction of other cells, such as monocytes, to the site of inflammation. This inflammatory process can also be initiated by activation of the complement system by bacterial cell surface antigens (described in section 1.1.3). Bacterial elimination via the complement system is based

on the coating of bacterial surfaces with soluble complement proteins that are then recognised and internalised by phagocytic cells [1].

1.1.2. Adaptive immunity

When the innate immune system is not sufficient for the elimination of pathogens, an adaptive immune response is mounted. Adaptive immunity is slower, but targeted to a specific antigen and results in the generation of immunological memory. The adaptive immune system involves T and B lymphocytes, but the initiation of this response depends on cells of the innate immune system [1, 3]. For example, antigen presenting cells (APC) in the infected tissues, internalise pathogens by macropinocytosis and receptor-mediated phagocytosis and present the pathogen antigens to naïve T cells in the lymph nodes [1, 3]. T cells are responsible for the cell-mediated immune responses. T cells that hold a T cell receptor (TCR) on the surface for the specific antigen presented by APC become activated and differentiate into effector T cells that will then induce B cells to expand and differentiate into antibody producing cells. B cells are involved in the humoral immune response but can also act as APC and activate specific T cells. [3, 5]. The B cell antibody response will target specific antigens and lead to the elimination of the pathogen [3, 5]. Once the immune response is resolved, most of the activated T and B cells die [1]. However, some of these cells differentiate into memory cells and after a second exposure to the antigen they are able to trigger a faster and stronger secondary immune response, known as immunological memory [3].

1.1.3. The complement system

The complement system consists of plasma proteins able to interact within themselves promoting the opsonisation of pathogens and the activation of inflammatory responses. Depending on the molecules involved in the activation of the complement system, this can be divided into three major pathways: classical, lectin and alternative (Figure 1.1).

The classical pathway is initiated via the binding of the C1 complex (C1q in complex with C1r and C1s serine proteases) to the Fc region of complement-fixing

antibodies attached to the surface of pathogens. The activation of C1r and C1s leads to the cleavage of C4 and C2 into C4b and C4a and C2b and C2a fragments, respectively. The fragments C4b and C2a associate and form the C4bC2a complex (C3 convertase) on the pathogen surface that is able to convert C3 into C3a and C3b, converging to the common point between all the complement activation cascades.

The lectin pathway depends on the recognition of pathogen-associated molecular patterns (PAMP) on the surface of pathogens by pattern-recognition receptors (PRR), such as mannose-binding lectin (MBL). The binding of MBL complexed with MBL-associated serine proteases (MASP)-1, MASP-2 and MASP-3 to the pathogen surface triggers the activation of MASP, the cleavage of C4 and C2 and consequent formation of the C3 convertase, as in the classical pathway.

The alternative pathway is activated by the hydrolysis of C3 into C3b and C3a by components present on the pathogens' cell surface. The fragment C3b promotes the cleavage of Factor B into Bb and Ba by Factor D, allowing the formation of the C3bBb complex (C3 convertase). This C3 convertase is analogue to the one produced via the classical and lectin pathways and is able to convert C3 into C3b and C3a.

The conversion of C3 into C3b, common to the three pathways, exposes an internal thioester bond that identifies pathogens as non-self to the host, triggering further complement activation via the binding of C3b to the C3 convertase, forming the C5 convertase. The conversion of C5 into C5a and C5b, via C5 convertase, leads to the formation of the membrane-attack complex (MAC) through the binding of C5b to terminal complement components (C6-C9).

The success of the complement system in the elimination of pathogens is based on different mechanisms: production of fragments, such as C3b and C4b, that opsonise the pathogen targeting it to phagocytosis; production of fragments, such as C5a and C3a, that act as chemoattractants and activators to phagocytes; formation of the terminal complement component MAC that creates pores in the bacterial membrane, leading to cell lysis [1, 6].

In addition to its roles in the innate immune system, the complement system has also been related with the modulation of adaptive immunity, in particular with T cell responses. Complement factors produced upon T cell contact with APC are involved in the co-stimulation of the TCR and are also associated in the maintenance of naïve T cells' viability [7]. To date, the mechanism involved in the modulation of T cell responses by the complement system is not fully understood. However, it was suggested that C3a and C5a receptors are upregulated in the surface of T cells and APC during contact at the immunological synapse. The signalling induced by the binding of C3a and C5a to their respective receptors activates phosphatidylinositol-4,5-bisphosphate 3-kinase (PI-3K) and Akt intracellular signalling pathways, which leads to enhanced T cell proliferation and reduced T cell apoptosis [7-9].

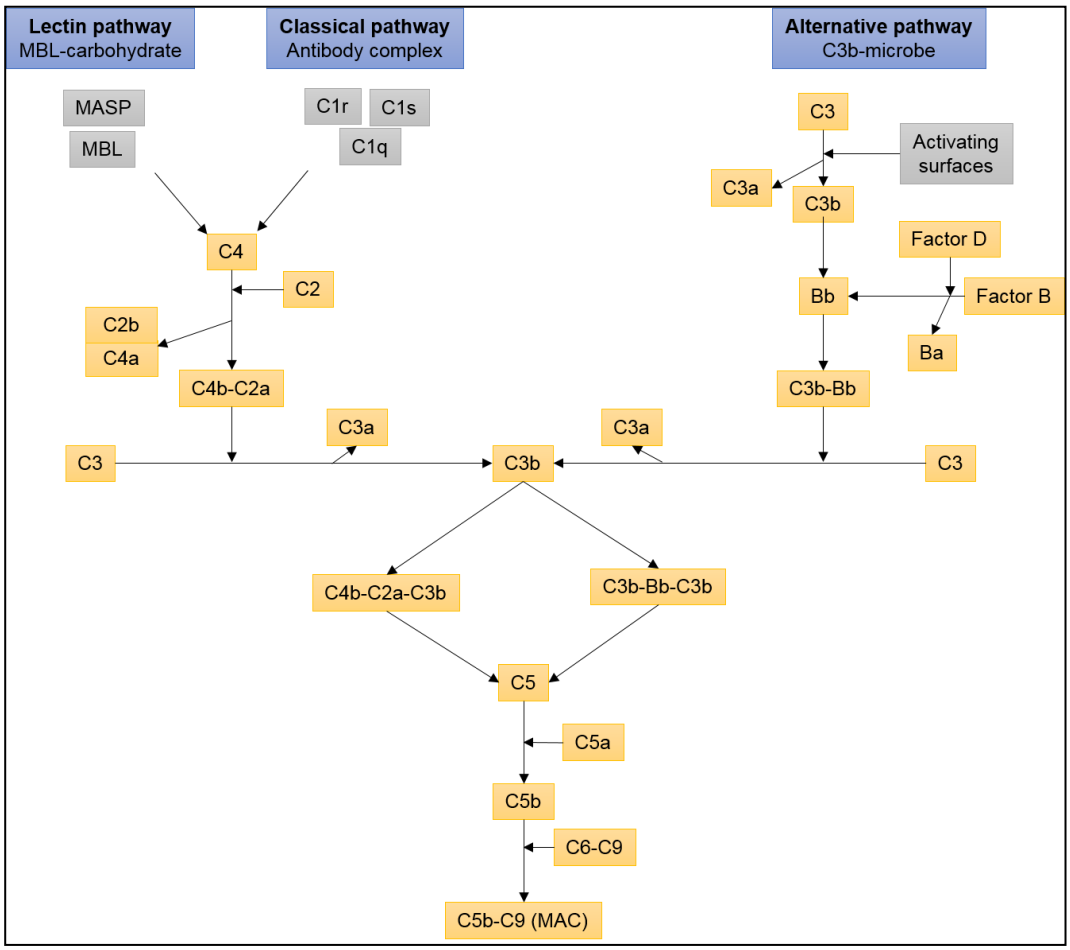

Figure 1.1 Schematic representation of the activation of the complement system through the three different pathways: classical, lectin and alternative. Adapted from periobasics.com.

1.1.4. Cell surface proteins and inflammatory response

The inflammatory response combines the action of immune cells, blood vessels and molecular mediators in a regulated orchestration of events. These events involve: leakage of water, salt and proteins from the vascular compartment; activation of endothelial cells; adhesive interactions between leukocytes and the vascular endothelium; recruitment of leukocytes; activation of tissue macrophages; activation and aggregation of platelets; activation of complement, clotting and fibrinolytic systems; and release of proteases and production of free radical species via nicotinamide adenine dinucleotide phosphatase (NADPH) oxidases and nitric oxide synthases from phagocytic cells, like neutrophils, monocytes/macrophages and resident tissue macrophages with concomitant activation of nuclear factor-κB (NF-κB) and pro-inflammatory gene expression [10, 11]. Proteins present at the surface of cells are key players on the complex cascade of events involved in the inflammatory response.

Cell surface proteins are components of the cellular membrane consisting of hydrophobic and hydrophilic regions. Hydrophobic residues are often buried within the lipid bilayer while hydrophilic residues are located at the membrane surface (intra- or extracellular) [12]. Cell surface proteins can be classified according to their topology as integral membrane proteins, peripheral membrane proteins or polypeptide toxins (Figure 1.2). Integral membrane proteins are permanent constituents of the cellular membrane and can be classified into polytopic (if they span across the membrane) or monotopic (attached to only one side of the membrane) proteins. Peripheral membrane proteins can be attached to the lipid components of the membrane or to integral proteins. Polypeptide toxins can associate with the lipid bilayer and be membrane-associated proteins [13].

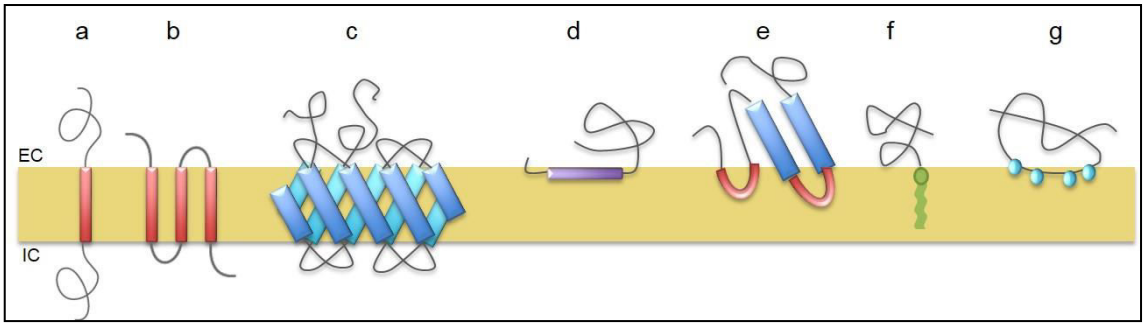

Figure 1.2 Schematic representation of the different categories of cell surface proteins according with their topology and interactions. a) Bitopic transmembrane α-helical protein; b) Polytopic transmembrane α-helical protein; c) Polytopic transmembrane β-sheet protein; d) Parallel monotopic α-helical protein; e) Interaction of a cell surface protein via a hydrophobic loop; f) Interaction of a cell surface protein via a membrane lipid; g) Interaction of a cell surface protein via electrostatic or ionic interactions with membrane lipids. Yellow rectangle represents the cell membrane. EC – Extracellular side. IC – Intracellular side. Adapted from https://en.wikipedia.org/wiki.

Cell surface proteins can also be classified according to their functions as membrane receptor proteins, transport proteins, membrane enzymes and cell adhesion molecules (CAM) (Figure 1.3). Membrane receptor proteins are mainly involved in cell signalling [12]. Cell surface receptors have been categorised to several classes, where G protein-coupled receptors (GPCR), receptors protein-tyrosine kinases (RTK) and cytokine receptors are the main classes (Table 1.1). GPCR, the largest family of cell surface receptors, consists of seven membrane spanning α-helices and includes β-adrenergic receptors, prostaglandin E2 receptors and rhodopsin. The interaction of these receptors (extracellular domain) with ligands induces a conformational change that enables the receptor (intracellular domain) to bind and activate a G protein (guanine nucleotide-binding protein) associated with the inner face of the plasma membrane. The activated G protein further dissociates from the receptor and transmits the intracellular signal to enzymes, ion channels or second messengers, such as cyclic adenosine monophosphate (cAMP), diacylglycerol (DAG) and inositol 1,4,5-triphosphate (IP3) [12, 14]. RTK are directly linked to intracellular enzymes and are responsible for the phosphorylation of tyrosine residues on their target proteins. Structurally these receptors consist of an N-terminal extracellular ligand-binding domain, a single transmembrane α-helix and a cytosolic C-terminal domain containing

the protein-tyrosine kinase activity. Intracellular signalling by protein-tyrosine kinases is accomplished by the binding of ligands to the N-terminal extracellular domain. This binding induces receptor dimerisation, auto-phosphorylation of the receptor itself and phosphorylation of intracellular target proteins that propagate the initial signal [12, 15]. Cytokine receptors consist of interleukin receptors, chemokine receptors and granulocyte macrophage colony stimulating factor (GM-CSF) receptor, amongst others. These receptors contain an N-terminal extracellular ligand-binding domain, a single transmembrane α-helix and a cytosolic C-terminal domain that is associated with non-receptor protein-tyrosine kinases (nRTK). Intracellular signalling through cytokine receptors is initiated by the binding of ligands to the extracellular domain, leading to receptor dimerisation and cross-phosphorylation of the associated nRTK. Subsequently, the receptor is phosphorylated by the activated kinases and recruits signalling molecules containing Src homology 2 (SH2) domains that propagate the signal [12, 16]. Receptors on the surface of cells of the immune system are involved in the phagocytosis of recognised pathogens, in the chemotaxis of neutrophils mediated by bacterial components and in the induction of effector molecules, triggering the adaptive immune system [1].

Table 1.1 Summary of the main classes of cell surface receptors.

Category	Structure	Mechanism	Examples
GPCR	Seven TM domains	Ligand binding to the extracellular domain; Conformational change; Intracellular binding and activation of G protein; Signal transduction through cAMP, DAG and IP3.	β-adrenergic receptor; Prostaglandin E2 receptor; Rhodopsin.
RTK	Single TM α-helix	Ligand binding to the extracellular domain; Receptor dimerization and auto-phosphorylation; Intracellular phosphorylation of target protein.	Epidermal growth factor receptor; Fibroblast growth factor receptor; Vascular endothelial growth factor receptor.
Cytokine	Single TM α-helix	Ligand binding to the extracellular domain; Receptor dimerization; Cross-phosphorylation by activate kinases; Recruitment of intracellular signalling molecules.	GM-CSF receptor; Interleukin receptors.

CAM are involved in cell growth, differentiation, embryogenesis, immune cell transmigration and response and cancer metastasis. CAM consist of an extracellular domain that interacts with other CAM or the extracellular matrix, a transmembrane domain and an intracellular domain. CAM can be grouped in four classes: Ig superfamily, integrins, cadherins and selectins [17-20]. The Ig superfamily consists in calcium-independent transmembrane glycoproteins, like intracellular adhesion molecule (ICAM), vascular-cell adhesion molecule (VCAM-1), platelet-endothelial-cell adhesion molecule (PECAM-1) and neural-cell adhesion molecule (NCAM). Integrins are non-covalently linked heterodimers of α and β dimer CAM that need activation to bind to their ligand [17, 19-21]. Cadherins are calcium-dependent CAM. The classical cadherin subfamily include cadherins such as neural (N)-cadherin, placental (P)-cadherin and epithelial (E)-cadherin [17, 19, 22, 23]. Selectins are carbohydrate-binding proteins that depend on divalent cations. Selectins can be grouped in endothelial (E)-selectin, leukocyte (L)-selectin and platelet (P)-selectin [17, 19-21]. CAM are also important players in the progress of an immune response. The recruitment of lymphocytes to inflammation depends on their passage from the blood stream to the specific tissue and this process is determined by the expression of CAM. The up-regulation of endothelial CAM promotes leukocyte adhesion to and rolling on the endothelial surface and the production of VCAM-1, which can bind to adhesion molecules on the leukocytes, consolidating the interaction between the vascular endothelium and leukocytes and allowing the leukocytes to infiltrate the tissue. Additionally to a general function of CAM in the recruitment of leukocytes to the inflammation site, CAM are also involved in the T cell response. Naïve T cells in the periphery are recruited into the lymph nodes through the interaction between ICAM-1 and ICAM-2 and lymphocyte function-associated antigen 1 (LFA 1) expressed on the surface of T cells. Furthermore, the homing of effector T cells to the inflamed site is also mediated by specific CAM, like integrin α_4:β_1, at the surface of T cells, that binds VCAM-1, promoting the extravasation of effector T cells [1].

Transport proteins include channel and carrier proteins. While channel proteins form pores in the membrane that allow free diffusion of molecules of an appropriate size, carrier proteins selectively bind and transport specific small molecules across the membrane in a conformational dependent manner [12]. Membrane enzymes are those involved in the metabolism of different membrane components. Examples of these cell surface proteins include phospholipases, cholesterol oxidases, glycosyltransferase, transglycosidases, signal peptidase, palmitoyl protein thioesterases and lipases [12].

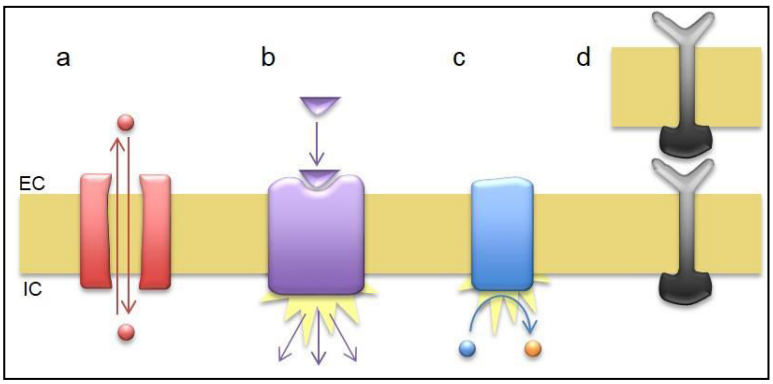

Figure 1.3 Schematic representation of the different categories of cell surface proteins according with their functions. a) Transport protein; b) Membrane receptor protein; c) Membrane enzyme; d) Cell adhesion molecule. Yellow rectangle represents the cell membrane. EC – Extracellular side. IC – Intracellular side. Adapted from [24].

1.2. T cell biology

1.2.1. T cell maturation

T cells derive from hematopoietic stem cell precursors that migrate from the bone marrow to the thymus. The thymus is localised in the upper anterior thorax and comprises several lobules that can be divided into peripheral cortex and central medulla. In the thymus, T cell precursors undertake different maturation steps that drive commitment to the T cell lineage and differentiation into the alternative T cell lineages.

The first development step involves the activation of the Notch signalling pathway and is the basis of the differentiation of hematopoietic precursors to the T cell lineage rather than the B cell lineage.

Developing thymocytes then undertake several maturation processes that involve the rearrangement of the TCR genes and the expression of different molecules at the surface of the cell, like cluster of differentiation (CD) 3 complex and co-receptor proteins CD4 and CD8. The changes at the thymocytes' surface are characteristic for each stage of maturation. Initially, thymocytes do not express any of the surface markers of mature T cells and the TCR genes are not rearranged. The first stage of differentiation involves cell proliferation and the expression of c-Kit, a stem cell growth factor receptor, CD44, an adhesion molecule, and CD25, α-chain of the IL-2 receptor (IL-2R). After this, TCR genes start rearranging, originating T cells bearing αβ or γδ TCR. At this point, the thymocytes do not express CD4 or CD8 T cell surface markers and are denominated double negative (DN) [25-27]. γδ thymocytes represent 10% of T lymphocytes of healthy adults and can be divided into three main populations based on the δ chain expression: Vδ1, Vδ2 and Vδ3. The initiation of the immune response in γδ T cells relies on cell-cell contact with APC. γδ T cells can recognise a variety of different ligands, including non-peptidic antigens, MHC and non-MHC cell surface molecules and soluble proteins. The thymocytes expressing αβ TCR differentiate into the CD4CD8 double positive (DP) stage, where both CD4 and CD8 co-receptors are expressed at the cell surface. At this phase, negative selection processes eliminate DP thymocytes that have a TCR incapable of binding MHC-I or MHC-II. Then, the DP thymocytes maturate into CD4 or CD8 single positive (SP) T cells. Thymocytes that recognise self-peptides complexed with MHC class I (MHC-I) become CD8 or cytotoxic T (Tc) cells, whereas thymocytes that recognise antigens presented via MHC-II become CD4 or T helper (Th) cells [2, 28-30]. Besides CD4 and CD8 T cells, other non-conventional lineages are also produced during the maturation process in the thymus. These include: natural regulatory T (Treg) cells, expressing FOXP3CD4CD25;

natural killer T (NKT) cells, reactive to CD1d; MHC1b CD8 T cells; and major histocompatibility molecule-related 1 (MR1)-restricted mucosa associated invariant T cells [31, 32].

Processes of negative and positive selection are again initiated. Mature T cells with TCR that strongly interact with self-MHC molecules are negatively selected and eliminated to prevent autoimmune reactions. Mature T cells that react too little to self-peptides are also eliminated. The T cells that bear αβ TCR capable of recognising self-peptides on thymic epithelial cells with intermediate level of TCR signalling are positively selected and leave the thymus to the periphery as mature naïve T cells [29].

1.2.2. T cell activation and T cell receptor signalling

Naïve T cells circulate in the periphery until they become activated through the presentation of antigens by APC. The contact between T cells and APC is highly specific. The TCR at the surface of T cells recognises a specific antigen bound to MHC molecules at the surface of the APC [3, 33]. The interface between APC and T cell, where the MHC molecules in APC interact with the TCR in T cells, is denoted as the immunological synapse. Additional to the binding between TCR and MHC, T cell activation depends on co-stimulatory molecules and chemical mediators expressed by APC. Co-stimulatory molecules, such as CD80 (or B7-1) and CD86 (or B7-2), engage with counter-receptors on the surface of T cells and transmit important signals for T cell proliferation and survival. Chemical mediators, like interleukins, act on T cells promoting their differentiation into effector cells [33].

The TCR, as outlined in the schematic in figure 1.4, is a transmembrane protein and consists of a peptide-MHC recognition unit (α and β chains) and a signal transduction unit (γ, δ, ε and ζ chains, or CD3 complex) [34]. When the antigen presented by MHC binds to the TCR at the immunological synapse, intracellular protein tyrosine kinases (PTK) of the Src, Syk and Tec families are recruited and activated. Lymphocyte-specific protein tyrosine kinase (LCK), a Src family PTK member,

phosphorylates ITAM on the γ-, δ-, ε- and ζ-CD3 chains, leading to the recruitment and activation of the Syk family PTK zeta-chain-associated protein kinase 70 (ZAP70). Phosphorylated and activated ZAP70, in turn, phosphorylate the adaptors linker of activated T cells (LAT) and SH2 domain containing lymphocyte protein of 76 kDa molecules (SLP-76). LAT and SLP-76 form platforms that allow signal transduction molecules to arrange in the correct intracellular location and execute their functions. LAT recruits signalling molecules that include phospholipase Cγ1 (PLCγ1), growth factor receptor-bound protein 2 (GRB2), GRB2-related adaptor protein (GADS), adhesion- and degranulation-promoting adaptor protein (ADAP), interleukin-2-inducible T cell kinase (ITK), non-catalytic region of tyrosine kinase adaptor protein 1 (NCK1) and guanine nucleotide exchange factor (VAV1). This cascade of events leads to the TCR signal propagation and activation of intracellular pathways, like the mitogen-activated protein kinase (MAPK), the nuclear factor-κB (NF-κB) and the Ras signalling pathways, which are involved in cytoskeletal reorganisation, calcium signalling and mobilisation of transcription factors [34-36]. The mobilisation of NF-κB, activator protein 1 (AP1) and nuclear factor of activated T cells (NFAT) to the nucleus, consequently promotes the transcription of IL-2, IL-4, GM-CSF and TNF-α genes essential for T cell growth and differentiation into effector T cells [37, 38].

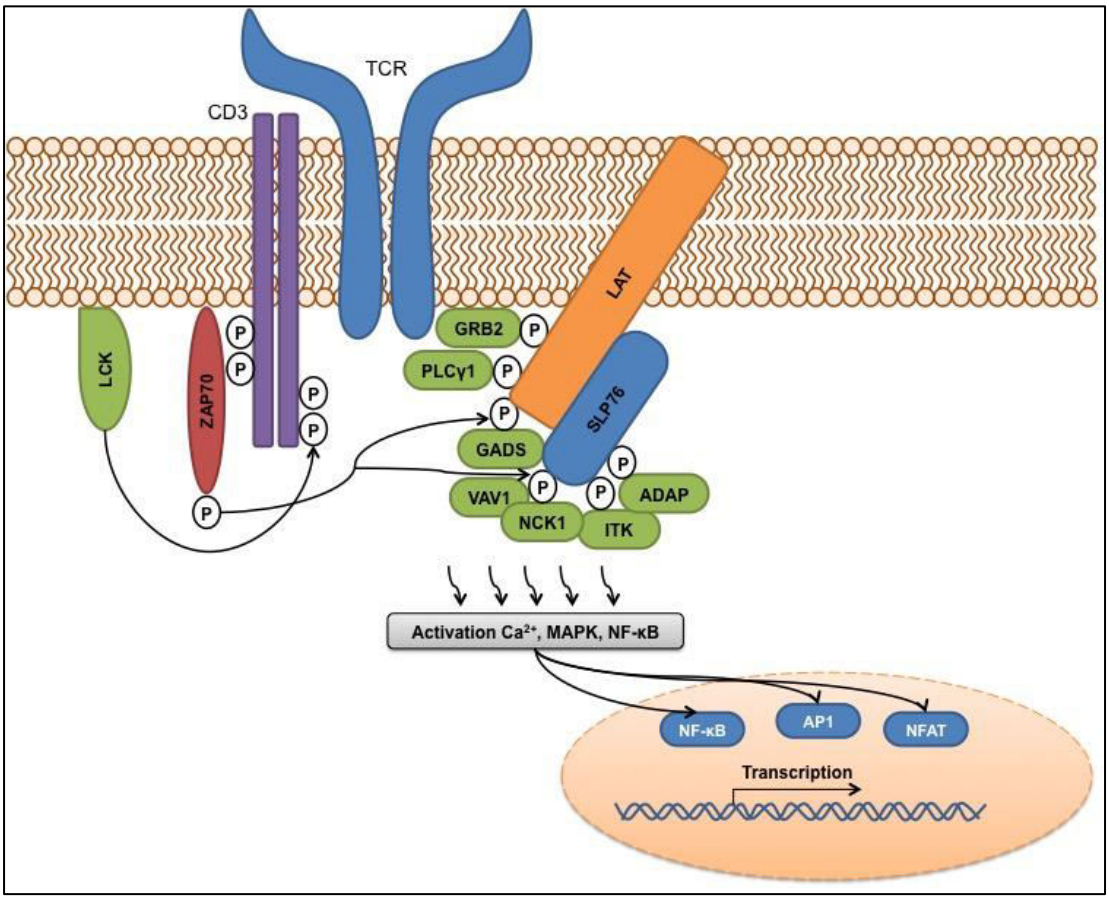

Figure 1.4 Schematic representation of TCR signalling. ADAP – adhesion- and degranulation-promoting adaptor protein; Ca^{2+} - calcium divalent ion; CD3 – cluster of differentiation 3; GADS – grb2-related adaptor downstream of Shc; GRB2 – growth factor receptor-bound protein 2; ITK – tyrosine-protein kinase; LAT – linker of activated T cells; LCK – lymphocyte-specific protein tyrosine kinase; MAPK – mitogen-activated protein kinase; NCK1 – non-catalytic region of tyrosine kinase adaptor protein 1; NF-κB – nuclear factor-kappaB; PLCγ1 – phospholipase C, gamma 1; SLP76 – SH2 domain containing lymphocyte protein of 76 kDa molecules; TCR – T cell receptor; VAV1 – guanine nucleotide exchange factor; ZAP70 – zeta-chain-associated protein kinase 70.

1.2.3. Interleukin-2 signalling pathway

IL-2 is a 15 kDa quaternary α-helical glycoprotein produced mainly by activated CD4 T cells, but also by CD8 and NKT cells and NK cells [39]. Besides being recognised as a T cell growth factor, IL-2 is also involved in activation-induced cell death (AICD), development of Treg and CD8 T cells, secondary expansion of memory CD8 T cells and modulation of CD4 T cell differentiation. Depending on the cytokine environment following antigen presentation, naïve T cells can differentiate into different T cell effector subsets (as detailed in 1.2.4). IL-2 was shown to be involved in the regulation of this process by priming cells for differentiation or helping cells to maintain a

differentiated state [40]. The production of IL-2 in T cells is potentiated by activation through antigen presentation. Secreted IL-2 acts on cells expressing the IL-2R. The IL-2R consists of three subunits (IL-2Rα or CD25, IL-2Rβ or CD122 and γc or CD132) and three classes of IL-2R exist: low-, intermediate- and high-affinity for IL-2. The mechanism of IL-2 interaction with the trimeric high-affinity IL-2R, consisting of subunits IL-2Rα, IL-2Rβ and γc, involves an initial contact between IL-2 and IL-2Rα through a large hydrophobic binding surface surrounded by a polar periphery, inducing a small conformational change in IL-2 that allows IL-2Rβ to associate with IL-2 through a distinct polar region. The γc unit is then recruited through a weak interaction with IL-2 and a stronger interaction with IL-2Rβ, forming the stable quaternary high-affinity IL-2-IL-2R complex. The dimeric intermediate-affinity IL-2R, consisting of IL-2Rβ and γc subunits, has weak affinity to IL-2 but is able to propagate the signal [41-43]. The monomeric IL-2R is formed by the IL-2Rα solely and, although it can bind IL-2 with low affinity, it is not competent for signal transduction [43]. The trimeric IL-2R can be found in Treg cells or recently antigen-activated T lymphocytes, whereas the dimeric IL-2R is almost undetectable on naïve CD4 T cells, but it is expressed at low levels on naïve CD8 and memory CD4 T cells and at high levels on memory CD8 T cells and NK cells [44].

At the cellular level, IL-2R subunits are selectively located in lipid micro domains or rafts [45, 46], facilitating the oligomerisation of the receptor and the intracellular signalling machinery [47]. Following IL-2-IL-2R complex formation the signal transduction process involves the phosphorylation of tyrosine residues on the cytoplasmic tail of IL-2Rβ by tyrosine kinases Jak1 and Jak3, which leads to the recruitment of the adaptor Shc [48]. MAPK, PI-3K and signal transducer and activator of transcription (STAT) 5 signalling pathways are then activated, leading to STAT5-dependent gene regulation [43]. The activation of STAT5 is similar in CD4 and CD8 effector T and Treg cells but the activation of S6 kinase (a downstream target of the PI-3K-protein kinase B and mammalian target of rapamycin – mTOR – kinase pathways)

is distinctive for the cell populations [49]. Furthermore, in Treg cells the expression of phosphatase and tensin homolog (PTEN) protein suppresses the activation of PI-3K-protein kinase B pathway and consequently, IL-2-dependent cell proliferation is not observed *in vitro* [50]. The activation of these signalling pathways promotes T cell growth, survival, AICD and differentiation [51, 52]. The signal induced by IL-2 can also stimulate the expression of IL-2Rα and IL-2Rβ, acting as a positive feedback loop [53, 54]. Following signal transduction, the IL-2-IL-2R complex is internalised, IL-2, IL-2Rβ and γc are rapidly degraded and IL-2Rα is recycled to the cell surface [55, 56].

1.2.4. T cell differentiation into different subsets

The activation of naïve T cells by APC induces T cell proliferation and differentiation into specific effector cells.

CD8 T cells turn into CD8 effector T cells after interaction with APC that present antigens via MHC-I molecules. The major transcription factors involved in the regulation of CD8 T cell differentiation are T-box transcription factor (T-bet), B lymphocyte-induced maturation protein 1 (Blimp1) and inhibitor of DNA binding (ID) 2. [57, 58]. CD8 effector T cells act on infected cells by releasing cytotoxins, such as perforin, granzymes and granulysin, which can penetrate the lipid bilayer and trigger an intrinsic cell death program. Effector cytokines, like IFN-γ and TNF-α, are also released by effector CD8 T cells and contribute to infection control [59].

CD4 T cells that become activated via antigen presentation by MHC-II molecules can differentiate into Th1, Th2, Th9, Th17, Th22, follicular helper (Tfh) and induced regulatory T (iTreg) cells. The cytokine microenvironment is the major contributor for the specific lineage differentiation, but other factors, such as the concentration of antigens, type of APC and co-stimulatory molecules, are also involved [60, 61] (Figure 1.5 and table 1.2).

Th1 response is initiated by IL-12 and IFN-γ. IL-12 is secreted by activated APC and induces the production of IFN-γ by NK cells. These cytokines are responsible for

the activation of several transcription factors, including T-bet, STAT1, STAT4, runt-related transcription factor (Runx) 3, eomesodermin (Eomes) and H2.0-like homeobox (Hlx), where T-bet is the central regulator in the differentiation of Th1 cells. IFN-γ released by NK cells activates STAT1 that in turn induces the expression of T-bet. T-bet further induces the production of more IFN-γ and the suppression of the Th2 and Th17 lineages. T-bet suppression of Th2 cells occurs by inhibiting IL-4 gene expression and suppressing the functions of Th2 principal transcription factor GATA binding protein 3 (GATA3). Th17 cells are inhibited by the suppression of the Th17 principal transcription factor, retinoic acid receptor-related orphan receptor gamma-T (RORγt). Th1 cells are particularly important against intracellular pathogens and are also associated with organ-specific autoimmunity. Th1 cells secrete IFN-γ, lymphotoxin α (LTα) and IL-2. IFN-γ increases phagocytic activity by promoting the activation of mononuclear phagocytes, like macrophages. LTα, a member of the TNF family, was shown to be associated with autoimmunity. IL-2 induces proliferation of CD8 T cells, development of CD8 memory T cells, enhancing a secondary immune response, and survival and activation of Treg cells.

The differentiation of Th2 cells depends on IL-4 and IL-2 cytokines. The principal transcription factors involved in Th2 response are GATA3, STAT6, STAT5, STAT3, growth factor independent 1 transcription repressor (Gfi-1), avian musculoaponeurotic fibrosarcoma (c-Maf) and interferon regulatory factor (IRF) 4, where GATA3 plays the major role. GATA3 expression, up-regulated by IL-4-induced STAT6, induces Th2 cytokine production, selective proliferation of Th2 cells and inhibition of Th1 cells differentiation. Th2 cells produce B-cell growth factors and interleukins IL-4 and IL-5. The main effector functions of Th2 cells are the induction of B cell proliferation, mediation of the immune response against extracellular parasites and induction and persistence of allergic inflammation [2, 32, 62, 63].

Th9 cells are described as a differentiated branch of Th2 cells. Transforming growth factor (TGF)-β is the factor responsible for the diversion of the differentiation of

Th2 towards the development of Th9 cells. However, the differentiation of Th9 cells can be directly induced by TGF-β and IL-4. Th9 cells secrete IL-9 in large quantities and are mainly involved in tissue inflammation against helminths and are also associated with the pathogenic process of allergy [32, 64, 65].

Th17 differentiation depends on TGF-β and IL-6 for the differentiation stage; IL-21 for the self-amplification stage; and IL-23 for the stabilisation stage. The main transcription factor affected by these signalling cytokines is RORγt, which is responsible for the production of IL-17A and IL-17F cytokines. Th17 cells are involved in the immune response against extracellular bacteria and fungi and are also related to the immune response observed in several autoimmune diseases, such as multiple sclerosis and rheumatoid arthritis (RA). The main effector cytokines involved in the Th17 response are IL-17A, IL-17F, IL-21 and IL-22. [63, 66]. IL-17A and IL-17F signalling occurs through the IL-17A receptor and promotes the production of pro-inflammatory cytokines, including IL-6, IL-1 and TNF-α, and pro-inflammatory chemokines, responsible for the chemotaxis of inflammatory cells to the inflammation site. IL-21 is essential for the amplification of Th17 development and is also involved in the differentiation of B cells into plasmocytes and memory cells and in the activation of NK cells. IL-22 promotes mucosal host defence against bacterial pathogens and exhibits tissue protective properties [32].

Th22 cells differentiate in the presence of TNF-α and IL-6 cytokines but the mechanism of signal transduction is not fully understood. The main cytokine expressed by these cells is IL-22, which is involved in wound repair and tissue regeneration. Th22 cells also express chemokine receptors CCR4, CCR6 and CCR10 that promote the migration of these cells to particular tissues, such as skin [67].

Tfh differentiation occurs in the presence of IL-6 and IL-21 cytokines, which are responsible for the induction of STAT3 and B-cell lymphoma (Bcl)-6 transcription factors. Inducible co-stimulator (ICOS) is also necessary for Tfh development. Tfh cells

participate in the development of B cell response, by regulating the differentiation of B cells into plasma cells [32, 65].

Induced Treg (iTreg) cells differentiate from naïve T cells in the presence of TGF-β and IL-2 cytokines. TGF-β and IL-2 signalling promote the activation of FOXP3 and STAT5 transcription factors, respectively. STAT5 enhances the expression of FOXP3 and, consequently, the FOXP3 signalling and iTreg cell differentiation. The main function of iTreg cells is to maintain the immune system tolerance to self-antigens. iTreg cells secrete TGF-β, IL-10 and IL-35, and they also induce immune responses through cell-cell interactions [32, 63].

Once the immune response is resolved, effector T cells are able to generate different subsets of memory T cells with diverse phenotypic and functional properties and gene expression profiles.

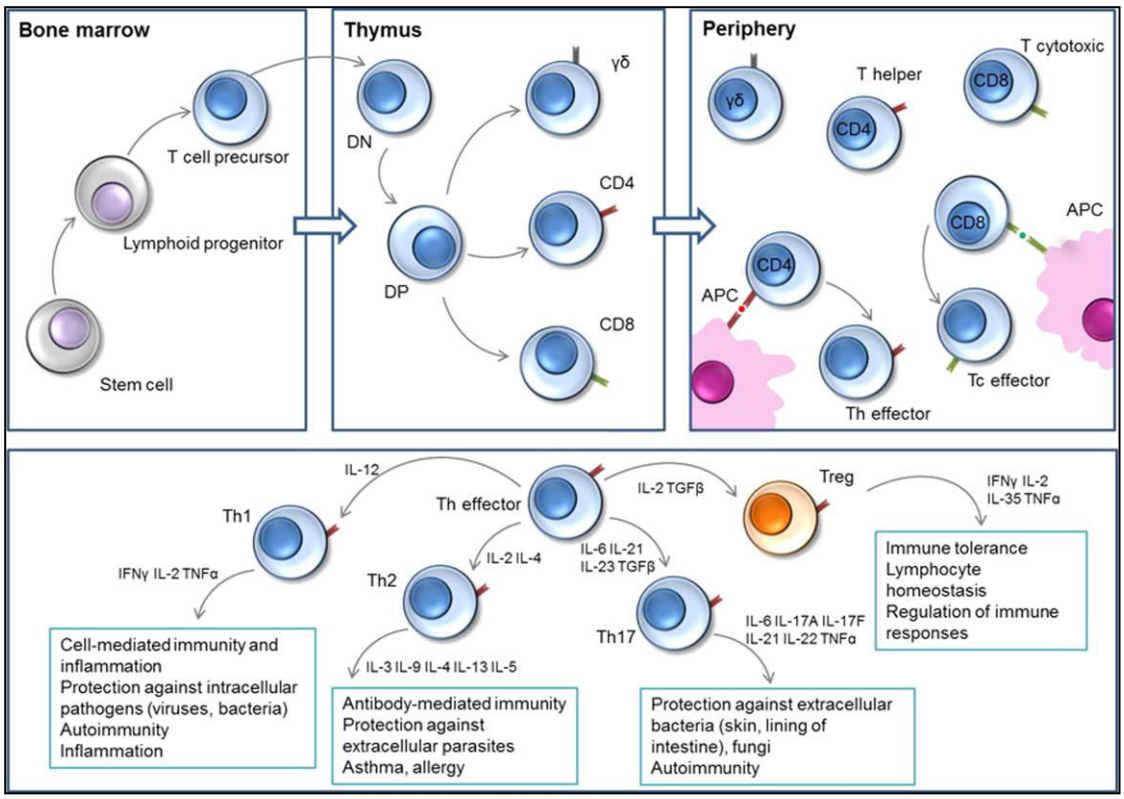

Figure 1.5 Schematic representation of T cell maturation and differentiation.

Table 1.2 Cytokines and transcription factors involved in the differentiation of the different Th cell subsets. The master regulators are highlighted in bold.

Th Subset	Differentiation cytokines	Transcription factors	Effector cytokines
Th1	IL-12, **IFN-γ**	**T bet**, STAT1, STAT4, Runx 3, Eomes, Hlx	IFN-γ, LTα, IL-2
Th2	**IL-4**, IL-2	**GATA3**, STAT6, STAT5, STAT3, Gfi-1, c-Maf, IRF4	IL-4, IL-5
Th17	IL-6, **IL-21**, IL-23, TGF-β	**RORγt**, STAT3, RORα, Runx1, Batf, IRF4, AHR	IL-17A, IL-17F, IL-21, IL-22
Th22	TNF-α, IL-6	Unknown	IL-22
Tfh	IL-6, IL-21	Bcl6, STAT3	IL-21, IL-4
iTreg	TGF-β, IL-2	**FOXP3**, Smad2, Smad3, STAT5, NFAT	TGF-β, IL-10, IL-35
Th9	TGF-β, IL-4	IRF4	IL-9

1.2.5. T cell metabolism

Cellular metabolism plays an important role in the regulation of immune cell functions and cell differentiation [68-71]. The regulation of the uptake and utilisation of nutrients, such as glucose, fatty acids and amino acids, is crucial for the control of the immune cell number and functional activity [72].

Glucose is the major energy source for mammalian cells and is also a substrate for protein and lipid synthesis (Figure 1.6). Glucose uptake from the extracellular medium occurs via two families of structurally related glucose transporters and it is metabolised via glycolysis. In glycolytic metabolism, each glucose molecule is converted into two molecules of pyruvate with the concomitant production of two adenosine triphosphate (ATP) molecules. Pyruvate can be further oxidised via the tricarboxylic acid (TCA) cycle to generate nicotinamide adenine dinucleotide (NADH) and flavin adenine dinucleotide ($FADH_2$) that fuel mitochondrial oxidative phosphorylation (OXPHOS) generating thirty-six ATP molecules per glucose molecule. Pyruvate can also be converted into lactate by lactate dehydrogenase enzyme, regenerating NAD^+ that can subsequently participate in glycolysis [73]. The conversion

of glucose into lactate is particularly important in hypoxic conditions and when mitochondria are damaged and cannot oxidise pyruvate. The conversion of pyruvate into lactate in normoxic conditions was first demonstrated by Otto Warburg in cancer cells and is described as aerobic glycolysis [74]. In this pathway a high flux of glycolysis meets increased cellular energy needs.

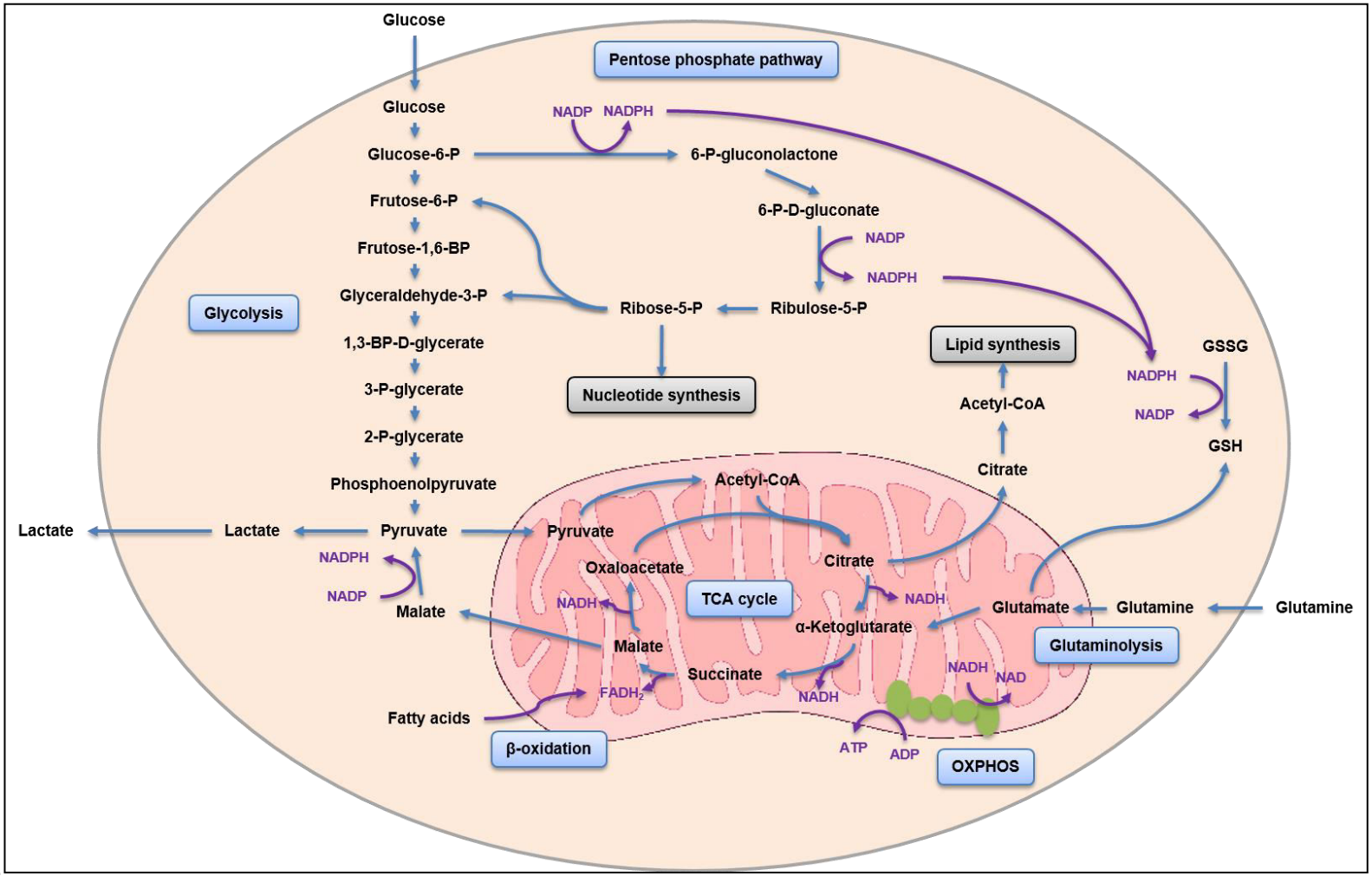

Figure 1.6 Schematic representation of glucose and glutamine metabolism. ADP – adenosine biphosphate; ATP – adenosine triphosphate; $FADH_2$ – flavin adenine dinucleotide; GSH – reduced glutathione; GSSG – oxidised glutathione; NAD^+ – nicotinamide adenine dinucleotide ion; NADH – nicotinamide adenine dinucleotide; $NADP^+$ – nicotinamide adenine dinucleotide phosphate ion; NADPH – nicotinamide adenine dinucleotide phosphate.

T cells alternate through states of metabolic quiescence and activation during their development and differentiation. Quiescent T cells require generation of ATP to meet their metabolic demands, whereas effector T cells need high metabolic flux proliferation-promoting pathways to be activated. The different T cell subsets rely on different energetic and biosynthetic pathways to meet their specific functional requirements [72].

In the thymus, DN thymocytes switch from quiescence to anabolic metabolism for the creation of biomass and proliferation. This phase is characterised by high levels of expression of glucose transporter 1 (GLUT1) promoting glycolytic metabolism used to support cell growth and proliferation. When thymocytes reach DP or SP stages, GLUT1 expression is downregulated and the intracellular pool of ATP molecules is originated from the breakdown of glucose, lipids and amino acids during OXPHOS [72, 75, 76].

Resting naïve T cells in the periphery, as quiescent cells, rely on OXPHOS or fatty acid oxidation for the synthesis of ATP [77-81]. Upon activation, T cells start clonal expansion and reprogram their metabolic machinery into aerobic glycolysis and increased OXPHOS and glutaminolysis for the rapid production of macromolecules required for anabolic cell growth [72, 77, 82]. Although glycolysis is less efficient in the production of energy-equivalents compared to OXPHOS, activated T cells engage in glycolysis since it is a rapid process for the generation of ATP and it also releases other metabolites required for productive cell growth [83]. The increase in glycolytic flux, observed in activated T cells, depends on the translocation of GLUT1 from the cytoplasmic pool to the cell surface in a PI-3K-Akt pathway-dependent process [84]. The metabolic reprogramming of T cells following activation is also regulated by mTOR pathway [85, 86] and, to a lesser extent, by extracellular signal-related kinase (ERK) [87], STAT5 [88], some MAP kinases [89] and hexokinase II [90]. Additionally to changes in the ATP source supply, the activation of T cells also induces changes in the

localisation of cations, like calcium, from intracellular stores (like endoplasmic reticulum – ER) to the cytosol, where they are involved in intracellular signalling [77, 91].

Once the immune response is terminated, most of the T cells die. The T cells that survive become memory T cells, but for that they need to return to a resting metabolic state, where lipid oxidation is the main energy-supply pathway [92].

1.3. Immune tolerance and autoimmunity

The immune system has as its main function to protect the organism against internal and external harmful *stimuli*, like bacteria, viruses and damaged cells. Additionally, the immune system has to be able to discriminate between self-antigens from foreign-antigens, in order to prevent inflammatory responses against the host's own cells and tissues [5]. The main tolerance mechanism develops during T cell maturation in the thymus, where newly generated T cells whose TCR strongly recognises self-antigens are eliminated by negative selection [3]. However, some T cells evade this mechanism and are released to the blood stream, where they are reactive to self-antigens. The main function of Treg cells is to maintain the organism's self-tolerance in the periphery and consequently Treg cells are able to detect, inhibit the induction of effector function and eliminate T cells that escaped the negative selection in the thymus [93, 94]. Impaired control of autoreactive T cell responses due to defects in the development, stability or function of Treg cells can trigger an immune response against the host organism described as autoimmunity [95].

Autoimmune diseases, resulting from autoimmune responses, affect distinct organs and present different clinical manifestations. Examples of autoimmune diseases are RA, periodontitis (PID), multiple sclerosis and psoriasis. At cellular level, the chronic inflammation and tissue damage observed in autoimmune diseases are due to cytokine production, epitope spreading and a disrupted effector T cell/Treg cell balance [96].

Risk factors for autoimmunity include genetic predisposition and environmental triggers combined with impaired immune regulatory functions that enable the escape, activation and proliferation of autoreactive lymphocytes. Genome-wide association studies (GWAS) focusing on autoimmune diseases have identified a large number of disease-associated *loci* that are usually located in regulatory regions of genes, whose products are involved in immunity, like human leukocyte antigen (HLA), cytokines/receptors and those involved in central tolerance [97, 98]. The HLA corresponds to the human variant of the MHC, which occurs in many species, and is responsible for the expression of more than 200 genes. The products of MHC genes are highly polymorphic transmembrane glycoproteins expressed at the surface of lymphocytes. The products of the *HLA/MHC* genes can be divided into class I (HLA-A, -B and -C) and class II (HLA-DR, -DQ and -DP), according to their structure, tissue distribution and characteristics in peptide presentation to T cells. MHC-I genes are expressed in all cells but red blood cells; MHC-I protein derived from them are responsible for the presentation of intracellular peptides to the immune system. MHC-II genes are expressed mainly on APC, such as DC, B cells and macrophages; MHC-II proteins usually present exogenous proteins that were taken up by endocytosis and fragmented by proteases in an endosome, to other immune cells [99]. MHC-I and -II molecules that bind with high affinity to self-peptides are eliminated to prevent autoimmunity. However, this is not a faultless process and some HLA alleles have different abilities to present auto-antigens to T cells, being associated with the breakdown of the immune system observed in autoimmune diseases. Environmental triggers for autoimmunity are suggested to include smoking, infections, the microbiome and tissue injuries and are responsible for the generation of a pro-inflammatory environment that allows the activation of autoreactive lymphocytes [96].

In addition to the risk factors and the impairment of the regulatory processes of the immune system mentioned previously, autoimmunity can be associated with modifications on self-antigens presented to the immune system. Post-translational

modifications (PTM) occur in proteins during ageing as part of physiological and pathological processes and can be responsible for the generation of neo-epitopes from self-proteins. In addition, PTM can be catalysed by enzymes or occur by chemical reaction and can contribute to alterations in the protein backbone, charge and differential three-dimensional folding pattern [100]. Examples of PTM that can affect amino acids are described in table 1.3. These modifications can generate neo-self epitopes and, consequentely, affect the affinity of MHC molecules or TCR binding or the activity of proteolytic enzymes involved in antigen processing [101].

Table 1.3 Amino acid post-translational modifications.

Amino acid	Modification
Arginine	Citrullination (deimination), methylation
Asparagine	N-linked glycosylation, deamidation (and isomerisation)
Aspartic acid	Isomerisation
Glutamic acid	Methylation
Glutamine	Deamidation
Histidine	Methylation
Lysine	Hydroxylation (and subsequent O-linked glycosylation), methylation
Proline	Hydroxylation
Serine and threonine	Phosphorylation, *O*-linked glycosylation

1.3.1. Citrullination

Citrullination (or deimination) is the enzymatic conversion of peptidylarginine into peptidylcitrulline mediated by peptidylarginine deiminase (PAD) enzymes (Enzyme Commission number 3.5.3.15.) (Figure 1.7). This reaction catalysed by PAD enzymes is calcium dependent and involves the hydrolysis of guanidinium groups on arginine residues, by a nucleophilic cysteine, to form citrulline. The complete substrate guanidinium group hydrolysis is mediated by a second histidine active site, where ammonia and water are released [102-107]. PAD enzymes were first described in 1977 by Rogers [108]. In humans, five isoforms of PAD enzymes (PAD1–4 and PAD6) have

been identified in chromosome 1p36 [109]. Additionally, a bacterial PAD enzyme can be expressed by *Porphyromonas gingivalis* (*P. gingivalis*) [110]. The structure of all PAD isoforms have not yet been achieved, but work on PAD2 and PAD4 enzymes revealed the presence of several regulatory calcium binding sites that are responsible for the correct positioning of the catalytic cysteine residue (Figure 1.8) [111-114].

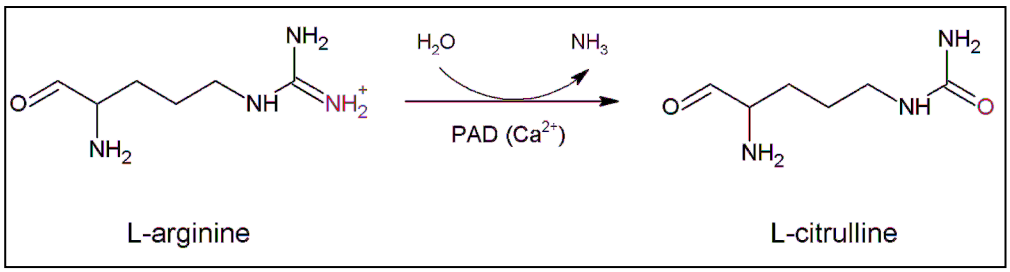

Figure 1.7 Conversion of protein arginine residues into citrulline by PAD enzymes. PAD – peptidylarginine deiminase; Ca^{2+} – calcium; H_2O – water; NH_3 – ammonia.

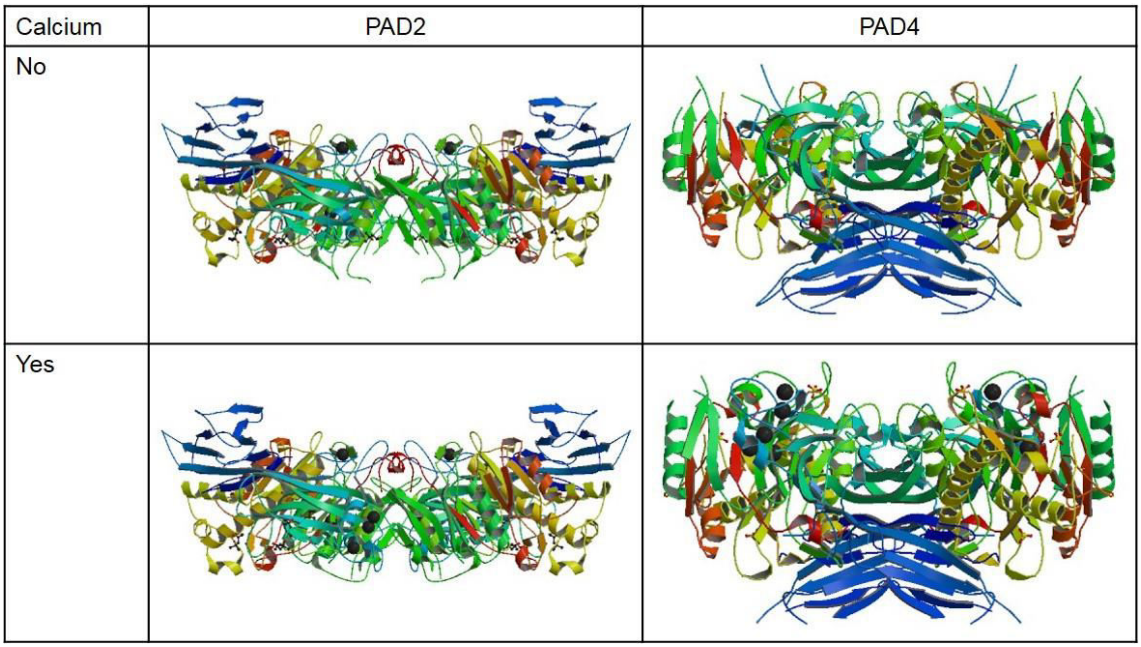

Figure 1.8 Schematic representation of PAD2 and PAD4 enzymes structures in the presence and absence of calcium. The crystal structures of PAD2 enzyme (Protein data bank – PDB – entity: 4N20, 4N2B) were determined at 1.6–1.7 Å resolution [113]. The crystal structures of PAD4 enzyme (PDB: 1WD8, 1WD9) were determined at 2.6–2.8 Å resolution [111].

Physiologically, citrullination is an essential PTM since citrulline is a non-standard amino acid. Human PAD enzyme isoforms are highly conserved (70–95% identical

amino acids) amongst themselves. However, factors like the physicochemical features (structure, charge, size, flexibility and the amino acids flanking the arginine residues) of the target protein, the subcellular localisation of the enzyme and its microenvironment influence the susceptibility of arginine residues for citrullination by PAD enzymes [115]. PAD1 enzyme is predominantly expressed in the epidermis and uterus [116-119]. The citrullination of keratin and keratin-associated protein filaggrin during keratinocyte differentiation reduces the flexibility of the keratin cytoskeleton, stimulating the cornification of the epidermis and maintaining the physical resistance of the epidermis [120-124]. The PAD2 enzyme is the most abundant PAD isoform and is expressed in several tissues, like skeletal muscle, brain, spleen and secretory glands [118, 125-131]. The PAD2 enzyme is regulated at transcriptional and translational levels [132, 133] and the levels of this enzyme are also under hormonal regulation [119, 125, 134-136]. In the nervous system, PAD2 is expressed in the grey matter, hypothalamus and also in the cerebellum, in oligodendrocytes, astrocytes, microglial cells and Schwann cells [137]. The citrullination of filament proteins like myelin basic protein (MBP), the major component of the myelin sheath in nerve cells, and glial fibrillary acidic protein (GFAP) is associated with the plasticity of the central nervous system [138, 139]. PAD2 messenger ribonucleic acid (mRNA) is expressed in monocytes and macrophages but the protein form is just observed in macrophages [133]. In macrophages, PAD2 mRNA expression and protein form of PAD2 enzyme are observed, however, the intracellular calcium levels are not sufficient for the enzymatic reaction to occur. So, activation of intracellular PAD2 enzyme depends on the increase of cytosolic calcium concentration, which is observed in situations of apoptosis and antigen uptake/processing [133, 140]. Vimentin, an intermediate filament protein, was found to be citrullinated in apoptotic macrophages, suggesting that the citrullination of this protein is involved in the disassembly of the vimentin filaments and consequent collapse of the vimentin cytoskeleton, observed in apoptotic conditions [141]. PAD3 expression is restricted to hair follicles [118, 142-144], where it is able to act on trichohyalin (a structural protein

of inner root sheath cells of hair follicles) [108, 144]. Citrullination of trichohyalin opens its α-helical structure, allowing the cross-linking of this protein with keratin filaments, forming a firm tube to guide the directional growth of the hair fibre [145, 146]. PAD4 enzyme is expressed by cells of the hematopoietic lineage, in particular granulocytes [147-149] and monocytes [133, 150] and can be detected intracellularly at nuclear level [149] in different tissues [130, 151]. PAD4 enzyme citrullinates nuclear proteins, such as histones and nucleophosmin/B23 [148, 149]. The high content of arginine residues in histones renders a strong net positive charge, which is essential for the interaction with the negatively charged DNA. Citrullination of histones changes their conformation and their net charge, consequently impairing the interaction with deoxyribonucleic acid (DNA) and increasing DNA susceptibility to degradation. PAD5 enzyme was initially described as a new PAD enzyme isoform but was later confirmed to correspond to PAD4 enzyme [147, 149]. PAD6 enzyme is found in early embryos and ovaries, where it is responsible for the reorganisation of egg cytoplasmic sheets during early embryo development [152] (Table 1.4).

Table 1.4 Tissue distribution, substrates and biological functions of PAD enzyme isoforms.

Isoform	Protein distribution	Substrates	Biological functions
PAD1	Epidermis, uterus	Keratin K1, filaggrin	Cornification of epidermal tissues
PAD2	Nervous system, skeletal muscle, spleen, uterus, pituitary gland	MBP, vimentin, β and γ-actins	Plasticity of the nervous system, transcription regulation, innate immune defence, female reproduction
PAD3	Epidermis, hair follicles	Filaggrin, trichohyalin	Regulation of epidermal functions
PAD4	Neutrophils, monocytes, macrophages, mammary gland epithelial cells	Histones H2A, H3 and H4, p300/CBP, nucleophosmin, nuclear lamin C	Chromatin decondensation, transcription regulation
PAD6	Eggs, ovary, early embryo	Unknown	Oocyte cytoskeletal sheet formation and female fertility

P. gingivalis is a major periodontal pathogen involved in PID [153]. *P. gingivalis* PAD (PPAD) can be observed as a secreted or a cell/membrane vesicle-associated

enzyme. This bacterial PAD enzyme isoform (AAF06719) is not calcium dependent and, contrary to human isoforms, is able to convert both free L-arginine and peptidyl-bound arginine residues [110, 154]. Citrullination by PPAD enzyme affects complement activity [155], inactivates epidermal growth factors [156] and contributes to infection of gingival fibroblasts and stimulation of the prostaglandin E2 synthesis [157], promoting the survivability of *P. gingivalis*. Furthermore, the production of ammonia, as a bi-product of the citrullination reaction, increases the environmental pH of the mouth and impairs neutrophil responses [110, 158]. The PPAD enzyme is able to citrullinate bacterial and host proteins [158], suggesting its involvement in the breakdown of the immune system associated with autoimmune diseases.

Generally, citrullination results in a decrease in the net positive charge of the protein, as arginine is a positively charged amino acid and citrulline is a neutral amino acid. Arginine is involved in the maintenance of ionic interactions with other amino acid side chains and in the establishment of hydrogen bonds with the peptide backbone and other amino acid side chains, being a key amino acid in the three-dimensional structure of proteins and in the interaction with other molecules. Consequently, the conversion of arginine into citrulline via citrullination results in the loss of potential ionic bonds and interferes with hydrogen bonds. These changes induce partial unfolding of the protein, leading to the formation of new motifs and the generation of neo-epitopes [146]. The involvement of citrullination in the breakdown of the immune system in RA and PID is detailed in the next sections.

1.3.2. Rheumatoid arthritis

RA is a chronic autoimmune disease, characterised by the accumulation of inflammatory cells (T and B cells, neutrophils and monocytes) in the synovial membrane. The inflammatory response in RA is mediated by the activation of T cells, macrophages and fibroblast-like synoviocytes, leading to the production of pro-inflammatory cytokines, like TNF and IL-6, and, ultimately, to tissue and bone

destruction [159, 160]. Clinically, RA is marked by pain, deformity and impaired functionality of the joints. According with the World Health Organisation (WHO) RA affects 0.3–1% of the adult population worldwide and has a higher incidence in women and in developed countries. The initiating event in the origin of RA is not known but genetic and environmental factors are involved in the pathogenesis of this disease [161-163]. Fifty to sixty per cent (50–60%) of RA susceptibility is associated with genetic factors, in particular with the presence of a specific allele in the HLA-DR gene [159, 164-166]. The first evidence for this association was demonstrated by Gregersen *et al*. in 1987 [167]. These authors proposed that a specific amino acid motif (Arginine, Alanine, Alanine – RAA) was shared by HLA-DR1 alleles associated with RA. Later, this shared epitope (SE) was shown to correlate with RA susceptibility and severity [166, 168, 169]. The presence of this SE motif induces the expression of MHC-II molecules with a different anchoring pocket that, consequently, will affect the interaction between MHC-II molecules and CD4 T cells [167, 170-172].

The environmental influence on RA pathogenesis is based on factors such as smoking, infections, caffeine intake and exposure to silica [109]. Smoking is the most established environmental risk factor for RA and increases by 50% the risk of developing RA [159, 162, 173-177].

The autoimmune nature of RA has been associated with the presence of autoantibodies in the serum and synovial fluid of RA patients, in particular rheumatoid factors (RF) and anti-citrullinated protein antibodies (ACPA) [178-182]. RF are antibodies directed against the Fc region of immunoglobulin G. Most of the ACPA-positive RA patients are also positive for RF, but ACPA are more specific and sensitive for the diagnosis of RA and are better predictors of poor prognostic outcomes [183]. Moreover, the presence of ACPA is related to the expression of SE, suggesting that a MHC-II:CD4 T cell response may be involved in the initiation of the immune reaction observed in RA [170, 184]. ACPA also appear to be associated with the early development of RA [185] and the severity and progression of the disease [186].

Dysregulation of PAD enzyme activity has been implicated in the origin of multiple disorders, such as psoriasis, multiple sclerosis, tumorigenesis and RA [109]. In RA, PAD2 and PAD4 enzymes were found in the synovial membrane of RA patients [187-189] and in synovial fluid cells [133]. Neutrophils and monocytes/macrophages are sources of PAD2 and PAD4 enzymes in RA. The activation of neutrophils leads to the amplification of the disease due to the production of reactive oxygen species (ROS), proteolytic enzymes and pro-inflammatory cytokines. Neutrophil immune responses include engulfing and degradation of microorganisms or opsonised particles, release of lytic enzymes to destroy extracellular pathogens and release of neutrophil extracellular traps (NET) that can trap and kill microbes [190, 191]. NET consist of nuclear chromatin associated with nuclear histones, granular antimicrobial proteins and cytoplasmic proteins [192]. The formation of NET, known as NETosis, was shown to depend on the citrullination of histones by PAD4 [193, 194]. In addition, PAD2 and PAD4 enzymes can be found attached to NET in the synovial fluid of RA patients [195]. PAD2 and PAD4 enzymes have also been reported in activated macrophages that infiltrate the synovium of RA patients [133]. Under normal physiological conditions, cytosolic calcium concentration is not sufficient for PAD activity, suggesting that intracellular citrullination only occurs when calcium homeostasis is lost, in situations like cell stimulation or after membrane disintegration resultant from apoptosis or NETosis [196]. Both intracellular and extracellular proteins have been reported to be citrullinated in RA, such as vimentin, fibronectin, fibrinogen, fibrin and α-enolase [184, 197-201]. Citrullinated fibrin, for example, was detected in the synovial membrane of RA patients [202] and ACPA were observed in the serum of RA patients. ACPA described so far include: anti-perinuclear factor [203, 204] and anti-keratin autoantibodies [205, 206] against citrullinated fillagrin [207]; anti-Sa autoantibodies against citrullinated vimentin [199, 208]; and anti-cyclic citrullinated peptide autoantibodies [209, 210]. Moreover, plasma cells with the ability to produce ACPA were found in the synovial membrane of RA patients [211]. This evidence

strongly suggests that the occurrence of citrullination in the synovium has a major role in driving the production of ACPA and, consequently, in triggering the immune response and chronic inflammation observed in RA [212].

1.3.3. Periodontitis

PID is a chronic inflammatory disease that affects the periodontal tissue and is characterised by the accumulation of lymphocytes and monocytes, tissue oedema, endothelial cell proliferation and matrix degradation. Clinically, PID is manifested by gingival bleeding, increased pocket depth, periodontal bone loss, increased tooth mobility and, ultimately, tooth loss [213]. PID affects 10–15% of the worldwide adult population [214]. PID susceptibility is also related with genetic and environmental factors. A genetic risk factor for PID is the presence of the SE and the environmental risk factors associated with PID are mainly smoking and stress [215],216]. PID can be categorised from gingivitis to aggressive periodontitis according with the composition of the subgingival microbial flora and also the factors that influence the host response to the microbial attack [161, 213]. A subgingival biofilm consisting of hundreds of anaerobic Gram-negative bacterial species is the source of the chronic inflammation responsible for the clinical manifestations of PID [213, 216]. Recent metagenomics, metatranscriptomic and mechanistic studies data [217-222] suggested that PID pathogenesis results from polymicrobial synergy and dysbiosis, which perturb the balanced biofilm associated with periodontal tissue homeostasis [223-225]. Bacteria implicated in the origin of PID include *Aggregatibacter actinomycetemcomitans*, *Porphyromonas gingivalis*, *Prevotella intermedia*, *Parvimonas micra*, *Treponema species* and *Tannerella forsythia* [153, 226]. Among these, *P. gingivalis* appears to be the major infectious agent associated with PID, since it is detected in higher abundance in patients with aggressive forms of PID [227]. The virulence associated with *P. gingivalis* is caused by fimbriae, degradative enzymes (like PPAD and gingipains), exopolysaccharide capsule and atypical lipopolysaccharide [228, 229].

PPAD is able to citrullinate both bacterial and host proteins, inducing an autoimmune response [230]. The amino acid sequence of PPAD and human PAD enzymes is very distinctive and the main difference in the mechanism of action of these enzyme is the fact that PPAD citrullinates preferentially C-terminal arginine residues and does not require calcium for activity, in contrast to human PAD enzymes that citrullinate internal arginine residues on a calcium-dependent manner [110]. PPAD is able to citrullinate human fibrinogen and α-enolase after the cleavage of these proteins by gingipains, which exposes target C-terminal arginine residues [231]. This particular processing induces the formation of neoepitopes and consequent generation of autoantibodies. In addition, the citrullination of epidermal growth factor (EGF) by PPAD was found to inhibit EGF-induced fibroblast proliferation and migration, affecting the healing process on periodontal tissue and consequently delaying the resolution of inflammation [156]. Other substrates of PPAD enzyme include fibrin, vimentin and bradykinin [110].

The autoimmune nature of PID involves autoreactive T cells, NK cells, anti-neutrophil cytoplasmic autoantibodies, heat shock proteins, autoantibodies and genetic factors. Since 1970, when Ivanyi and Lehner first suggested a cell-mediated immunity in PID [232], several studies have found evidence for the role of T cells in the homeostasis of periodontal tissues [233], modulation of the immune responses [234] and mediation of the bone loss characteristic from PID [235]. Periodontopathic bacteria have been shown to be involved in the suppression of lymphocyte induction [236-240], in particular *P. gingivalis* was shown to down-regulate over one thousand genes and up-regulate about thirty genes in both CD4 and CD8 subsets of T cells in mice. From the total of down-regulated genes most are metabolism-associated genes but some encode for proteins involved in the immune response, in particular for cytokines and cytokine receptors [241]. Furthermore, T cells with decreased ability to respond in an autologous mixed lymphocyte reaction and reduced production of IL-2 and IL-2R expression were extracted from PID patients' tissues [242, 243]. The association between different T cell subsets and PID progression has also been investigated.

Decreased CD4:CD8 ratio was found on T cells isolated from PID patients' gingival tissues [242, 244] and in histological samples from PID patients [245, 246]. However, there is no consensus from studies on T cell subset involvement in PID and no differences [247, 248] and increases [249, 250] in the CD4/CD8 T cell ratio have also been reported.

The impact of PID spreads from the oral cavity to the systemic circulation. PID has been associated with increased susceptibility of PID patients to diseases such as atherosclerosis [251, 252], adverse pregnancy outcomes [253], RA [254] and cancer [255]. High levels of bacterial pro-inflammatory components and Gram-negative bacteria were found in circulation in patients with severe PID compared with healthy individuals [256-258]. In particular, *P. gingivalis* DNA was detected in plasma and synovial fluid from RA patients [259]. Furthermore, antibodies against oral pathogens can also be found in the plasma of patients with pancreatic cancer, correlating PID with increased risk of this type of cancer [260]. Although PID is an irreversible chronic inflammatory disease, the levels of *P. gingivalis* present in the gingival tissue of PID patients decreased after non-surgical periodontal treatment and the general periodontal health of these patients was increased [261]. Furthermore, plaque removal treatment through improved oral hygiene reduces the rate of tooth loss and improves general quality of life [262].

1.4. Rheumatoid arthritis and periodontitis: a link through citrullination

The association between RA and PID dates back from 400 BC, when Hippocrates reported the treatment of a patient with joint pain after the extraction of a single tooth [263]. Recently, several epidemiological studies showed that RA patients have a significantly increased prevalence in PID, strengthening the link between these two diseases [264-272]. Also, the severity of RA is related with the severity of PID and vice-versa [273-275]. RA and PID are both chronic destructive inflammatory diseases characterised by the production of pro-inflammatory cytokines and tissue destruction,

in the synovium and periodontium, respectively [197, 216, 276, 277]. Other common features between these diseases include increased susceptibility to PID in RA patients and vice-versa and increased RA and PID susceptibility in genetically predisposed individuals (SE carriers) and the impact of similar environmental risk factors, like smoking [216].

Accumulating evidence support the initiation of an immune response between PID and RA: the use of antibiotics against anaerobic bacteria for the successful treatment of RA [278]; the presence of *P. gingivalis* DNA in the plasma and synovial fluid of RA patients [259]; the occurrence of high levels of antibodies against oral bacteria in the serum and synovial fluid of RA patients [279]. The main theory for the link between RA and PID is based on the production of PPAD enzyme by *P. gingivalis*. *P. gingivalis* is able to impair the epithelial integrity, invade human endothelial cells and modify transcription and protein synthesis [254]. The localisation of PPAD at the bacterial surface promotes the interaction with host proteins via bacterial adhesins. The PPAD enzyme induces the citrullination of host and bacterial proteins in the inflamed periodontium, triggering an immune response against self-proteins and promoting the production of ACPA in susceptible individuals [280]. ACPA have been extensively reported to associate with the early development of RA [185] and are also associated with worse outcomes of disease [186]. Increased levels of ACPA have been reported in patients with PID when compared with healthy controls [281]. Furthermore, ACPA levels in RA patients also correlate with the presence of PID [282]. For example, autoantibodies against citrullinated α-enolase, an established RA autoantigen, were found to cross-react with α-enolase citrullinated by PPAD [254]. Moreover, increased levels of antibodies against citrullinated α-enolase were detected in animal models of PID [283]. Immune complexes consisting of ACPA and citrullinated antigens that are formed lead to the activation and stimulation of phagocytic cells, like neutrophils and macrophages. Activated neutrophils and macrophages, in turn, release inflammatory mediators like cytokines, metalloproteinases, eicosanoids and reactive oxygen and

nitrogen species, perpetuating the inflammatory response and ultimately leading to tissue destruction [284]. After the initial break in the immune tolerance to PPAD-citrullinated peptides, processes of epitope spreading and molecular mimicry are responsible for cross-reactivity of ACPA with joint proteins and formation of immune complexes in the inflamed joint, leading to the exacerbation and perpetuation of the inflammatory response observed in RA [231, 285]. The chronic inflammation is further perpetuated by the citrullination of host proteins by human PAD enzymes, in particular PAD2 and PAD4 isoforms [277].

1.5. Hypothesis and aims

Citrullination studies have previously been focused in the generation of neoepitopes that drive an autoimmune response through the formation of immune complexes between ACPA and citrullinated antigens. Less importance has been attributed to the effects of PAD enzymes on the cells responsible for the immune response. T cells have shown to have important roles in the development of the immune response observed in RA and PID. Furthermore, the citrullination of HLA binding peptide was shown to increase the peptide-MHC affinity, leading to the activation of CD4 T cells in animal models [286]. Considering this evidence, this thesis aims to investigate the hypothesis that citrullination, as observed in RA and PID, modulates T cell activation. To address this question the main objectives established were as it follows:

- To optimise conditions to detect and identify cellular protein targets of citrullination;
- To establish a functional and biochemical competent T cell model to perform citrullination studies;
- To investigate the effects of PAD enzymes on the activation T cells;
- To analyse the inflammatory, citrullination and redox status and to compare the expression of genes of interest in PID patients.

Chapter 2 Materials and methods

2.1. Materials

2.1.1. Consumables

Cell culture and general plasticware were obtained from Thermo Fisher Scientific Inc. (Loughborough, UK). Plasticware for gene expression studies was obtained from VWR International Ltd. (Lutterworth, UK). Needles and syringes for blood collection were from BD (Becton, Dickinson and Company, Oxford, UK). VACUETTE® ethylenediaminetetraacetic acid (EDTA) and VACUETTE® heparin tubes were from Greiner Bio-One Ltd. (Stonehouse, UK). All salts, buffers and chemicals were obtained from Sigma-Aldrich Co. (Dorset, UK) unless stated. Protein inhibitor cocktail consisted of 4-(2-aminoethyl)benzenesulphonyl fluoride hydrochloride (AEBSF, 104 mM), aprotinin (80 μM), bestatin (4 mM), E-64 (1.4 mM), leupeptin (2 mM) and pepstatin A (1.5 mM). Recombinant human PAD2 and 4 (hPAD2 and hPAD4) enzymes purified from bacterial cell lysate using nickel (II)-beads were obtained from ModiQuest Research B. V. (Oss, Netherlands).

2.1.2. Antibodies

Table 2.1 Details of antibodies used.

Antigen	Application	Description	Product code	Company
CD25	FC	Mouse monoclonal [BC96] conjugated with APC	ab134477	Abcam plc. (Cambridge, UK)
CD28	FS	Mouse monoclonal [CD28.2] functional grade purified	16-0289	eBioscience Ltd. (Hatfield, UK)
CD3	FS	Mouse monoclonal [OKT3] functional grade purified	16-0037	eBioscience Ltd. (Hatfield, UK)
CD3	IB	Rabbit polyclonal IgG	ab16044	Abcam plc. (Cambridge, UK)
CD38	FC	Mouse monoclonal [HB7] conjugated with FITC	11-0388	eBioscience Ltd. (Hatfield, UK)
CD4	FC	Mouse monoclonal [EDU-2] conjugated with PE	ab1155	Abcam plc. (Cambridge, UK)
CD8	FC	Mouse monoclonal [RPA-T8] conjugated with PE-Cy5.5	35-0088	eBioscience Ltd. (Hatfield, UK)
NF-κB p65	IB	Rabbit polyclonal IgG	ab7970	Abcam plc. (Cambridge, UK)
Rabbit IgG	IB	Goat polyclonal conjugated with peroxidase	A6154	Sigma-Aldrich Co. (Dorset, UK)

APC – allophycocyanin; Cy – cyanine; CD – cluster of differentiation; FC – flow cytometry; FITC – fluorescein isothiocyanate; FS – functional studies; IB – immunoblotting; IgG – immunoglobulin; NF-kB – nuclear factor-kappa B; PE – phycoerythrin.

2.2. Fibrinogen citrullination

2.2.1. Reagents

FNG isolated from human plasma, containing more than 80% clottable protein, was obtained from Merck Millipore Ltd. (Watford, UK) and Sigma-Aldrich Co. (Dorset, UK). Roswell Park Memorial Institute (RPMI) medium (RPMI 1640 with stable L-glutamine) was from Gibco^{TM} (Thermo Fisher Scientific Inc., Loughborough, UK).

2.2.2. Background

Citrullination is an enzymatic post-translational modification catalysed by PAD enzymes (EC 3.5.3.15.). In humans, there are five isoforms of PAD (PAD1–4 and PAD6). Citrullination is responsible for the conversion of L-arginine residues into L-citrulline in the polypeptide chain, in a calcium dependent manner (Figure 1.7) [1]. FNG is one of the proteins that has been described as citrullinated *in vivo* in the context of RA [184, 197, 198]. Therefore, FNG was used as an *in vitro* model to develop methods for the detection of citrullination.

2.2.3. Protocol

FNG (100 µg) was dissolved in either phosphate buffer saline (PBS) or RPMI and citrullinated with 50 mU of hPAD2 or hPAD4 enzymes in 100 µL reaction buffer (100 mM Tris-HCl, pH 7.5, 5 mM dithiothreitol – DTT, 10 mM calcium chloride – $CaCl_2$). The controls used in the experiment included 1) no enzyme, 2) addition of EDTA immediately after addition of PAD enzymes and 3) heat inactivated (HI – 30 minutes at 63°C) PAD enzymes. The reaction was performed for 2 hours at 37^0 C and was stopped by boiling the samples with Laemmli buffer for 3 minutes or by adding 200 mM EDTA, according to the follow-up method.

2.3. Studies on Jurkat E6.1 T cells

2.3.1. Reagents

Jurkat E6.1 T cells were from American Type Culture Collection (ATCC®, Teddington, UK). Fetal bovine serum (FBS), penicillin/streptomycin and RPMI medium were from Gibco™ (Thermo Fisher Scientific Inc., Loughborough, UK). RPMI complete medium (RPMI 1640 supplemented with 10% FBS and 1% penicillin/streptomycin) was stored at 4^0 C and used within a month.

2.3.2. Background

Jurkat E6.1 T cells are a subclone of the original Jurkat cells that were derived from a 14-year-old boy with T cell acute lymphoblastic leukaemia. Jurkat E6.1 T cells have the characteristics of immature thymocytes and are regularly used to study TCR signalling and cytokine production [287]. Here, we studied the T cell activation response by treating Jurkat E6.1 T cells with phytohaemagglutinin-L (PHA-L) or with anti-CD3/anti-CD28 antibodies. PHA-L is the subunit L of PHA and is responsible for the leukocytic activity of this lectin. By crosslinking glycosylated proteins on the surface of T cells PHA-L is able to induce TCR activation. Antibodies against CD3 and CD28 receptors were used here to mimic the two-step TCR activation by APC.

2.3.3. Protocol: activation of Jurkat E6.1 T cells

Jurkat E6.1 T cells were cultured at 37^0 C in 5% carbon dioxide (CO_2) using RPMI complete medium. Medium was changed every 4 days and cells were re-seeded at a density of 2–5 x 10^5 cells/mL. On the day of the experiment, cells were washed with complete RPMI 1640 medium and 1 mL was added into 24-well plates at a density of 1 x 10^6 cells/mL. Cells were then stimulated with PHA-L or with anti-CD3/anti-CD28 antibodies at 37^0 C in 5% CO_2 for 24, 48 or 72 hours. A non-activated control was also included. The concentrations of PHA-L ranged from 0 to 10 µg/mL. The anti-CD3 and anti-CD28 antibodies were prepared in sterile PBS and the concentrations of anti-CD3

ranged between 0 and 5 μg/mL and the concentration of anti-CD28 was 2 μg/mL. In the antibodies activation method, anti-CD3 antibody was pre-coated into a 24-well plate. After overnight incubation at 4^0 C, the plate was washed three times with PBS and the cells were seeded. Anti-CD28 antibody was added to the plate immediately after addition of the cells. Following incubation, cells were collected and cell viability assessed with CellTiter-Blue® cell viability assay (Promega Co., Southampton, UK), as described in 2.14, or trypan blue exclusion assay (described in section 2.15).

2.4. Studies on primary T cells in peripheral blood mononuclear cells population

2.4.1. Reagents

Lymphoprep™ was purchased from Axis-Shield (Dundee, UK). FBS, penicillin/streptomycin and RPMI medium were from Gibco™ (Thermo Fisher Scientific Inc., Loughborough, UK). Bovine serum albumin (BSA) was from Thermo Fisher Scientific Inc. (Loughborough, UK). RPMI complete medium was stored at 4^0 C and used within a month.

2.4.2. Volunteers

Blood was collected from healthy volunteers aged between 25 and 55 years old. Ethical approval was granted by Aston University research ethics committee (ethics reference 802). Volunteers were free to withdraw from the study at any time point.

2.4.3. Background

Peripheral blood includes many different cells. Peripheral blood mononuclear cells (PBMC) are defined as the fraction of the blood that contains round cells with round nucleus, including lymphocytes and monocytes. By layering whole blood on top of a density gradient of Lymphoprep™ (Axis-Shield, Dundee, UK) PBMC and platelets can

be separated from granulocytes and erythrocytes according to their different densities [288].

2.4.4. Protocol: optimisation of peripheral blood mononuclear cells isolation

Blood from healthy volunteers was collected by venepuncture into VACUETTE® EDTA tubes (Greiner Bio-One Ltd., Stonehouse, UK) and PBMC were isolated by centrifugation over Lymphoprep™. Briefly, 20 mL of blood was diluted 1:2.5 with sterile filtered 0.1% (w/v) BSA in PBS and layered over Lymphoprep™. Different isolation conditions and batches of Lymphoprep™ were compared (Table 2.2) in order to maximise the yield of recovered cells. After centrifugation, the layer between plasma and Lymphoprep™, consisting of PBMC, was collected and washed twice with 0.1% (w/v) BSA in PBS. Based on the number of PBMC collected from each condition (Table 2.3), determined by the trypan blue exclusion assay (described in section 2.15), the system selected for further experiments with PBMC was a two-step centrifugation for the separation of diluted blood over Lymphoprep™ (ratio 25:11) and a spin of 400 x g for 10 minutes to further pellet the cells. After the first centrifugation, the top clear layer, consisting of platelets, was removed. It was also noted that using older batches of Lymphoprep™ could affect the separation, so Lymphoprep™ solution was used within 1 month after opening.

Table 2.2 Conditions compared to isolate PBMC from blood (2.5 mL per condition). Batch 1 refers to Lymphoprep™ solution open and used for more than one month; batch 2 refers to Lymphoprep™ solution used within one month after opening.

Condition	Lymphoprep™	Ratio Lymphoprep™:blood	First spin	Second spin	Spin to pellet cells
1	Batch 1	3:6	800 x g, 20', 20^0 C	---	250 x g, 10'
2	Batch 1	3:6	800 x g, 20', 20^0 C	---	400 x g, 10'
3	Batch 2	3:6	800 x g, 20', 20^0 C	---	250 x g, 10'
4	Batch 2	3:6	800 x g, 20', 20^0 C	---	400 x g, 10'
5	Batch 1	11:25	160 x g, 20', 20^0 C	381 x g, 20', 20^0 C	250 x g, 10'
6	Batch 1	11:25	160 x g, 20', 20^0 C	381 x g, 20', 20^0 C	400 x g, 10'
7	Batch 2	11:25	160 x g, 20', 20^0 C	381 x g, 20', 20^0 C	250 x g, 10'
8	Batch 2	11:25	160 x g, 20', 20^0 C	381 x g, 20', 20^0 C	400 x g, 10'

Table 2.3 Total number of PBMC recovered with each of the tested conditions. Cell number was determined by the trypan blue exclusion assay.

Condition	Cell count (x 10^6)
1	2.0
2	1.8
3	2.1
4	1.1
5	2.1
6	1.5
7	2.9
8	3.3

2.4.5. Protocol: activation of primary T cells from peripheral blood mononuclear cells

Blood from healthy volunteers was collected by venepuncture into VACUETTE® EDTA tubes (Greiner Bio-One Ltd., Stonehouse, UK) and PBMC were isolated by centrifugation over Lymphoprep^{TM}. Briefly, 20 mL of blood was diluted 1:2.5 with sterile filtered 0.1% (w/v) BSA in PBS and 25 mL was layered over 11 mL of Lymphoprep^{TM}. After two centrifugation steps (160 x g at 20^0 C for 20 minutes; 381 x g at 20^0 C for 20 minutes), the layer between plasma and Lymphoprep^{TM}, consisting of PBMC, was collected and washed twice with 0.1% (w/v) BSA in PBS. The cells were resuspended into complete RPMI 1640 medium at a density of 0.5 x 10^6 cells/mL in a 24-well plate (1 mL per well) and stimulated with PHA-L or antibodies against CD3 and CD28 for 24, 48 or 72 hours at 37^0 C in 5% CO_2. The concentrations of PHA-L ranged from 0 to 5 µg/mL, the concentrations of anti-CD3 ranged between 0 and 5 µg/mL and the concentration of anti-CD28 was 2 µg/mL. After the incubation period, cells were collected and further analysed.

2.4.6. Protocol: citrullination of peripheral blood mononuclear cells

PBMC (5 x 10^5) isolated from healthy volunteers, as previously described in 2.4.5, were pre-treated with 125, 250, 500 or 1000 mU of hPAD2 or hPAD4 enzymes in RPMI complete medium. After 2 hours of incubation at 37^0 C in 5% CO_2, enzymes were washed off from the cell culture (by centrifuging at 400 x g for 5 minutes) and replacing with fresh medium then cells were activated with 1 µg/mL of anti-CD3 antibody and 2 µg/mL of anti-CD28 antibody at 37^0 C in 5% CO_2 for 24 hours. Controls without the enzymes and without activation were also included. After the activation period, cells were collected for further analysis.

2.5. Clinical samples

2.5.1. Reagents

FBS, PBS (without calcium and magnesium) and RPMI medium were from Gibco™ (Thermo Fisher Scientific Inc., Loughborough, UK). BSA, Dynabeads® CD4 positive isolation kit and Dynabeads® CD8 positive isolation kit were from Thermo Fisher Scientific Inc. (Loughborough, UK). Periopaper™ strips were obtained from Oraflow Inc. (Plainview, NY, USA).

2.5.2. Volunteers

Blood and gingival crevicular fluid (GCF) samples from chronic PID patients were collected from patients attending the periodontal clinic at Birmingham Dental Hospital. Age-matched, periodontally healthy controls were collected from staff of the Birmingham Dental Hospital (Table 2.4). Both patient and healthy samples were prepared and kindly provided by Professor Iain Chapple and Dr Paul Weston, Birmingham Dental Hospital. Chronic PID, as previously described [289], was defined as the presence of at least two non-adjacent sites per quadrant with probing pocket depths ≥ 5 mm which bled on probing and which demonstrated radiographic bone loss ≥ 30% of the root length (non-first molar or incisor sites). All study participants were systemically healthy, did not use recreational drugs and had no special dietary requirements. Ethical approval was granted by South Birmingham Local Research Ethics Committee (ethics reference 14/SW/1148). Volunteers were free to withdraw from the study at any time point.

Table 2.4 Demographics of the sample population.

Parameter	HC group	PID group
N	6	6
Gender (M/F)	1/5	3/3
Age (years)	49.0 ± 10.1	49.5 ± 9.4

HC – healthy controls; M/F – male/female gender; N – number of subjects in each group; PID – periodontitis patients; Age is expressed as mean ± SD.

2.5.3. Background

Plasma is the extracellular matrix of blood cells. Plasma consists of molecules absorbed from the gut and secreted from the cells, including proteins, lipids, glycans, nutrients and salts. To obtain plasma, whole blood is treated with an anticoagulant and the cells are removed by centrifugation [290].

GCF is found at the gingival margin or within the gingival crevice. In periodontal disease GCF is rich in bacterial enzymes, bacterial degradation products, connective tissue degradation products, host-derived enzymes, inflammatory mediators and extracellular matrix proteins making this fluid an important source for biochemical analysis [291].

Isolation of CD4 and CD8 T cells was performed using a positive isolation method. This technique consists of the separation of cells from a mixed population by immunoaffinity. In this case, CD4 and CD8 T cells were isolated from the PBMC population by incubating the entire cell population with magnetic beads conjugated with an antibody specific for CD4 or CD8, respectively. The unbound cell population is then removed and the cells of interest are detached from the magnetic beads.

2.5.4. Solutions

- Buffer 1:
    - PBS, without calcium and magnesium
    - 0.1% (w/v) BSA
    - 2 mM EDTA
    - pH 7.4
- Buffer 2:
    - RPMI 1640
    - 1% (v/v) FBS

2.5.5. Protocol: CD4 and CD8 T cells positive isolation from whole blood

CD4 T cells were isolated from whole blood using Dynabeads® CD4 positive isolation kit according to the manufacturer's instructions. Briefly, 5 mL of whole blood was diluted with 10 mL of buffer 1 and centrifuged at 600 x g for 10 minutes at 4^0 C. The upper layer, consisting of plasma and platelets, was discarded and the blood resuspended in 5 mL of buffer 1. Pre-washed anti-CD4 Dynabeads (12.5 µL per mL of blood) were added to the blood and incubated for 30 minutes at 4^0 C with gentle tilting and rotation. Bead-bound cells were isolated using a magnet and resuspended in 100 µL buffer 2 per mL blood in the original sample. The remaining cells were used for CD8 T cell isolation using Dynabeads® CD8 positive isolation kit in accordance with the manufacturer's instructions. Briefly, pre-washed anti-CD8 Dynabeads (12.5 µL per mL of blood) were added to CD4 T cell-depleted blood and incubated for 30 minutes at 4^0 C with gentle tilting and rotation. Bead-bound cells were isolated using a magnet and resuspended in 100 µL buffer 2 per mL of blood in the original sample. To separate CD4 or CD8 T cells from Dynabeads, 10 µL DETACHaBEAD solution was added per mL of initial blood used and cells incubated for 45 minutes at room temperature (RT) with gentle mixing. Dynabeads were recovered using a magnet while supernatants containing released CD4 or CD8 T cells were transferred to a new tube and washed from DETACHaBEAD with 10 mL buffer 2. CD4 and CD8 T cells were resuspended in 1 mL buffer 2, counted with trypan blue exclusion assay (described in section 2.15) and collected for further analysis.

2.5.6. Validation of CD4 and CD8 T cells isolation

To assess the purity of CD4 and CD8 T cell isolated from whole blood, 1 x 10^6 cells in buffer 2 were incubated on ice for 15 minutes and then with anti-CD4-PE (130 ng) or anti-CD8-PE-Cy5.5 (125 ng) antibodies, respectively, for 30 minutes on ice. Cells were then analysed by flow cytometry on a Cytomics FC 500 and CXP® software (Beckman Coulter Inc., London, UK). The respective isotype controls (mouse IgG2a PE and

mouse IgG1 PE-Cy5.5) were also used. Data were analysed using Flowing software v 2.5.

2.5.7. Protocol: plasma collection

After collection, 4 mL of whole blood was centrifuged twice at 1600 x g for 10 minutes to remove cells and the plasma was aliquoted into new tubes and stored at -80^0 C until analysis. Plasma (99 µL) to be analysed for GSH quantification was mixed with 1 µL of sulfosalicylic acid (SSA), centrifuged at 13,000 x g for 90 seconds and stored at -80^0 C until further analysis.

2.5.8. Protocol: gingival crevicular fluid collection

GCF samples were collected from a mesio-buccal and disto-lingual site on each of three teeth (a molar, pre-molar and canine or incisor) in the left and right quadrant, providing four samples. GCF samples were collected for 30 seconds on Periopaper™ strips (Oraflow Inc., Plainview, NY, USA) from volunteers with chronic periodontitis and matched controls, GCF volumes were measured using a pre-calibrated Periotron 8000™ (Oralflow Inc., Plainview, NY, USA) equipment, as described previously [289], snap frozen in liquid nitrogen and stored at -80^0 C until analysed. GCF was extracted from the strips into 180 µL PBS with 1% protease inhibitor cocktail for 30 minutes at RT.

2.6. Protein quantification by bicinchoninic acid assay (BCA)

2.6.1. Background

Protein determination by BCA assay is based on a 2-step process. In the first step, biuret reaction, peptide bonds in proteins reduce divalent copper ions (Cu^{2+}) from copper sulphate ($CuSO_4$) to monovalent copper ions (Cu^{+}), in an alkaline environment, forming a coloured chelate complex. In the second step, colour development reaction, each cuprous cation (from step one) reacts with two molecules of BCA forming a

purple-coloured product that absorbs light at 562 nm. The amino acids responsible for the Cu^{2+} reduction are cysteine, tyrosine and tryptophan, and the amount of Cu^{2+} reduced is proportional to the amount of protein present in solution (Figure 2.4) [292].

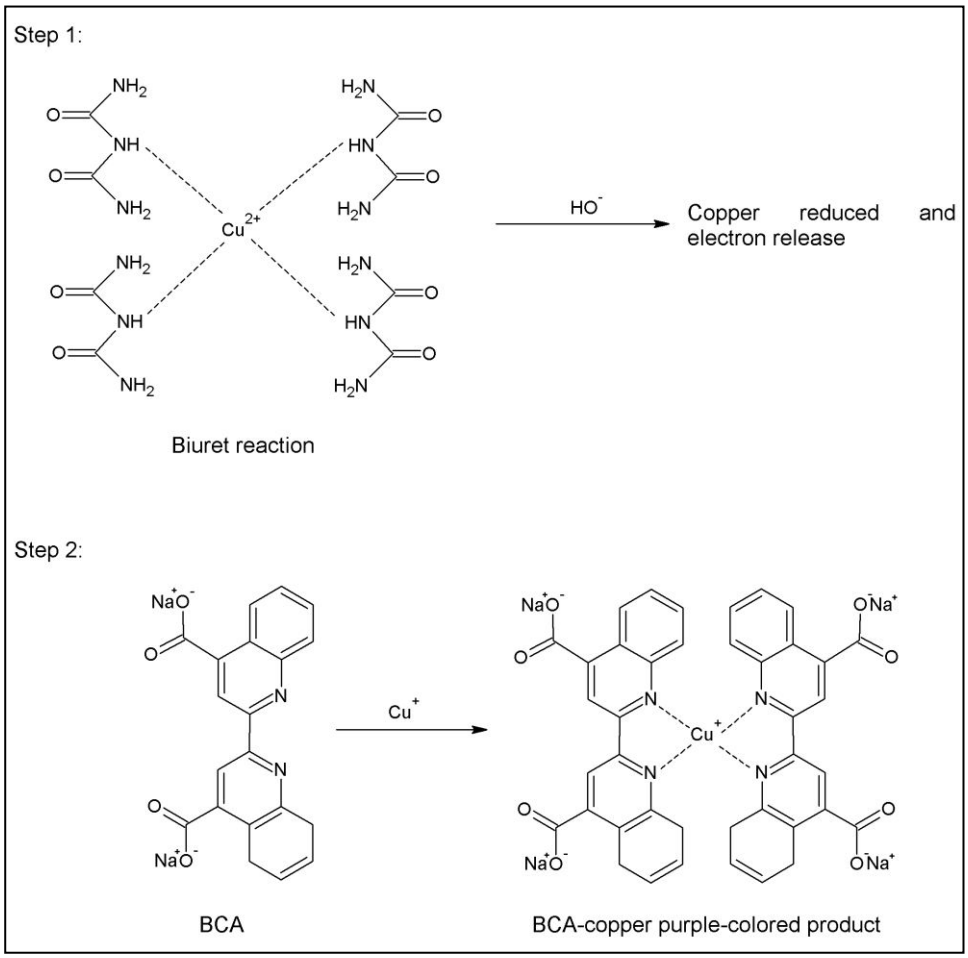

Figure 2.1 Schematic representation of the BCA 2-step reaction for protein quantification.

2.6.2. Protocol

Protein content was determined by adding 200 µL $CuSO_4$:BCA solution (1:50 – v/v) to 10 µL of sample or BSA standards (ranging from 0 to 1 mg/mL) in a 96-well plate. After incubating the plate for 30 minutes at 37^0 C the absorbance was measured at 570 nm on a microplate reader (BioTek Instruments Inc., Swindon, UK) and protein content in unknowns was determined by interpolating from the standard curve.

2.7. Protein quantification by Bradford assay

2.7.1. Reagents

Bradford reagent was from Pierce (Thermo Fisher Scientific Inc., Loughborough, UK).

2.7.2. Background

In the Bradford assay protein content determination is based on the formation of a protein-Coomassie Brilliant Blue (CBB) G250 complex, in acidic conditions, that shifts the absorption maximum of CBB G250 from 465 to 595 nm. The increase of absorbance at 595 nm is proportional to the amount of protein in solution. The main amino acids responsible for the colour development in this method are arginine, lysine and histidine. The main advantage of this method is its compatibility with most salts, solvents, buffers, thiols and reducing agents present in protein samples [293].

2.7.3. Protocol

Protein content was determined by adding 200 µL Bradford reagent to 10 µL of sample or BSA standards (ranging from 0 to 1 mg/mL) in a 96-well plate. After incubating the plate for 10 minutes at RT the absorbance was measured at 595 nm on a microplate reader (BioTek Instruments Inc., Swindon, UK) and protein content in unknowns was determined by interpolating from the standard curve.

2.8. Protein separation by sodium dodecyl sulphate polyacrylamide gel electrophoresis (SDS-PAGE)

2.8.1. Reagents

Precision Plus Protein™ Kaleidoscope™ Standards were obtained from Bio-Rad Laboratories Ltd. (Hemel Hempstead, UK). Acetic acid and methanol were from Fisher Chemicals (Thermo Fisher Scientific Inc., Loughborough, UK).

2.8.2. Background

SDS-PAGE is a protein separation method, where the electrophoretic mobility reflects length, conformation and charge of a protein. SDS-PAGE involves the denaturation of the protein with a reducing agent, usually β-mercaptoethanol (β-ME), and the binding of SDS to the linear protein, providing a uniform negative charge. Subsequently, negatively charged proteins are forced to pass through a gel containing acrylamide by applying an electrical field. Polymerised acrylamide creates pores that confer resistance to protein migration and allow proteins to be separated according to their molecular weight (MW) [294, 295].

Proteins separated by SDS-PAGE can be detected by staining the gel with dyes such as CBB R250 or CBB G250, or by immunoblotting. Furthermore, electrophoresed proteins can be extracted, digested and identified by mass spectrometry (MS) [296].

CBB R250 and CBB G250 are disulphonated triphenylmethane compounds that, in acidic conditions, bind to proteins through basic amino acids (primarily arginine, lysine and histidine) enabling their visualisation on a gel. CBB G250 has two additional methyl groups compared with to CBB R250, allowing it to be used as a colloidal stain [297]. Immunoblotting technique will be addressed and described later (section in 2.9).

2.8.3. Solutions

- Resolving gel buffer:
    - 1.5 M Tris-base
    - 0.4% (w/v) SDS
    - pH 8.4

- Stacking gel buffer:
    - 0.5 M Tris-base
    - 0.4% (w/v) SDS
    - pH 6.8

- Ammonium persulphate (APS):
    - 10% (w/v) APS in double-distilled water

- Electrophoresis running buffer:
    - 20 mM Tris-base
    - 192 mM glycine
    - 0.1% (w/v) SDS

- CBB R250 staining solution:
    - 0.05% (w/v) CBB R250
    - 50% (v/v) methanol
    - 10% (v/v) acetic acid

- Destaining solution:
    - 50% (v/v) methanol
    - 10% (v/v) acetic acid

2.8.4. Protocol

A fixed amount of protein was mixed with Laemmli buffer (1:1 ratio) and incubated at 95^0 C for 3 minutes. Samples were resolved in 7.5, 10 or 12% acrylamide gels, after being concentrated in a 3% stacking gel (composition of the gels is described in table 2.5). Electrophoresis was performed at 115 V for 105 minutes in electrophoresis running buffer using a Mini-PROTEAN Tetra cell (Bio-Rad Laboratories Ltd., Hemel Hempstead, UK). Following electrophoresis, gels were stained overnight with CBB R250 staining solution, destained at least three times for one hour with destaining solution and visualised and analysed using a G:BOX Chemi HR 1.4 imaging system and GeneTools 4.03 image analysis software (Syngene, Cambridge, UK).

Table 2.5 Composition of SDS-PAGE resolving and stacking gels (volumes are per gel).

Reagent	7.5% resolving	10% resolving	12% resolving	3% stacking
Bi-distilled water	6 mL	5 mL	7.2 mL	4.87 mL
Resolving gel buffer	3 mL	3 mL	3 mL	-
Stacking gel buffer	-	-	-	1.87 mL
Acrylamide/bis-acrylamide (29:1) 30% solution	3 mL	4 mL	4.8 mL	0.75 mL
APS	100 µL	100 µL	100 µL	100 µL
Tetramethylethylenediamine (TEMED)	10 µL	10 µL	10 µL	10 µL

2.9. Immunoblotting

2.9.1. Reagents

Methanol was obtained from Fisher Chemicals (Thermo Fisher Scientific Inc., Loughborough, UK). Amersham enhanced chemiluminescence (ECL) Prime Western Blotting detection reagent and Amersham Hybond P 0.45 µm polyvinylidene difluoride (PVDF) were from GE Healthcare Life Sciences Ltd. (Little Chalfont, UK).

2.9.2. Background

Immunoblot or Western blot is a technique that uses antibodies to specifically detect targeted proteins. Proteins are first separated by electrophoresis, then transferred to a nitrocellulose or PVDF membrane and finally probed with specific antibodies. Transfer of proteins usually occurs by electroblotting, where an electric current forces proteins to move from the gel to the membrane, maintaining the same organisation and being exposed on a thinner surface. Before incubating the membrane with the antibody of interest, non-specific interactions between the membrane and the antibody are blocked using BSA or non-fat dry milk. The membrane is then probed for a specific antigen using an antibody conjugated with a reporter enzyme or a combination of primary and secondary antibodies, where the second is directed to a species-specific portion of the first and is conjugated with a reporter enzyme. Usually, secondary antibodies are

conjugated with horseradish peroxidase (HRP), which enables the chemiluminescence detection of the proteins of interest [296].

2.9.3. Solutions

- Transfer buffer:
    - 20 mM Tris-base
    - 192 mM glycine
    - 25% (v/v) methanol

- Tris buffered saline (TBS) solution:
    - 150 mM sodium chloride (NaCl)
    - 20 mM Tris-HCl
    - pH 7.5

- Washing solution (TTBS):
    - 0.05% (v/v) Tween-20 in TBS

- Blocking solution:
    - 3% (w/v) BSA in TTBS

2.9.4. Protocol

Proteins separated by SDS-PAGE were electro-transferred into a PVDF membrane using a Criterion™ blotter wet system (Bio-Rad Laboratories Ltd., Hemel Hempstead, UK) at 240 mA for 105 minutes in transfer buffer. PVDF membrane was soaked in 100% methanol for 1 minute and washed in transfer buffer for 5 minutes prior to transfer. Following transfer, membranes were incubated with blocking solution overnight at 4^0 C or 2 hours at RT and probed with an antibody targeted to a specific protein and subsequently the adequate secondary antibody conjugated with HRP. Antibodies were diluted in blocking solution and incubations were either overnight at 4^0 C or for 2 hours at RT. After the incubation steps, membranes were washed 6 times

for 5 minutes each with TTBS. Bands were detected with ECL and visualized on a G:BOX Chemi HR 1.4 imaging system and GeneTools 4.03 image analysis software (Syngene, Cambridge, UK).

2.10. Protein separation by two-dimensional isoelectric focusing/SDS-PAGE (2D IEF/SDS-PAGE)

2.10.1. Materials and reagents

10% Criterion™ Tris-HCl gel, Bio-Lyte® 3/10 ampholyte, Flamingo™ fluorescent gel stain solution, Precision Plus Protein™ Kaleidoscope™ standards, ReadyPrep™ 2-D clean-up kit, ReadyStrip™ immobilized pH gradient (IPG) strips (+3–10) and TGS buffer were obtained from Bio-Rad Laboratories Ltd. (Hemel Hempstead, UK). Acetic acid and ethanol were from Fisher Chemicals (Thermo Fisher Scientific Inc., Loughborough, UK). Amberlite resin and DeStreak™ reagent were from GE Healthcare Life Sciences Ltd. (Little Chalfont, UK).

2.10.2. Background

2D IEF/SDS-PAGE is one of the most widely used analytical techniques to separate mixtures of proteins. The principle of 2D IEF/SDS-PAGE is the separation of proteins in two dimensions: 1) based on their net charges by IEF and 2) based on their MW by SDS-PAGE. In IEF, proteins are applied into IPG strips containing a fixed pH gradient. When an electrical field is applied, proteins migrate through the pH gradient becoming immobilized when they approach their specific isoelectric point (pI). Following IEF, IPG strips can be applied to SDS-PAGE, allowing separation of the proteins in a second dimension, according with their MW. After 2D separation, gels can be stained for protein visualisation and analysis. With 2D IEF/SDS-PAGE, hundreds of proteins can be separated and detected. However, one of the major drawbacks of this technique is

the difficulty to separate low abundant and hydrophobic proteins [298]. This will be of particular relevance when analysing MP.

2.10.3. Solutions

- Solubilisation buffer:
    - 8 M urea
    - 2 M thiourea
    - 4% (w/v) 3-[(3-Cholamidopropyl)dimethylammonio]-1-propanesulphonate hydrate (CHAPS)

- Rehydration buffer:
    - 8 M urea
    - 2 M thiourea
    - 2% (v/v) CHAPS
    - 0.2% (v/v) Bio-Lyte® 3/10 ampholyte
    - 1% (v/v) DeStreak™ reagent

- Equilibration buffer:
    - 6 M urea
    - 2% (w/v) SDS
    - 30% (v/v) glycerol
    - 1% (w/v) DTT
    - 50 mM Tris-HCl, pH 8.6

- Fixative buffer:
    - 40% (v/v) ethanol
    - 10% (v/v) acetic acid

2.10.4. Protocol

Proteins were prepared for 2D IEF/SDS-PAGE using ReadyPrep™ 2-D clean-up kit according with the manufacturer's instructions. Briefly, 125 µg of protein were transferred into a new tube and incubated with 300 µL precipitating agent 1 for 15

minutes on ice. Proteins were then mixed with precipitating agent 2 and centrifuged at 12,000 x g for 5 minutes. Supernatant was discarded and samples were centrifuged briefly (approximately thirty seconds) to collect residual liquid. Wash reagent 1 (40 µL) was added to the pellet and centrifuged at 12,000 x g for 5 minutes. Supernatant was discarded and the pellet was resuspended with 25 µL ultrapure water, followed by 1 mL of wash reagent 2 (pre-chilled at -20^0 C for at least 1 hour) and 5 µL of wash 2 additive. The tubes were then incubated at -20^0 C for 30 minutes (vortexed for 30 seconds every 10 minutes). After the incubation period, the tubes were centrifuged at 16,000 x g for 5 minutes and the supernatant was discarded. The pellet was briefly centrifuged again to remove residual liquid and air-dried at RT for 5 minutes. Protein pellets were then solubilised overnight at 20^0 C in solubilisation buffer with gentle agitation. Protein concentration was determined by Bradford assay (described in section 2.7). Urea/thiourea solutions were deionised before use by incubating with 1% (w/v) Amberlite mixed bed resin for 10 minutes. Samples (50 µg) were diluted in rehydration buffer, applied to IPG strips and incubated overnight at 20^0 C. After rehydration, IPG strips were focused using a Protean i12 IEF apparatus (Bio-Rad Laboratories Ltd., Hemel Hempstead, UK) with the following programme: 0–800 V for 800 Vh, 800–8,000 V for 8,000 Vh and 8,000 V for 96,000 Vh at 20^0 C. The IPG strips were incubated in equilibration buffer for 15 minutes and then in equilibration buffer with 4.7% (w/v) iodoacetamide (IAM) for 15 minutes. For the second dimension, samples were resolved by SDS-PAGE on 10% Criterion^{TM} Tris-HCl gels in TGS buffer. Electrophoresis was performed at 150 V for 85 minutes using a Criterion™ Cell (Bio-Rad Laboratories Ltd., Hemel Hempstead, UK). Following electrophoresis, gels were fixed for 16 hours in fixative buffer and stained with Flamingo fluorescent gel stain solution for 8 hours. The stained gels were visualised and analysed using a molecular imager PharosFX^{TM} and Quantity One software (Bio-Rad Laboratories Ltd., Hemel Hempstead, UK).

2.11. Protein separation by 2D blue native (BN)/SDS-PAGE

2.11.1. Reagents

8–16% Mini-PROTEAN® TGX Stain-Free® precast gels and Precision Plus Protein™ Kaleidoscope™ Standards were from Bio-Rad Laboratories Ltd. (Hemel Hempstead, UK). CBB G250, n-dodecyl-beta-maltoside (DDM), NativeMark™ protein standards and NativePAGE™ Novex® 4–16% Bis-Tris gels were obtained from Thermo Fisher Scientific Inc. (Loughborough, UK).

2.11.2. Background

2D BN/SDS-PAGE is an electrophoresis technique that enables the separation of associated proteins in native and denaturing conditions. Combinations of different techniques and dimensions enable analysis of various characteristics of the separated proteins. BN-PAGE was first applied to separate protein complexes from mitochondrial extracts and then applied to biological membranes and total cell and tissue homogenates. Protein complexes are initially separated by size in a first native dimension. This provides information about native protein or protein complexes size and relative abundance, since protein complexes are not disturbed [299, 300]. The incorporation of CBB G250 in the samples prior to separation confers the negative charge that will allow the complexes to migrate into the gel. After the first dimension, native complexes can be extracted and used for 2D crystallisation, electron microscopy, in-gel activity assays or native electroblotting and immunodetection. Alternatively, protein complexes can be further separated in a second dimension by SDS-PAGE followed by immunoblotting (3D) or IEF followed by SDS-PAGE (3D) for the separation of the complexes' subunits. The combination of second and third dimensions allow to obtain information about different complexes that share common subunits, presence of free monomeric forms of individual subunits, and whether these parameters change upon cell stimulation or treatment [301-303].

2.11.3. Solutions

- BN sample buffer (BN SB):
    - 750 mM aminocaproic acid (ACA)
    - 50 mM Bis-Tris pH 7.0
    - 0.5 mM disodium EDTA (EDTA-Na_2)
- Loading buffer (LB):
    - 750 mM ACA
    - 50 mM Bis-Tris pH 7.0
    - 5% (w/v) CBB G250
    - Stored at -20^0 C
- Dialysis buffer:
    - Loading buffer without CBB G250 10x diluted
    - Stored at 4^0 C
- DDM solution:
    - 10% (w/v) DDM in BN SB
- BN cathode running buffer (10x):
    - 500 mM tricine
    - 150 mM Bis-Tris pH 7.0
    - 0.2% (w/v) CBB G250
    - Stored at 4^0 C
- BN anode running buffer (10x):
    - 500 mM tricine
    - Stored at 4^0 C
- SDS-PAGE running buffer (10x):
    - 250 mM Tris
    - 1.92 M glycine
    - 1% (w/v) SDS

- Overlay solution:
    - 0.5% (w/v) agarose in 1x SDS-PAGE running buffer
    - Microwave to dissolve
- Fixing solution:
    - 40% (v/v) methanol
    - 10% (v/v) acetic acid
- Destaining solution:
    - 8% (v/v) acetic acid
- CBB high sensitivity staining solution:
    - 0.02% (w/v) CBB G250
    - 5% (w/v) aluminium sulphate hydrate
    - 10% (v/v) ethanol
    - 2% (v/v) *o*-phosphoric acid
    - Stored at RT
- CBB high sensitivity destaining solution:
    - 10% (v/v) ethanol
    - 2% (v/v) *o*-phosphoric acid
    - Stored at RT

2.11.4. Protocol

BN-PAGE and 2D BN/SDS-PAGE were performed as previously described by Reisinger and Eichacker [304]. First dimension BN-PAGE was performed using NativePAGE™ Novex® 4–16% Bis-Tris gels assembled on an XCell SureLock™ Mini-Cell Electrophoresis System from Thermo Fisher Scientific Inc. (Loughborough, UK). For the second dimension 8–16% Mini-PROTEAN® TGX Stain-Free® precast gels assembled on a Mini-PROTEAN Tetra Cell (Bio-Rad Laboratories Ltd., Hemel Hempstead, UK) were used.

MP were isolated from 5 x 10^5 cells as further described in section 2.13 and dialysed against 10x diluted BN loading buffer using Slide-A-Lyzer™ Dialysis Cassettes, 3.5K MWCO, 0.5 mL (Thermo Fisher Scientific Inc., Loughborough, UK). Protein concentration after dialysis was determined by the BCA method (described in section 2.8) and samples were further evaporated in a centrifugal concentrator (Eppendorf AG, Loughborough, UK). FNG (10 µg) and MP (25 µg) were resuspended in 20 µL of BN SB and mixed with DDM solution to a final concentration of 0.625% (v/v) of DDM. Samples were vortexed every 5 minutes while incubating on ice for 1 hour. Insolubilized material was pelleted by centrifuging at 16,900 x g for 30 minutes at 4^0 C. The supernatant was transferred to a new tube containing 5 µL of LB (with 1% protease inhibitor cocktail) and incubated on ice for 5 minutes. After assembling the electrophoresis apparatus, 1x BN cathode running buffer and 1x BN anode running buffer were poured into the upper and lower chambers, respectively. Samples and protein markers were loaded and BN-PAGE performed at 4^0 C at 150 V for 60 minutes. After 60 minutes, the voltage was increased to 250 V and the electrophoresis continued for 30–60 minutes until the blue front reached the bottom of the gel. 1D BN-PAGE gels were fixed with 100 mL of fixing solution for 15 minutes at RT, destained with 100 mL of destaining solution until the desired background was obtained and visualized and analysed using a G:BOX Chemi HR 1.4 imaging system and GeneTools 4.03 image analysis software (Syngene, Cambridge, UK).

To perform 2D BN/SDS-PAGE, 1D gel strips of interest were excised and the proteins denatured with Laemmli buffer (incubation at 95^0 C for 15 minutes followed by incubation at RT for 1 hour, in 15 mL conical tubes). After denaturation, 1D strips were assembled in the 2D gels on the top of a layer of overlay solution and sealed with another layer of overlay solution. 2D SDS-PAGE was performed at 150 V for approximately 1 hour at RT. 2D BN/SDS-PAGE gels were washed thrice with water for 10 minutes and stained overnight with CBB high sensitivity staining solution. Gels were then rinsed twice with water and destained with CBB high sensitivity destaining solution

for 1 hour. After a final rinse with water the gels were visualized and analysed using a G:BOX Chemi HR 1.4 imaging system and GeneTools 4.03 image analysis software (Syngene, Cambridge, UK) and SameSpots software (TotalLab ltd., Newcastle upon Tyne, UK), respectively. In the SameSpots analysis software (TotalLab ltd., Newcastle upon Tyne, UK), gel images were cropped to the area containing the proteins spots. A reference image was then selected according with the conditions under study. The software matches the spots, the spot volumes are normalised to the reference gel and the resultant up- or down-regulated spots are statistically analysed using analysis of variance (ANOVA) test. The resultant spots can then be filtered for fold changes higher or equal to two and *p-values* higher or equal to 0.05.

2.12. Protein identification by mass spectrometry

2.12.1. Reagents

Acetic acid, acetonitrile (ACN) and methanol were from Fisher Chemicals (Thermo Fisher Scientific Inc. (Loughborough, UK). Trypsin gold and chymotrypsin were from Promega Co. (Southampton, UK).

2.12.2. Background

Proteomic studies depend on the separation of proteins, usually by electrophoresis, cleavage of polypeptide chains into small peptides by proteases, separation of digested peptides by liquid chromatography (LC) and ionisation and detection of the ions according with their mass/charge (m/z) ratio by MS. This combination of techniques allows the identification of proteins in a complex mixture, detection of PTM in a protein and it can also provide quantitative information about the analysed molecules [305].

Commonly, proteins are converted into small peptides after being separated by SDS-PAGE. Gel bands are excised and proteins digested with proteases. Trypsin is the most common protease used in proteomics, but others can be used, such as

chymotrypsin or Glu-C. Trypsin cleaves polypeptide chains at the carboxyl side of lysine or arginine residues, except when these are followed by proline. Chymotrypsin cleaves at the carboxyl side of tyrosine, phenylalanine, tryptophan and leucine amino acids. Glu-C cleaves peptide bonds at the carboxyl side of glutamic residues but it can also cleave at both glutamic and aspartic residues, depending on the buffer used. The original procedure for in-gel digestion, first introduced in 1992 by Rosenfeld [306], underwent several modifications during the years. The method developed by Shevchenko in 2006 is currently one of the most commonly used and comprises of destaining the gel bands, reduction and alkylation of the cysteine residues in the protein, proteolytic cleavage of the protein and extraction of the generated peptides [307]. After protein digestion, peptides can be analysed by MS. This technique allows the acquisition of MW and structural information of a compound with high sensitivity, being the most comprehensive and versatile technique in proteomics. A mass spectrometer is organised in sample introduction device, ionisation source (for ion generation), mass analyser (for ion separation) and ion detector (to transform analogue signals into digital signals and record a mass spectrum). The equipment used in this study by Dr Creese at University of Birmingham was a linear trap quadrupole (LTQ)-Orbitrap Velos electron transfer dissociation (ETD) mass spectrometer (Thermo Fisher Scientific Inc., Loughborough, UK) coupled to a Dionex Ultimate 3000 high performance liquid chromatography (HPLC) system (Sunnyvale, USA). The mass spectrometer components described here are based on this equipment.

Coupling MS to a reversed phase (RP)-HPLC system allows the separation and simplification of complex biological samples prior to mass analysis. HPLC allows the separation of peptides according to their hydrophobicity. After separation, peptides are ionised by electrospray ionisation (ESI) transferring the analytes into the gas phase maintaining their non-covalent interactions [308]. ESI involves the application of a high voltage to a flow of liquid creating an electrically charged spray, formed by small charged drops. The solvent on these drops is further evaporated, creating charged ions

in the interface with the mass spectrometer [309]. In the mass analyser, the ions are separated by electric or magnetic fields. LTQ-Orbitrap is a hybrid mass analyser that combines linear and orbital trapping of ions in its electrostatic fields, featuring high resolution, high mass accuracy, high speed and high sensitivity and enabling tandem MS [308]. In ion trap equipment, ions are imprisoned inside while the MS operations (full scan, precursor selection, fragmentation and product ion analysis) take place [309]. Tandem MS mass analysis is carried out on intact molecular ions (full scan) or on collision induced dissociation (CID) fragmented precursor ions (MS^n scan). CID fragmentation is a thermal process that leads to the cleavage of the amine bond on peptide ions producing *b* and *y* fragment ions (Figure 2.2), that provides sequence information, which can be searched against protein databases [310]. Peptide fragmentation spectra (plot of ion abundance versus m/z ratio) are matched against *in silico* calculated spectra leading to protein identification [308]. Alternatively to CID, ETD, which involves radical ion chemistry, randomly cleaves along the peptide backbone, producing *c* and *z* fragment ions (Figure 2.2) that leave side chains and modifications intact [310]. In a variant of ETD, supplemental activation ETD (saETD), the charge-reduced ion is activated by collision, thus disrupting any non-covalent bonding [311].

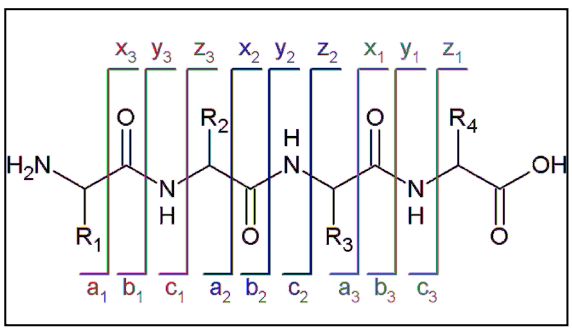

Figure 2.2 Schematic representation of a, b, c, x, y and z ions during peptide fragmentation in tandem MS.

Characterisation of citrullination by direct tandem MS is very challenging due to the low abundance of this modification in complex samples and also because the 0.98 Da mass difference between citrulline and arginine can be misidentified by other

modifications, such as deamination (removal of an amine group from a molecule), or the simple MS sample processing [312]. To counteract this, Creese and colleagues developed a method based on the occurrence of neutral loss of isocyanic acid (43 Da) from citrullinated peptides (Figure 2.3) that enables differentiating citrullination from deamination. In this method, if neutral loss of isocyanic acid is observed in the CID spectrum, saETD of the parent ion is performed, improving the identification and localisation of the modification site [310].

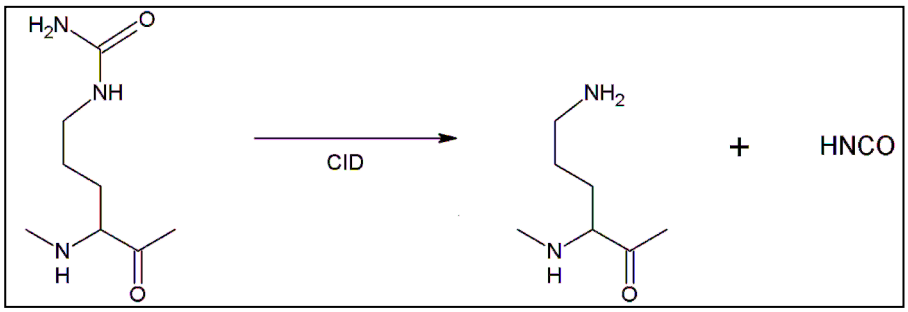

Figure 2.3 Schematic representation of the neutral loss of isocyanic acid (HNCO) (43 Da) from citrullinated peptides by CID.

2.12.3. Solutions

- Reducing solution: 10 mM DTT in 100 mM ammonium bicarbonate (ABC)
- Alkylating solution: 55 mM iodoacetamide (IAM) in 100 mM ABC
- Digestion solution 1: 10 mM ABC, 10% (v/v) ACN
- Digestion solution 2: 100 mM Tris-HCl
- Extraction buffer: 5% (v/v) formic acid/ACN (1:2 ratio)

2.12.4. Protocol: in-gel protein digestion for mass spectrometry analysis

Proteins separated on gels were stained with either CBB R250 or CBB G250 (as previously described in sections 2.8 and 2.11) and the selected bands excised, destained and dehydrated prior to proteolytic digestion using standard protocols [307]. Briefly, gel pieces were washed twice with 100 mM ABC/100% (v/v) ACN (1:1 ratio) for 30 minutes with agitation. Washed gel pieces were incubated with 100% (v/v) ACN for

10 minutes at RT. Supernatants were discarded and gel pieces were reduced with reducing solution for 30 minutes at 56°C. Reducing solution was discarded and gel pieces incubated with 100% (v/v) ACN for 10 minutes. Subsequently, supernatants were discarded and gel pieces alkylated with alkylating solution for 30 minutes at RT. Alkylating solution was discarded and gel pieces incubated with 100% (v/v) ACN for 10 minutes. Reduced and alkylated gel pieces were enzymatically digested with 30 µL of trypsin solution (13 ng/mL) solubilised in digestion solution 1 or α-chymotrypsin (13 ng/mL) solubilised in digestion solution 2 and incubated for 2 hours on ice. Following, 20 µL of 100 mM ABC was added to activate the enzymes and samples were incubated overnight at 37^0 C. The digests were extracted from the gel pieces by incubating with 100 µL extraction buffer for 15 minutes at 37^0 C. Supernatants were dried in a centrifugal concentrator for 1–2 hours and the precipitate resuspended in 20 µL of 0.5% (v/v) trifluoroacetic acid (TFA). Peptides were desalted and concentrated using ZipTip® pipette tips (Merck Millipore Ltd., Watford, UK) according with the manufacturer's instructions. Briefly, the tips were sequentially washed with 20 µL ACN, 2 x 0.1% (v/v) TFA, ACN/0.1% (v/v) TFA (1:1 ratio) and 2 x 0.1% (v/v) TFA. Samples were then aspirated with the tips (15–20 times) and after the tips were washed twice with 20 µL 0.1% (v/v) TFA. Finally, the peptides were eluted with 20 µL ACN/0.1% (v/v) TFA (1:1 ratio), dried in a vacuum centrifuge and stored at -20^0 C for further MS analysis.

2.12.5. Protocol: analysis of protein digests by LC-CID-saETD-MS/MS

Digested peptides were resuspended in 10 µL 0.1% (v/v) formic acid prior to LC-MS analysis. Peptides were separated and analysed using a Dionex Ultimate 3000 HPLC system (Sunnyvale, USA) and a LTQ-Orbitrap Velos ETD mass spectrometer (Thermo Fisher Scientific Inc., Loughborough, UK) as described previously [310]. This work was performed in collaboration with Dr Andrew Creese, Advanced Mass Spectrometry Facility, School of Biosciences, University of Birmingham.

Samples (5 µL) were loaded onto a 75 µm (internal diameter) Acclaim PepMap100 (LC Packings, Sunnyvale, USA) C18 column (length 10 cm) and separated over a 30 minute gradient from 3.2% to 44% acetonitrile [0.1% (v/v) formic acid]. Peptides were infused by use of an Advion Triversa Nanomate (Ithaca, USA) ESI source directly into a Thermo Fisher Scientific Inc. (Loughborough, UK) LTQ-Orbitrap Velos ETD mass spectrometer (Bremen, Germany), at a flow rate of 350 $nLmin^{-1}$, applied at a voltage of 1.7 keV. The mass spectrometer alternated between a full Fourier transform mass spectrometry (FTMS) scan (m/z 380–1600) and subsequent MS/MS scan(s) of the most abundant precursor ions. Survey scans were acquired in the Orbitrap with a resolution of 60,000 at m/z 400. Precursor ions were isolated and subjected to CID in the linear ion trap. Isolation width was 2 Th. Automatic gain control (AGC) was used to accumulate sufficient precursor ions (target value 1 x 10^5 charges, maximum fill time 25 ms). CID was performed with helium gas at a normalised collision energy of 35%. Parent ions were activated for 10 ms. Dynamic exclusion was used (60 seconds exclusion window). If one of the three most abundant fragment ions in the CID mass spectrum corresponded to a neutral loss of 43 Da (isocyanic acid) from the precursor peptide, saETD of the precursor ion was triggered. saETD was performed in the ion trap and detected in the Orbitrap with a resolution of 7500 at m/z 400. Precursor ions were isolated in the ion trap with an isolation width of 3 Th. AGC target value was 2 x 10^5 charges, maximum fill time 1000 ms with 2 microscans co-added per mass spectrum. saETD was performed for 130 ms with a normalised supplemental activation energy of 25%.

Data were analysed by Xcalibur 2.1 software. Data from the samples containing the singly citrullinated peptides were searched against the IPI human database (v3.66, containing 86,850 sequences) added using the SEQUEST algorithm within the Proteome Discoverer 1.0 SP1 software package (Thermo Fisher Scientific Inc., Loughborough, UK). Mono-isotopic precursor and fragment ions were searched with a mass tolerance of 5 ppm (precursor) and 0.1 Da (fragment) for CID and 0.02 Da for

saETD. Proteome Discoverer separated the CID and ETD data prior to searches. For CID data, b and y ions were considered. For saETD data, c and z ions were considered. Carboxymethylation of cysteine was specified as a fixed modification and phosphorylation (serine, threonine and tyrosine), oxidation (methionine), acetylation (lysine), deamidation (asparagine and glutamine) and citrullination (arginine) were set as variable modifications in the search. The maximum number of missed cleavages allowed was 2.

The results were filtered using XCorr versus charge state (2+ ions with a score less than 2 were rejected, 3+ ions with scores <2.25 were rejected and 4+ ions with scores <2.5 were rejected). XCorr is a measure of how close an experimental MS/MS spectrum is to the theoretical MS/MS spectrum. Higher scores equate to greater confidence in a peptide match. XCorr values were calculated by Proteome Discoverer 1.0 SP1 software package (Thermo Fisher Scientific Inc., Loughborough, UK).

2.13. Membrane proteins extraction

2.13.1. Reagents

Mem-PER Plus membrane protein extraction kit was obtained from Pierce (Thermo Fisher Scientific Inc., Loughborough, UK).

2.13.2. Background

MP are key components of biological membranes, being involved in processes such as cell signalling, molecule and ion transport and cell adhesion [12]. To study the effects of PAD enzymes on MP, MP were isolated from PBMC after treatment with PAD enzymes and activation with anti-CD3/anti-CD28 antibodies.

The Mem-PER Plus membrane protein extraction kit uses a mild detergent-based selective extraction protocol for the separation between cytosolic and membrane proteins. The cells are first permeabilised with a mild detergent, allowing soluble

cytosolic proteins to be released. After, a second detergent is used to solubilise the MP.

2.13.3. Protocol

Jurkat E6.1 T cells (5 x 10^6) or PBMC (5 x 10^5) were harvested by centrifugation at 300 x g for 5 minutes and washed twice with cell wash solution. Washed cells were resuspended in 0.75 mL of permeabilisation buffer (with 1% protease inhibitor cocktail) and incubated 10 minutes at 4^0 C with constant mixing. The permeabilised cells were centrifuged for 15 minutes at 16,000 x g. Supernatant containing cytosolic proteins (CP) was collected and the pellet resuspended with 0.5 mL of solubilisation buffer (with 1% protease inhibitor cocktail) and incubated 1 hour at 4^0 C with constant mixing. The solubilised MP were centrifuged for 15 minutes at 16,000 x g and stored at -80^0 C for further analysis.

2.13.4. Membrane proteins extraction validation

To validate the efficacy of MP extraction 5 x 10^6 Jurkat E6.1 T cells were harvested and CP and MP fractions isolated according with the protocol described above (section 2.13.3). Fractions were dialysed against 75 mM ACA, 50 mM Bis-Tris pH 7.0 as outlined in section 2.11 and analysed by immunoblotting with antibodies against CD3 and NF-κB p65. Briefly, 15 µg of CP or MP were separated by SDS-PAGE on an 11% gel and electro transferred to a PVDF membrane. After, the membrane was blocked with 3% (w/v) BSA in TTBS overnight at RT and probed for CD3 or NF-κB with specific antibodies diluted 1:1000 in blocking solution for 2 hours at RT. After a second incubation with goat anti-rabbit antibody (1:5000 in blocking solution), the signal was developed with ECL reagent and visualised in a G:BOX Chemi HR 1.4 imaging system and GeneTools 4.03 image analysis software (Syngene, Cambridge, UK). The immunoblot on figure 2.4 validates the efficiency of the separation between CP and MP, since CD3 was detected in the MP fraction and the p65 subunit of NF-κB was detected in the CP fraction.

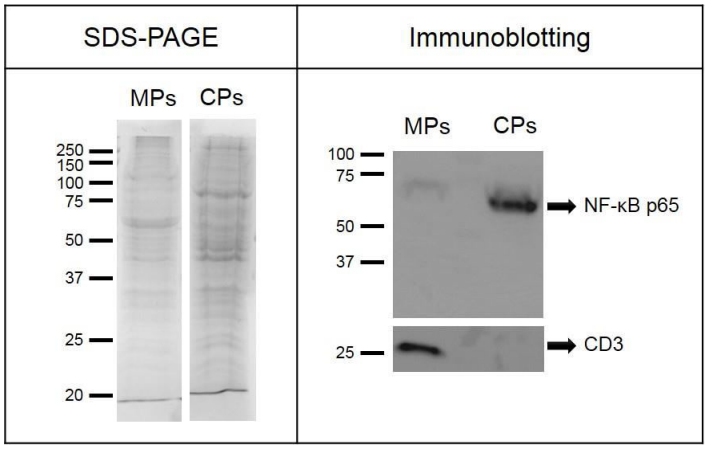

Figure 2.4 Validation of CP and MP fractioning using Mem-PER Plus membrane protein extraction kit. CP and MP were isolated from 5 x 10^6 Jurkat E6.1 T cells and dialysed against 75 mM ACA, 50 mM Bis-Tris pH 7.0. Immunoblotting was performed after running 15 µg protein in an 11% gel and transferring to a PVDF membrane. Anti-CD3 and anti-NF-κB p65 were diluted 1:1000 in blocking solution and incubated with the membrane for 2 hours at RT. Proteins were detected after incubation with goat anti-rabbit antibody (1:5000 in blocking solution) and ECL reagent. The gels and immunoblots are representative of two independent experiments.

2.14. Determination of cell viability using CellTiter-Blue® cell viability assay

2.14.1. Reagents

CellTiter-Blue® cell viability assay was obtained from Promega Co. (Southampton, UK).

2.14.2. Background

The CellTiter-Blue® assay relies on the ability of living cells to convert resazurin, a redox dye, into resorufin. Nonviable cells, due to the loss of metabolic capacity, are not able to produce resorufin. The reduction of resazurin to resorufin is responsible for a shift in the visible light absorbance properties of the CellTiter-Blue® reagent, which can be monitored by spectrophotometry (Figure 2.5).

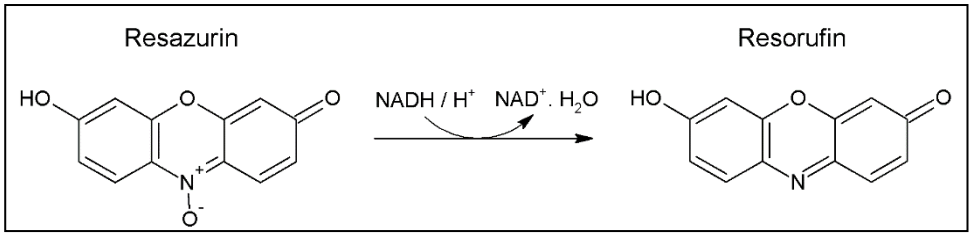

Figure 2.5 Schematic representation of the metabolic conversion of resazurin into resorufin in live cells.

2.14.3. Protocol

After treating Jurkat E6.1 T cells and PBMC, cell viability was determined with CellTiter-Blue® cell viability assay, according with the manufacturer's instructions. Briefly, 20 µL of CellTiter-Blue® reagent were added to 100 µL of each cell condition, into a 96-well plate, in duplicate, and shaken for 10 seconds. After overnight incubation at 37^0 C in 5% CO_2 the optical density at 490 nm of each well was measured using a spectrophotometric plate reader (BioTek Instruments Inc., Swindon, UK). Cell viability was calculated using the following equation, where control corresponds to the control condition:

$$\frac{OD_{490nm}\ \text{sample}}{OD_{490nm}\ \text{control}} \times 100$$

Equation 1 Determination of cell viability (%) using CellTiter-Blue® cell viability assay.

2.15. Determination of cell viability using trypan blue exclusion assay

2.15.1. Background

Trypan blue is a vital stain that dyes cells with damaged cellular membranes. The trypan blue exclusion method is based on the principle that live cells have intact membranes and, therefore, exclude the dye, whereas dead cells, with compromised membranes, are not able to do that [313].

2.15.2. Protocol

Viable and nonviable cells were counted on a haemocytometer after performing a 1:1 dilution with 0.4% trypan blue solution. Cell viability was determined using the following equation:

$$\text{Viability (\%)} = \frac{\text{n.° of viable cells}}{\text{n.° of viable cells + n.° of non-viable cells}} \times 100$$

Equation 2 Determination of cell viability (%) using trypan blue exclusion assay.

2.16. Cytokine quantification by sandwich enzyme linked immunosorbent assay (ELISA)

2.16.1. Reagents

BSA was obtained from Thermo Fisher Scientific Inc. (Loughborough, UK). Human IL-2 ELISA development kit was obtained from Peprotech EC Ltd. (London, UK). Human IL-6 and IL-8 ELISA kits were obtained from R&D systems (Abingdon, UK).

2.16.2. Background

Sandwich ELISA, or ELISA, is a detection and quantification plate-based method that can be used with peptides, proteins and antibodies. By immobilizing specific antigens between two antibodies it is possible to detect them in a complex mixture. Typically the second antibody is conjugated with an enzyme or fluorophore that allows signal detection. In Peprotech ELISA development kits, the detection antibody is conjugated with biotin. By adding avidin conjugated with HRP and HRP chromogenic substrate (as *o*-phenylenediamine dihydrochloride – OPD – or 3,3',5,5'-Tetramethylbenzidine – TMB) in consequent steps, the amount of antigen in the plate can be detected and interpolated from a standard curve.

2.16.3. Protocol

Secretion of IL-2 by cells was quantified by ELISA using human IL-2 development kit (Peprotech EC Ltd., London, UK), according to the manufacturer's instructions. Briefly, a monoclonal capture antibody (2 µg/mL in PBS) was coated onto a NUNC MaxiSorp™ 96-well plate overnight at RT. The following day, the wells were blocked with 1% (w/v) BSA in PBS for 1 hour at RT and triplicates of standards or samples were incubated 2 hours at RT. After, the plate was incubated for 2 hours with a biotinylated polyclonal detection antibody (6.25 µg/mL in 0.1% BSA in 0.05% Tween-20 in PBS) and 30 minutes with 1:2000 Avidin-HRP (protected from light). Four washes with 0.05% (v/v) Tween-20 in PBS were performed between each incubation step. The amount of bound avidin was assessed using SIGMAFAST™ OPD and the reaction stopped with 2 M sulphuric acid (H_2SO_4). Absorbance of each well at 490 nm was measured in a plate spectrophotometer (BioTek Instruments Inc., Swindon, UK) and concentration of cytokine interpolated from a standard curve (0.06 to 4 ng/mL).

IL-6 and IL-8 levels in the plasma of HC and PID patients were quantified with IL-6 and IL-8 Quantikine ELISA kits (R&D systems, Abingdon, UK), respectively, according with the manufacturer's instructions. Briefly, duplicates of standards or samples were added to a monoclonal antibody specific for IL-6 or IL-8, respectively, pre-coated 96-well plate and incubated for 2 hours at RT. After, the plate was incubated with human IL-6 or IL-8 conjugate, respectively, for 1 hour at RT. Four washes with wash buffer were performed between incubation steps. The plate was then incubated with substrate solution for 30 minutes at RT and protected from light and the colorimetric reaction stopped with stop solution. Absorbance of each well at 450 nm was measured in a plate spectrophotometer (BioTek Instruments Inc., Swindon, UK) and concentration of the cytokines interpolated from a standard curve (IL-6: 3.1 to 300 pg/mL; IL-8: 31.3 to 2000 pg/mL). Correction of wavelength was performed at 570 nm.

2.17. Analysis of membrane protein expression by flow cytometry

2.17.1. Reagents

FC antibodies and respective isotype controls were obtained from Abcam plc. (Cambridge, UK), eBioscience Ltd. (Hatfield, UK) and AbD Serotec® (Bio-Rad Laboratories Ltd., Hemel Hempstead, UK) according with table 2.6.

Table 2.6 Details of the antibodies use to detect membrane protein expression by flow cytometry.

Antigen	Description	Product code	Company	Volume per 1 x 10^6 cells (µL)
CD25	Mouse monoclonal [BC96] conjugated with APC	ab134477	Abcam plc.	5
CD38	Mouse monoclonal [HB7] conjugated with FITC	11-0388	eBioscience Ltd.	5
CD4	Mouse monoclonal [EDU-2] conjugated with PE	ab1155	Abcam plc.	10
CD8	Mouse monoclonal [RPA-T8] conjugated with PE-Cy5.5	35-0088	eBioscience Ltd.	5
IC	Mouse IgG1 isotype control conjugated with RPE	MCA928PE	AbD Serotec®	10
IC	Mouse F(ab')2 IgG1 [15H6] conjugated with APC	ab37391	Abcam plc.	10
IC	Mouse IgG1 K isotype control conjugated with FITC	11-4714	eBioscience Ltd.	5
IC	Mouse IgG1 K isotype control conjugated with PE-Cy5.5	35-4714	eBioscience Ltd.	10

APC – allophycocyanin; CD – cluster of differentiation; Cy – cyanine; FITC – fluorescein isothiocyanate; IC – isotype control; PE – phycoerithirn.

2.17.2. Background

FC is a laser-based technique that allows to measure size, granularity and fluorescence intensity of cells. A flow cytometer is composed by fluidics, optics and electronics systems. The fluidics system is responsible for the transport of single particles such as cells, on a stream of fluid to the laser beam. The optics system consists of lasers that illuminate the particles on the stream and of optical filters that direct the light signals to the detectors. As particles pass through the laser beam, light is scattered according to the physical properties of the particle. Forward-scatter light (FSC) depends on the size of the particle while side-scattered light (SSC) is proportional to cell granularity or internal complexity. Additionally, a flow cytometer can be used to detect fluorescence emitted from fluorescent dyes or fluorophores that have

been excited by the lasers. Using antibodies conjugated with fluorophores allows the detection and quantification of specific antigens on cells. Finally, the electronics system is responsible for the conversion of light signals into electronic signals that can be processed and analysed by a computer. Here, antibodies conjugated with specific fluorophores were used to analyse the expression of specific markers on the surface of the studied cells [314].

2.17.3. Protocol

After the treatments, cells in RPMI complete medium were collected into 1.5 mL tubes and incubated on ice for 15 minutes. Samples were then incubated with a specific antibody conjugated with a fluorophore or a negative isotype control according with table 2.7, for 30 minutes on ice and analysed on a Cytomics FC 500 and CXP® software (Beckman Coulter Inc., London, UK). Data were analysed using Flowing software v 2.5. MFI represents median fluorescence intensity. Median is a more robust statistic measure than the mean, since it is less influenced by skew or outliers. Details of the antibodies used are described on table 2.7.

Table 2.7 Fluorescence details of the antibodies used for flow cytometry.

Antigen	Fluorophore	Excitation (nm)	Emission (nm)	Laser
CD25	APC	645	660	FL4
CD38	FITC	488	517	FL1
CD4	PE	488	575	FL2
CD8	PE-Cy5.5	488	690	FL4

APC – allophycocyanin; CD – cluster of differentiation; Cy – cyanine; FITC – fluorescein isothiocyanate; FL – fluorescence; PE – phycoerithirn.

2.18. Quantification of reduced glutathione in plasma by the recycling assay

2.18.1. Background

GSH is the major antioxidant system in living organisms and is present in cells mainly on its reduced form. GSH is a tripeptide (γ-glutamylcysteinylglycine) and its oxidation leads to the formation of GSSG. The recycling assay for the detection of GSH involves the oxidation of GSH to GSSG by 5', 5'-dithio-bis(2-nitrobenzoic acid) (DTNB), generating 2-nitro-5-thiobenzoic acid (TNB) that can be detected by spectrophotometry at 412 nm. Generated GSSG can be recycled to GSH by GSR in the presence of NADPH, being available for further oxidation by DTNB (Figure 2.6). The colour development will be proportional to the amount of glutathione present in the samples and can be interpolated from a standard curve.

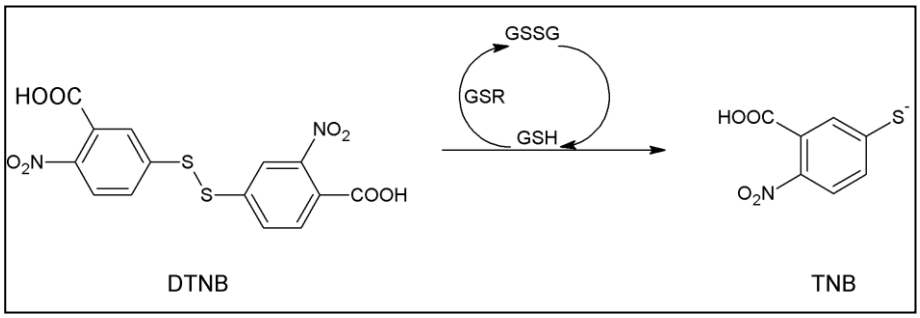

Figure 2.6 Schematic representation of the recycling assay for the quantification of reduced glutathione. DTNB – 5,5'-dithiobis-(2-nitrobenzoic acid); GSH – reduced glutathione; GSSG – oxidised glutathione; GSR – glutathione reductase; TNB – trinitrobenzene.

2.18.2. Solutions

- Stock buffer:
    - 125 mM sodium phosphate
    - 6.3 mM disodium EDTA (monobasic anhydrous)
    - pH 7.5
- Daily buffer:
    - 3 mg NADPH in 10 mL stock buffer

- SSA solution:
    - 1 g SSA in 1 mL bi-distilled water

2.18.3. Protocol

Plasma samples stored with 1% SSA were analysed for GSH content by the recycling assay. Briefly, 25 µL plasma and standards (0–80 µM) were loaded into a 96-well plate in triplicate and incubated with 150 µL daily buffer and 50 µL of 6 mM DTNB for 5 minutes. Immediately after, 25 µL GSR (4 U/mL in stock buffer) were added and the absorbance at 410 nm was measured in a microplate reader (BioTek Instruments Inc., Swindon, UK) at 5 time points. GSH concentration was interpolated from the standard curve.

2.19. Antibody based assay for peptidylarginine deiminase activity (ABAP)

2.19.1. Reagents

ABAP kit assay was obtained from Modiquest Research B. V. (Oss, Netherlands). BSA was obtained from Thermo Fisher Scientific Inc. (Loughborough, UK).

2.19.2. Background

ABAP is a commercial 96-well plate ELISA based assay for determination of PAD enzyme activity. The wells of the plate were coated with peptides containing arginine. As positive control, well H of each strip was coated with a deiminated arginine-containing peptide. When solutions containing PAD enzymes are added to the plate, the arginines coated to the plate are deiminated and can then be detected by a monoclonal antibody specific for deiminated arginine. Subsequently, a second HRP-labelled polyclonal anti-mouse immunoglobulin antibody is added to the plate, followed by HRP substrate what allows colour development to occur. Optical density is directly

proportional to the amount of arginines that have been deiminated and can be measured by spectrophotometry [315].

2.19.3. Protocol

PAD enzyme activity was measured using the ABAP assay (Modiquest Research B. V., Oss, Netherlands) according with the manufacturer's instructions. Briefly, deimination buffer (100 µL) was incubated in the ABAP plate for 30 minutes at 37^0 C. After incubation, the ABAP plate was emptied by inversion and placed on ice. Samples and standards (prepared in deamination buffer) were then added to the ABAP plate and incubated for 1 hour and 15 minutes at 37^0 C in a humidified chamber. After five washes with wash buffer [0.05% (v/v) Tween-20 in PBS], MQR mouse anti-deiminated arginine antibody [1:1000 in 1% (w/v) BSA in wash buffer] was added and the ABAP plate was incubated for 1 hour at 37^0 C in a humidified chamber. Next, the ABAP plate was washed five times with wash buffer, HRP-labelled anti-mouse Ig antibody [1:2000 in 1% (w/v) BSA in wash buffer] was added and the plate was incubated for 1 hour at 37^0 C in a humidified chamber. After five washes with wash buffer and three washes with PBS, OPD reagent was added to the ABAP plate for colour development and the reaction was stopped with 2 M H_2SO_4. Absorbance of each well at 450 nm was measured in a plate spectrophotometer (BioTek Instruments Inc., Swindon, UK) and PAD enzyme activity interpolated from a standard curve.

2.20. Determination of endotoxin content by limulus amebocyte lysate (LAL) assay

2.20.1. Reagents

Pierce™ LAL Chromogenic Endotoxin Quantitation Kit was obtained from Thermo Fisher Scientific Inc. (Loughborough, UK). Acetic acid was from Fisher chemicals (Thermo Fisher Scientific Inc., Loughborough, UK).

2.20.2. Background

Endotoxins are lipopolysaccharides naturally present in the outer cell membrane of Gram-negative bacteria that can influence growth and functionality of a different range of cells. LAL assay allows the quantification of Gram-negative bacterial endotoxins in a chromogenic detection method based on the ability of endotoxins to catalyse the activation of a proenzyme. The activated proenzyme can then catalyse the removal of coloured *p*-nitroaniline (pNA) from a colourless substrate (Ac-lle-Glu-Ala-Arg-pNA). The amount of pNA released can be measured by spectrophotometry (405–410 nm) and the amount of endotoxin interpolated from a standard curve [316].

PAD enzymes used in this work were recombinant produced in bacterial cells, so it was vital to test the presence of endotoxin in PAD enzyme samples.

2.20.3. Protocol

Endotoxin levels in PAD enzymes were determined using LAL Chromogenic Endotoxin Quantitation Kit (Pierce, Thermo Fisher Scientific Inc., Loughborough, UK) according with the manufacturer's instructions. Briefly, a 96-well plate was equilibrated for 10 minutes at 37ºC. Duplicates of standards and samples (50 µL) were dispensed into the plate and incubated for 5 minutes at 37ºC. After, 50 µL LAL was added, the plate was shaken for 10 seconds and then incubated at 37ºC for 10 minutes. After exactly 10 minutes, 100 µL of substrate solution was added, then the plate was shaken for 10 seconds and incubated at 37ºC for 6 minutes. The reaction was stopped by adding 50 µL of 25% acetic acid, the absorbance at 405–410 nm was read on a plate reader (BioTek Instruments Inc., Swindon, UK) and the concentration of endotoxin in EU/mL was interpolated from a standard curve.

2.21. Gene expression analysis

2.21.1. Reagents

miRNeasy Micro Kit, mRNeasy Plus Mini Kit, QuantiTect® primers and trizol lysis solution were obtained from Qiagen Ltd. (Manchester, UK). qScriptTM complementary DNA (cDNA) Synthesis Kit and PerfeCTa® SYBR® Green SuperMix were obtained from Quanta Biosciences (Gaithersburg, MD, USA). Chloroform and ethanol were from Fisher chemicals (Thermo Fisher Scientific Inc., Loughborough, UK). Nuclease free-water was obtained from Thermo Fisher Scientific Inc. (Loughborough, UK).

2.21.2. Background

Studying the expression of mRNA coding for particular genes is a pivotal area in molecular biology. The detection of changes in the expression of a specific gene in response to specific treatments allows collecting important information about cellular functions [317]. Two methods were used here to quantify mRNA and, consequently, obtain information about gene expression: 1) microarray and 2) real time – quantitative polymerase chain reaction (RT-QPCR).

Isolation of RNA from the cells is a critical step for both microarray and RT-QPCR. Qiagen RNA isolation kits supply lysis buffer containing guanidine thiocyanate. This chemical disrupts non-covalent interactions leading to protein denaturation. Consequently, ribonucleases (RNase) that possibly degrade RNA will be inactivated. After this, lysed solutions are passed through a silica gel membrane where nucleic acids are retained and other contaminants are removed. In a final step, nucleic acids are eluted from the membrane and RNA concentration and integrity can be determined by a bioanalyser or a spectrophotometer. Both techniques were used here. The Agilent® 2100 Bioanalyzer™ instrument (Agilent Technologies LDA UK Ltd., Stockport, UK) was used at University of Birmingham prior to microarray experiments. This equipment allows evaluation of the RNA concentration and extent of degradation through a combination of microfluidics, capillary electrophoresis and fluorescent

labelling. To spectrophotometrically quantify mRNA, a NanoDrop 1000 (Thermo Fisher Scientific Inc., Loughborough, UK) analyser was used. This instrument relies on the principles of light absorption and has the advantage of using a small volume of sample (microliter range). Nucleic acids, proteins and other contaminants have specific absorbance maxima at 260, 280 and 230, respectively. The ratio of absorbances at these wavelengths is commonly used to infer the purity of the nucleic acid extraction. A260/A280 and A260/A230 ratios of approximately 2 are considered as “pure” RNA [318].

mRNA expression profiling using microarrays allows to analyse the expression of thousands of genes in a quick and efficient manner. This technique is based on the ability of complementary nucleic acid sequences in two different DNA strands to specifically pair with each other. A typical microarray experiment involves the isolation of RNA, its conversion to complementary deoxyribonucleic acid (cDNA) by reverse transcription and consequent hybridisation on a solid support where cDNA probes had been pre-immobilised. Hybridisation extent can be fluorescent-determined using labelled target sequences and fluorescence intensity can be used to assess the expression of a particular gene.

RT-QPCR technique is based on the same principle as microarray (hybridisation) but primers for targeted genes are used individually. This is a sensitive and robust method to evaluate gene expression and is particularly useful when genes of interest have been identified (for instance by microarray). RT-QPCR principle is based on two stages. The first involves the reverse transcription of mRNA into cDNA. In the second stage, the cDNA template is amplified by QPCR. The heating of the sample leads to the denaturation of the original double stranded cDNA. Following, new DNA is synthesised in the presence of DNA polymerase, deoxyribonucleoside triphosphates (dNTP) and specific PCR primers. Repeating these steps in a cycler equipment through temperatures that allow denaturation, annealing and synthesis, leads to exponential amplification of the initial product. Analysing the fluorescent signal

resultant from the introduction of SYBR Green, a DNA-intercalating dye, into the reaction mixture allows evaluating the PCR product synthesis [319]. Quantitative gene expression can be analysed by absolute or relative quantification. In absolute quantification the copy number of the gene is interpolated from a standard curve. In relative quantification the copy number of the gene of interest is relative to a calibrator or internal control (housekeeper) gene. The relative quantification method adopted here was the comparative threshold cycle (C_T) or 2(-$\Delta\Delta C_T$) method. In this method, the difference between the C_T values (ΔC_T) of the gene of interest and the housekeeping gene is first calculated for each experimental sample. Then, the difference between the ΔC_T values ($\Delta\Delta C_T$) of the experimental and control samples is calculated. The fold-change in the expression of the gene of interest is then equivalent to 2^(-$\Delta\Delta C_T$) [320, 321].

2.21.3. Protocol: RNA extraction

Total RNA was isolated from 5 x 10^5 PBMC using RNase-free plasticware and the miRNeasy Micro Kit according with the manufacturer's instructions. Briefly, 5 x 10^5 PBMC were harvested by centrifugation at 300 x g for 5 minutes and lysed with 700 µL QIAzol Lysis Reagent. The homogenate was then mixed with 140 µL chloroform and the phases separated by centrifugation for 15 minutes at 12,000 x g at 4^0 C. The upper aqueous phase was mixed with 1.5 volumes of 100% ethanol in a new collection tube and transferred into an RNeasy MinElute spin column. The column was then washed with 700 µL buffer RWT, 500 µL buffer RPE and 80% ethanol. RNA was eluted from the RNeasy MinElute spin column by adding 14 µL of RNase-free water and centrifuging for 1 minute at full speed.

Total RNA was isolated from an average of 1.1 x 10^6 CD4 and CD8 T cells using RNase-free plasticware and the RNeasy Plus Mini Kit according to the manufacturer's instructions. Briefly, after isolation of cells, they were counted, collected by centrifugation at 300 x g for 5 minutes and lysed with 350 µL of buffer RLT Plus with

1% (v/v) β-ME. The lysate was then transferred to a QIAshredder spin column and centrifuged for 2 minutes at maximum speed. The homogenised lysate was transferred to a gDNA Eliminator spin column and centrifuged for 30 seconds at 8000 x g. The flow-through was mixed with 1 volume of 70% ethanol and transferred to an RNeasy spin column that was then washed with 700 µL buffer RW1 and twice with 500 µL buffer RPE. RNA was eluted from the RNeasy membrane by adding 30–50 µL of RNase-free water and centrifuging for 1 minute at 8000 x g.

Total RNA quality and quantity were assessed spectrophotometrically using NanoDrop 1000 (Thermo Fisher Scientific Inc., Loughborough, UK). The ratio of A260/A280 of approximately 2 and A260/A230 between 2 and 2.2 were considered as "pure" RNA.

2.21.4. Protocol: cDNA synthesis

cDNA was synthesised according with the manufacturer's instructions (Quanta Biosciences Inc., Gaithersburg, MD, USA). Briefly, RNA samples were mixed with water to a final concentration of 100 ng (in 20 µL) in PCR tubes and cDNA master mix was prepared according with the number of reactions + 1 [for 1 reaction: 4 µL qScript Reaction Mix (5x), 1 µL qScript RT]. RNA samples or water as control (20 µL) were mixed with 5 µL cDNA master mix and reversed transcribed in a thermal cycler with the following program: 1 cycle – 22^0 C, 5 minutes; 1 cycle – 85^0 C, 5 minutes; 4^0 C, hold. After completion of cDNA synthesis, samples were stored at -20^0 C.

2.21.5. Protocol: RT-QPCR

cDNA products were diluted 1/5 and reaction mix was prepared according with the number of reactions + 3 (for 1 reaction: 5.5 µL nuclease-free water, 5.0 µL specific primer, 12.5 µL PerfeCTa® SYBR® Green SuperMix). cDNA samples (2 µL) were dispensed into PCR plate wells and 23 µL of reaction mix added. A negative control with 2 µL nuclease-free water instead of cDNA was also included. RT-QPCR was performed in an Agilent Mx3000P™ QPCR System (Agilent Technologies LDA UK Ltd,

Stockport, UK) using the MxPro QPCR software with the following protocol: 1 cycle – 95^0 C, 2 minutes; 45 cycles – 95^0 C, 10 sec + 60^0 C, 30 sec; 1 cycle – 60^0 C, 30 sec + 95^0 C, 30 sec.

The results obtained were then analysed using the comparative C_T method and the mRNA levels were normalised to *18S* or *YWHAZ* mRNA.

2.21.6. Protocol: microarray

RNA quantity was validated using an Agilent® 2100 Bioanalyzer™ instrument (Agilent Technologies LDA UK Ltd, Stockport, UK) and microarray experiment was performed at University of Birmingham according with the manufacturer's instructions. Fluorescent array images were collected using Agilent DNA microarray scanner and microarray data was analysed using GeneSpring GX software (Agilent Technologies LDA UK Ltd, Stockport, UK). Shift to 75.0 percentile was used as normalisation and median of all samples was applied as baseline transformation. Venn diagrams were used to identify the up- and down-regulated genes against an experimental control, based on entities with a *p*-value equal or lesser than 0.05 and a fold-change equal or higher than two.

2.22. L-lactate quantification

2.22.1. Reagents

The L-lactate assay kit was purchased from Abcam plc. (Cambridge, UK).

2.22.2. Background

Lactate is a by-product of glycolysis, and is a metabolic indicator of cell metabolic activity.

In the L-lactate assay kit from Abcam plc. (Cambridge, UK) the levels of L-lactate are detected by the oxidation of this compound into pyruvate that can then interact with water soluble tetrazolium salts to produce formazan. Formazan can then be spectrophotometrically detected (Figure 2.7).

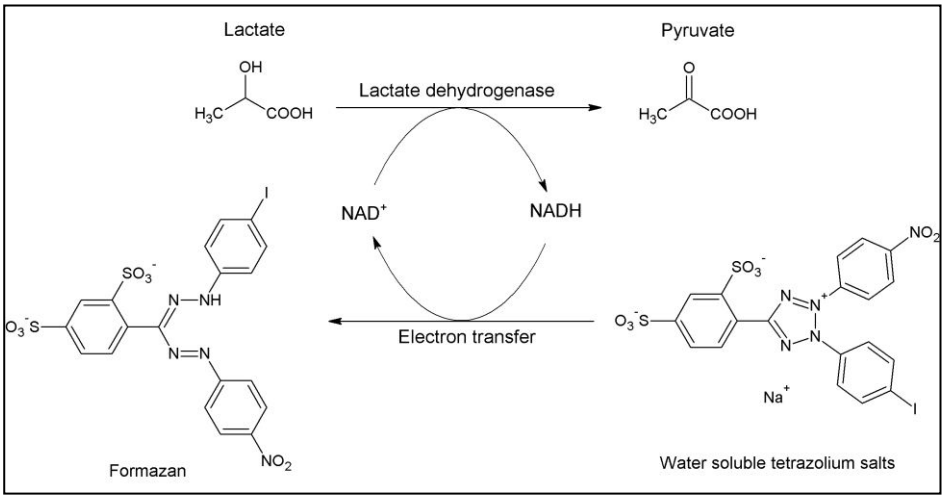

Figure 2.7 Schematic representation of the detection of L-lactate by the L-lactate assay kit from Abcam plc.. NAD^+ – nicotinamide adenine dinucleotide ion; NADH – nicotinamide adenine dinucleotide.

2.22.3. Protocol

L-lactate levels in the supernatant of PBMC pre-treated with PAD enzymes and activated with anti-CD3/anti-CD28 antibodies were quantified using a L-lactate assay kit (Abcam plc., Cambridge, UK) according with the manufacturer's instructions. Briefly, cells were harvested by centrifugation at 300 x g for 5 minutes and the supernatant collected into a new tube and deproteinised. For deproteinisation, samples (200 µL) were mixed with 4 M perchloric acid (PCA) to a final concentration of 1 M and incubated on ice for 5 minutes. After centrifuging at 13,000 x g for 2 minutes at 4^0 C, supernatants were transferred to a fresh tube and the excess of PCA was precipitated with 200 µL of ice-cold 2 M potassium hydroxide (KOH). The pH of the samples was then adjusted to 6.5–8 with 0.1 M KOH and the supernatants were collected after centrifugation at 13,000 x g for 15 minutes at 4^0 C. Next, 50 µL of samples and standards (ranging from 0 to 10 nmol) were loaded in duplicates into the wells of a 96-well plate and after preparing a master mix according to the number of samples + 1 (for 1 reaction: 46 µL lactate assay buffer, 2 µL lactate probe and 2 µL lactate enzyme mix), 50 µL lactate reaction mix was added to the plate. Background sample wells (without lactate enzyme) were also included. The plate was incubated for 30 minutes at

RT, the absorbance was read at 450 nm in a microplate reader (BioTek Instruments Inc., Swindon, UK) and the concentration of L-lactate was interpolated from a standard curve.

2.23. Statistical analysis

Data obtained was analysed using GraphPad Prism (v6.02) and presented as mean ± standard error of the mean (SEM), unless otherwise specified. Experiments were performed in duplicate or triplicate. Comparison between two groups was performed using Mann-Whitney test. Comparison between three or more groups was performed using Kruskal-Wallis test followed by Dunn's multiple comparison test or one-way ANOVA followed by Tukey's multiple comparison test, according with non-parametric or parametric distribution of the data, respectively. Statistical significance was defined as * p-value < 0.05, ** p-value < 0.01, *** p-value < 0.001 and **** p-value < 0.0001.

Chapter 3 Methodological optimisation: analysing citrullination and isolating T cell membrane proteins

3.1. Preface

This chapter describes the optimisation of a method to detect and identify citrullination modifications in human FNG, as a model protein. Proteomics techniques, such as, SDS-PAGE, 2D IEF/SDS-PAGE, 2D BN/SDS-PAGE and MS were used in this chapter to detect citrullination by PAD enzymes. Furthermore, methods were optimised for the separation of T cell MP by 2D BN/SDS-PAGE. The optimised methods have been applied in later chapters.

3.2. Introduction

3.2.1. Fibrinogen

FNG is a soluble 340 kDa glycoprotein [322]. Human FNG comprises of three pairs of non-identical polypeptide chains: Aα, Bβ and γ [323] (Figure 3.1), that are encoded by gene loci *FGA*, *FGB* and *FGG*, respectively, located in chromosome 4 [324]. The three-dimensional structure of FNG is arranged in three main domains: two terminal D domains consisting of a triple-stranded array of α helical coiled coils and a central E domain which is stabilised by 29 disulphide bonds (Figure 3.1) [325]. FNG molecules show high variability resulting from alternative splicing [324], PTM (including phosphorylation, sulphation, glycosylation and hydroxylation), proteolytic degradation and polymorphic variation of Aα and Bβ [323]. The predominant Aα, Bβ and γ chains contain 610 amino acids (70 kDa), 461 amino acids (56 kDa) and 411 amino acids (48 kDa), respectively [323] (Figure 3.2). FNG is synthesised in the liver and is secreted into the blood stream, where it can be found at a concentration of 9 μM with a half-life of approximately 100 hours [323].

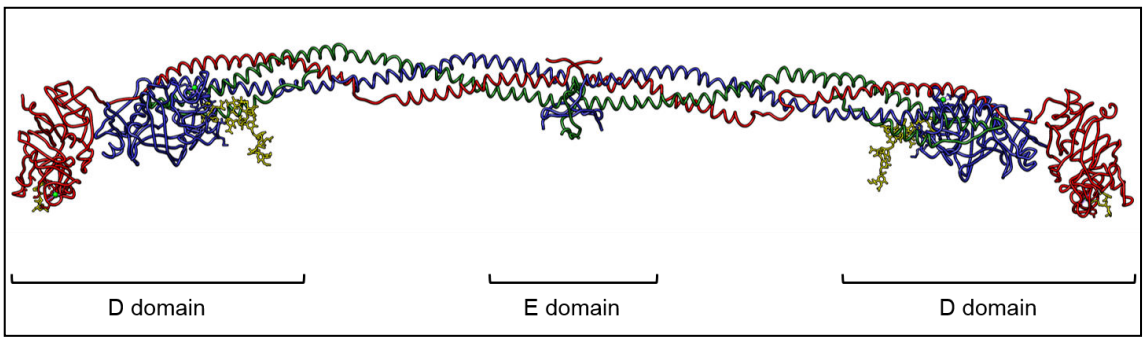

Figure 3.1 Schematic representation of human fibrinogen (Protein data base – PDB – reference: 3GHG). The crystal structure of human FNG, isolated from human blood plasma, was determined at approximately 3.3 Å resolution. Blue – α-chain; green – β-chain; red – γ-chain; yellow – carbohydrate ligand; grey – synthetic peptide knob; light green – calcium ion.

Figure 3.2 Human fibrinogen amino acid sequence. a – α-chain; b – β-chain; c – γ-chain. Residues highlighted in red indicate arginines available for citrullination.

Biologically, the main function of FNG is clot formation. Following vascular damage and blood leakage in the perivascular space, tissue factor (TF), a transmembrane glycoprotein of the perivascular tissue, is activated. TF associates with factor VII and activates factor X, directly or through the activation of factor IX. The activation of factor X mediates the cleavage of prothrombin into thrombin that can then act on fibrinogen. Thrombin releases fibrinopeptides A and B from the amino-terminal ends of Aα and Bβ chains of FNG, respectively, leading to the conversion of FNG into fibrin monomers [323]. The fibrin clot is then formed by spontaneous polymerisation of fibrin monomers followed by intermolecular cross-linking catalysed by transglutaminase (factor XIIIa) (Figure 3.3) [326].

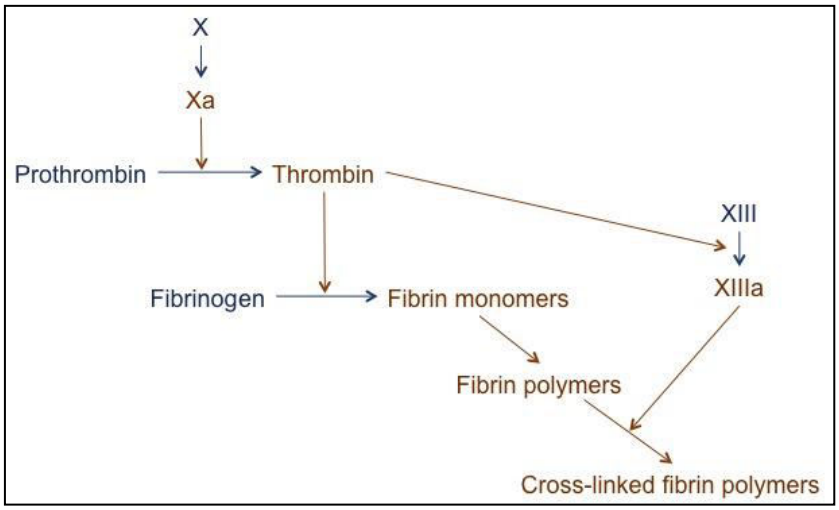

Figure 3.3 Schematic representation of the coagulation cascade. The activated factor Xa converts prothrombin to thrombin. Thrombin then activates factor XIII to XIIIa and converts fibrinogen into fibrin monomers. Fibrin monomers associate spontaneously forming polymers that can then cross-link and form a clot.

In addition to its role in coagulation, FNG is also involved in the regulation of cell adhesion, spreading, migration and proliferation [323], with particular emphasis in inflammatory processes. Inflammation and coagulation are activated by the same stimuli and occur in the same tissues and diseases [327]. FNG expression is regulated at the transcriptional level and is increased during inflammation which is induced by IL-6, glucocorticoids and oncostatin M [323]. FNG has several interaction sites but their accessibility depends on the molecular state of FNG (native FNG versus fibrin and

fibrin polymers) [326]. FNG or its derivatives can interact with other haemostatic factors, with pro- and anti-fibrinolytic proteins and with extracellular matrix proteins and cellular receptors [328]. In the context of inflammation, the interaction of FNG with its integrin receptor promotes leukocyte adhesion to the vascular endothelium, infiltration into the affected site [329, 330] and chemotactic responses by monocytes and neutrophils [331-333]. Importantly, pro-inflammatory and pro-coagulation functions that result from FNG signalling are regulated through different domains and, consequently, do not restrict each other [334].

3.2.2. Peptidylarginine deiminase enzymes and citrullination

Citrullination, as described previously in section 1.3.1, is an enzymatic post-translational modification mediated by PAD (EC 3.5.3.15.) enzyme. In humans, five isoforms of PAD enzymes (PAD1–4 and PAD6) have been identified on chromosome 1p36. Citrullination is responsible for the conversion of peptidylarginine into peptidylcitrulline in a calcium dependent manner (Figure 1.7) [109]. This conversion results in the loss of positive charge in the protein, affecting the protein structure and leading to the formation of new motifs and the generation of neoepitopes [109, 335]. Physiologically, citrullination is essential since citrulline is a non-standard amino acid. PAD enzyme isoforms are differentially expressed in specific tissues and have discrete roles, however, they are highly conserved (70–95% identical amino acids). PAD1 enzyme is mainly expressed in the epidermis and is involved in the flexibility of the keratin cytoskeleton [109, 277, 336, 337]. PAD2 enzyme is the most abundant isoform, being expressed in skeletal muscle, brain, spleen, secretory glands, macrophages and monocytes. In the brain, PAD2 enzyme is associated with the plasticity of the central nervous system. In macrophages, PAD2 enzyme citrullinates the intermediate filament vimentin, associating citrullination with apoptosis mechanisms [133]. PAD3 enzyme expression is restricted to hair follicles and is linked to the firmness of the tube that guide hair fibre growth. PAD4 enzyme is expressed by the cells of the hematopoietic

lineage and can be detected intracellularly and in the nucleus in different tissues. The PAD4 enzyme is involved in gene regulation; it has been implicated in cell apoptosis and negative feedback processes associated with histone functionality and p53 and oestrogen pathway regulation. The PAD6 enzyme is found in early embryos and ovaries and is associated with the reorganisation of egg cytoplasmic sheets during early embryo development [109, 277, 336]. The PAD5 enzyme was initially described as a new PAD enzyme isoform but was then confirmed to be the same as PAD4 enzyme [336].

3.2.3. Citrullination in rheumatoid arthritis

RA is an autoimmune disease characterised by chronic inflammation, oedema, augmented angiogenesis and extensive fibrin deposition in the synovial tissue. These processes lead to degeneration and impairment of the affected joints [338]. The presence of fibrin and fibrin degradation products in the joints and synovial fluid of patients with RA [338-341] suggests the importance of this molecule in the pathophysiology of RA. The role of FNG and its products in RA inflammation have been extensively documented in *in vitro* and *in vivo* studies [342-354].

In addition to the local pro-inflammatory role of FNG and its derivatives in RA, antibodies against citrullinated FNG are also strong markers of RA. ACPA were first described in the context of RA by Schellekens G. and colleagues in 1998 [355]. Following the initial finding, many studies have shown the relevance and connection of these antibodies with RA. ACPA are highly specific for RA [356], can appear before the clinical onset of RA [186, 357, 358] and are correlated with the disease persistence and joint destruction observed [359, 360]. Additional to the presence of ACPA, isoforms 2 and 4 of the PAD enzyme were also found in the synovial membrane [187-189, 361] and in synovial fluid cells [133] of RA patients. FNG is amongst the proteins found to be citrullinated and involved in the production of ACPA in RA [201, 211, 362, 363]. Anti–citrullinated fibrinogen antibodies were also shown to induce the production

of TNF by macrophages, via co-ligation of Toll-like receptor 4 (TLR4) and Fc-γ receptors, suggesting that citrullination potentiates the role of FNG as an endogenous innate immune ligand [358]. Furthermore, citrullination of fibrin α and β chains was also detected in the synovium of RA patients [201, 202, 361, 364].

3.2.4. T cell surface proteins

Cell membranes are key elements to maintain cellular homeostasis within subcellular compartments and between the intra- and the extra-cellular environment. Approximately 50% of the cell surface membrane consists of proteins (MP) responsible for cell-cell contact, surface recognition, cytoskeleton contact, signalling, enzymatic activity and transport across the membrane functions [12]. These proteins at the cell membrane with exposed domains towards the extracellular space constitute the cell surfaceome [365]. In T cells, the immune response relies on MP as it requires the engagement of the TCR/CD3 complex and the co-receptor, CD4 or CD8, with antigens presented through MHC-I or MHC-II molecules by antigen presenting cells (APC) [366]. So far, approximately 300 proteins have been identified in the T cell surfaceome [365]. Additionally, it is known that T cell MP can undergo modifications such as glycosylation [367, 368], phosphorylation [369] and ubiquitination [370] that affect the development, survival or reactivity of these cells. However, there is no information in the literature about citrullination of T cell MP or the effects of PAD enzymes on the activation of these cells.

In order to be able to study the effects of citrullination on T cell MP in future chapters, analytical methods were first optimised and are described in this chapter. Therefore, the aims of this chapter are as follows:

- To optimise conditions to detect citrullination in FNG;
- To optimise conditions to identify the FNG arginine residues modified by PAD enzymes;
- To optimise conditions to separate and detect MP isolated from T cells.

3.3. Methods

3.3.1. Fibrinogen citrullination

Endotoxin content of hPAD enzymes was determined by the chromogenic LAL assay as described in section 2.20.

FNG was citrullinated with hPAD2 and hPAD4 enzymes as outlined in section 2.2.

3.3.2. Analysis of fibrinogen citrullination

Fibrinogen citrullinated with hPAD2 and hPAD4 enzymes was analysed by SDS-PAGE, 2D IEF/SDS-PAGE and 2D BN/SDS-PAGE as outlined in sections 2.8, 2.10 and 2.11, respectively.

3.3.3. Identification of fibrinogen and citrullinated peptides by LC-CID-saETD-MS/MS

Citrullinated FNG separated by SDS-PAGE was further analysed by MS to identify the protein bands and the residues modified by citrullination, as detailed in section 2.12.

3.3.4. Membrane proteins analysis

MP were isolated from Jurkat E6.1 T cells as described in section 2.13 and analysed by 2D BN/SDS-PAGE (section 2.11).

3.3.5. Statistical analysis

Data obtained was analysed as described in section 2.23.

Citrullinated FNG separated by 2D BN/SDS-PAGE was analysed using the SameSpots (TotalLab ltd., Newcastle upon Tyne, UK) analysis software as described in section 2.11. Non-citrullinated FNG was selected as the reference gel.

3.4. Results

3.4.1. Peptidylarginine deiminase enzyme purity

The presence of endotoxin on hPAD enzyme solutions was assessed using the LAL assay (described in section 2.20). The results from this assay showed that hPAD2 and hPAD4 enzyme solutions contained high levels of endotoxin (hPAD2: 3.91e5 EU/mL; hPAD4: 0.93e5 EU/mL). To counteract this obstacle PAD enzymes were HI (30 minutes at 63^0 C) and their effects on all outcomes studied, e.g. citrullination of FNG in this chapter, was compared with the non-inactivated enzymes in order to identify whether any effects observed were due to PAD enzyme activity or LPS contamination (presented in section 3.4.3).

3.4.2. Fibrinogen source comparison

Two commercially available forms of FNG (Sigma-Aldrich Co. and Merck Millipore Ltd.) and two commonly used solutions (phosphate buffer saline – PBS and RPMI) were compared in an initial study (Figure 3.4).

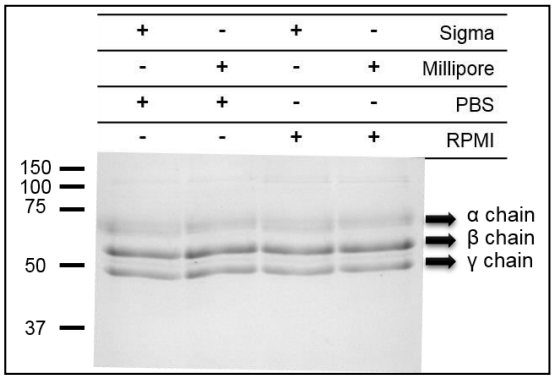

Figure 3.4 Comparison of commercially available FNG (Sigma-Aldrich Co. and Merck Millipore Ltd.) dissolved in PBS or RPMI. Ten micrograms (10 µg) of FNG (Sigma-Aldrich Co. or Merck Millipore Ltd.) dissolved in PBS or RPMI (serum free) were separated by SDS-PAGE in a 12% acrylamide gel. After electrophoresis, the gel was stained with CBB R250. The gel is representative of three independent experiments.

The bands corresponding to the three chains of FNG were identified in the gel, according with their MW (α – 70 kDa; β – 56 kDa; γ – 48 kDa). No differences were found between the two commercial sources of FNG or the two solutions used. For further studies, FNG from Sigma-Aldrich Co. was dissolved in PBS.

3.4.3. Detection of fibrinogen citrullination by SDS-PAGE

FNG was citrullinated *in vitro* with hPAD2 and hPAD4 enzymes in the presence of calcium and analysed by SDS-PAGE. As previously shown, it was possible to detect the bands corresponding to the three polypeptide chains of FNG, according to their MWs. Citrullination of FNG with hPAD2 enzyme did not reveal any changes in the profile of the FNG bands when compared with the control lane (Figure 3.5a). However, when FNG was incubated with hPAD4 enzyme it was possible to observe a shift to a high MW on the band corresponding to the α-chain of FNG (Figure 3.5b). The addition of EDTA (a calcium chelator) immediately after the start of the reaction and the use of HI PAD enzymes did not affect the profile of FNG separation by SDS-PAGE compared to untreated FNG (Figure 3.5).

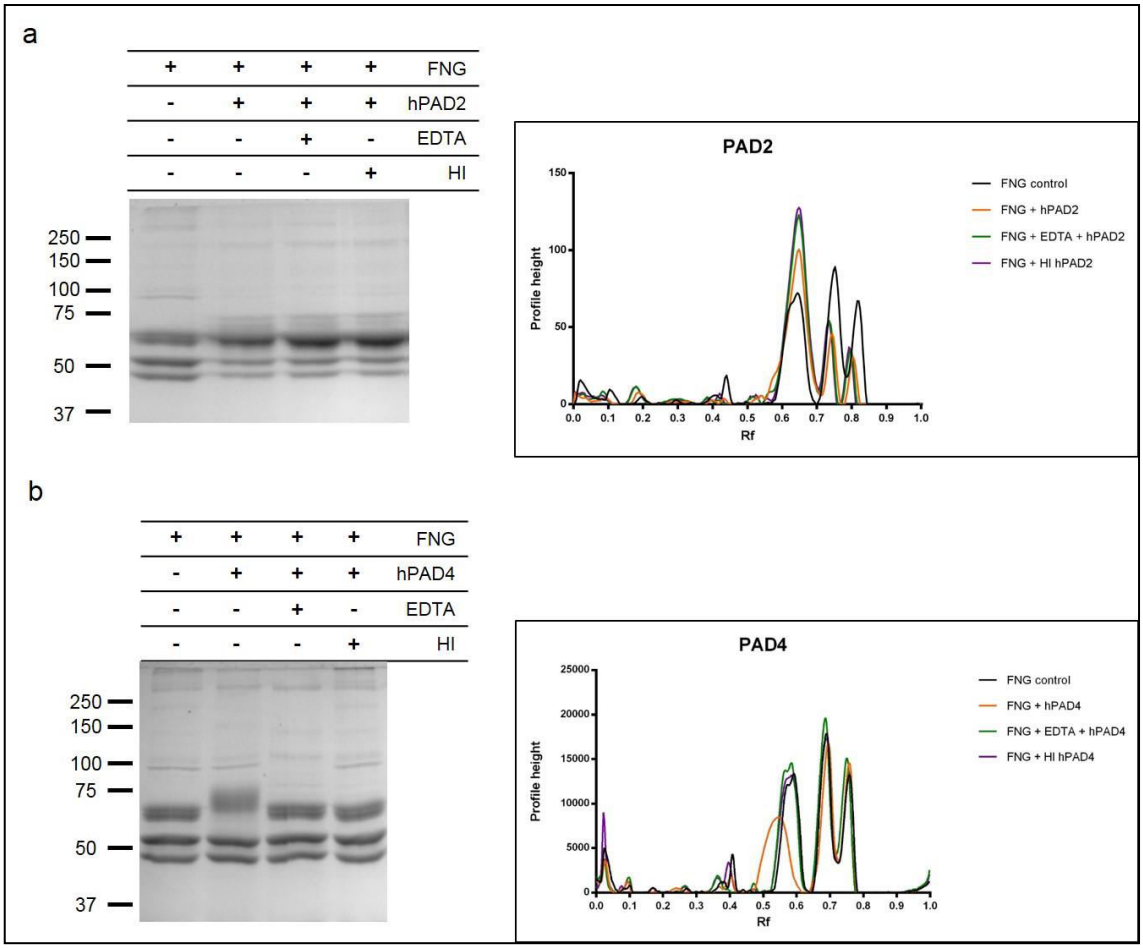

Figure 3.5 *In vitro* citrullination of FNG by hPAD2 and hPAD4 enzymes. One hundred micrograms (100 µg) of FNG was citrullinated with 50 mU of hPAD2 enzyme (a) or hPAD4 enzyme (b) at 37°C for 2h. The reaction was stopped with 200 mM EDTA. Twenty micrograms (20 µg) of protein were separated by SDS-PAGE in a 7.5% acrylamide gel. After electrophoresis, the gel was stained with CBB R250. Controls with only FNG, with the addition of EDTA immediately after the addition of the enzyme and with the heat inactivation (63^0 C for 30 minutes) of the enzymes were included. The right panels represent the densitometry histogram for each lane. The gels are representative of three independent experiments.

3.4.4. Identification of fibrinogen citrullination by mass spectrometry

The identification of citrullinated proteins involved: detection of citrullination, identification of target proteins and possible citrullination sites. FNG was initially used as a model to study the detection of citrullination. hPAD2- and hPAD4-citrullinated FNG was studied by MS to confirm the identification of the polypeptide chains and also to identify the citrullination sites on each subunit. The bands identified 1–9 in figure 3.6 were excised, digested with trypsin and chymotrypsin enzymes and analysed by MS using the neutral loss method (described in section 2.12).

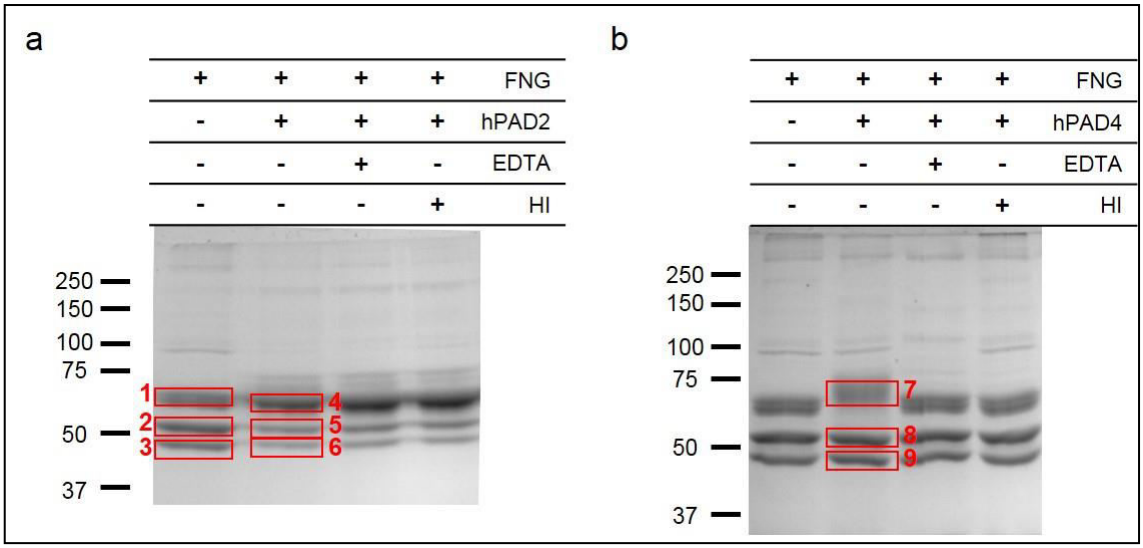

Figure 3.6 *In vitro* citrullination of FNG by hPAD2 and hPAD4 enzymes. One hundred micrograms (100 µg) of FNG was citrullinated with hPAD2 and hPAD4 enzymes at 37°C for 2h. The reaction was stopped with 200 mM EDTA. Twenty micrograms (20 µg) of protein were separated by SDS-PAGE in a 7.5% acrylamide gel. After electrophoresis, the gel was stained with CBB R250. Controls with only FNG, with the addition of EDTA immediately after the addition of the enzyme and with the heat inactivation (63^0 C for 30 minutes) of the enzymes were included. Numbered bands (1–9) represent the bands that were excised for polypeptide digestion and MS analysis.

The analysis of the samples by the neutral loss method (LC-CID-saETD-MS/MS) after digestion with trypsin and chymotrypsin allowed the identification of the bands corresponding to α-, β- and γ-chain of FNG. Additionally, it was possible to identify the arginine residues that were converted into citrulline by the PAD enzymes. In total twenty-three arginine residues were found to be citrullinated, fourteen of which were found in the α-chain, six in the β-chain and two in the γ-chain of FNG (Table 3.1). However, four of these arginine residues were also found to be citrullinated in FNG that was not treated with PAD enzymes, hence these considered as false positives. The coverage of the FNG sequences was lower for the α-chain (56.27%), possibly due to its bigger size, but it was similar for the β- (81.94%) and γ-chain (90.6%).

The detection and identification of FNG subunits and citrullinated sites provides evidence that this method can be applied for further studies.

Table 3.1 Protein identification of the bands excised from the *in vitro* citrullination of human FNG by hPAD2 and hPAD4 enzymes by LC-CID-saETD-MS/MS.

Band	Sample	Identification	Sequence coverage (%) (high confidence)	Citrullinated sites (high confidence)
1	FNG	α-chain	52.89	R353, R394, R573, R510
2	FNG	β-chain	84.11	R121
3	FNG	γ-chain (isoform A)	92.68	-
4	FNG+hPAD2	α-chain	59.58	R123, R263, R271, R287, R367, R394, R404, R425, R426, R510, R512, R547, R573
5	FNG+hPAD2	β-chain	81.87	R60, R121, R196, R410
7	FNG+hPAD4	α-chain	56.35	R271, R367, R425, R426, R547, R573, R591
8	FNG+hPAD4	β-chain	79.84	R53, R60, R376
9	FNG+hPAD4	γ-chain	88.52	R31, R282

Data from the MS experiment was analysed with Proteome Discoverer software (Thermo Fisher Scientific Inc., Loughborough, UK) and the protein identification determined by comparison with the IPI human database. Sequence coverage is a measure of how close an experimental MS/MS spectrum is to the theoretical MS/MS spectrum. Citrullination sites were identified using the neutral loss method and the data was validated by sequence analysis (Appendix 1). High confidence interval corresponds to 1% false discovery rate.

3.4.5. Detection of fibrinogen citrullination by 2D IEF/SDS-PAGE

Citrullination of FNG was also analysed by 2D IEF/SDS-PAGE. After citrullination with hPAD4 enzyme, the sample was de-salted, quantified and focused on IPG strips. The IPG strips were then equilibrated and the proteins resolved by SDS-PAGE. After staining the gels with Flamingo solution it was possible to visualise alterations in the profile of FNG after citrullination with hPAD4 enzyme (Figure 3.7). When observing citrullinated FNG, it is possible to detect spots that were absent from FNG control and hPAD4 enzyme control (Red circles on figure 3.7c). These results suggest that modifications in the chains of FNG due to citrullination occurred and could be visually detected by 2D IEF/SDS-PAGE.

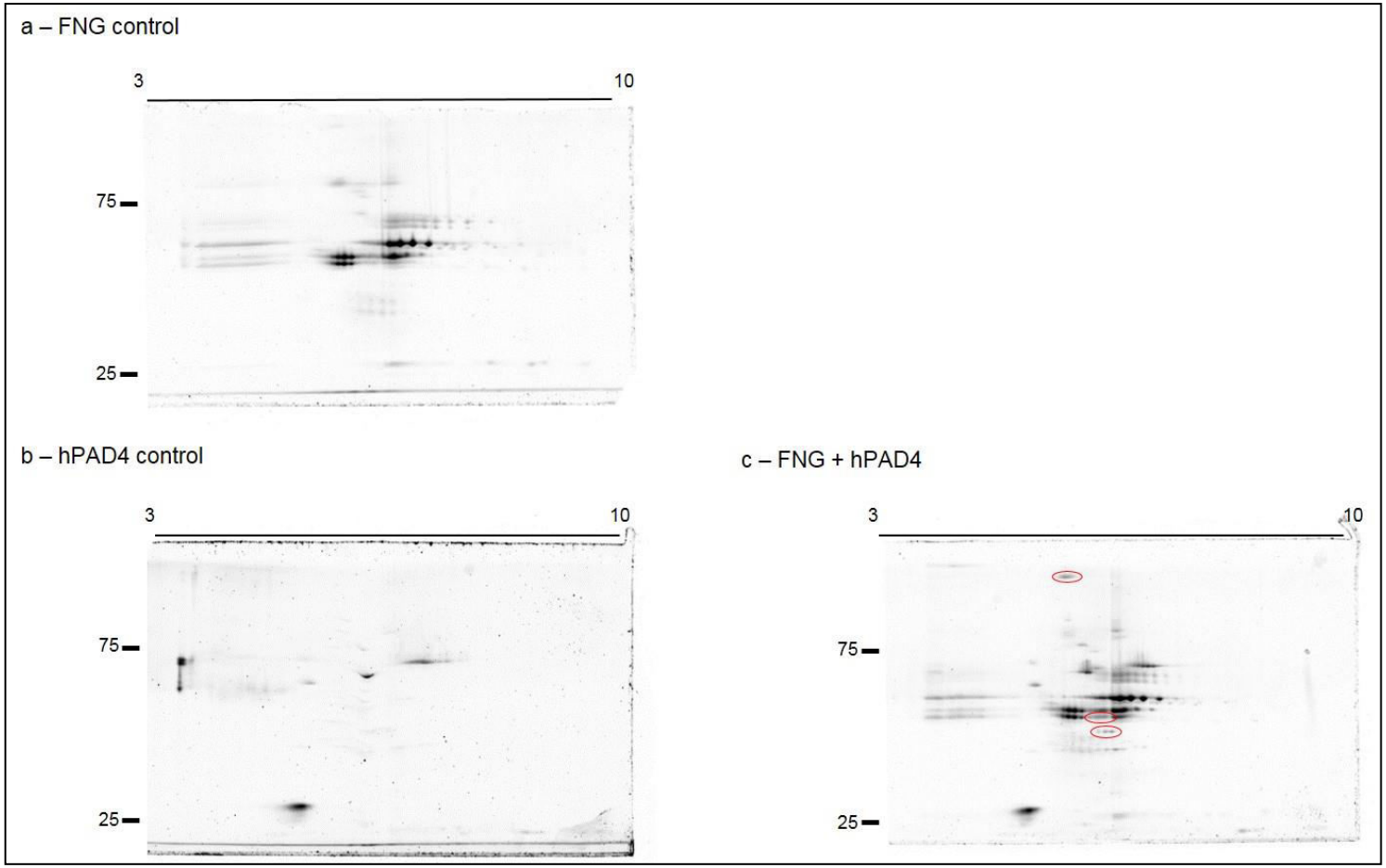

Figure 3.7 *In vitro* citrullination of FNG by hPAD4 enzyme. One hundred micrograms (100 µg) of FNG was citrullinated with 50 mU of hPAD4 enzyme at 37°C for 2h. The reaction was stopped with 200 mM EDTA. Fifty micrograms (50 µg) of protein were prepared for 2D IEF/SDS-PAGE using ReadyPrep™ 2-D clean-up kit. The protein pellets were solubilised and quantified by Bradford assay. Ten micrograms (10 µg) of protein were rehydrated, loaded into IPG strips (11 cm, pH 3–10) and focused in a Protean i12 IEF equipment (Bio-Rad Laboratories Ltd., Hemel Hempstead, UK). In the second dimension, samples were resolved by SDS-PAGE on 10% Criterion pre-cast gels and stained with Flamingo solution. The gel is representative of two independent experiments. Red circles identify the spots that were present in citrullinated FNG but absent on the controls.

3.4.6. Detection of fibrinogen citrullination by 2D BN/SDS-PAGE

Changes in FNG citrullinated with PAD enzymes can be detected by 2D IEF/SDS-PAGE, however, the effectiveness of this technique for the separation of MP is arguable. 2D IEF/SDS-PAGE is a powerful technique to separate complex mixtures of proteins, but due to the high content of hydrophobic amino acid residues, MP show low solubility and a high tendency for aggregation that makes 2D IEF/SDS-PAGE separation impractical [371]. To counteract this, feasibility of 2D BN/SDS-PAGE separation was assessed and implemented to analyse FNG modification by PAD enzymes. BN-PAGE, as previously described in section 2.11, has been used for the separation of microgram amounts of MP from biological membranes [372-376].

First, the separation of native FNG was titrated by 1D BN-PAGE (Figure 3.8). For the three concentrations of FNG tested a band at around 700 kDa was detected. Although native FNG has a MW of 340 kDa the band detected might represent dimeric forms of the protein or the occurrence of PTM. It is also important to notice that some of the sample did not migrate into the gel and consequently was not separated. This can be observed by the staining of the bottom of the wells (Figure 3.8). After separation of different concentrations of native FNG by 1D BN-PAGE, 10 µg was selected as the concentration to use in further optimisation studies.

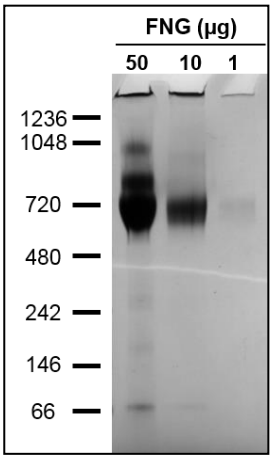

Figure 3.8 FNG analysis by 1D BN-PAGE. FNG (50, 10 and 1 µg) was separated by 1D BN-PAGE in a NativePAGE™ Novex™ 4–16% Bis-Tris gel. After electrophoresis, the gel was fixed and destained with 8% acetic acid. The gel is representative of two independent experiments.

Next, native FNG was separated in two dimensions by 2D BN/SDS-PAGE (Figure 3.9). In figure 3.9 it is possible to observe the separation of native FNG in one band (Figure 3.9a) followed by the SDS-PAGE separation in a second dimension (Figure 3.9b). This combination of dimensions enabled the separation of FNG into its three subunits. As observed previously (Figure 3.8), some of the protein did not migrate into the gel. This is more obvious on figure 3.9b where spots corresponding to the three subunits of FNG can be observed in the left hand side of the gel.

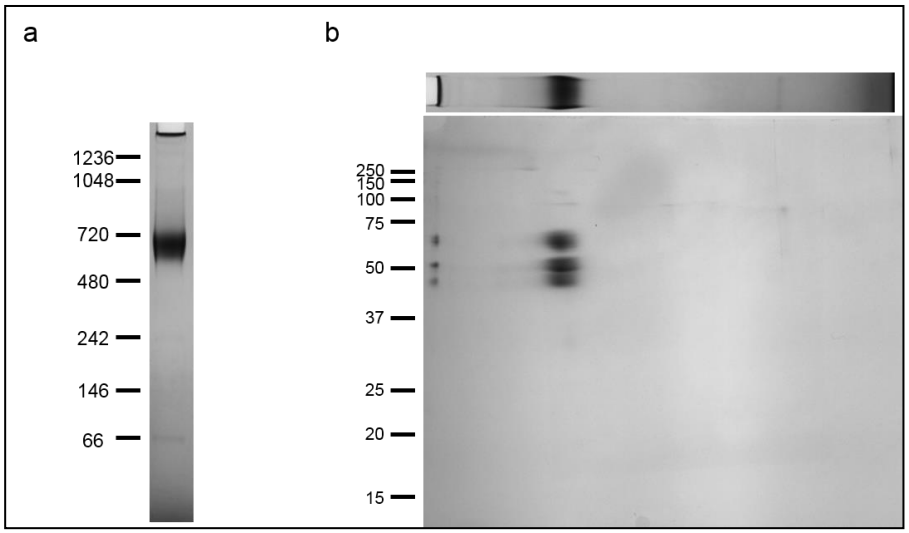

Figure 3.9 FNG analysis by 2D BN/SDS-PAGE. FNG (10 µg) was separated by 2D BN/SDS-PAGE. In the first dimension a NativePAGE™ Novex™ 4–16% Bis-Tris gel was used (a). In the second dimension, the 1D strip was separated in TGX Mini-PROTEAN® TGX™ 8–16% pre-cast gel (b). After 1D electrophoresis, the gel was fixed and destained with 8% acetic acid. The 2D gel was stained with high sensitivity CBB G250. The gels are representative of two independent experiments.

After evidence that native FNG could be detected by 2D BN/SDS-PAGE, the next step was to apply this technique to FNG that had been citrullinated by PAD enzymes. FNG was citrullinated with hPAD2 and hPAD4 enzymes and analysed by 2D BN/SDS-PAGE. On figure 3.10a it is possible to observe the 1D BN-PAGE separation of FNG and citrullinated FNG into three bands with equivalent migration to proteins with MW of approximately 900, 700 and 400 kDa. It is also possible to observe that all the three bands are shifted to higher MW equivalencies on citrullinated FNG samples. Furthermore, hPAD4-citrullinated FNG presented an extra band at a lower MW that

was also present on the lane of hPAD4 enzyme only control and is probably derived from the enzyme itself.

Figure 3.10b–f represents the 2D BN/SDS-PAGE of FNG samples separated in the second dimension. On figure 3.10b, as before in figure 3.9, it is possible to observe the separation of native FNG into its three subunits.

Figures 3.10c and 3.10d represent the separation of the enzymes hPAD2 and hPAD4 enzymes by 2D BN/SDS-PAGE. These figures represent controls for figures 3.10e and 3.10f where citrullinated FNG was separated by 2D BN/SDS-PAGE.

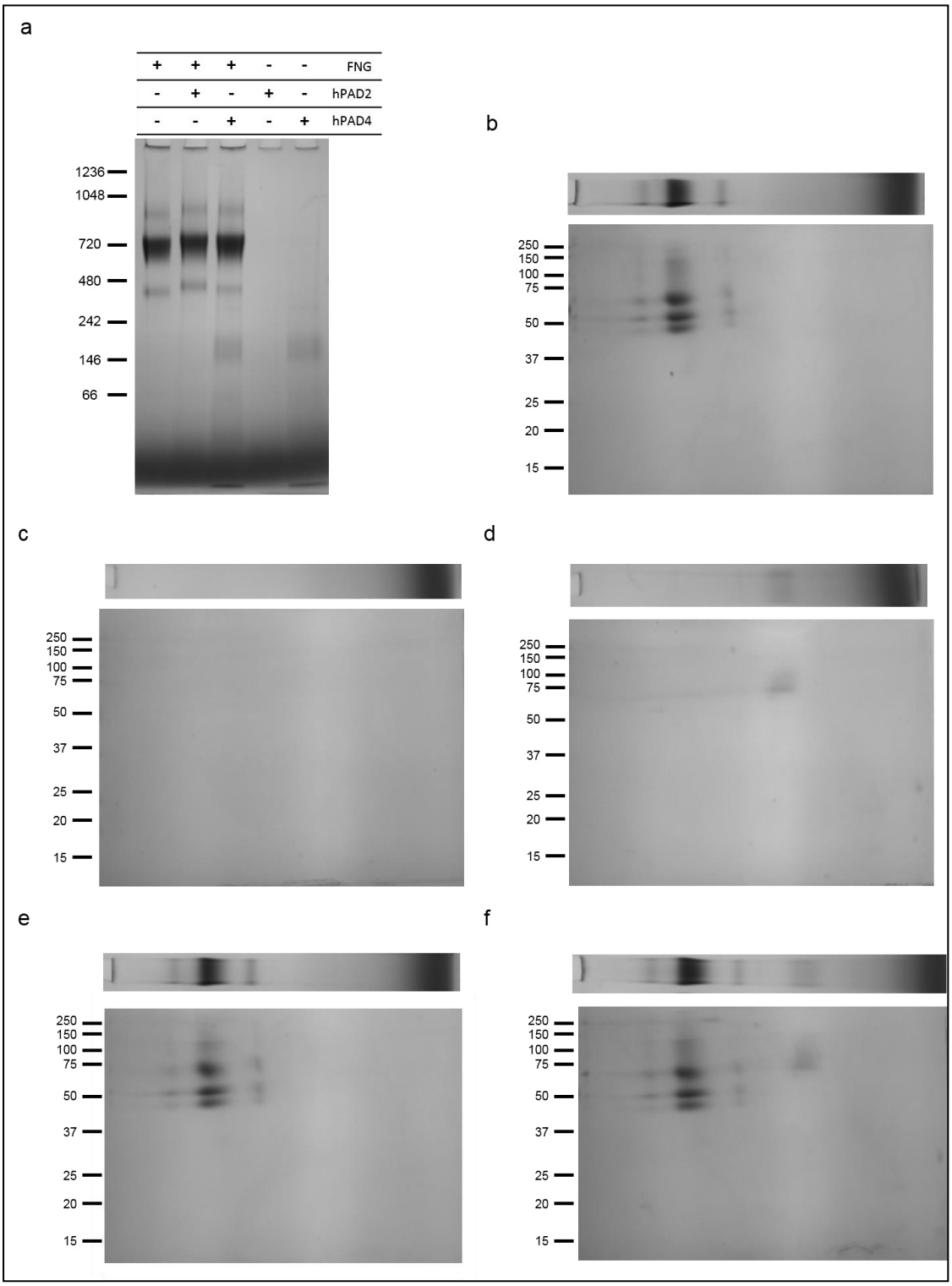

Figure 3.10 *In vitro* citrullination of FNG by hPAD2 and hPAD4 enzymes analysed by 2D BN/SDS-PAGE. One hundred micrograms (100 µg) of FNG was citrullinated with 50 mU of hPAD2 or hPAD4 enzymes at 37°C for 2h. The reaction was stopped with 200 mM EDTA. Ten micrograms (10 µg) of protein were separated by 2D BN/SDS-PAGE. In the first dimension a NativePAGE™ Novex™ 4–16% Bis-Tris gel was used (a). In the second dimension, the 1D strip was separated in TGX Mini-PROTEAN® TGX™ 8–16% pre-cast gel (b–f). b) FNG 1D strip separated by 2D BN/SDS-PAGE. c) hPAD2 enzyme 1D strip separated by 2D BN/SDS-PAGE. d) hPAD4 enzyme 1D strip separated by 2D BN/SDS-PAGE. e) FNG + hPAD2 enzyme 1D strip separated by 2D BN/SDS-PAGE. f) FNG + hPAD4 enzyme 1D strip separated by 2D BN/SDS-PAGE. After 1D electrophoresis, the gel was fixed and destained with 8% (v/v) acetic acid. The 2D gel was stained with high sensitivity CBB G250. The gels are representative of two independent experiments.

The five 2D gels were then analysed using the SameSpots (TotalLab ltd., Newcastle upon Tyne, UK) analysis software in order to detect differences in the FNG profile according with the tested conditions, where non-PAD enzyme treated FNG was considered as the reference gel for normalisation effects. As only one replicate was performed it was not possible to perform statistical analysis of the identified spots, however it was possible to identify the spots with fold changes higher than 2. In total nineteen spots were identified across the four test conditions (hPAD2, hPAD4, FNG + hPAD2 and FNG + hPAD4) with fold changes higher than 2 relative to the control (Figure 3.11 displays the spot position on the reference gel – FNG control), however only spots 190, 213, 217, 227, 233, 401, 402, 404, 405, 406, 407, 408, 409 and 413 were considered for further analysis as the remaining ones were considered speckles or protein streaks.

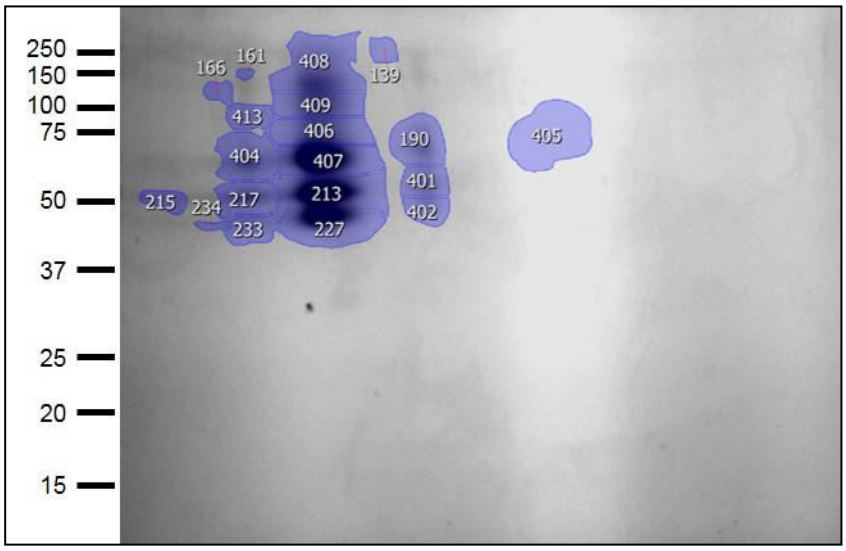

Figure 3.11 SameSpots (TotalLab ltd., Newcastle upon Tyne, UK) software spots identification from *in vitro* citrullination of FNG separation by 2D BN/SDS-PAGE. Ten micrograms (10 µg) of FNG were separated by 2D BN/SDS-PAGE. The gels images were loaded into the software, the spots were matched across gels using FNG control as the reference gel and the spots with fold change higher than 2 between conditions identified in the reference gel.

In accordance with the previous 1D SDS-PAGE (Figure 3.5) and 2D BN/SDS-PAGE (Figure 3.10) gels and based on the MW of the different FNG chains, figure 3.11 suggests that: spots 404, 407 and 190 correspond to the α-chain of FNG; spots 217,

213 and 401 correspond to the β-chain of FNG; spots 233, 227 and 402 correspond to FNG γ-chain; spot 405 corresponds to hPAD4 enzyme. From the graphical representation of the normalised spots it is possible to compare the different intensity profiles according with the conditions tested (Figures 3.12 to 3.17). However, as this analysis results from only one experiment, careful interpretation of the results has to be taken into account. Figure 3.12 suggests that spots 404, 407 and 190 are nearly absent from conditions where only PAD enzymes were analysed. This can be confirmed on the SameSpots software (TotalLab ltd., Newcastle upon Tyne, UK) analysis for spot 407. In addition, it can also be inferred that the treatment of FNG with hPAD2 induced a shift corresponding to higher MW in 404, 407 and 190 spots. Using the same approach, figure 3.13 suggests the absence of FNG from spots 217, 213 and 401 in non-FNG samples what could be confirmed by the software analysis for spot 213. Figure 3.14, once again, suggests the absence of FNG on spots 233, 227 and 402 from PAD only gels, which can be confirmed by software analysis for spot 227. Furthermore, the MW of spots 213 and 227, corresponding to β- and γ-chain of FNG, respectively, appears to have a lower MW (Figure 3.13 and 3.14). Spot 405 was only present on hPAD enzyme treatments and was considered to result from the hPAD4 enzyme itself (Figure 3.15). The presence of spots 413, 409 and 406 were only observed in conditions where FNG was present. Furthermore, it was also possible to observe an increase in the correspondent MW of spot 406 on FNG treated with hPAD2 (Figure 3.16). In figure 3.17, representing spot 408, it is possible to observe the presence of this spot only in conditions where FNG was present. A lower MW of spot 408 in FNG was observed after treatment by both PAD enzymes.

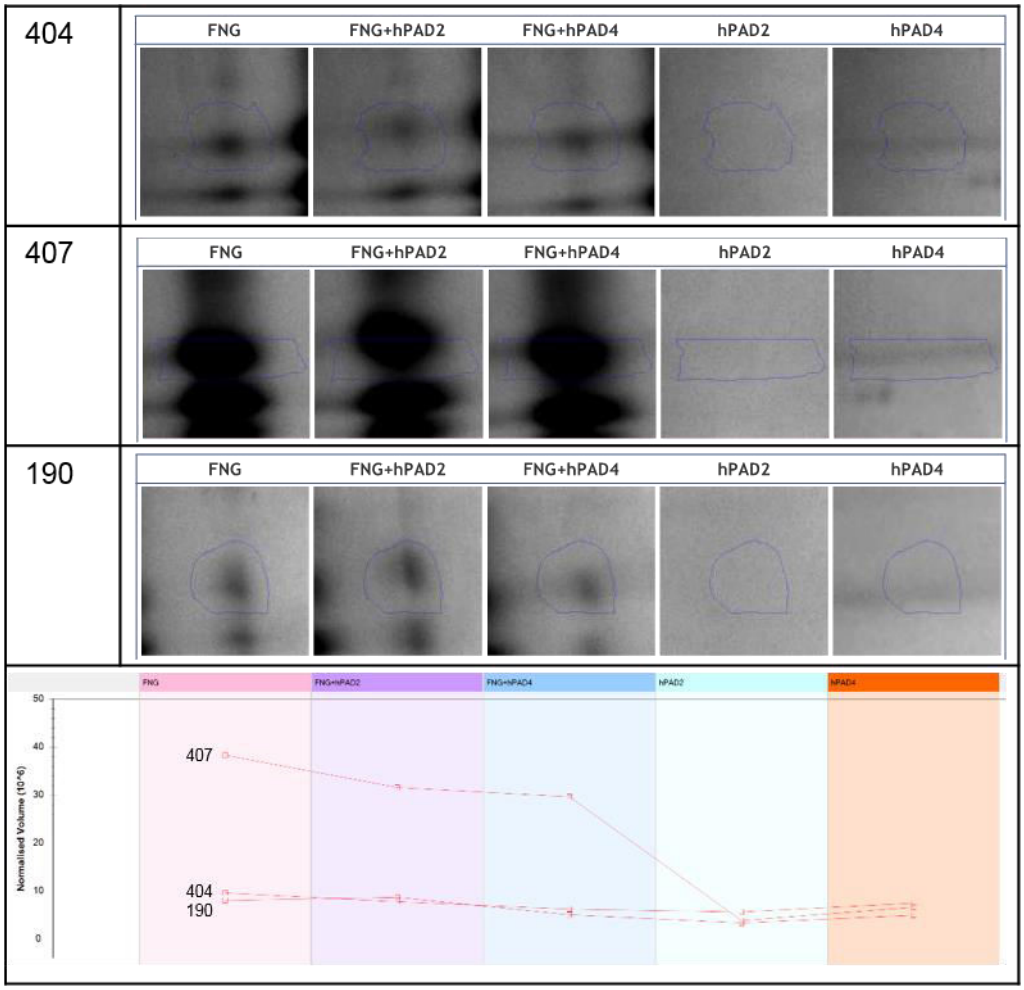

Figure 3.12 Graphical representation of normalised intensity profile of spots 404, 407 and 190 using the SameSpots (TotalLab ltd., Newcastle upon Tyne, UK) analysis software.

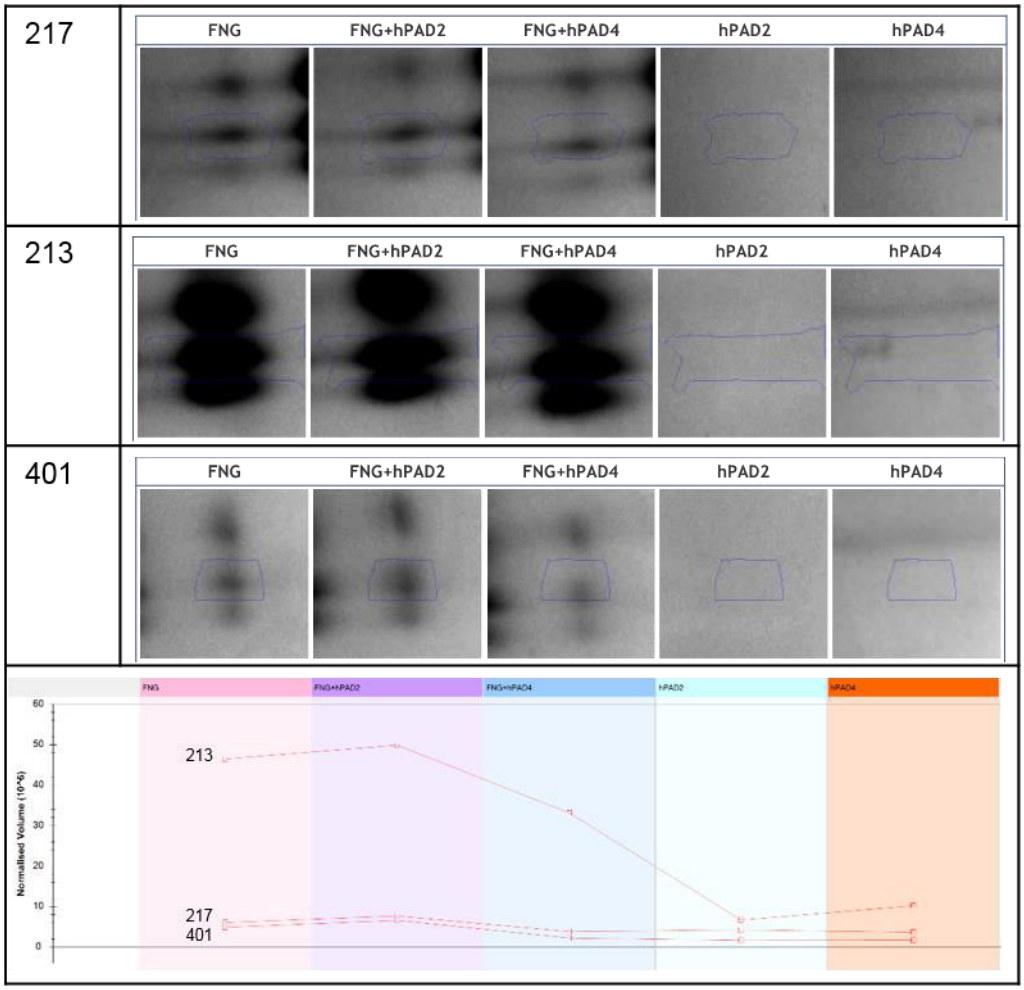

Figure 3.13 Graphical representation of normalised intensity profile of spots 217, 213 and 401 using the SameSpots (TotalLab ltd., Newcastle upon Tyne, UK) analysis software.

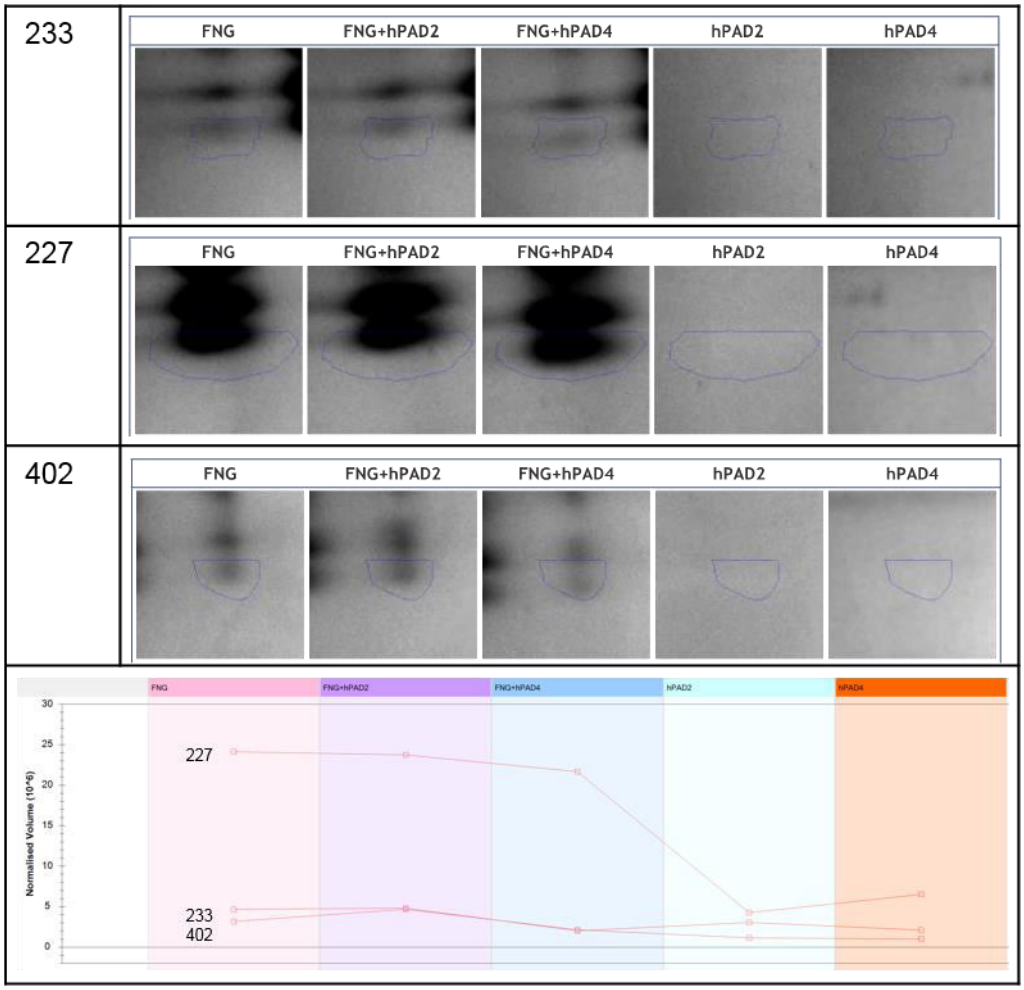

Figure 3.14 Graphical representation of normalised intensity profile of spots 233, 227 and 402 using the SameSpots (TotalLab ltd., Newcastle upon Tyne, UK) analysis software.

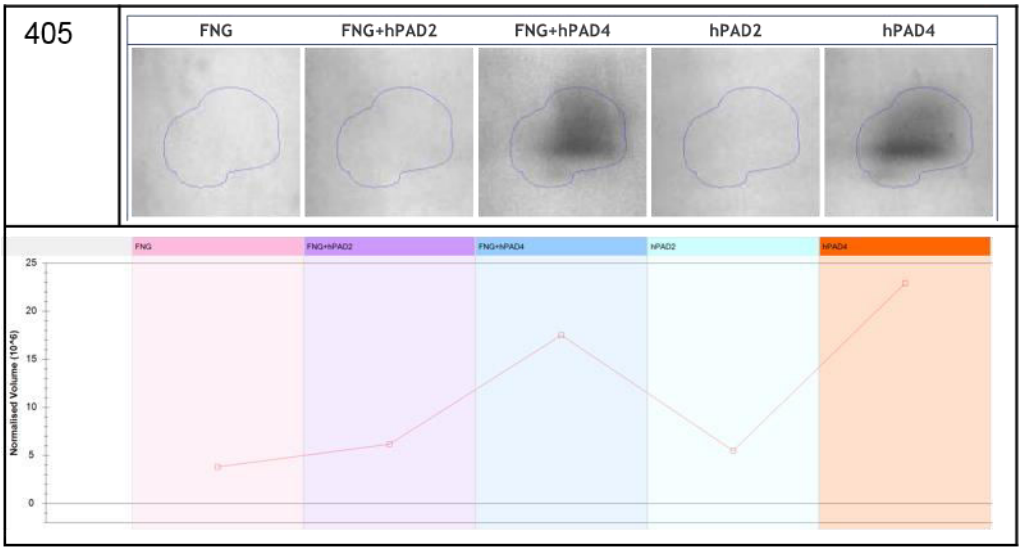

Figure 3.15 Graphical representation of normalised intensity profile of spot 405 using the SameSpots (TotalLab ltd., Newcastle upon Tyne, UK) analysis software.

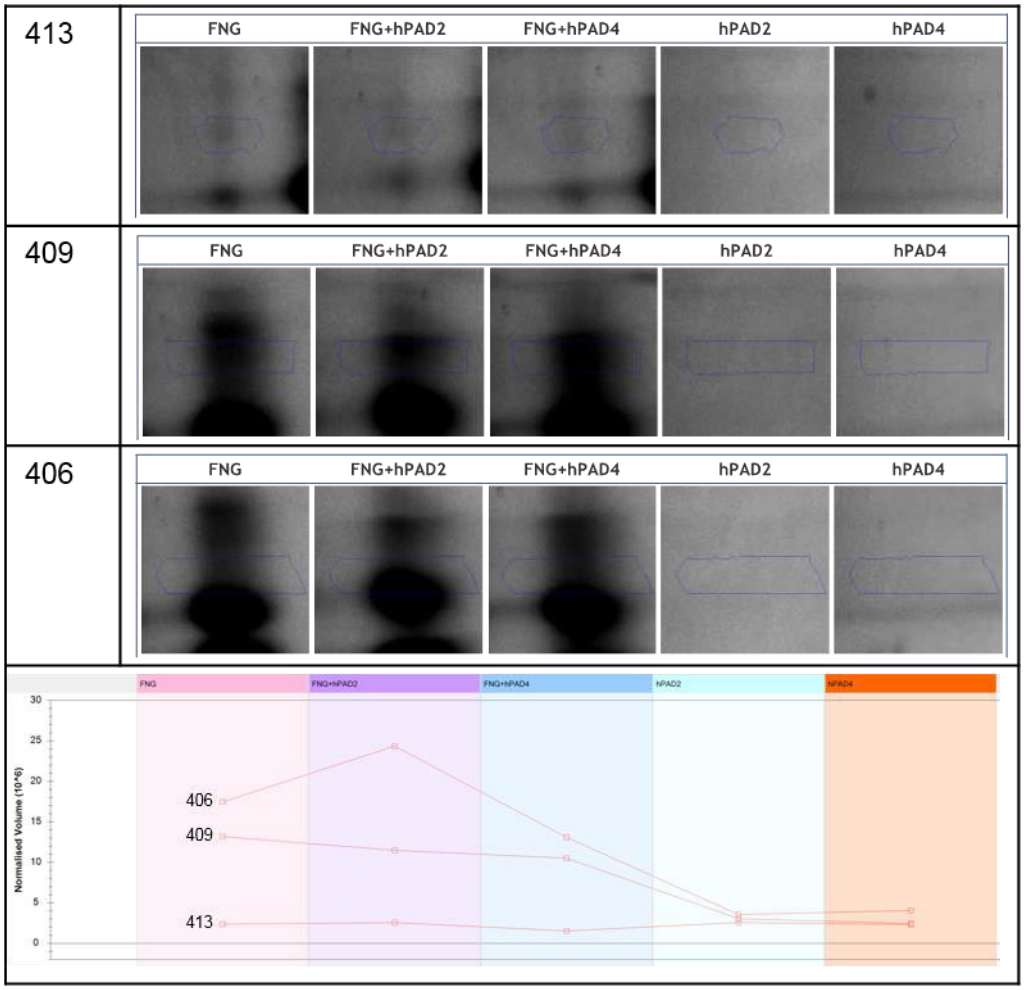

Figure 3.16 Graphical representation of normalised intensity profile of spots 413, 409 and 406 using the SameSpots (TotalLab ltd., Newcastle upon Tyne, UK) analysis software.

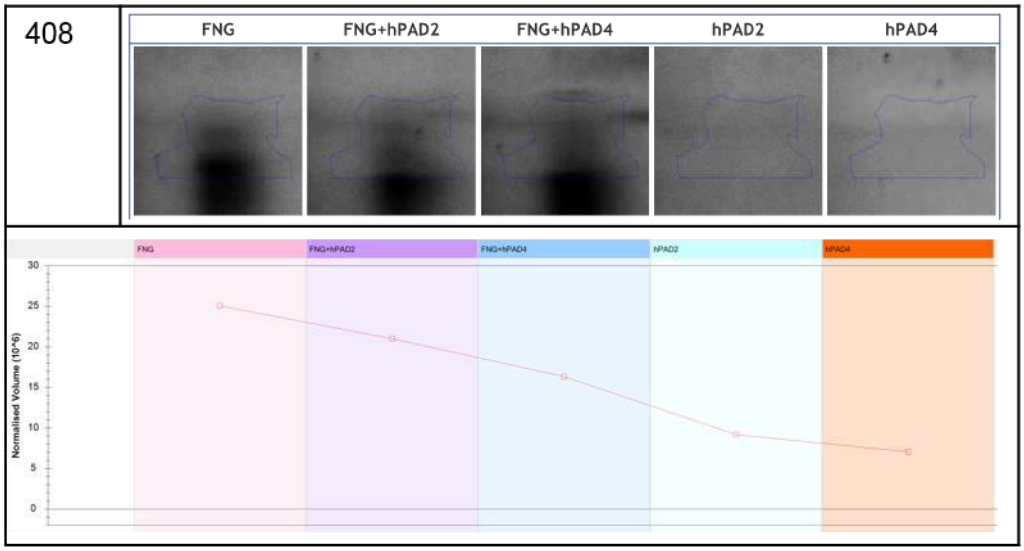

Figure 3.17 Graphical representation of normalised intensity profile of spot 408 using the SameSpots (TotalLab ltd., Newcastle upon Tyne, UK) analysis software.

3.4.7. Detection of membrane proteins by 2D BN/SDS-PAGE

Once it was established that modifications in citrullinated FNG can be detected by 2D BN/SDS-PAGE, the next step was to apply this methodology to a more complex model. As the main purpose of this work is to identify citrullinated T cell surface proteins, MP from Jurkat E6.1 T cells were isolated as described in 2.13 and analysed by 2D BN/SDS-PAGE.

Initially MP were separated in 1D BN-PAGE in the presence of increased concentrations of DDM. DDM is a water soluble nonionic detergent commonly used to solubilise hydrophobic membrane proteins [300-302]. As shown in figure 3.18 the addition of DDM improved the separation of MP by 1D BN-PAGE. The smear and narrowing of the bands observed on the first lane of the gel (0% DDM) disappeared once the detergent was introduced. The resolution of the bands, however, did not seem to improve greatly, probably due to the low amount of protein loaded in the gels (15 µg). For further studies, 0.625% DDM was used and the amount of total protein loaded was increased to 25 µg.

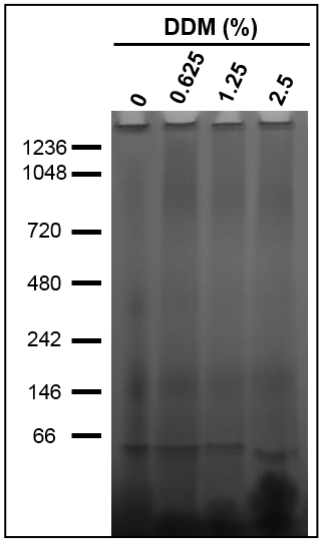

Figure 3.18 MP separation by 1D BN-PAGE. Fifteen micrograms (15 µg) of MP extracted from Jurkat E6.1 T cells were separated by 1D BN-PAGE in a NativePAGE™ Novex™ 4–16% Bis-Tris gel in the presence of increased concentrations of DDM. After electrophoresis, the gel was fixed and destained with 8% (v/v) acetic acid.

MP (25 µg) from Jurkat E6.1 T cells were then separated by 2D BN/SDS-PAGE in the presence of 0.625% DDM. Figure 3.19a shows the 1D separation of the proteins and several bands can be observed. Figure 3.19b illustrates the 2D BN/SDS-PAGE separation of MP. As previously, there were some proteins that did not migrate into the gel and, consequently, were not separated. It is also important to refer the presence of some degree of smear. However, the MP seemed to have been separated and clear spots can be identified in the gel. This approach is showed as viable to separate MP from T cells and will be further used to compare MP from PBMC citrullinated with PAD enzymes (chapter 4).

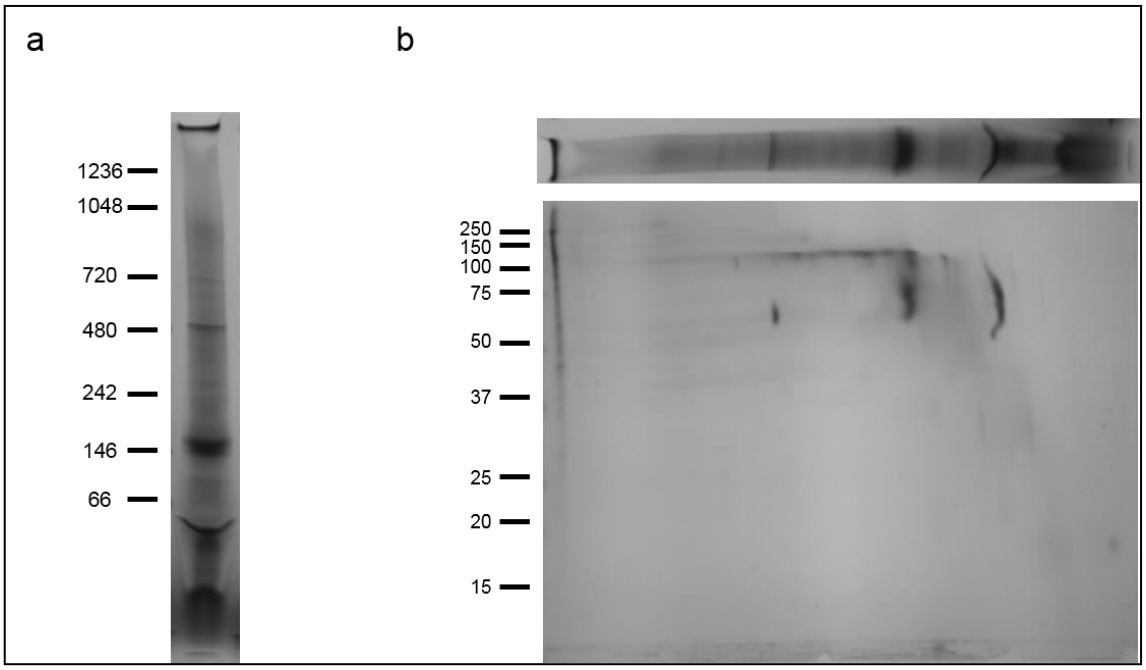

Figure 3.19 MP separation by 2D BN/SDS-PAGE. Twenty-five micrograms (25 µg) of MP extracted from Jurkat E6.1 T cells using the Mem-PER Plus kit (Pierce, Thermo Fisher Scientific Inc., Loughborough, UK) were separated by 2D BN/SDS-PAGE in the presence of 0.625% (v/v) DDM. In the first dimension a NativePAGE™ Novex™ 4–16% Bis-Tris gel was used (a). In the second dimension, the 1D strip was separated in TGX Mini-PROTEAN® TGX™ 8–16% pre-cast gel (b). After 1D electrophoresis, the gel was fixed and destained with 8% (v/v) acetic acid. The 2D gel was stained with high sensitivity CBB G250. The gels are representative of two independent experiments.

3.5. Discussion

Citrullination is an important PTM. Physiologically, the conversion of peptidylarginine to peptidylcitrulline by PAD enzymes is associated with an increase stiffness of the cellular cytoskeleton (citrullination of keratin and fillagrin), the myelin sheets and the hair fibres (citrullination of trichohyalin) and is also involved in regulation of gene expression, through the modification of arginine residues on histones. Pathologically, citrullination is associated with several diseases, including RA and PID [336]. The loss of immune tolerance to self-proteins by the human body and consequent production of ACPA is the main indicator of the involvement of citrullination in RA. In PID, citrullination is linked to the expression of a bacterial PAD enzyme isoform, that is able to modify bacterial and human proteins that can trigger an immune response [109].

The aim of this chapter was to develop a methodology to detect and identify citrullinated proteins. FNG was selected to perform *in vitro* citrullination studies, since it is one of the proteins found to be citrullinated in RA [184, 197, 198]. Autoantibodies against citrullinated forms of the α- and β-chain of FNG were reported in the serum and synovial fluid of RA patients [170, 201]. Additionally, PAD2 and PAD4 enzymes were also identified in the synovium of RA patients [187-189, 361]. Isoforms 2 and 4 of PAD enzymes share sequence homology (Appendix 2) and can both be detected in the synovium of RA patients. However, these two isoforms are expressed by different cells in the synovial tissue, their intracellular localisation is also different and their expression and activation are separately regulated at transcription, translation and enzyme activation [133]. Furthermore, PAD2 and PAD4 enzyme stability, calcium dependency, optimal pH range and substrate specificity are significantly different [377, 378].

FNG isolated from whole blood plasma can be obtained commercially and different sources are available. The first step of this study was to compare the separation of native FNG obtained from two different companies (Sigma-Aldrich Co.

and Merck Millipore Ltd.) by SDS-PAGE. The original buffer system was also addressed, by comparing PBS and RPMI. The separation of native FNG by SDS-PAGE did not show differences either between the commercial sources or the buffer systems studied and it was possible to observe three bands corresponding to the MW of FNG subunits in all conditions. FNG was then citrullinated with hPAD2 and hPAD4 enzyme and separated by three different techniques, SDS-PAGE, 2D IEF/SDS-PAGE and 2D BN/SDS-PAGE. Considering that the conversion of peptidylarginine into peptidylcitrulline only accounts for 1 Da increase in the MW of the protein [335] it was considered unlikely to detect changes in citrullinated FNG by SDS-PAGE. However, it was possible to detect differences between unmodified and citrullinated FNG in all the separations performed.

In 1D SDS-PAGE separation the difference between FNG control and hPAD4 enzyme modified FNG was more obvious than between FNG control and hPAD2 enzyme citrullinated FNG. The opposite was observed by van Beers and colleagues [379], who reported that citrullination of FNG with hPAD2 enzyme was more evident than with hPAD4 enzyme based on the mobility shift of the FNG bands by SDS-PAGE and the number of citrullinated residues identified by MS. Here, after 1D SDS-PAGE separation, citrullinated FNG was digested with two different proteolytic enzymes (trypsin and chymotrypsin) to optimise the sequence coverage and minimise the influence of citrullination on cleavage. In MS studies, trypsin is the most common used protease for the digestion of proteins, once it has high proteolytic activity and cleavage specificity. Trypsin is a serine protease that cleaves polypeptide chains at the C-terminal of arginine and lysine residues. The main drawbacks of the use of this protease for protein digestion are the incomplete digestion, the resistance to proteolysis by tightly folded proteins and its inhibition by some reagents used in protein preparation. As here, the study of citrullination implies the modification of arginine residues, this will contribute to lower efficiency rates of trypsin cleavage, once the digested peptides will be larger and have lower probabilities to be detected by MS

equipment. The combination of proteolytic enzymes is a common approach to improve the digestion of larger proteins or proteins suggested to PTM and increase the sequence coverage of the resultant peptides [380].

The analysis of the digests by MS using CID and ETD fragmentation allowed the identification of eighteen arginine residues citrullinated by hPAD2 or hPAD4 enzymes amongst the three polypeptide chains of FNG. Eleven of these were associated with the α-chain of FNG, five with the β-chain and two with the γ-chain. In total, 28% of the arginines in FNG were found to be citrullinated by either hPAD2 or hPAD4 enzymes. From the total eighteen citrullinated arginine residues, the majority was found in FNG treated with hPAD2 enzyme, this time in agreement with van Beers and colleagues [379]. Six of the eighteen arginine residues were found citrullinated by the two hPAD enzymes, while seven were found to be citrullinated only by hPAD2 enzyme and five only by hPAD4 enzyme.

A fact to consider is that PAD enzymes were also present in FNG citrullinated samples and consequently they were expected to be separated with FNG. As a control for this, controls with just the enzymes in solution were performed. The separation of hPAD2 and hPAD4 enzymes by 1D SDS-PAGE and 2D BN/SDS-PAGE indicated that hPAD4 enzyme was possible to be detected by these techniques, suggesting that in the FNG citrullinated conditions, bands corresponding to this enzyme were also expected to be visualised. The presence of hPAD2 enzyme was not evident, because the amount of hPAD2 enzyme to the FNG solutions was smaller than the amount of hPAD4 enzyme added, due to different intrinsic activity presented by each enzyme.

Another point to take into account in this study is the contamination of recombinant expressed PAD enzymes with endotoxin (lipopolysaccharide – LPS). To clarify the effects of contaminating LPS in mediating effects of PAD enzymes on different proteins and cell functions, a control with HI (63^0 C for 30 minutes) PAD enzymes was performed. Endotoxins are highly heat-stable and can only be inactivated when exposed at temperature of 250^0 C for more than 30 minutes or

180^0 C for more than 3 hours [381]. However, as PAD enzymes have optimal activity at 37ºC [158], by incubating them at 63^0 C for 30 minutes, the enzymes will lose their ability to citrullinate arginine residues. Using HI PAD enzymes did not show any differences on the protein profile of FNG compared to controls which suggests that endotoxin has no effects on the change in MW observed after treatment with PAD enzymes. This control will still need to be performed in further cellular experiments, as the presence of endotoxin is likely to cause immune cell activation and affect T cell responses.

The results from this chapter suggest that citrullination of FNG by hPAD2 and hPAD4 enzymes can be detected by different electrophoretic techniques. The separation of citrullinated FNG by 1D SDS-PAGE allowed to identify the three chains of this protein and it was also possible to identify arginine residues citrullinated by hPAD2 and hPAD4 enzymes by MS analysis. The separation of citrullinated FNG by 2D BN/SDS-PAGE allowed detection of native FNG in the first dimension and the three chains of the protein in the second dimension, allowing the gathering of more information. 2D BN/SDS-PAGE has been extensively used for the analysis of respiratory protein complexes of the electron transfer chains of animals and plants, providing insight into their native interactions. Recently, this technique has been applied to the identification of protein complexes in whole cell lysates from human cell lines [382-388]. Applying this technique to the study of MP addressed here, will allow the separation of the protein complexes and provide information about protein-protein interactions. To corroborate the feasibility of 2D BN/SDS-PAGE in further studies, the level of protein complexity was increased, progressing from FNG, a single protein, to MP isolated from Jurkat E6.1 T cells. By using this mixture of proteins it was possible to assess and validate the applicability of 2D BN/SDS-PAGE to complex samples but also in particular to MP, that have been investigated as a target for citrullination in following Chapters of this thesis. As biological membranes result from complex associations between lipids and proteins, the solubilisation of the lipid components is

essential to extract and analyse the protein fraction. However, the complexity here was to maintain the native structure and subunit composition of the membrane components. The use of detergents has been widely accepted for the extraction and analysis of MP by BN-PAGE. Detergents are amphipatic molecules that have the ability to dissolve the lipid bilayer and form stable micelles with hydrophobic cores in aqueous media, allowing the dissolution of hydrophobic molecules like proteins. DDM is one of the most commonly used detergents in BN-PAGE and has hydrophobic/hydrophilic properties that facilitate lipid solubilisation and at the same time provide a lipid-like environment for MP. The detergent choice is crucial for the solubilisation of MP. DDM was selected for this study and showed to improve the separation of MP but other detergents can be used, according with the protein nature.

The combination of proteomic techniques used in this study allowed the detection of modifications on FNG citrullination by hPAD2 and hPAD4 enzymes. It was possible to identify the three subunits of FNG as well as the arginine residues that were modified by citrullination using a MS method specially developed for the detection of citrullination (LC-CID-saETD-MS/MS) [310]. 2D BN/SDS-PAGE was also confirmed as a valid approach for a complex mixture of MPs. The use of 2D BN/SDS-PAGE and LC-CID-saETD-MS/MS is a suitable approach for further studies on the detection and identification of T cell surface proteins targets of citrullination.

Chapter 4 Analysis of the effects of citrullination of PBMC on T cell activation

4.1. Preface

The aim of this chapter was to study the effects of citrullination by PAD enzymes on the activation of T cells. Initially, the secretion of IL-2 and the expression of IL-2R (CD25) on the surface of cells were used as readouts to select a functional T cell activation model. The activation of T cells was compared using PHA-L and anti-CD3/anti-CD28 antibodies in Jurkat E6.1 T cells and PBMC. After the identification of a functional T cell model, the effects of PAD (hPAD2 and hPAD4) enzymes on the activation of T cells was studied using gene and cell surface protein expression analysis.

4.2. Introduction

The immune system has two main functions, to initiate an inflammatory response when the organism is injured and to distinguish between self- and non-self-proteins. Extreme importance is attributed to the relationship between these two functions. If the organism is not able to identify the self-proteins an inflammatory response can be triggered against the self-organism, leading to autoimmune diseases, such as RA [2, 3]. T cells play a critical role in this differentiation between self and non-self and in the initiation of the adaptive immune response. The principal function of T cells is to promote efficient removal of foreign material by mounting an effective adaptive immune response [12]. The recognition of citrullinated self-peptides as foreign by T cells has been suggested as the trigger for the B cell production of ACPA, a major hallmark of RA, and the breakdown of the immune system. Furthermore, a genetic association between RA susceptibility and severity and the HLA-DR gene that encodes for MHC-II molecules has been suggested [159, 164-172]. It has been established that citrullination plays a key role triggering the autoimmune response observed in RA [159, 170, 171, 184, 211, 389, 390].

T cell functions are influenced by alterations in redox homeostasis, depending on the oxidation state of the cell surface and cytoplasmic protein-thiols. At the T cell surface level, proteins with cysteine (Cys) residues have free thiol groups available for oxidation/reduction by a network of redox regulating peptides, proteins and enzymes, such as GSH, thioredoxins and thioredoxin reductase (TrxR) and protein disulphide isomerase (PDI) [391, 392]. GSH, a cysteine containing tri-peptide, is the most abundant non-protein thiol, and, in combination with its oxidised dimer (GSSG), plays a key role in the maintenance of redox balance and thiol groups. GSH synthesis depends on the activity of γ-glutamylcysteinyl ligase (GCL) enzyme and Cys availability. The expression of GCL is coupled to the cellular redox state through the nuclear factor erythroid 2–related factor 2 – Kelch-like ECH-associated protein 1 (Nrf2-

KEAP1) system, constituting an oxidative stress sensing mechanism that can induce de novo GSH synthesis and restore redox homeostasis [393]. Thioredoxins are a group of small redox enzymes involved in cellular functions such as redox control [394], protection of proteins from oxidative aggregation and inactivation [394-397], helping cells to cope with ROS [398], regulation of programmed cell death [399, 400], modulation of the inflammatory response [401-403] and promotion of protein folding [404]. PDI is a redox active protein that reduces disulphide bonds in cell surface proteins, like β3 integrin on the surface of platelets [405, 406], and it was also shown to be involved in facilitating human immunodeficiency virus (HIV) entry into T cells by forming complex with HIV gp120, CD4 and CXCR4 on the surface of T cells [407-411]. At intracellular level, redox homeostasis is achieved through three major redox couples: NADH/NAD^+, NADPH/$NADP^+$ and GSH/GSSG [412, 413].

OXPHOS and glycolysis are the key cellular metabolic pathways and are intimately related to redox biology. Glycolysis is the main source for NADPH, which is an essential cofactor for NADPH oxidase and for the regeneration of GSH and Trx through their respective reductases (Figure 4.1) [414]. Furthermore, the activity of PAD enzymes, involved in the citrullination of self-antigens in RA, is also influenced by the redox status of the surrounding environment, since the thiol group of Cys351 is essential for the catalytic process [415].

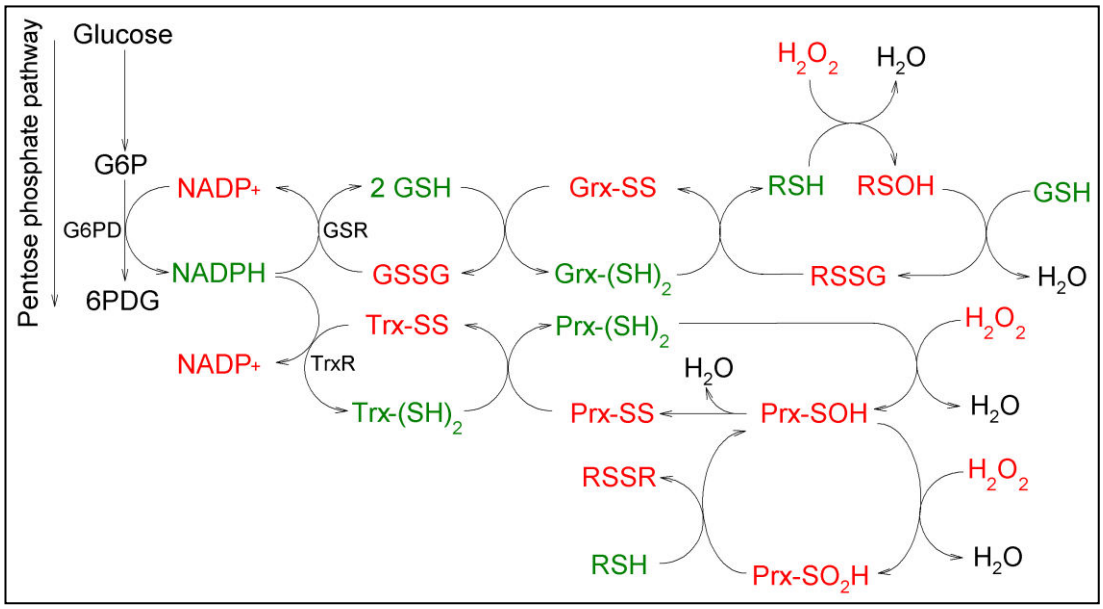

Figure 4.1 Link between reducing nucleotides derived from the pentose phosphate pathway and maintenance of cellular redox state through reduction of hydrogen peroxide and oxidised proteins. Reduced molecules are highlighted in green and oxidised molecules are highlighted in red. GR – glutathione reductase; Grx – glutaredoxin; Grx-$(SH)_2$ – reduced glutaredoxin ; Grx-SS – oxidised glutaredoxin; GSR – glutathione reductase; GSH – glutathione; GSSG – glutathione disulphide; H_2O – water; H_2O_2 – hydrogen peroxide; $NADP^+$ – oxidised nicotinamide adenine dinucleotide phosphate; NADPH – reduced nicotinamide adenine dinucleotide phosphate; Prx – peroxiredoxin; Prx-$(SH)_2$ – reduced peroxiredoxin; Prx-SOH – peroxiredoxin sulphenate; Prx-SO_2H – peroxiredoxin sulphinate; Prx-SS – oxidised peroxiredoxin; RSH – protein; RSSG – glutathionylated protein; RSOH – protein sulphenate; RSSR – protein disulphide; Trx – thioredoxin; TrxR – thioredoxin reductase.

T cells vary in energetic requirements, according to their activity. During maturation and exit from the thymus, naïve T cells depend on OXPHOS for their metabolic needs [77-81], whereas for proliferation after TCR rearrangement T cells rely on glycolysis and glutaminolysis. Once in the periphery (lymphoid organs or in circulation), T cell activation induces metabolic reprogramming of the naïve T cell to a program of anabolic growth and biomass accumulation that is dependent on aerobic glycolysis (conversion of glucose into lactate) [72, 416]. Aerobic glycolysis is less efficient than OXPHOS in the production of energy; however, importantly it yields rapid energy and metabolic intermediates for cell growth and proliferation. Furthermore, aerobic glycolysis also provides a way to maintain cellular redox homeostasis (NAD^+/NADH) [416-418].

Although T cell surface proteins are susceptible to PTM [367-370], there is no information in the literature about citrullination of these proteins or the effects of PAD

enzymes on the activation of T cells. Therefore, it is important to understand whether citrullination occurs on T cells, and how this protein modification affects T cell activation. The aims of this chapter are as follows:

- To compare the activation of Jurkat E6.1 T cells and PBMC with PHA-L and antibodies against CD3/CD28 and select a functional T cell model;
- To investigate the effects of hPAD2 and hPAD4 enzymes on the activation of T cells;
- To explore the effects of hPAD2 and hPAD4 enzymes on gene expression of activated T cells;
- To investigate the effects of PAD enzymes on the citrullination of cell surface proteins.

4.3. Methods

4.3.1. Studies on Jurkat E6.1 T cells

Activation of Jurkat E6.1 T cells with PHA-L and antibodies against CD3 and CD28 was performed as outlined in section 2.3. Following activation, cell viability was assessed and cells were collected for further experiments.

4.3.2. Studies on peripheral blood mononuclear cells population

PBMC were isolated, pre-treated with PAD enzymes and activated with PHA-L and antibodies against CD3 and CD28 as detailed in section 2.4. Following activation, cell viability was assessed and cells were collected for further analysis.

4.3.3. Determination of cell viability

Following the treatments, the viability of Jurkat E6.1 T cells or PBMC was assessed using the CellTiter-Blue® cell viability assay or the trypan blue exclusion assay, as detailed in sections 2.14 and 2.15, respectively.

4.3.4. Quantification of interleukin-2 secretion levels

IL-2 levels secreted by Jurkat E6.1 T cells and PBMC were quantified by sandwich ELISA, as described in section 2.16.

4.3.5. Quantification of extracellular L-lactate levels

The levels of L-lactate in the supernatant of PBMC activated with anti-CD3/anti-CD28, with and without PAD enzyme treatment were quantified using the L-lactate assay kit as described in section 2.22.

4.3.6. Analysis of the expression of the interleukin-2 receptor in the surface of T cells

Flow cytometry was used to quantify the expression of CD4 and CD25 (IL-2Rα) at the surface of PBMC, as detailed in section 2.17.

4.3.7. Identification of membrane proteins

Twenty-five micrograms of MP were isolated from PBMC with and without treatment with PAD enzymes and activated with anti-CD3/anti-CD28 antibodies, as described in section 2.13 and analysed by 2D BN/SDS-PAGE (section 2.11). Following 2D BN/SDS-PAGE separation, selected spots from non-PAD treated, hPAD2- and hPAD4-treated conditions were pooled together alkylated, digested with trypsin and analysed by LC-CID-saETD-MS/MS for the protein and citrullinated residues identification, as outlined in section 2.12.

4.3.8. Quantification of gene expression

Total RNA was isolated from 5 x 10^5 PBMC following treatment with PAD enzymes and activation with anti-CD3/anti-CD28 antibodies, converted to cDNA and analysed by microarray hybridisation and by RT-QPCR, as outlined in section 2.21. The mean of unactivated PBMC was used as a control condition for the comparison of gene expression between unactivated and activated PBMC. The mean of activated PBMC was used as a control condition for the comparison of gene expression between activated PBMC and PAD-treated PBMC followed by activation.

4.3.9. Statistical analysis

Data obtained was analysed as described in section 2.23.

Citrullinated protein spots previously separated by 2D BN/SDS-PAGE were analysed using the SameSpots (TotalLab ltd., Newcastle upon Tyne, UK) analysis

software as described in section 2.11. A non-citrullinated sample was selected as the reference gel.

4.4. Results

4.4.1. Comparison between Jurkat E6.1 T cells and peripheral blood mononuclear cells as a model for T cell activation

In order to study the activation of T cells, an initial comparison with two models of T cells and two models of T cell activation was performed. Jurkat E6.1 T cells and PBMC were used as a model of T cell activation and PHA-L and antibodies against CD3 and CD28 were used as *stimuli* to induce T cell activation. Activation studies were performed for 24, 48 and 72 hours. Following incubation with PHA-L or anti-CD3/anti-CD28 antibodies, Jurkat E6.1 T cells and PBMC were collected and assessed for viability, expression of CD25 at the surface and secretion of IL-2 to the extracellular medium.

Cell viability is an important readout to evaluate if the treatment is associated with any cell toxicity. Expression of CD25 at the surface of T cells and secretion of IL-2 to the extracellular medium are key markers of T cell activation. CD25 is the α-chain of the IL-2R and *in vivo* is highly expressed at the surface of T cells when these are proliferating in the thymus [2]. Later, when naïve CD4 T cells become activated in the periphery, through the presentation of antigen by APC, the secretion of IL-2 to the extracellular medium and the expression of the CD25 are stimulated. The interaction between IL-2 and IL-2R induces T cell growth, differentiation and survival [419].

The cell viability results, using the trypan blue exclusion assay, showed that a high percentage of Jurkat E6.1 T cells lost viability with the PHA-L treatment (Figure 4.2a). Using increasing concentrations of PHA-L (0, 0.5, 1, 2 µg/mL) for 24 hours the viability of Jurkat E6.1 T cells decreased from 96.9 ± 0.4% (0 µg/mL PHA-L) to 81.55 ± 8.35% (1 µg/mL PHA-L) and to 80.15 ± 5.85% (2 µg/mL PHA-L), but this difference was not statistically significant (*p*-value = 0.267). Treating the Jurkat E6.1 T cells with PHA-L for longer periods (48 and 72 hours) had a similar effect on the viability of the cells. Jurkat E6.1 T cells stimulated with 0 to 10 µg/mL of PHA-L for 48 hours showed

a non-statistically significant decrease of 20.56% (*p*-value = 0.210) between the minimum and maximum concentrations, but a statistically significant decrease of 29.06% (*p*-value = 0.03) was observed when Jurkat E6.1 T cells stimulated with 0 to 10 µg/mL of PHA-L for 72 hours, suggesting that treating Jurkat E6.1 T cells for longer periods with high concentrations of PHA-L can be toxic and lead to cell death. However, at lower concentrations this toxic effect was not observed. Data from Jurkat E6.1 T cells treated with 1 µg/mL of PHA-L for 24, 48 and 72 hours show that cell viability was similarly reduced to 81.55 ± 8.35% at 24 hours, 79.70 ± 6.2% at 48 hours and 88.5 % at 72 hours (*p*-value = 0.600).

PBMC were only stimulated with PHA-L for 24 hours. The viability of these cells remained above 86% with the increased concentrations of PHA-L (Figure 4.2b). When PBMC were stimulated with increased concentrations (from 0 to 5 µg/mL) of anti-CD3 antibody in combination with an antibody against CD28 the viability of these cells was not affected (lowest value of 89.54 ± 4.08%), even after 72 hours of incubation (Figure 4.2c).

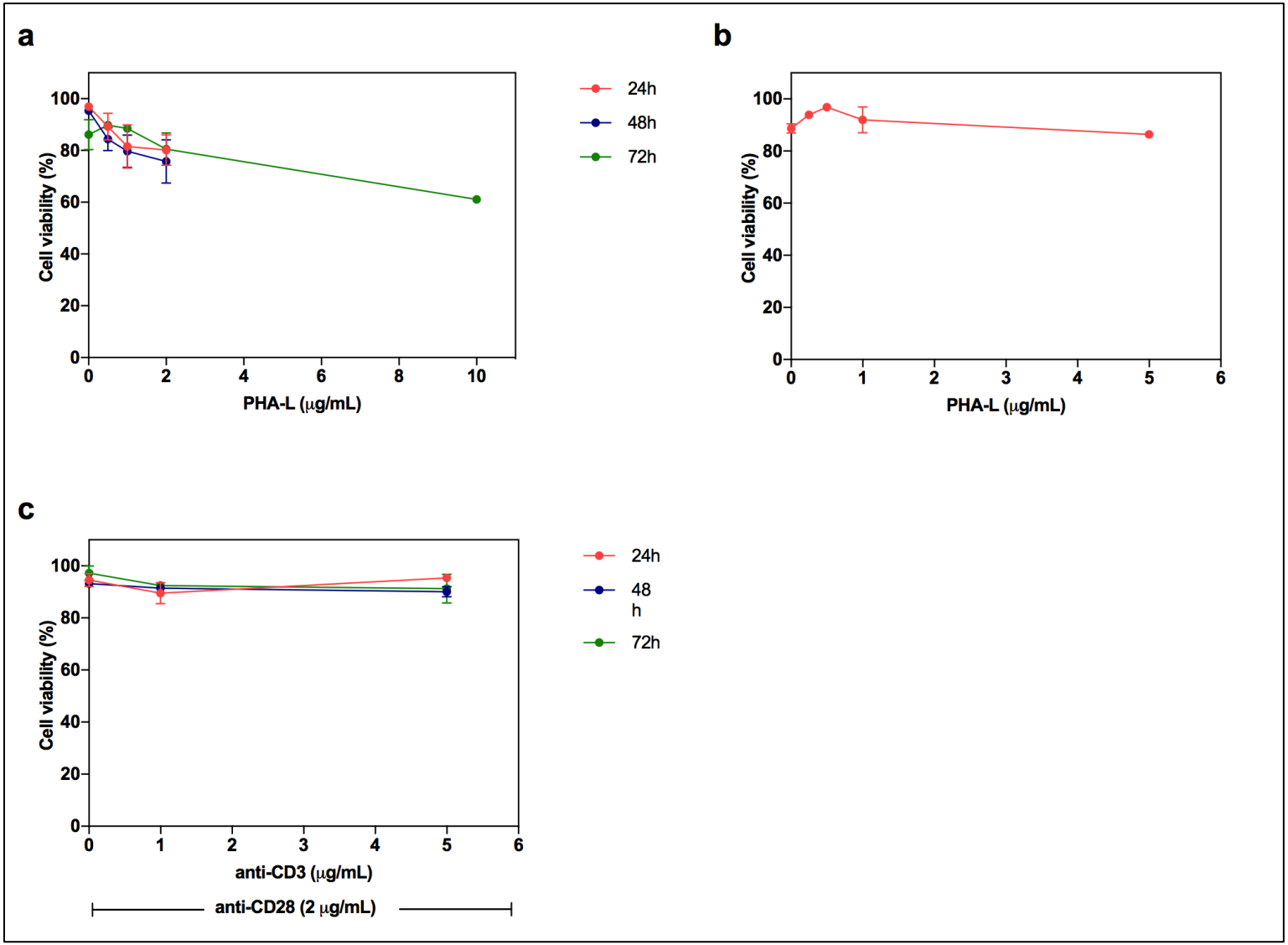
a
Cell viability (%)
PHA-L (μg/mL)
24h
48h
72h
b
Cell viability (%)
PHA-L (μg/mL)
c
Cell viability (%)
anti-CD3 (μg/mL)
anti-CD28 (2 μg/mL)
24h
48 h
72h

Figure 4.2 Jurkat E6.1 T cells and PBMC viability after activation with PHA-L or anti-CD3/anti-CD28. Jurkat E6.1 T cells were cultured in complete RPMI medium. PBMC were isolated from healthy volunteers. a) Jurkat E6.1 T cells (1 x 10^6 cells/mL) were stimulated with concentrations of PHA-L ranged from 0 to 10 µg/mL and incubated at 37^0 C for 24, 48 and 72 hours. b) PBMC (5 x 10^5 cells/mL) were stimulated with concentrations of PHA-L ranged from 0 to 5 µg/mL and incubated at 37^0 C for 24 hours. c) PBMC (5 x 10^5 cells/mL) were stimulated with concentrations of anti-CD3 antibody ranged from 0 to 5 µg/mL, followed by incubation with antibody against CD28 (2 µg/mL), and incubated at 37^0 C for 24, 48 and 72 hours. Cell viability was assessed by the trypan blue exclusion assay. Mean values are shown with SEM. The values are the results from three independent experiments with Jurkat E6.1 T cells and two independent experiments with PBMC. Kruskal-Wallis test followed by Dunn's multiple comparison test were performed and revealed no statistical significance.

As previously mentioned, IL-2 secreted into the extracellular medium constitutes a relevant readout of T cell activation. The levels of IL-2 in the supernatant of Jurkat E6.1 T cells and PBMC incubated with PHA-L and anti-CD3/anti-CD28 antibodies was assessed by ELISA. When comparing the levels of IL-2 secreted by Jurkat E6.1 T cells activated with PHA-L (Figure 4.3a) and anti-CD3/anti-CD28 antibodies (Figure 4.3b) it is possible to observe a trend towards increased levels of IL-2 as a response to increasing concentrations of PHA-L and anti-CD3 antibody. However, this response was more obvious with the antibodies activation method. Nevertheless, the IL-2 levels were only increased when the concentration of anti-CD3 antibody was 5 µg/mL and the cells were incubated for more than 48 hours. When comparing the activation of T cells within the PBMC population with PHA-L and anti-CD3 antibody, both for 24 hours, it was again possible to observe that the IL-2 secretion was greater when the combination of antibodies against CD3 and CD28 was used instead of PHA-L. Even using 5 µg/mL of PHA-L the IL-2 secretion only reached 0.61 ± 0.06 ng/mL, while using 1 µg/mL of anti-CD3 antibody in combination with 2 µg/mL of anti-CD28 antibody it was possible to detect 1.33 ± 0.04 ng/mL of IL-2 (Figure 4.3c). The activation of T cells on PBMC with anti-CD3/anti-CD28 antibodies was also compared for 24, 28 and 72 hours. In figure 4.3d it is possible to observe than IL-2 secretion increased substantially when PBMC were activated with 1 µg/mL of anti-CD3 antibody for 24 (0.65 ± 0.03 ng/mL) or 48 hours (0.90 ± 0.03 ng/mL), when comparing with no activation levels (0.02 ± 0.01 ng/mL at 24 hours and 0.04 ± 0.01 ng/mL at 48 hours). However, the IL-2 levels did not increase proportionally when 5 µg/mL were used instead of 1 µg/mL,

changing to 0.69 ± 0.03 ng/mL at 24 hours and to 0.9 ± 0.03 ng/mL at 48 hours. The stimulation of the PBMC for 72 hours did not reproduce the increase in IL-2 secretion observed in 24 or 48 hours (Figure 4.3d).

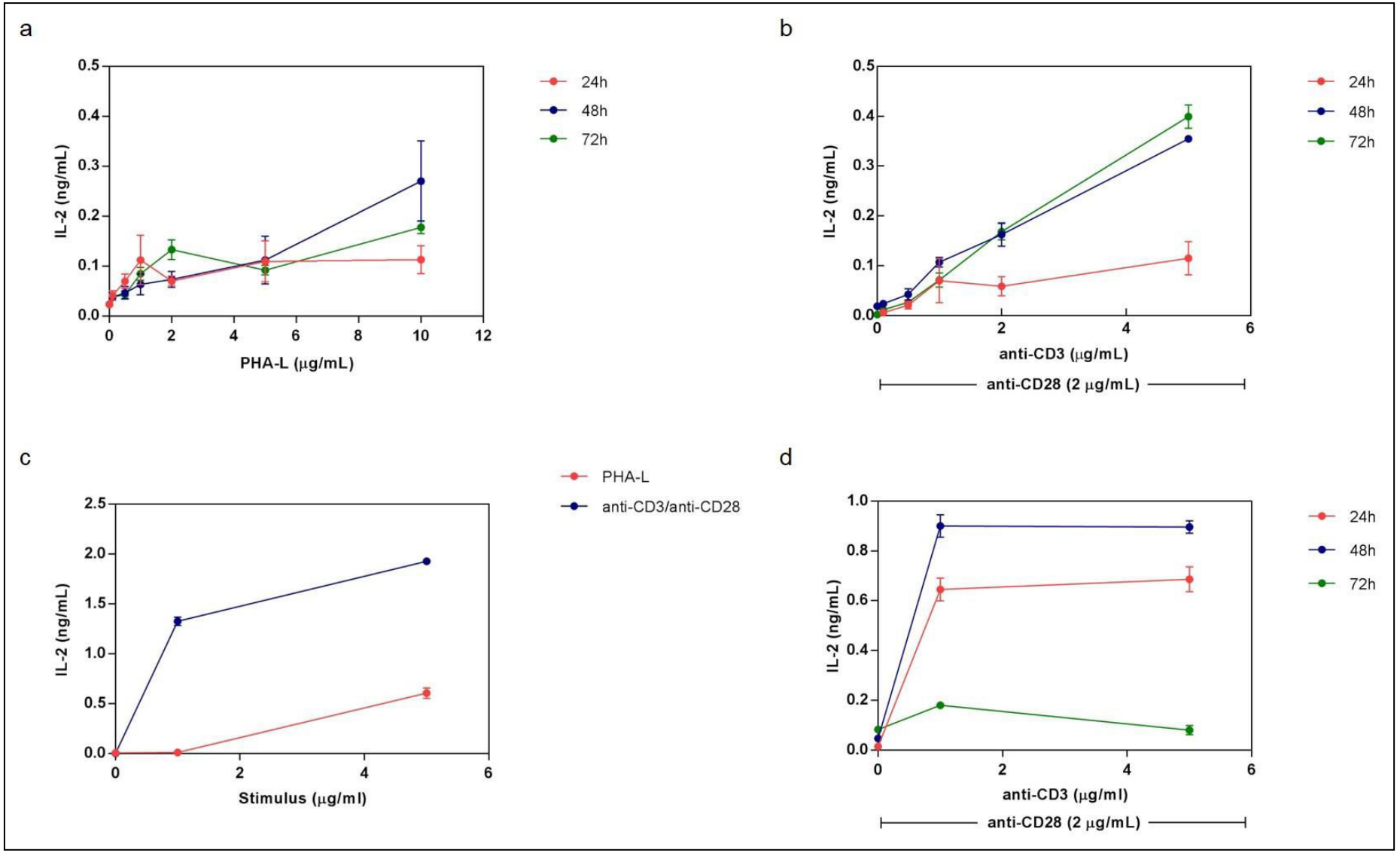
a
IL-2 (ng/mL)
PHA-L (μg/mL)
24h
48h
72h
b
IL-2 (ng/mL)
anti-CD3 (μg/mL)
anti-CD28 (2 μg/mL)
24h
48h
72h
c
IL-2 (ng/mL)
Stimulus (μg/ml)
PHA-L
anti-CD3/anti-CD28
d
IL-2 (ng/mL)
anti-CD3 (μg/ml)
anti-CD28 (2 μg/mL)
24h
48h
72h

Figure 4.3 IL-2 secretion from Jurkat E6.1 T cells and PBMC after activation with PHA-L or anti-CD3/anti-CD28. Jurkat E6.1 T cells were cultured in complete RPMI medium. PBMC were isolated from healthy volunteers. a) Jurkat E6.1 T cells (1 x 10^6 cells/mL) were stimulated with 0 to 10 µg/mL of PHA-L and incubated at 37^0 C for 24, 48 or 72 hours. b) Jurkat E6.1 T cells (1 x 10^6 cells/mL) were stimulated with 0 to 5 µg/mL of anti-CD3 antibody, followed by incubation with anti-CD28 antibody (2 µg/mL) and incubated at 37^0 C for 24, 48 or 72 hours. c) PBMC (5 x 10^5 cells/mL) were stimulated with 0 to 5 µg/mL of PHA-L or anti-CD3 antibody, followed by incubation with anti-CD28 antibody (2 µg/mL) and incubated at 37^0 C for 24 hours. d) PBMC (5 x 10^5 cells/mL) were stimulated with 0 to 5 µg/mL of anti-CD3 antibody, followed by incubation with anti-CD28 antibody (2 µg/mL) and incubated at 37^0 C for 24, 48 or 72 hours. Supernatants from each tested condition were collected after the incubation time and the levels of IL-2 determined using an IL-2 ELISA kit (Peprotech EC Ltd., London, UK). Mean values are shown with SEM. The values are the results from three independent experiments with Jurkat E6.1 T cells and two independent experiments with PBMC. ANOVA followed by Tukey's multiple comparison test were performed and the significant differences are identified in tables 4.1 and 4.2.

Table 4.1 Resume of statistical significance obtained for Figure 4.3a. Statistical significance was defined as * *p*-value < 0.05; ** *p*-value < 0.01; *** *p*-value < 0.001.

Significance		
*	**	***
1 µg/mL vs 10 µg/mL (48h) 24h vs 48h (10 µg/mL)	0.5 µg/mL vs 10 µg/mL (48h)	2 µg/mL vs 10 µg/mL (48h)

Table 4.2 Resume of statistical significance obtained for Figure 4.3b. Statistical significance was defined as * *p*-value < 0.05; ** *p*-value < 0.01; *** *p*-value < 0.001; **** *p*-value < 0.0001.

Significance			
*	**	***	****
0.1 µg/mL vs 5 µg/mL (24h) 1 µg/mL vs 2 µg/mL (72h)	0 µg/mL vs 2 µg/mL (72h)	0.1 µg/mL vs 2 µg/mL (24h) 0.1 µg/mL vs 2 µg/mL (48h) 0.5 µg/mL vs 2 µg/mL (48h) 0.5 µg/mL vs 2 µg/mL (72h)	0 µg/mL vs 5 µg/mL (48h) 0.1 µg/mL vs 5 µg/mL (48h) 0.5 µg/mL vs 5 µg/mL (48h) 1 µg/mL vs 5 µg/mL (48h) 2 µg/mL vs 5 µg/mL (48h) 0.1 µg/mL vs 2 µg/mL (72h) 0 µg/mL vs 5 µg/mL (72h) 0.1 µg/mL vs 5 µg/mL (72h) 0.5 µg/mL vs 5 µg/mL (72h) 1 µg/mL vs 5 µg/mL (72h) 48h vs 72h (5 µg/mL)

The levels of CD25 expressed at the surface of PBMC were analysed by flow cytometry after T cell activation. As previously observed in figure 4.3c, the activation of T cells within the PBMC population with antibodies against CD3 and CD28 was more effective than the use of PHA-L (Figure 4.4a). When testing different concentrations of anti-CD3 antibodies and increased incubation times for the activation of T cells there was a trend to increased levels of CD25 expressed at the surface of CD4 T cells when incubating the cells with 1 and 5 µg/mL of anti-CD3 antibody in combination with anti-CD28 antibody. Even though there seemed to be an increase in the CD25 expressed by these cells when incubation with anti-CD3 antibody was performed for 24 or 48 hours, a longer incubation of 72 hours did not seem to have such a pronounced effect (Figure 4.4b). As this data results from only one experiment, interpretation has to be carefully made. However, these observations support those in the literature [420], that activation of T cells within PBMC population with antibodies against CD3 and CD28 results in increased levels of CD25 expressed at the surface of CD4 T cells.

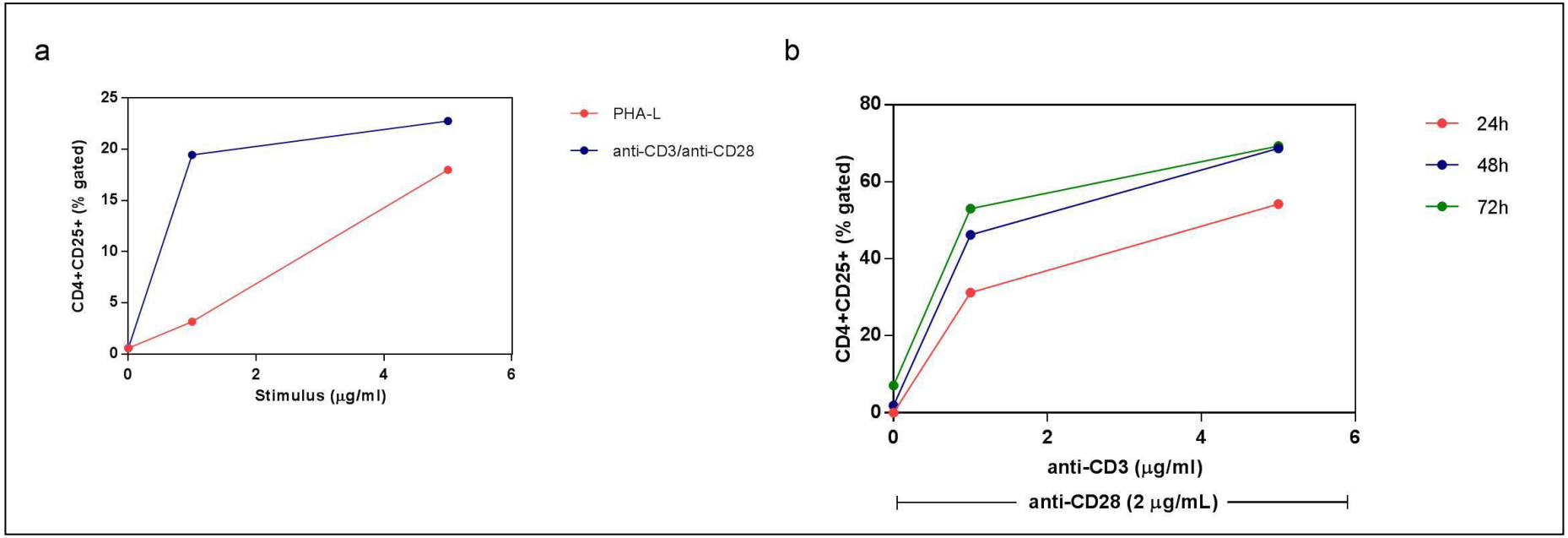

Figure 4.4 $CD4^+CD25^+$ T cells on the PBMC population after activation with PHA-L or anti-CD3/anti-CD28. PBMC were isolated from healthy volunteers. a) PBMC (5 x 10^5 cells/mL) were stimulated with 0 to 5 µg/mL of PHA-L or anti-CD3 antibody, followed by incubation with anti-CD28 antibody (2 µg/mL) and incubated at 37^0 C for 24 hours. b) PBMC (5 x 10^5 cells/mL) were stimulated with 0 to 5 µg/mL of anti-CD3 antibody, followed by incubation with anti-CD28 antibody (2 µg/mL) and incubated at 37^0 C for 24, 48 or 72 hours. One hundred thousand PBMC were used in combination with anti-CD4-PE and anti-CD25-APC conjugated antibodies on a Beckman Coulter flow cytometer. The values are the result from one experiment performed in triplicate.

The results presented so far in this chapter confirm that, in the conditions used here, both Jurkat E 6.1 T cells and T cells within the PBMC population can be activated with PHA-L and with the antibodies against CD3 and CD28. These results also show that activation by anti-CD3/anti-CD28 antibodies is more effective in the activation of T cells, in particular when using PBMC as a T cell source. Therefore, further studies on the effects of PAD enzymes in the activation of T cells were performed using PBMC activated with anti-CD3 and anti-CD28 antibodies.

4.4.2. Functional effects of peptidylarginine deiminase enzymes on T cell activation

Isolated PBMC were pre-treated with two isoforms of PAD, hPAD2 and hPAD4, enzymes followed by activation with the combination of anti-CD3/anti-CD28 antibodies, and then they were analysed for T cell activation indicators (IL-2 secretion and CD25 expression) and also cell viability. Different amounts of the PAD enzymes were tested (125, 250, 500 and 1000 mU). Furthermore, in order to investigate whether any activation could be attributed to non-enzyme contaminants, a control where PAD enzymes had been HI beforehand was also included.

As previously, cell viability was investigated as a measure of the toxic effect of the treatment in use. After incubation with PAD enzymes and activation by anti-CD3/anti-CD28 antibodies, PBMC viability was not altered in any of the tested conditions (Figure 4.5).

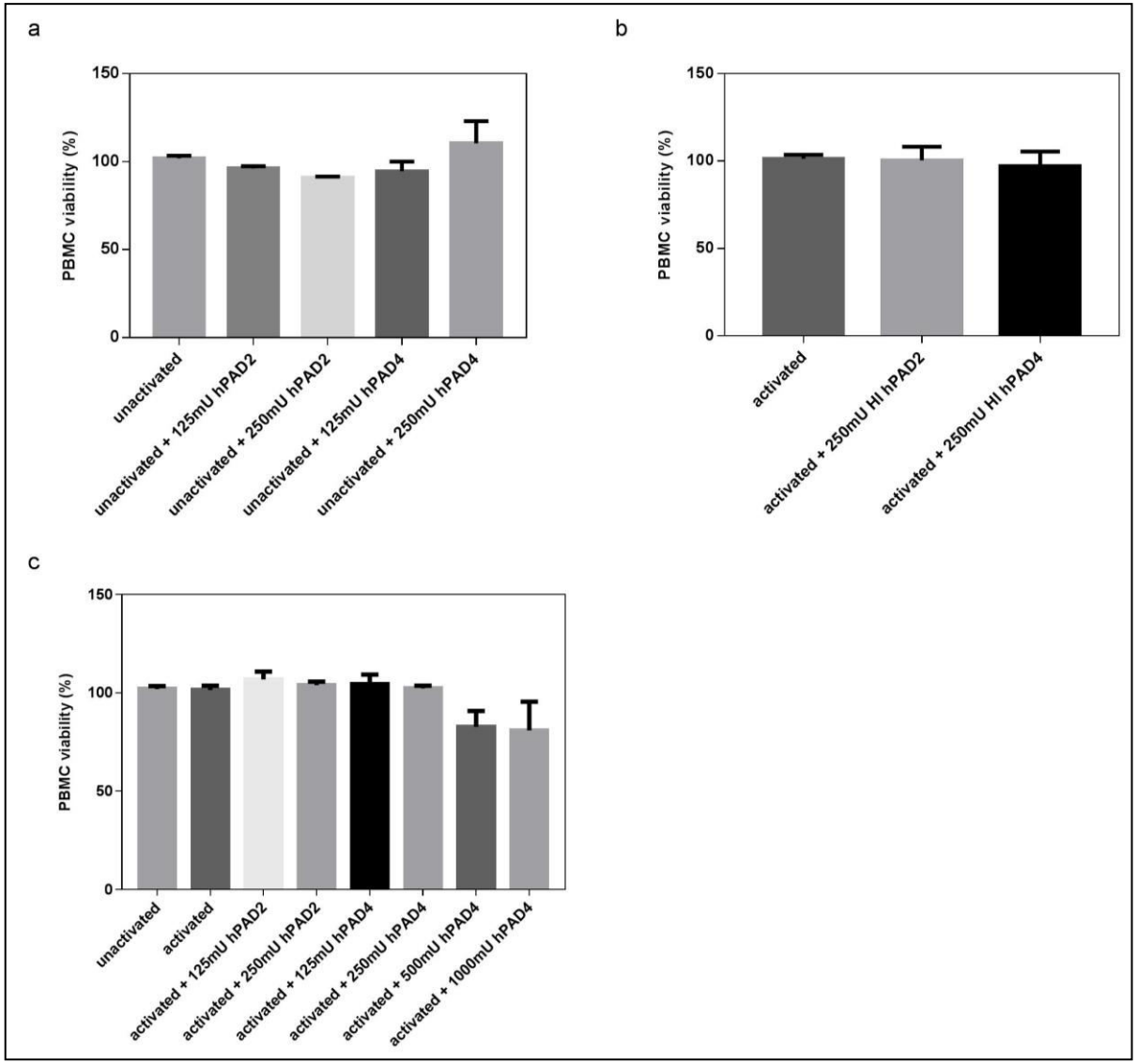
a
PBMC viability (%)
150
100
50
0
unactivated
unactivated + 125mU hPAD2
unactivated + 250mU hPAD2
unactivated + 125mU hPAD4
unactivated + 250mU hPAD4
b
PBMC viability (%)
150
100
50
0
activated
activated + 250mU HI hPAD2
activated + 250mU HI hPAD4
c
PBMC viability (%)
150
100
50
0
unactivated
activated
activated + 125mU hPAD2
activated + 250mU hPAD2
activated + 125mU hPAD4
activated + 250mU hPAD4
activated + 500mU hPAD4
activated + 1000mU hPAD4

Figure 4.5 Effects of PAD enzymes on PBMC viability after activation with anti-CD3/anti-CD28 antibodies. PBMC were isolated from healthy volunteers and seeded at a density of 5 x 10^5 cells/mL. Five hundred thousand cells/mL were incubated with PAD enzymes (2 hours at 37^0 C), followed by activation with 1 µg/mL anti-CD3 antibody and 2 µg/mL anti-CD28 antibody for 24 hours at 37^0 C. a) Control with PAD enzymes treatment but no activation. b) Control with HI PAD enzymes. c) PBMC incubated with increasing amounts (0, 125, 250, 500, 1000 mU) of PAD enzymes. Cell viability was assessed using the CellTiter-Blue® cell viability assay (Promega Co., Southampton, UK) considering non-treated PBMC as a reference control (100%). Mean values are shown with SEM. The values are the results from two independent experiments with HI PAD enzymes and 500 and 1000 mU hPAD4 enzyme and at least three independent experiments for the other conditions. Kruskal-Wallis test followed by Dunn's multiple comparison test were performed and revealed no statistical significance.

In accordance with previous data, the activation of T cells within the PBMC population with anti-CD3/anti-CD28 antibodies resulted in a significant increase in the IL-2 levels secreted by these cells (Figure 4.6a). The treatment of PBMC with PAD enzymes without further activation did not induce changes in the levels of IL-2 secreted into the supernatant (Figure 4.6a). When PBMC were incubated with active hPAD2 and hPAD4 enzymes prior to activation with antibodies against CD3 and CD28, the levels of IL-2 secreted by these cells decreased significantly more than 50% (Figure 4.6b). In particular, when PBMC were pre-treated with 125mU and 250 mU of hPAD2 and hPAD4 enzymes before being activated with anti-CD3/anti-CD28 antibodies, the levels of IL-2 secreted into the supernatant decreased by about 50% from 1.4 ± 0.06 ng/mL to 0.66 ± 0.03 ng/mL and 0.067 ± 0.04 ng/mL, respectively. Empirically, 23 – 138 mU of PAD enzymes would be necessary to citrullinate MP from PBMC isolated from 20 mL of whole blood, so 250 mU was the amount of PAD enzyme selected to be used in further studies. Due to the high amount of endotoxin detected on the PAD enzyme solutions (result in chapter 3), it was important to assess whether the effects induced by hPAD2 and hPAD4 enzymes were due to enzymatic or endotoxin activity. HI enzymes were used to test the effects of non-enzymatic contaminants, such as endotoxin, on the activation of T cells within the PBMC population with antibodies against CD3/CD28. In figure 4.6c it is possible to observe that the heat inactivation of PAD enzymes did not significantly alter the secretion of IL-2 by activated PBMC. Moreover, the secretion of IL-2 by PBMC was significantly decreased in PBMC pre-treated with hPAD2 and hPAD4 enzymes prior to activation when compared to pre-

treatment with HI PAD enzymes. These facts suggest that the decrease in the IL-2 levels secreted by activated PBMC is due to the enzymatic activity of PAD enzymes and not other non-enzymatic contaminants such as LPS.

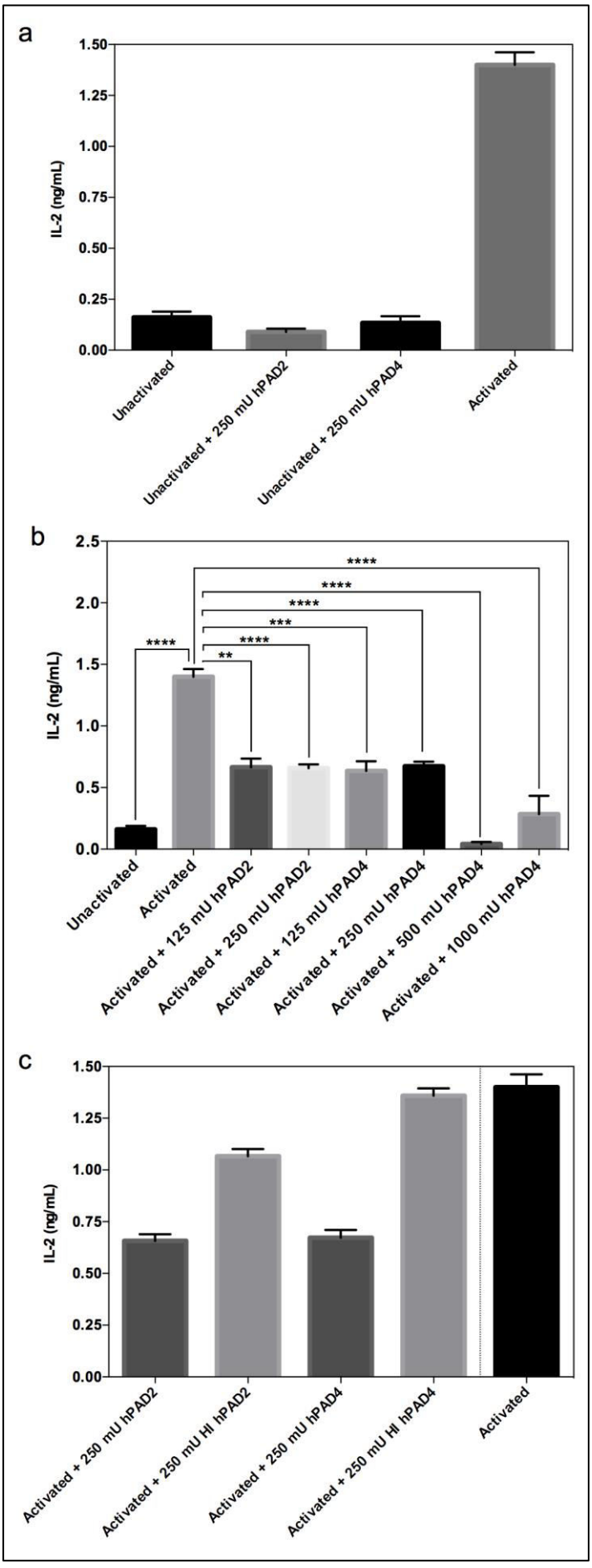
a
IL-2 (ng/mL)
1.50
1.25
1.00
0.75
0.50
0.25
0.00
Unactivated
Unactivated + 250 mU hPAD2
Unactivated + 250 mU hPAD4
Activated
b
IL-2 (ng/mL)
2.5
2.0
1.5
1.0
0.5
0.0
****
****
****
***
****
**
Unactivated
Activated
Activated + 125 mU hPAD2
Activated + 250 mU hPAD2
Activated + 125 mU hPAD4
Activated + 250 mU hPAD4
Activated + 500 mU hPAD4
Activated + 1000 mU hPAD4
c
IL-2 (ng/mL)
1.50
1.25
1.00
0.75
0.50
0.25
0.00
Activated + 250 mU hPAD2
Activated + 250 mU HI hPAD2
Activated + 250 mU hPAD4
Activated + 250 mU HI hPAD4
Activated

Figure 4.6 Effects of PAD enzymes on the secretion of IL-2 by PBMC after activation with anti-CD3/anti-CD28 antibodies. PBMC were isolated from healthy volunteers. Five hundred thousand cells/mL were pre-incubated with PAD enzymes (2 hours at 37^0 C), followed by activation with 1 µg/mL anti-CD3 antibody and 2 µg/mL anti-CD28 antibody for 24 hours at 37^0 C. a) PAD enzymes treatment on PBMC. b) PBMC incubated with increasing amounts (0, 125, 250, 500 and 1000 mU) of PAD enzymes. c) HI PAD enzymes treatment on PBMC followed by activation. Supernatants from each tested condition were collected after the incubation time and the levels of IL-2 determined using an IL-2 ELISA kit (Peprotech EC Ltd., London, UK). Mean values are shown with SEM. The values are the results from two independent experiments for a) and c) and at least three independent experiments for b). Kruskal-Wallis test followed by Dunn's multiple comparison test were performed. Statistical significance was defined as: ** *p*-value < 0.01, *** *p*-value < 0.001, **** *p*-value < 0.0001.

The effects of PAD enzymes on the expression of CD25 at the surface of $CD4^+$ PBMC was also assessed. In line with the IL-2 data presented above, the median fluorescence intensity (MFI) of expression of CD25 at the surface of $CD4^+$ PBMC was increased in 2 out of 3 donor cell populations after the cells have been activated with anti-CD3/anti-CD28 antibodies (Figures 4.7a and 4.7c). In addition to this, the number of $CD4^+$ T cells expressing CD25 significantly increased on activation (Figure 4.7b). When PBMC from four independent donors were pre-treated with PAD enzymes prior to activation, the effect of activation to increase the percentage of positive cells was lost and no significant differences were observed in the expression of CD25 after anti-CD3/anti-CD28 activation (Figures 4.7b and 4.7d).

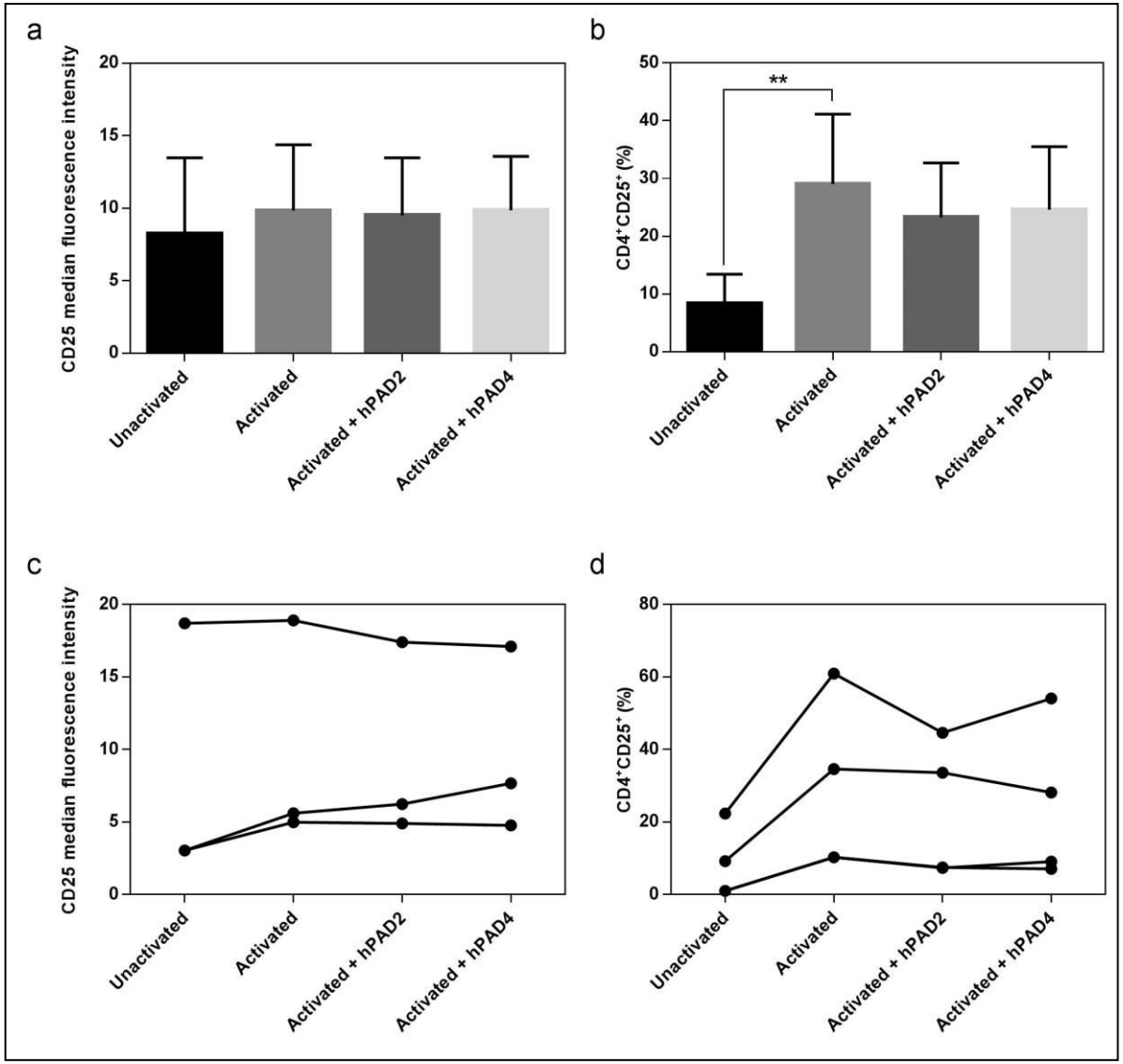
a
CD25 median fluorescence intensity
0
5
10
15
20
Unactivated
Activated
Activated + hPAD2
Activated + hPAD4
b
CD4+CD25+ (%)
0
10
20
30
40
50
**
Unactivated
Activated
Activated + hPAD2
Activated + hPAD4
c
CD25 median fluorescence intensity
0
5
10
15
20
Unactivated
Activated
Activated + hPAD2
Activated + hPAD4
d
CD4+CD25+ (%)
0
20
40
60
80
Unactivated
Activated
Activated + hPAD2
Activated + hPAD4

Figure 4.7 Effects of PAD enzymes on the expression of CD25 on $CD4^+$ T cells within the PBMC population after activation with anti-CD3/anti-CD28 antibodies. PBMC were isolated from healthy volunteers. Five hundred thousand cells/mL were pre-incubated with 250 mU PAD enzymes (2 hours at 37^0 C), followed by activation with 1 µg/mL anti-CD3 antibody and 2 µg/mL anti-CD28 antibody for 24 hours at 37^0 C. One hundred thousand PBMC were used in combination with anti-CD4-PE and anti-CD25-APC conjugated antibodies on a Beckman Coulter flow cytometer. a) CD25 MFI. b) Percentage of $CD4^+$ T cells expressing CD25 at the surface. c) CD25 MFI for the three independent experiments performed. b) Individual values for the percentage of $CD4^+$ T cells expressing CD25 at the surface for the four independent experiments performed. Friedman test followed by Dunn's multiple comparison test were performed. Statistical significance was defined as: ** p-value < 0.01.

These results suggest that PAD enzyme modification prior to activation may affect the IL-2 response observed from activated T cells within the PBMC population.

4.4.3. Effects of peptidylarginine deiminase enzymes on the levels of L-lactate on activated T cells

T cells rely on metabolic changes to fulfil the energy requirements essential for T cell proliferation [82, 414]. Lactate is an important by-product of aerobic glycolysis. In order to ascertain whether pre-treatment with PAD enzymes affected the PBMC metabolic switch after activation, the levels of extracellular lactate were assessed on supernatants collected from PBMC pre-treated with PAD enzymes and then activated for 24 hours. The activation of T cells in the PBMC population led to a decrease in the secretion of lactate to the supernatant. When PBMC were pre-treated with hPAD2 enzyme prior to activation, the levels of lactate resemble the levels of lactate on unactivated cells. The treatment of PBMC with hPAD4 enzyme prior to activation of T cells did not show significant alterations in lactate accumulation compared to unactivated cells (Figure 4.8).

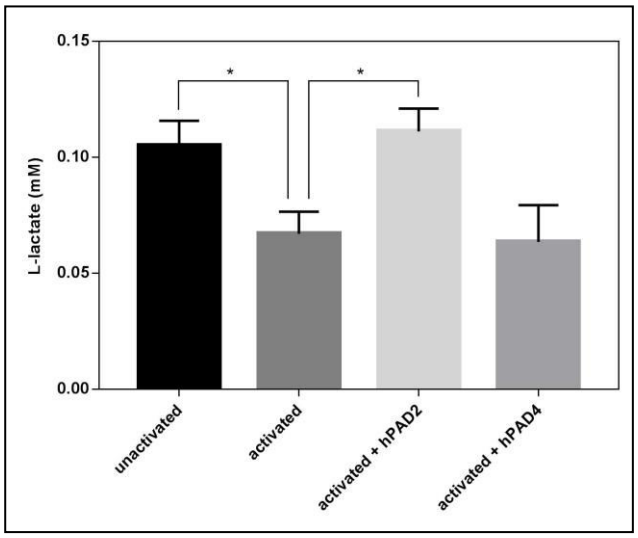

Figure 4.8 Effects of PAD enzymes on L-lactate levels on the supernatant of PBMC after activation with anti-CD3/anti-CD28 antibodies. PBMC were isolated from healthy volunteers. Five hundred thousand cells/mL were incubated with 250 mU PAD enzymes (2 hours at 37^0 C), followed by activation with antibodies against CD3 and CD28 at 37^0 C for 24 hours. The concentration of anti-CD3 antibody was 1 µg/mL and the concentration of anti-CD28 antibody was 2 µg/mL. Supernatants from each tested condition were collected after the incubation time and the levels of L-lactate determined using a L-lactate assay kit (Abcam plc., Cambridge, UK). Mean values are shown with SEM. The values are the results from three independent experiments. Kruskal-Wallis test followed by Dunn's multiple comparison test were performed. Statistical significance was defined as: * *p*-value < 0.05.

4.4.4. Effects of peptidylarginine deiminase enzymes on gene expression of activated T cells

The previous data has shown that T cell activation and metabolism are affected by pre-incubation with PAD enzymes. In order to provide insight into the mechanisms by which extracellular protein modifications can influence downstream intracellular pathways, gene expression array analysis was undertaken.

Genes with altered expression subsequent to citrullination of PBMC constitute a good indicator of signalling pathways affected by PAD enzymes. To investigate this, total RNA, including mRNA and micro RNA (miRNA), was isolated from PBMC pre-treated with and without PAD enzymes and activated with anti-CD3/anti-CD28 antibodies and analysed by microarray technology. By using this technology, thousands of target genes are analysed at the same time within different samples, producing complex and extend sets of data, which can be analysed by specific software to indicate key pathways that are affected by treatment with PAD enzymes.

GeneSpring GX software (Agilent Technologies LDA UK Ltd., Stockport, UK) was used to analyse the data produced by microarray and generate heat maps of entities determined to have a *p*-value less or equal to 0.05 and a fold change higher than 2 between activated cells and the remaining conditions. Clustering analysis was applied to organise genes and conditions in the dataset into clusters based on the similarity of their expression profiles. The three replicates of unactivated PBMC clustered together in one of the branches of the clustering tree, while all the activated replicates (pre-treated with PAD enzymes or not) clustered on a different branch. In terms of the PAD enzyme and activation treatments, the gene expression profile seemed to depend more on the replicate (donor) rather than on the treatment (Figure 4.9).

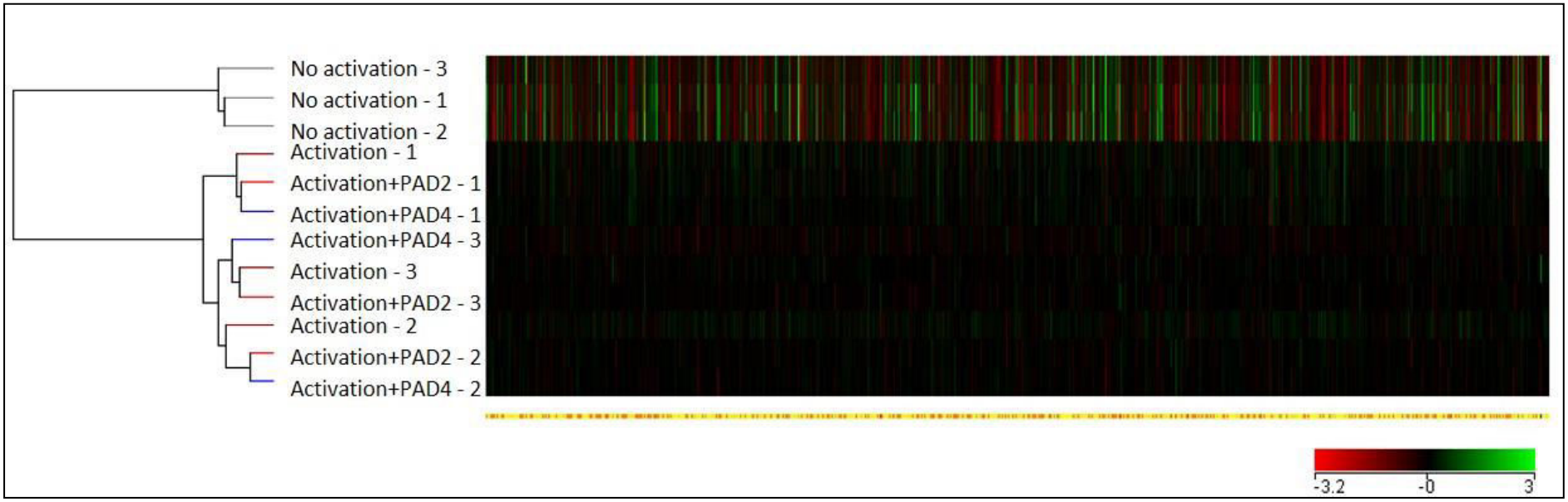

Figure 4.9 Clustered gene expression data of the effects of PAD enzymes on activated PBMC. PBMC were isolated from three healthy volunteers. Five hundred thousand cells/mL were pre-incubated with 250 mU PAD enzymes (2 hours at 37^0 C), washed and followed by activation with antibodies against CD3 and CD28 at 37°C for 24 hours. The concentration of anti-CD3 antibody was 1 µg/mL and the concentration of anti-CD28 antibody was 2 µg/mL. Following activation, mRNA was extracted using the miRNA micro kit (Qiagen Ltd., Manchester, UK) and the gene expression of three independent experiments analysed by microarray. Green and red indicate a positive and a negative log ratio, respectively. Clustering was carried out using a hierarchical algorithm. Tree diagrams group similar vectors into nodes; the height of each node indicates the overall similarity of its members.

When analysing the microarray data, activated PBMC were selected as the reference condition against which the effects of pre-incubation with PAD enzymes were compared. From this analysis, 1431 genes were detected as having increased expression on unactivated PBMC, whereas 2497 genes were identified as having decreased expression on unactivated PBMC. On PBMC pre-treated with hPAD2 enzyme prior to activation, 39 genes were identified as up-regulated and 78 as down-regulated. The treatment of PBMC with hPAD4 enzyme prior to activation led to the identification of 58 genes with up-regulated expression and 94 genes with down-regulated expression. To narrow the dataset results, Venn diagrams were applied in order to identify the genes similarly up- or down-regulated by the two PAD enzymes. Eight genes were identified as having their expression increased by both hPAD2 and hPAD4 enzymes (Figure 4.10a), while thirty-five genes were identified as down-regulated by the two enzymes (Figure 4.11a). Figures 4.10b and 4.11b represent the heat maps of the eight and thirty-five entities determined to be up- or down-regulated, respectively, by hPAD2 and hPAD4 enzymes, when compared with activated PBMC.

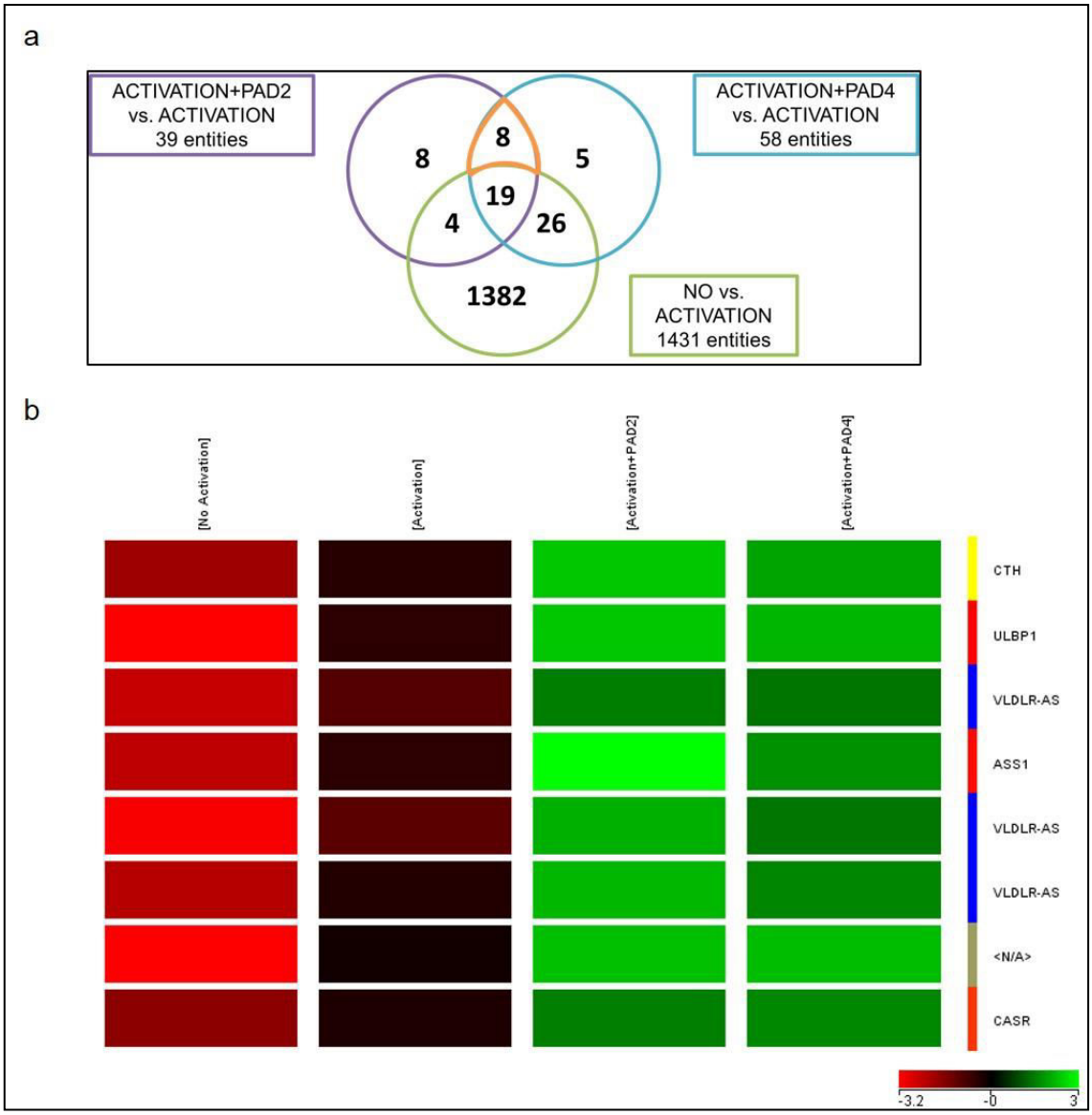

Figure 4.10 Up-regulated genes by hPAD2 and hPAD4 enzymes on activated PBMC. PBMC were isolated from three healthy volunteers. Five hundred thousand cells/mL were pre-treated with 250 mU of hPAD2 or hPAD4 enzymes, for 2 hours at 37^0 C, and then stimulated with antibodies against CD3 and CD28 at 37^0 C for 24 hours. The concentration of anti-CD3 antibody was 1 µg/mL and the concentration of anti-CD28 antibody was 2 µg/mL. Following activation, mRNA was extracted using the miRNeasy micro kit (Qiagen Ltd., Manchester, UK) and the gene expression of three independent experiments analysed by microarray using an Agilent DNA microarray scanner. Data was analysed using GeneSpring GX software (Agilent Technologies Inc.). Shift to 75.0 percentile was used as normalisation and median of all samples was applied as baseline transformation. a) Venn diagrams were used to identify the genes up-regulated by both hPAD2 and hPAD4 enzymes. b) Heat map of the eight up-regulated genes by hPAD2 and hPAD4 enzymes. Green and red indicate a positive and a negative log ratio, respectively.

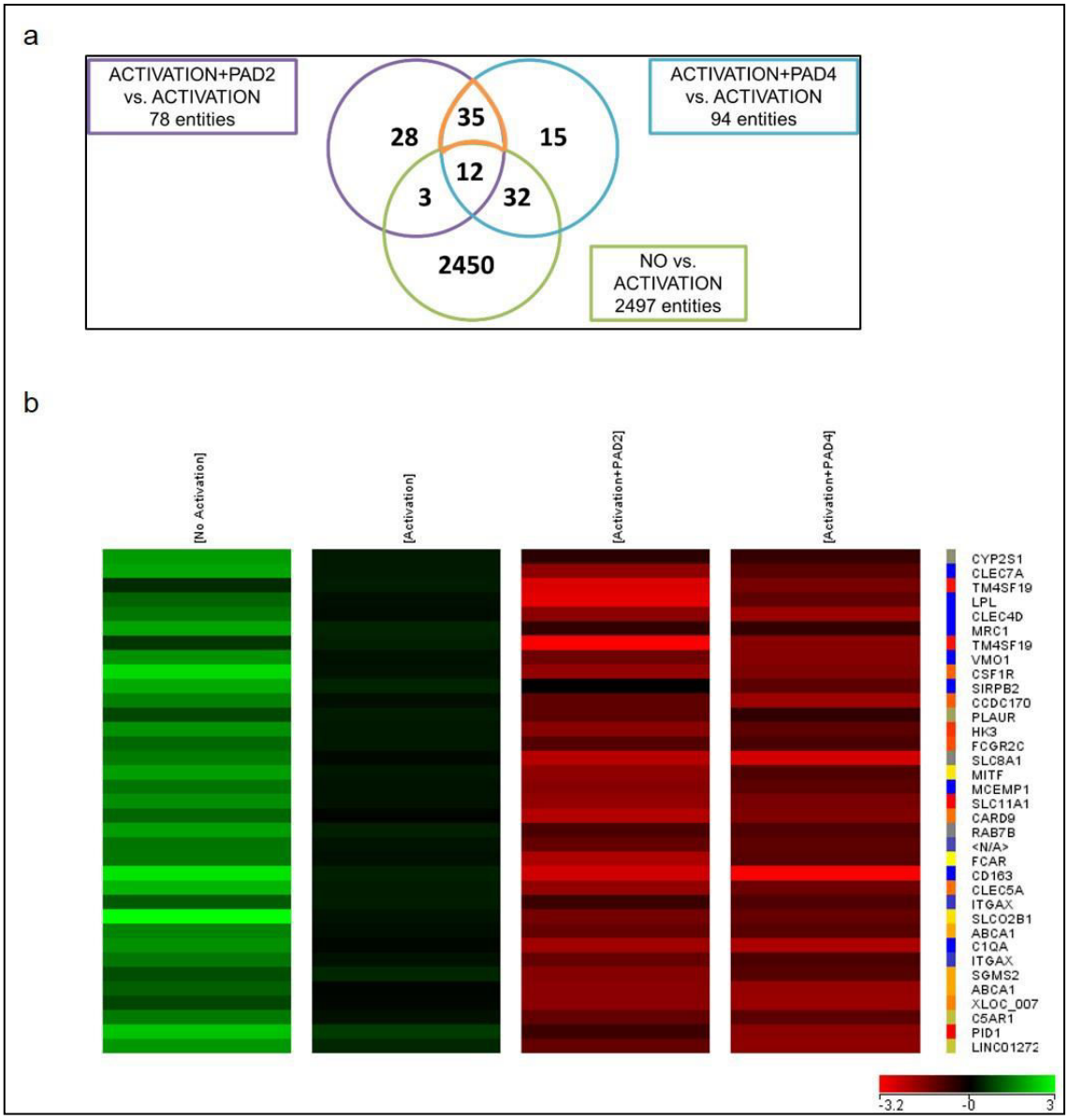

Figure 4.11 Down-regulated genes by hPAD2 and hPAD4 enzymes on activated PBMC. PBMC were isolated from three healthy volunteers. Five hundred thousand cells/mL were pre-treated with 250 mU of hPAD2 or hPAD4 enzymes, for 2 hours at 37^0 C, and stimulated with antibodies against CD3 and CD28 at 37^0 C for 24 hours. The concentration of anti-CD3 antibody was 1 µg/mL and the concentration of anti-CD28 antibody was 2 µg/mL. Following activation, mRNA was extracted using the miRNeasy micro kit (Qiagen Ltd., Manchester, UK) and the gene expression of three independent experiments analysed by microarray using an Agilent DNA microarray scanner. Data was analysed using GeneSpring GX software (Agilent Technologies LDA UK Ltd., Stockport, UK). Shift to 75.0 percentile was used as normalisation and median of all samples was applied as baseline transformation. a) Venn diagrams were used to identify the genes down-regulated by both hPAD2 and hPAD4 enzymes. b) Heat map of the thirty-five down-regulated genes by hPAD2 and hPAD4 enzymes. Green and red indicate a positive and a negative log ratio, respectively.

To understand what intracellular pathways may be affected by the PAD enzyme treatment of PBMC prior to activation, gene ontology (GO) analysis was performed. Pathways with a *p*-value equal or lower than 0.05 and more than one identified entity

were considered. Of particular interest, pathways involved in metabolism of amino acids and proteins and immune regulation between lymphoid and non-lymphoid were identified as being up-regulated by PAD enzymes in PBMC prior to activation (Table 4.5). The relevant pathways found to be down-regulated on PBMC by PAD enzymes prior to activation were associated with the complement system activation, lipid and glucose metabolism and the clot cascade (Table 4.6).

Table 4.3 Gene ontology analysis of pathways associated with genes up-regulated by hPAD2 and hPAD4 enzymes on PBMC prior to activation.

Pathway	*p*-value	Matched Entities	Pathway Entities of Experiment Type
Hs_Metabolism_of_amino_acids_and_derivatives_WP2693_76898	3,8E-03	2	184
Hs_Trans-sulfuration_pathway_WP2333_72015	0.0016	1	10
Hs_Alanine_and_aspartate_metabolism_WP106_74147	0.0020	1	40
Hs_GPCRs,_Class_C_Metabotropic_glutamate,_pheromone_WP501_79715	0.0025	1	15
Hs_Urea_cycle_and_metabolism_of_amino_groups_WP497_72142	0.0033	1	37
Hs_Trans-sulfuration_and_one_carbon_metabolism_WP2525_78541	0.0051	1	31
Hs_Selenium_Metabolism_and_Selenoproteins_WP28_71888	0.0079	1	48
Hs_Vitamin_B12_Metabolism_WP1533_79884	0.0082	1	53
Hs_Folate_Metabolism_WP176_79883	0.0107	1	67
Hs_Immunoregulatory_interactions_between_a_Lymphoid_and_a_non-Lymphoid_cell_WP1829_76993	0.0126	1	292
Hs_Selenium_Micronutrient_Network_WP15_79870	0.0135	1	84
Hs_Gastrin-CREB_signalling_pathway_via_PKC_and_MAPK_WP2664_76844	0.0227	1	147

Table 4.4 Gene ontology analysis of pathways associated with genes down-regulated by hPAD2 and hPAD4 enzymes on PBMC prior to activation.

Pathway	*p*-value	Matched Entities	Pathway Entities of Experiment Type
Hs_Human_Complement_System_WP2806_78589	8,12E+01	3	136
Hs_Complement_and_Coagulation_Cascades_WP558_79680	1,71E+02	3	61
Hs_Statin_Pathway_WP430_78268	2,65E+03	2	31
Hs_Lipid_digestion,_mobilization,_and_transport_WP2764_77026	4,33E+03	2	41
Hs_Dissolution_of_Fibrin_Clot_WP1802_76989	0.0066	1	8
Hs_Vitamin_D_Receptor_Pathway_WP2877_79998	0.0099	2	186
Hs_SREBF_and_miR33_in_cholesterol_and_lipid_homeostasis_WP2011_75253	0.0131	1	18
Hs_miR-targeted_genes_in_adipocytes_-_TarBase_WP2001_78529	0.0139	1	38
Hs_Complement_Activation,_Classical_Pathway_WP545_72062	0.0139	1	17
Hs_Farnesoid_X_Receptor_Pathway_WP2879_79602	0.0156	1	19
Hs_Sphingolipid_Metabolism_WP1422_79871	0.0172	1	21
Hs_Transport_of_vitamins,_nucleosides,_and_related_molecules_WP1937_77048	0.0188	1	24
Hs_Triacylglyceride_Synthesis_WP325_71223	0.0196	1	24
Hs_Post-translational_modification-_synthesis_of_GPI-anchored_proteins_WP1887_80028	0.0204	1	26
Hs_Latent_infection_of_Homo_sapiens_with_Mycobacterium_tuberculosis_WP2700_76907	0.0237	1	62
Hs_Phase_1_-_Functionalization_of_compounds_WP1879_76834	0.0261	1	33
Hs_Nuclear_Receptors_in_Lipid_Metabolism_and_Toxicity_WP299_78587	0.0269	1	35
Hs_Fatty_Acid_Beta_Oxidation_WP143_79783	0.0277	1	34
Hs_Nucleotide-binding_domain,_leucine_rich_repeat_containing_receptor_(NLR)_signaling_pathways_WP2763_77025	0.0285	1	38
Hs_DAP12_interactions_WP2694_76901	0.0285	1	45
Hs_NOD_pathway_WP1433_80018	0.0333	1	41
Hs_Complement_cascade_WP1798_77042	0.0333	1	192
Hs_Vitamin_A_and_Carotenoid_Metabolism_WP716_79968	0.0341	1	43
Hs_Sphingolipid_metabolism_WP2788_77079	0.0365	1	46
Hs_Binding_and_Uptake_of_Ligands_by_Scavenger_Receptors_WP2784_77068	0.0373	1	195
Hs_Aryl_Hydrocarbon_Receptor_WP2586_79995	0.0381	1	48

Table 4.4 Continuation.

Pathway	*p*-value	Matched Entities	Pathway Entities of Experiment Type
Hs_Differentiation_Pathway_WP2848_80009	0.0389	1	50
Hs_Glycolysis_and_Gluconeogenesis_WP534_78585	0.0397	1	49
Hs_Vitamin_B12_Metabolism_WP1533_79884	0.0405	1	53
Hs_Transport_of_glucose_and_other_sugars,_bile_salts_and_organic_acids,_metal_ions_and_amine_compounds_WP1935_76949	0.0421	1	52
Hs_RANKL-RANK_Signaling_Pathway_WP2018_79959	0.0444	1	55
Hs_Extracellular_matrix_organization_WP2703_76914	0.0468	1	58
Hs_Kit_receptor_signaling_pathway_WP304_78799	0.0476	1	59
Hs_Oxidation_by_Cytochrome_P450_WP43_79993	0.0492	1	64
Hs_Integrin_cell_surface_interactions_WP1833_77019	0.0499	1	64

Based on function and localisation of the protein products, five of the forty-three identified genes were selected for further investigation. The genes with up-regulation selected for further analysis were *ASS1* (encodes for argininosuccinate synthase 1 – ASS1) and *CTH* (encodes for cystathionine γ-lyase – CTH) and the genes with down-regulation selected were *HK3* (encodes for hexokinase 3 – HK3), *CD163* (encodes for CD163 molecule) and *SGMS2* (encodes for sphingomyelin synthase 2 – SGMS2). The individual expression profile of these genes can be found in appendix 3. The expression of these selected genes was confirmed by RT-QPCR, since this is a more specific and accurate technique. When assessing gene expression by RT-QPCR, the experimental control previously used (unactivated PBMC treated with PAD enzymes but not activated) was also incorporated in the analysis. However, only one independent experiment was performed with the unactivated PBMC treated with hPAD2 enzyme.

In general, the C_T values obtained from RT-QPCR for the genes of interest and the housekeeper used were high which corresponds to low levels of gene expression (Tables 4.5 and 4.6). The biggest differences in C_T values were observed in the expression of *CTH*, however, the expression levels of this gene were very low, with average C_T values of 35.2 (Table 4.6) from one donor PBMC only. Expression could not be detected in PBMC from other volunteers.

Table 4.5 Raw C_T values of the housekeeper *18S* in the plate of each of the selected genes analysed by RT-QPCR. After PBMC treatment with PAD enzymes and activation with anti-CD3/anti-CD28 antibodies, the mRNA was extracted, converted into cDNA and used to evaluate the levels of *ASS1*, *CTH*, *HK3*, *CD163*, *SGMS2* transcripts by RT-QPCR in a Agilent Max3000P QPCR system (Agilent Technologies LDA UK Ltd, Stockport, UK). Raw C_T values are presented. N = number of independent experiments (healthy donors) performed.

	18S C_T values for each primer plate														
	ASS1 primer			*CTH* primer			*HK3* primer			*CD163* primer			*SGMS2* primer		
	Mean	SEM	N	Mean	SEM	N	Mean	SEM	N	Mean	SEM	N	Mean	SEM	N
Unactivated	15.45	1.28	3	13.18	0.89	3	14.04	0.61	3	13.77	0.71	3	13.31	0.72	3
Unactivated + hPAD2	16.27	0.08	1	21.66	3.08	1	16.51	0.14	1	16.02	0.08	1	15.86	0.16	1
Unactivated + hPAD4	18.5	1.37	2	15.35	0.45	1	15.98	0.50	2	15.75	0.38	2	15.48	0.47	2
Activated	17.43	1.55	3	14.45	1.81	2	14.79	0.98	3	14.46	1.00	3	13.75	1.12	3
Activated + hPAD2	15.23	2.13	2	14.7	2.11	2	13.12	0.71	2	12.84	0.81	2	12.45	0.84	2
Activated + hPAD4	16.94	1.88	3	14.83	0.30	3	15.19	0.27	3	15.18	0.42	2	14.70	0.39	3

Table 4.6 Raw C_T values of selected genes analysed by RT-QPCR. After PBMC treatment with PAD enzymes and activation with anti-CD3/anti-CD28 antibodies, the mRNA was extracted, converted into cDNA and used to evaluate the levels of *ASS1*, *CTH*, *HK3*, *CD163*, *SGMS2* transcripts by RT-QPCR in a Agilent Max3000P QPCR system (Agilent Technologies LDA UK Ltd, Stockport, UK). Raw C_T values are presented. * values higher than thirty-five were obtained, but these were not included for the data analysis. N = number of independent experiments (healthy donors) performed.

	C_T values														
	ASS1 primer			*CTH* primer			*HK3* primer			*CD163* primer			*SGMS2* primer		
	Mean	SEM	N	Mean	SEM	N	Mean	SEM	N	Mean	SEM	N	Mean	SEM	N
Unactivated	29.81	0.51	3	32.88	1.01	3*	28.42	0.33	3	27.87	0.57	3	30.04	0.44	3
Unactivated + hPAD2	31.48	0.41	1	37.75	2.20	1*	30.10	0.07	1	30.76	0.22	1	32.93	0.99	1
Unactivated + hPAD4	36.86	1.84	2*	41.89	1.58	1*	29.47	0.61	2	30.10	0.57	2	31.60	0.79	2
Activated	32.41	1.67	3*	31.20	1.85	2*	29.86	0.21	3	31.25	0.56	3	31.81	0.39	3
Activated + hPAD2	29.15	0.89	2	32.66	3.30	2*	29.80	0.77	2	31.17	1.18	2	32.65	1.06	2*
Activated + hPAD4	29.91	0.93	3	34.85	1.68	3*	29.96	0.49	3	30.19	0.44	2	32.87	0.87	3*

The expression of the selected genes in unactivated PBMC treated with PAD enzymes was compared within the different conditions using the comparative C_T method. In addition, the expression of each gene was compared within the same donor that was used for all the conditions to access the variability within the same individual. From these results it was possible to observe that the gene expression showed high variation. The treatment of unactivated PBMC with hPAD4 enzyme showed a trend to an increase in the expression of *ASS1* and *HK3* and a decrease in the expression of *CD163*. The expression of *SGMS2* showed no consistency between the treatment with hPAD2 and hPAD4 enzymes, being decreased with hPAD2 and increased with hPAD4 (Figure 4.12).

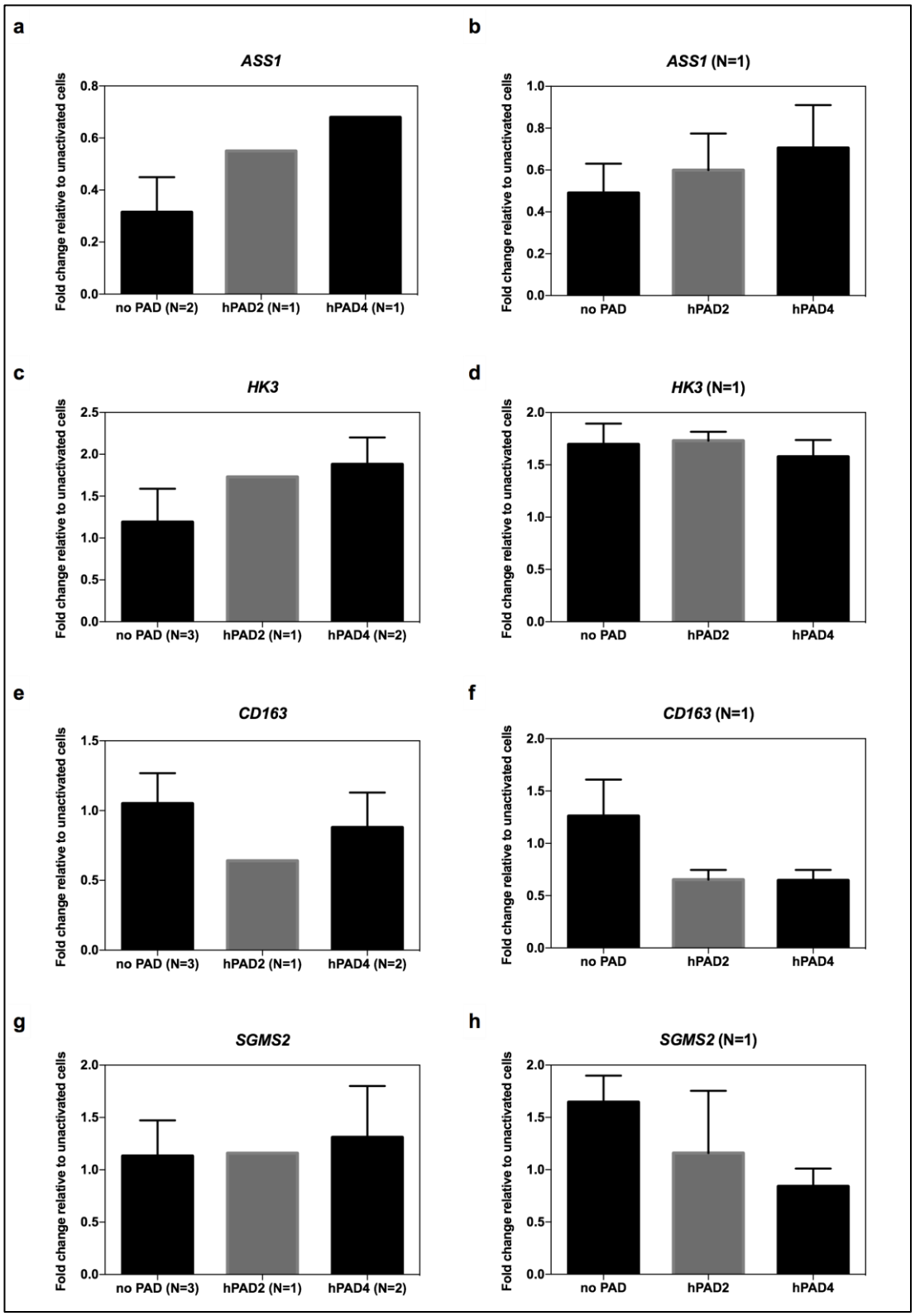

Figure 4.12 Effect of PAD enzymes in the expression of selected genes in unactivated PBMC. After PBMC treatment with PAD enzymes, the mRNA was extracted, converted into cDNA and used to evaluate the levels of *ASS1* (a, b), *HK3* (c, d), *CD163* (e, f), *SGMS2* (g, h) transcripts by RT-QPCR. Results were obtained with the comparative C_T method and are expressed as fold change relative to unactivated cells. Mean values are presented with SEM. The values are the result from the number of individual donors indicated, analysed in triplicate (Figures on the left). Same individual donor was analysed in triplicate to assess intra-assay variability (Figures on the right). One-way ANOVA followed by Tukey's multiple comparison test was performed and no statistical significant differences were found.

The activation of T cells within the PBMC population induced a decrease in the expression of *ASS1* and *CD163*, an increase in the expression of *HK3* and no differences in the expression of *SGMS2*. From one experiment only, *CTH* expression was increased after the activation of T cells with anti-CD3/anti-CD28 antibodies, in line with previous microarray experiments (Figure 4.13).

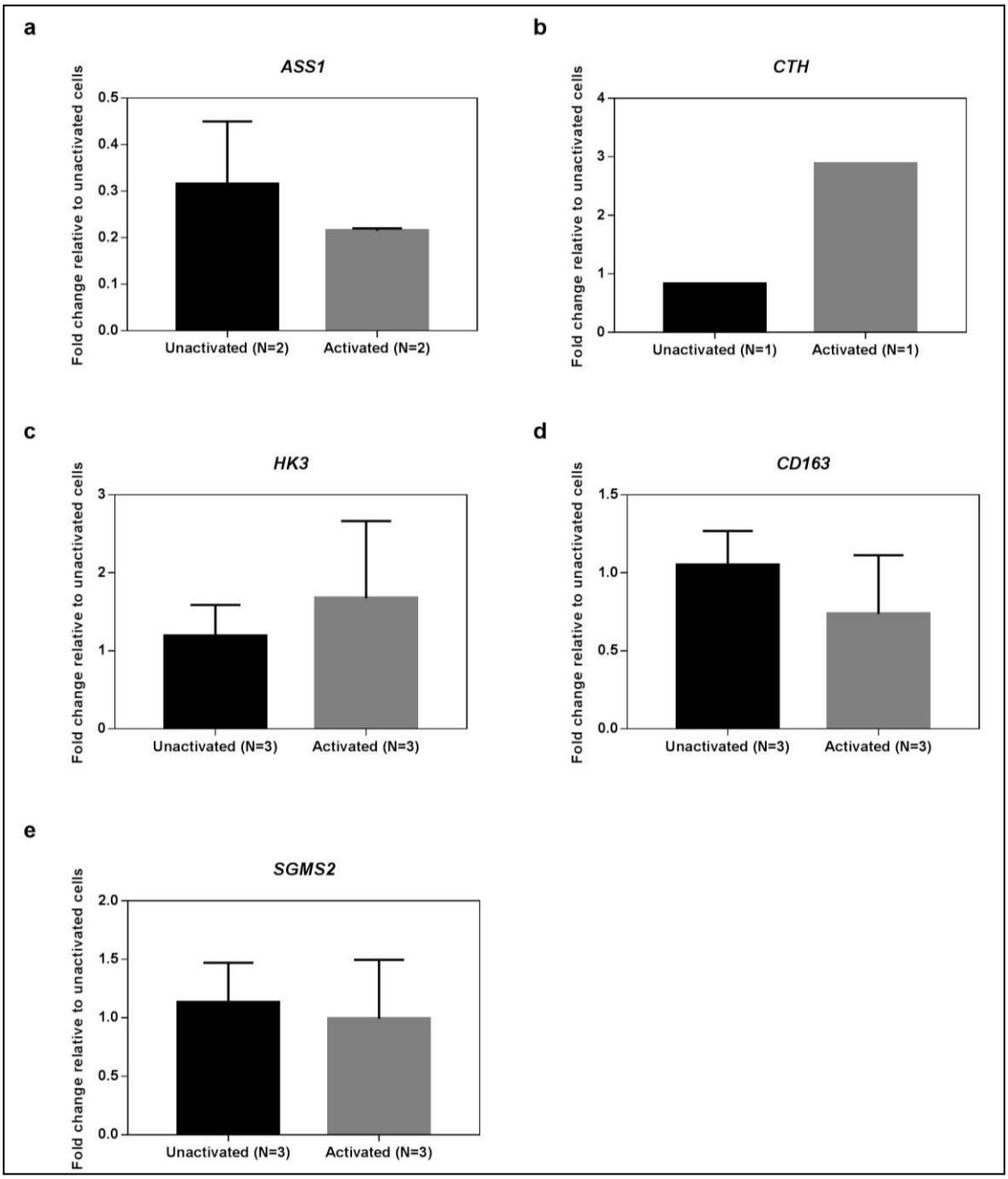

Figure 4.13 Fold changes in the expression of selected genes in activated PBMC. After PBMC treatment with PAD enzymes and activation with anti-CD3/anti-CD28 antibodies, the mRNA was extracted, converted into cDNA and used to evaluate the levels of *ASS1* (a), *CTH* (b), *HK3* (c), *CD163* (d), *SGMS2* (e) transcripts by RT-QPCR. Results were obtained with the comparative C_T method and are expressed as fold change relative to unactivated cells. Mean values are presented with SEM. The values are the result from the number of individual donors indicated, analysed in triplicate. Paired t-test was performed and no statistical significant differences were found.

When analysing the expression of the selected genes in PBMC pre-treated with PAD enzymes followed by activation with the anti-CD3/anti-CD28 antibodies, the level of variation in the results was again high, in particular in conditions where hPAD2 enzyme

was used (Figure 4.14). *ASS1* and *CTH* were the two genes selected after microarray analysis with increased expression in activated PBMC pre-treated with the two isoforms of PAD enzymes. When analysed by RT-QPCR, an increase in the expression of *ASS1* was observed in PBMC pre-treated with both PAD enzymes prior to activation, when compared with activated PBMC, which is not statistically significant (Figure 4.14a). An increase in the expression of *CTH* was also observed in PBMC pre-treated with both PAD enzymes prior to activation, when compared with activated PBMC. However, this resulted from the analysis of only one replicate data (Figure 4.14b). *HK3*, *CD163* and *SGMS2* were the selected genes for which down-regulation of expression was observed by microarray after PAD enzyme treatments. *HK3* expression was non-significantly decreased in PBMC pre-treated with PAD enzymes prior to activation when compared with activated PBMC (Figure 4.14c). The expression of *CD163* and *SGMS2* in PBMC prior to activation showed a trend to differential regulation by PAD enzymes, showing decreased levels with hPAD2 enzyme and increased levels with hPAD4 enzyme (Figure 4.14d and 4.14e). Overall, the effect of hPAD2 pre-treatment prior to activation was greater than hPAD4 pre-treatment.

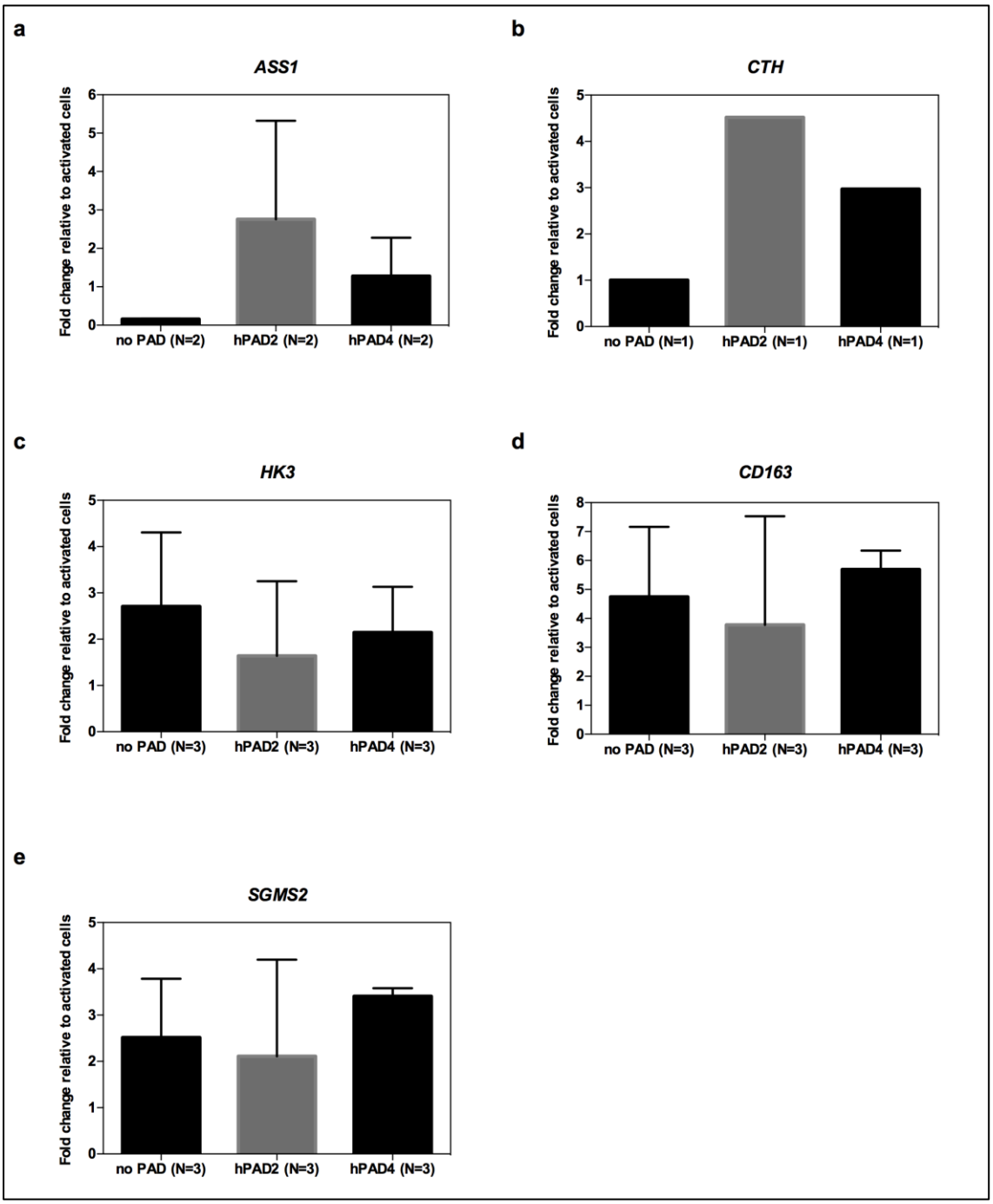

Figure 4.14 Effect of PAD enzymes in the expression of selected genes relative to activated PBMC. After PBMC treatment with PAD enzymes and activation with anti-CD3/anti-CD28 antibodies, the mRNA was extracted, converted into cDNA and used to evaluate the levels of *ASS1* (a), *CTH* (b), *HK3* (c), *CD163* (d), *SGMS2* (e) transcripts by RT-QPCR. Results were obtained with the comparative C_T method and are expressed as fold change relative to activated cells. Mean values are presented with SEM. The values are the result from the number of experiments indicated. One-way ANOVA followed by Tukey's multiple comparison test was performed and no statistical significant differences were found.

High variation in the expression levels of the selected genes was found in the RT-QPCR data. Individual donor variability and the use of the entire PBMC population are

possible explanations for this. For the study of these genes in clinical samples, in chapter 5, more samples will be analysed and the gene expression will be assessed in CD4 and CD8 T cell subsets instead of the total PBMC population.

4.4.5. Effects of peptidylarginine deiminase enzymes on cell surface proteins of PBMC after T cell activation

In order for PAD enzymes to exert any effects on activation pathways of T cells, modification of cell surface proteins or MP by citrullination is predicted. To investigate this, MP were extracted from unactivated PBMC, activated PBMC and activated PBMC pre-treated with PAD enzymes obtained from three healthy individuals, then they were pooled together and analysed by 2D BN/SDS-PAGE, as previously validated in chapter 3.

The gels of MP separated by 2D BN/SDS-PAGE from studied conditions were compared using the SameSpots (TotalLab ltd., Newcastle upon Tyne, UK) analysis software (Figure 4.15). “Activated PBMC” was the condition selected as reference and in figure 4.15a it is possible to observe two predominant spots in the right side of the gel with molecular weights in the region of 25–100 kDa. In the upper left region of all the gels, corresponding to proteins/complexes with lesser migration in the 1D BN-PAGE, a smear was visible, suggesting that high MW protein complexes were not completely separated or were not completely denatured to run accurately on the 2D BN/SDS-PAGE (Figure 4.15). Figures 4.15b–e represent the overlay between the reference gel (“activated PBMC”) and the other tested conditions. For all of them it is possible to observe some alterations in the two spots previously mentioned. However, the profile of the tested conditions was similar to the reference condition. Using the SameSpots (TotalLab ltd., Newcastle upon Tyne, UK) analysis software it was possible to compare the normalised intensity of particular spots in the different conditions tested. One hundred and fifty spots were identified by the software as having

normalised intensity with fold changes higher than two between the different conditions tested (Figure 4.16a). The large area of unresolved proteins at the top of the gel was excluded from the analysis as well as speckles and the borders of the gels. Comparison was then performed manually and nine spots were identified across the five conditions (Figure 4.16b). The top spot was divide into six smaller regions, identified by spots 260, 258, 249, 246, 247 and 250. The individual analysis of each spot did not show consistency between PAD treated and non-PAD treated conditions (Figures 4.17, 4.18 and 4.19). The bottom spot was divided into three smaller spots (242, 244 and 245) and the individual analysis of these revealed some difference between PAD-treated activated and non-PAD treated activated conditions for spots 244 and 245, where a decreased intensity was observed when PBMC were pre-treated with PAD enzymes (Figure 4.20). Spots 244 and 245 were then selected for identification by mass spectrometry.

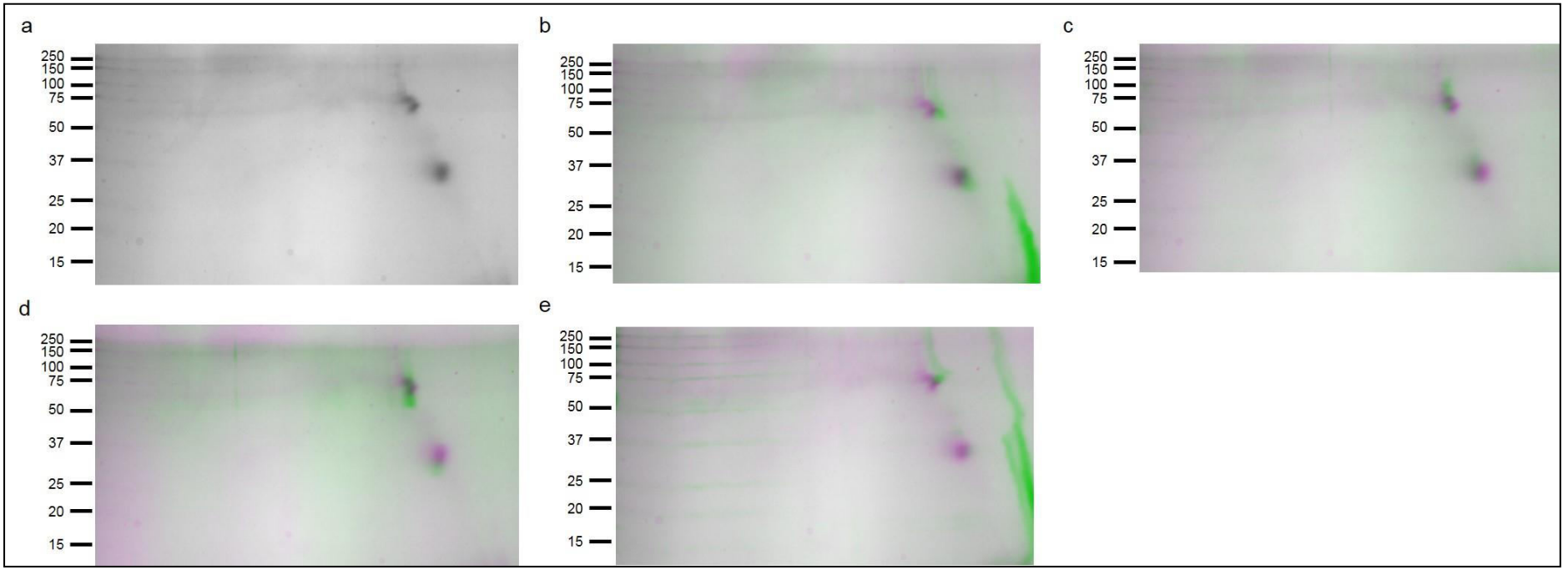

Figure 4.15 SameSpots software gels comparison from PBMC MP separation by 2D BN/SDS-PAGE. PBMC were isolated from healthy volunteers. Five hundred thousand cells/mL were incubated with 250 mU PAD enzymes (2 hours at 37^0 C), followed by activation with antibodies against CD3 (1 µg/mL) and CD28 (2 µg/mL) at 37°C for 24 hours. After, MP from three independent experiments were extracted using the Mem-PER Plus membrane protein extraction kit (Thermo Fisher Scientific Inc., Loughborough, UK) and pooled together. Twenty-five micrograms (25 µg) of MP were separated by 2D BN/SDS-PAGE in the presence of 0.625% (v/v) DDM. In the first dimension a NativePAGE™ Novex™ 4–16% Bis-Tris gel was used and in the second dimension, the 1D strip was separated in TGX Mini-PROTEAN® TGX™ 8–16% pre-cast gel. After separation, the gels stained with high sensitivity CBB G250 and analysed using SameSpots (TotalLab ltd., Newcastle upon Tyne, UK) software. Activated PBMC were used as the reference gel (a) and aligned with the unactivated PBMC gel (b), activated PBMC pre-treated with hPAD2 enzyme (c), activated PBMC pre-treated with hPAD4 enzyme (d) and unactivated PBMC treated with hPAD4 enzyme (e). Pink gel represents the reference gel (activated PBMC) and the green gel represents the comparison.

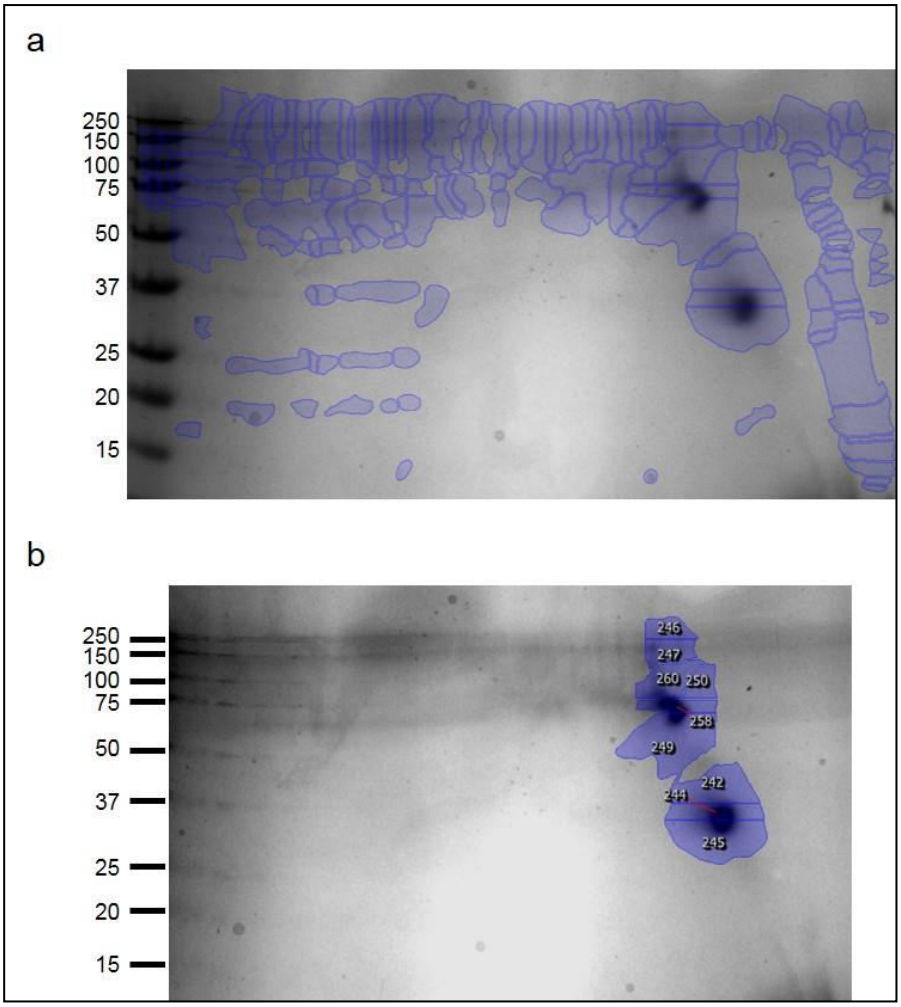

Figure 4.16 SameSpots software spots identification from PBMC MP separation by 2D BN/SDS-PAGE. After PBMC treatment with PAD enzymes and activation with anti-CD3/anti-CD28 antibodies, MP were extracted using the Mem-PER Plus membrane protein extraction kit (Thermo Fisher Scientific Inc., Loughborough, UK). Twenty-five micrograms (25 µg) of MP pooled together from three independent experiments were separated by 2D BN/SDS-PAGE in the presence of 0.625% (v/v) DDM. In the first dimension a NativePAGE™ Novex™ 4–16% Bis-Tris gel was used and in the second dimension, the 1D strip was separated in TGX Mini-PROTEAN® TGX™ 8–16% pre-cast gel. After separation, the gels stained with high sensitivity CBB G250 and analysed using SameSpots (TotalLab ltd., Newcastle upon Tyne, UK) software. Activated PBMC were used as the reference gel. (a) Initial spot detection by the SameSpots (TotalLab ltd., Newcastle upon Tyne, UK) software. (b) Spots manually selected for further investigation by visual analysis.

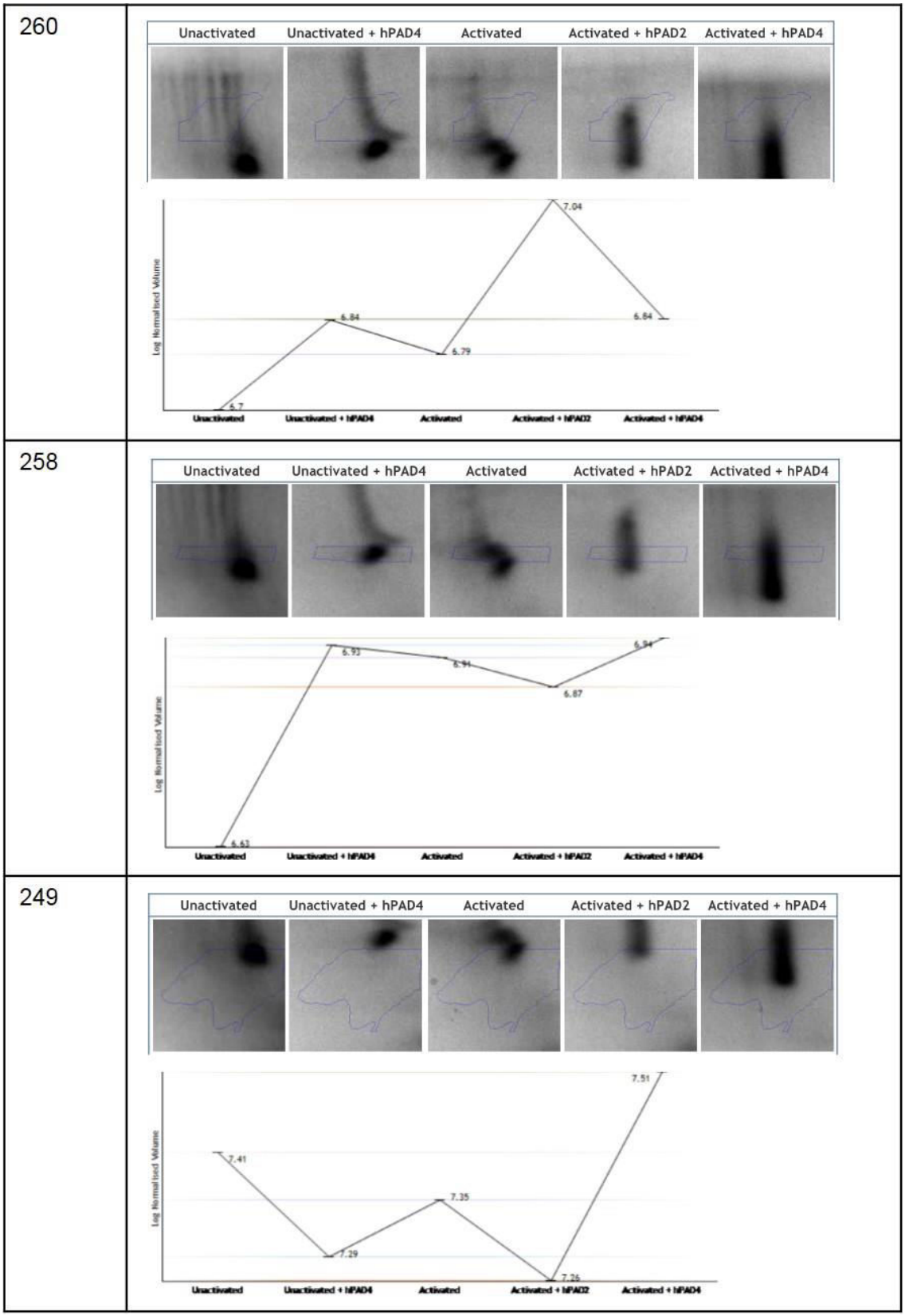

Figure 4.17 Graphical representation of normalised expression profile of spots 260, 258 and 249 using the SameSpots (TotalLab ltd., Newcastle upon Tyne, UK) analysis software.

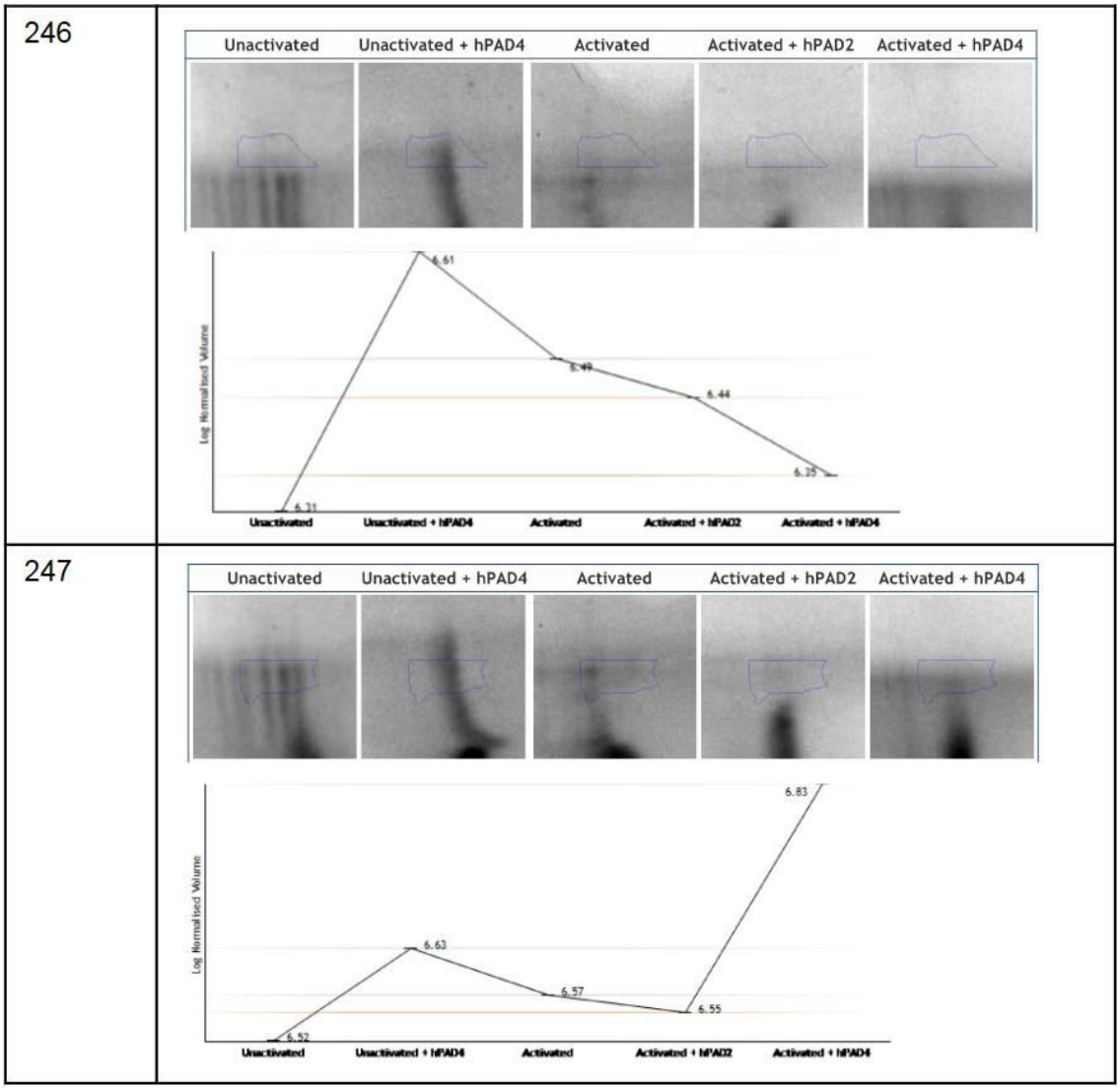

Figure 4.18 Graphical representation of normalised expression profile of spots 246 and 247 using the SameSpots (TotalLab ltd., Newcastle upon Tyne, UK) analysis software.

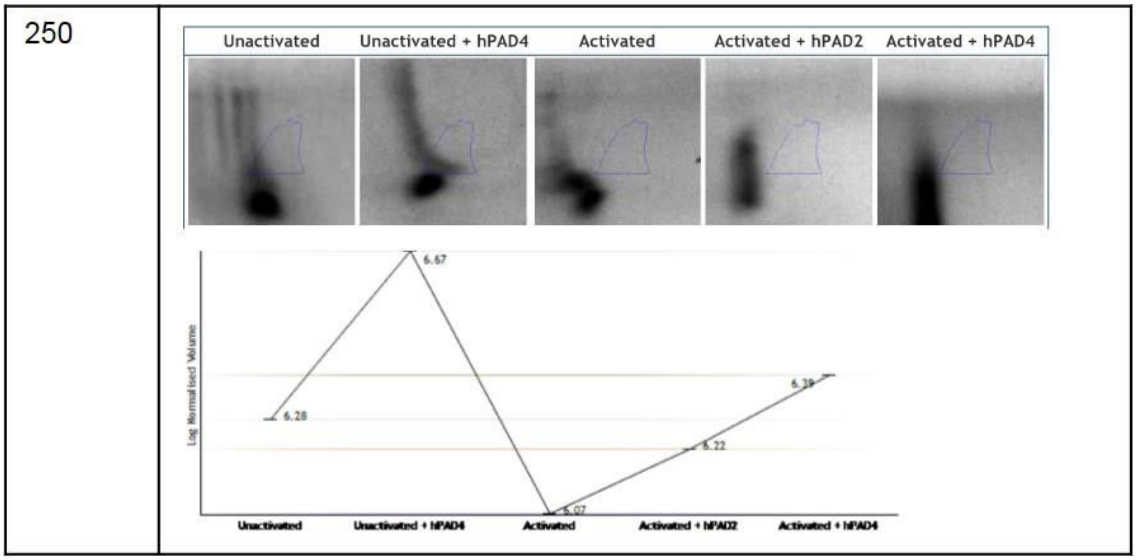

Figure 4.19 Graphical representation of normalised expression profile of spot 250 using the SameSpots (TotalLab ltd., Newcastle upon Tyne, UK) analysis software.

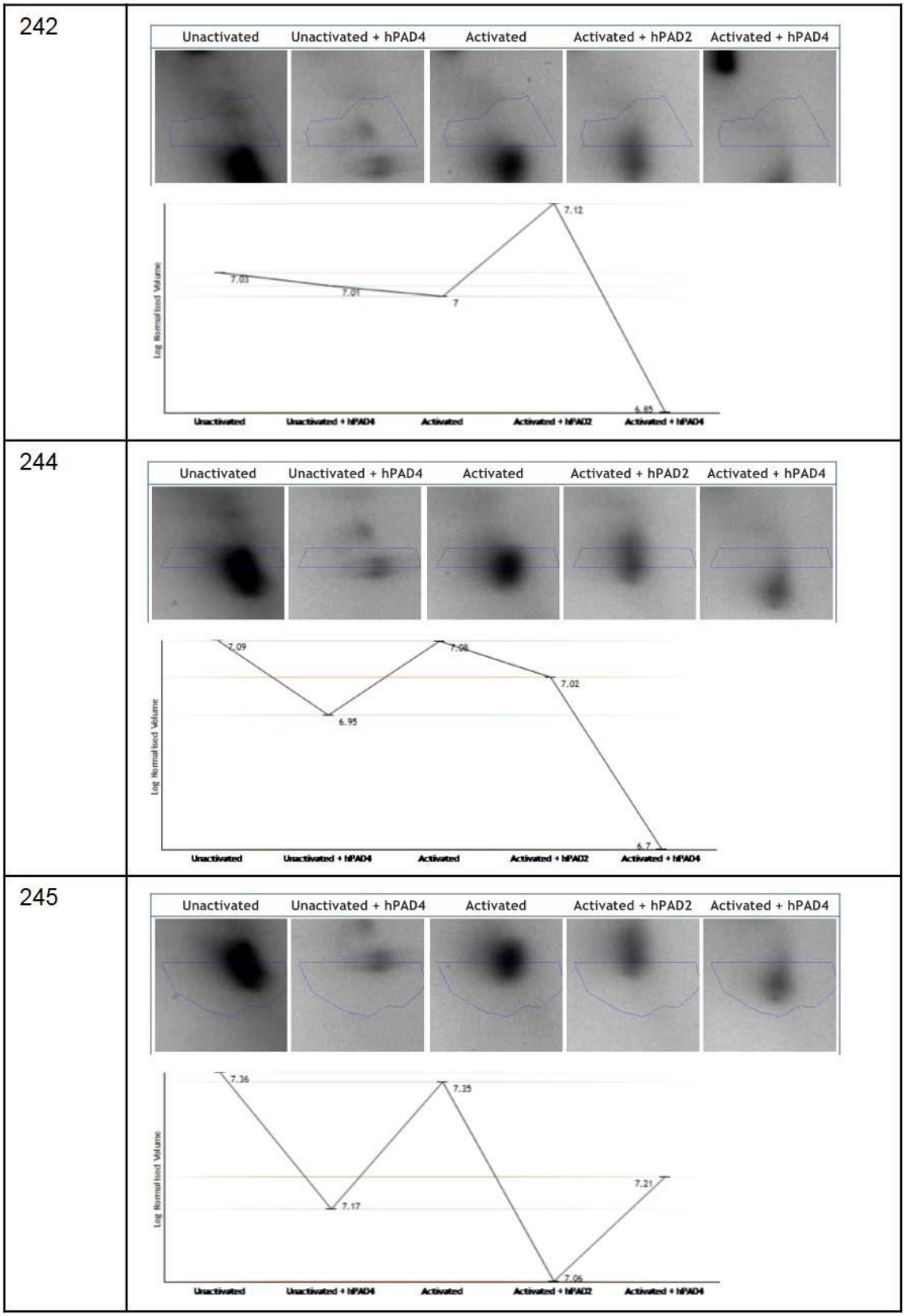

Figure 4.20 Graphical representation of normalised expression profile of spots 242, 244 and 245 using the SameSpots (TotalLab ltd., Newcastle upon Tyne, UK) analysis software.

4.4.6. Identification of membrane proteins modified by PAD enzymes by mass spectrometry

The analysis of the samples by the neutral loss method (LC-CID-saETD-MS/MS) after digestion with trypsin allowed the identification of several proteins for each of the spots analysed. The results obtained were filtered according with the number of unique peptides and the sequence coverage. Proteins with more than two peptides identified and sequence coverage higher than ten per cent were considered for analysis (Appendix 4). To note, the main hits for all the conditions were human keratin and human serum albumin and these were not further considered.

Plasma and intracellular organelle MP were identified in the analysed spots (244 and 245) from different conditions. In order to narrow down the dataset results, Venn diagrams were applied to identify the proteins exclusively associated with PAD enzymes. Despite the fact that all of the proteins identified exclusively associated with PAD enzymes on spots 244 and 245 can be found in the extracellular milieu or at the plasma membrane, some of them exert their main functions in the membrane of intracellular organelles, as described later on.

In spot 244, thirty-seven proteins were identified in all the conditions. From these, proteins complement component 1 Q subcomponent-binding protein (C1QBP), mitochondrial (fragment), Rho GDP-dissociation inhibitor 1 (RhoGDI) (fragment) and synaptogyrin-2 were only identified in the gels from PBMC treated with hPAD2 and hPAD4 enzymes (Figure 4.21a and table 4.7). C1QBP is an inhibitor of the classical pathway of the complement system since it binds to component C1q and consequently inhibits its association with C1r and C1s, suggesting a relationship with the innate immune system. RhoGDI is involved in the regulation of intracellular signalling through Rho GTPases. Synaptogyrin-2 is a membrane protein expressed with pre-synaptic vesicles in neuronal cells, being involved in synaptic plasticity.

In spot 245 it was possible to identify a total of thirteen proteins amongst all the conditions. Two proteins, ATP synthase subunit beta, mitochondrial (ATP5B), and

calreticulin (CRT), were only identified in the gels from PBMC treated with hPAD4 enzyme while no proteins were specifically identified in the gels from PBMC treated with hPAD2 enzyme (Figure 4.21b and table 4.8). ATP5B is part of the complex of ATPase that is responsible for the synthesis and/or hydrolysis of ATP combined with the transport of protons across the mitochondrial membrane. CRT is involved in the secretory pathway, where its main function is to prevent misfolded proteins from being exported from the endoplasmic reticulum to the Golgi apparatus.

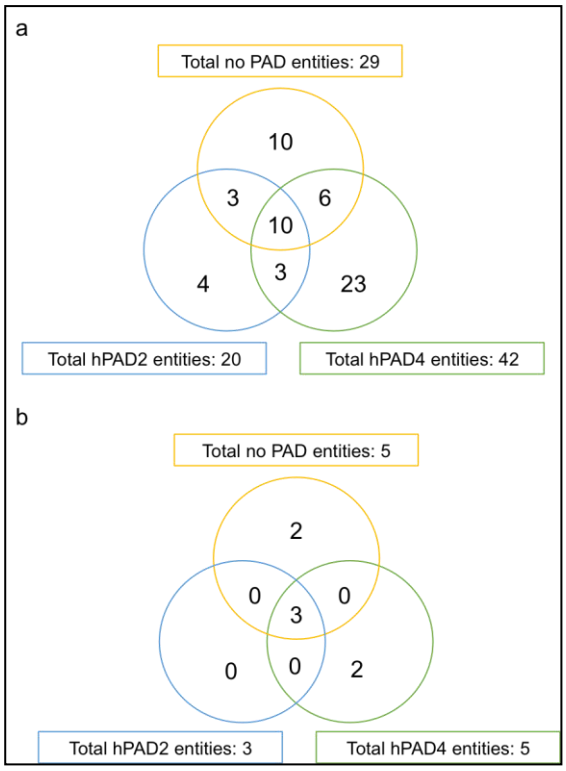

Figure 4.21 Venn diagrams representation of the proteins identified by LC-CID-saETD-MS/MS in spots 244 (a) and 245 (b). PBMC were isolated from healthy volunteers. Five hundred thousand cells/mL were pre-treated with 250 mU of hPAD2 or hPAD4 enzymes, for 2 hours at 37^0 C, and then stimulated with antibodies against CD3 and CD28 at 37^0 C for 24 hours. The concentration of anti-CD3 antibody was 1 µg/mL and the concentration of anti-CD28 antibody was 2 µg/mL. Following activation, MP from three independent experiments were extracted using the Mem-PER Plus membrane protein extraction kit (Thermo Fisher Scientific Inc., Loughborough, UK). Twenty-five micrograms (25 µg) of MP were separated by 2D BN/SDS-PAGE in the presence of 0.625% (v/v) DDM. In the first dimension a NativePAGE™ Novex™ 4–16% Bis-Tris gel was used and in the second dimension, the 1D strip was separated in TGX Mini-PROTEAN® TGX™ 8–16% pre-cast gel. After separation, the gels were stained with high sensitivity CBB G250 and spots 244 and 245 were collected, the proteins digested with trypsin gold and the resulting peptides extracted and analysed by LC-CID-saETD-MS/MS in a LTQ-Orbitrap Velos ETD mass spectrometer (Thermo Fisher Scientific Inc., Loughborough, UK) coupled to a Dionex Ultimate 3000 HPLC system (Sunnyvale, USA). Data were analysed using Proteome Discoverer 1.0 SPI software (Thermo Fisher Scientific Inc., Loughborough, UK).

Table 4.7 Proteins identified for spot number 244 exclusively associated with hPAD2 and hPAD4 enzymes treated PBMC. The accession number is the unique identifier used for the protein sequence.

Accession number	Protein	Function	Localisation
I3L3Q7	Complement component 1 Q subcomponent-binding protein, mitochondrial (Fragment)	Inhibition of C1 activation	Cytosol, extracellular, mitochondrion, nucleus, plasma membrane
J3KTF8	Rho GDP-dissociation inhibitor 1 (Fragment)	Regulation of signalling through Rho GTPases	Cytoskeleton, cytosol, extracellular
O43760	Synaptogyrin-2	Synaptic plasticity	Extracellular, plasma membrane

Table 4.8 Proteins identified for spot number 245 exclusively associated with hPAD4 enzyme treated PBMC. The accession number is the unique identifier used for the protein sequence.

Accession number	Protein	Function	Localisation
P06576	ATP synthase subunit beta, mitochondrial	ATP synthesis	Extracellular, mitochondrion, nucleus, plasma membrane
P27797	Calreticulin	Promotes folding, oligomeric assembly and quality control in the endoplasmic reticulum	Cytosol, endoplastic reticulum, extracellular, nucleus

Two citrullinated peptides were found in proteins from the two analysed spots (Appendix 4): actin, cytoplasmic 1; and complement component 1 Q subcomponent-binding protein. From these, the peptide where citrullination was detected in actin (spot 245 in hPAD2- and hPAD4-treated PBMC) was the same identified in non PAD-treated actin, cytoplasmic 1 (spot 244). The citrullinated peptide identified in complement component 1 Q subcomponent-binding protein (spot 244 in hPAD4-treated PBMC) was not identified in any of the non PAD-treated samples. However this is a mitochondrial protein and consequently, not one of the specific targets of this study.

These results suggest that the approach used here, 2D BN/SDS-PAGE followed by LC-CID-saETD-MS/MS, might not be the most effective method for the identification of citrullinated MP in the conditions studied here. The fact that MP contain less arginine residues than intracellular proteins is one of the limitations of this approach since the available sites for tryptic cleavage will be considerably decreased. The identification of only one citrullinated arginine residue might be reflection of this.

4.5. Discussion

Citrullination is the enzymatic PTM mediated by PAD enzymes, responsible for the conversion of peptidylarginine into peptidylcitrulline in a calcium dependent manner [109]. This conversion results in the loss of positive charge in the protein, affecting the protein structure and leading to the formation of new motifs and the generation of neoepitopes [109, 335]. Citrulline is a non-essential amino acid, consequently citrullination is a vital physiological reaction, being involved in keratinization of epithelial cells [120-124], inflammation [133, 147-150] and apoptosis [133, 140]. Five human isoforms of PAD enzymes (PAD1–4 and PAD6) have been described and are differentially expressed in specific tissues. Except for the PAD4 enzyme, which translocate to the nucleus, PAD enzymes are typically located in the cytoplasm of different cell types [336]. Of particular interest, PAD enzymes expressed in white blood cells recruited to inflammation sites, can be released to the extracellular environment when apoptosis occurs and act on extracellular proteins. This will lead to the formation of neoantigens and the triggering of an immune response through the production of ACPA. This mechanism of citrullination-induced autoimmunity has been described in RA [421] and PID [286]. RA and PID share similar pathological processes, including gene- and environmentally-associated disease susceptibility, soft and hard tissue destruction triggered from an exaggerated inflammatory response and the involvement of bacteria in the aetiology of the disease [284, 422]. Other key factors linking these two inflammatory diseases include the local and systemic production of autoantibodies [282, 355, 422-425] and the production of citrullinated peptides recognised by autoreactive T cells [285, 426].

FNG is an example of an extracellular protein that is found to be citrullinated in RA. ACPA against citrullinated FNG were found in the serum and synovial fluid of RA patients and constitute a well-known marker for RA with excellent sensitivity and specificity [363, 427].

It is then established that citrullination is involved in the breakdown of the immune system in diseases as RA and PID. However, to date, no studies have investigated the role of these enzymes in the activation of T cells.

The activation and proliferation of T cells induced by antigens are important characteristics of adaptive immune responses. The activation of T cells is triggered by the presentation of antigen peptides to TCR/CD3 through MHC molecules, but co-stimulatory molecules are also essential for the activation of T cells, such as CD28/B7 [428]. When T cells become activated, the secretion of IL-2 to the extracellular medium and the expression of the CD25 are up-regulated [429-431]. The interaction between IL-2 and CD25 induces T cell growth, differentiation and survival [419, 432].

In this chapter, different models of T cell activation were studied and the effects of PAD enzymes on T cell activation were investigated by analysing the secretion of IL-2 and the expression of CD25 at the cell surface. Furthermore, the consequences of PAD enzyme treatments were also assessed at nuclear (gene expression) and cell membrane (MP at the cell surface) levels.

Jurkat E6.1 T cells and PBMC were the two T cell models compared. Since Jurkat E6.1 T cells are an immortalised cell line it was important to compare their activation responses with primary immune cells. Primary T cell responses were studied within the PBMC population, where T cell activation is closer to physiological conditions. Furthermore, it was previously shown that essential stimulatory signals for T cell proliferation are provided by non-T cells [433-435]. PHA-L and anti-CD3/anti-CD28 antibodies were the two stimulation methods selected. PHA-L crosslinks glycosylated proteins on the surface of T cells, resembling what happens during TCR activation [436]. Antibodies against CD3 and CD28 activate T cells similarly to APC, proving the initial (CD3 binding) and the co-stimulatory (CD28 binding) signals. Secretion of IL-2, quantified by ELISA, and expression of CD25 at the cell surface, analysed by flow cytometry, were compared on the different tested combinations. From these data, PBMC stimulated with 1 µg/mL anti-CD3 and 2 µg/mL anti-CD28 for 24

hours were the combination selected for the subsequent citrullination studies. These were not the conditions that induced maximal changes in IL-2 and CD25 levels, however, as there was no indication on the effect of citrullination on the activation of T cells, a maximal T cell stimulation in control conditions without PAD enzymes was not the considered objective. Duarte *et al*., showed previously that T cells stimulated with PHA lose their ability to respond to allogenic stimulation or viral antigens *in vitro*, whereas immune functions are preserved on CD3/CD28-stimulated T cells. The hypothesised reason for this is the distribution of CCR7/CD45RA T cell functional subsets. The activation of T cells via CD3/CD28 mimics the lineage differentiation pattern induced by antigens in physiological conditions, while in PHA induced activation the distribution of the CCR7/CD45RA functional T cell subsets is skewed, with near disappearance of the subpopulations that display the effector phenotype [437].

Here, PBMC were incubated with PAD enzymes (isoforms 2 and 4), followed by activation with the conditions selected previously (1 µg/mL anti-CD3 and 2 µg/mL anti-CD28 for 24 hours) and analysed for IL-2 secretion and IL-2Rα expression. PBMC viability after the treatments was also assessed and showed no differences when compared with unactivated and untreated PBMC, suggesting that citrullination was not toxic for the cells. Flow cytometric analysis of CD4/CD25 double-stained PBMC allowed evaluation of the number of CD4 T cells expressing CD25 at their surface and also the amount of CD25 expressed by CD4 T cells. The PBMC population was narrowed to CD4 T cells in this case since these cells are involved in the humoral immune response associated with citrullination. The flow cytometry results showed an increase in the percentage of CD4 T cells expressing CD25 at the surface. PBMC from healthy individuals consist of 70–90% of lymphocytes (B and T cells) and within the lymphocyte population, approximately 75% consist of CD4 and CD8 T cells [438]. *In vivo*, CD25 is expressed by CD4 T cells upon activation, accounting for approximately

30–40% of the total population of PBMC. Here, an average 35% of CD4 T cells were found to express CD25 at their surface after activation with anti-CD3/anti-CD28.

In PBMC pre-treated with hPAD2 or hPAD4 enzymes, then activated the number of CD4 T cells expressing CD25 at the surface was lower than in activated PBMC. However, the level of CD25 expressed by CD4 T cells pre-treated with PAD enzymes did not show consistent results between the replicates. The levels of IL-2 secreted by the cells showed a significant increase when the cells were activated via CD3/CD28. However, no difference was observed when the cells were treated with hPAD2 or hPAD4 enzymes without activation, suggesting that PAD enzymes by themselves do not induce alterations in the secretion of IL-2 by T cells. PBMC pre-treated with hPAD2 and hPAD4 enzymes, then activated showed a significant decrease of more than 50% in the levels of secreted IL-2, when compared with activated cells. This was observed for all the tested concentrations of PAD enzymes. The HI-PAD enzyme pre-treatment effect on IL-2 secretion was not significantly different from activation alone. In chapter 3 it was shown that FNG treated with HI PAD enzymes had a similar SDS-PAGE profile to FNG treated with PAD enzymes in the presence of EDTA, suggesting that HI was effective for denaturing PAD.

Several studies have previously reported impairments in T cell responses in PID models [232, 236-240, 439]. Furthermore, deficits in the IL-2 response were reported in T cells from PID patients [243, 440].

Human PAD2 and hPAD4 enzymes share 50% of sequence homology. However, these two PAD enzyme isoforms localise differently inside the cell, are expressed by different cells and their expression and activation are separately regulated [133, 149, 441, 442]. Human PAD2 and hPAD4 enzymes also differ in stability, calcium dependency, optimal pH range and substrate specificity [377, 378]. These isoforms were chosen due to their increased expression in the synovium of RA patients [187] and their presence in the inflamed gingiva of periodontitis patients [443]. Darrah *et al*. suggested that substrate specificity and activity of different PAD enzymes

are linked with the specific distribution of each PAD enzyme isoform [442]. Physiologically these enzymes are localised intracellularly. However, in pathological conditions, apoptosis or necrosis of cells (macrophages and neutrophils) leads to the release of intracellular content, including intracellular PAD enzymes. Here, hPAD2 and hPAD4 enzymes were added to the extracellular medium of PBMC, to mimic pathological conditions. To estimate the amount of PAD enzyme necessary to citrullinate MP in the PBMC population it was calculated that from 40 x 10^6 PBMC obtained from 20 mL of blood, 200–1200 µg total protein should be achieved [444] and of this 23% would be membrane-spanning proteins [445]. ModiQuest Research B. V. (Oss, Netherlands), the commercial supplier of PAD enzymes, recommends the use of 50 mU of hPAD2 or hPAD4 enzyme for the citrullination of 100 µg of pure protein. According to this, 23–138 mU of PAD enzymes would be enough for the conversion of arginine residues on MP isolated from 20 mL of whole blood. The different concentrations of PAD enzymes used here showed similar results on the impairment of IL-2 secretion from T cells and, consequently, 250 mU was the concentration selected for further studies, since it is above the required amount estimated empirically, and was used for 2 hours, as this time was previously shown to be sufficient for PAD enzymatic activity, given the necessary cofactors are in place [196]. After treatment, PAD enzymes were removed by careful washing to minimise the risk of citrullination of the activation antibodies.

A key regulator of PAD enzyme activity is calcium. The binding of calcium changes the conformation of the catalytic site of PAD enzymes, affecting the enzyme-substrate interaction [111]. Half-maximal PAD enzyme activities are reached at calcium concentrations ranging from 40 µM to 3.3 mM [196, 315, 446, 447]. In resting cells, the levels of intracellular calcium are low and not sufficient for PAD enzyme activity. However, after cell stimulation or with membrane disintegration calcium reach maximum levels that allow PAD enzyme activation [448]. Calcium concentration of the RPMI medium used in this study is 0.4 mM, being sufficient for PAD enzyme activity.

The treatment of PBMC with hPAD2 and hPAD4 enzymes prior to T cell activation showed a significant decrease in the IL-2 secretion, suggesting alterations in the IL-2 T cell response. IL-2 is essential for T cell activation and proliferation. Decreased IL-2 production was previously reported in patients with autoimmune disease systemic lupus erythematosus (SLE) [449], in cultured lymphocytes from patients with SLE [450] and in SLE murine models [451]. The reduced IL-2 secretion in SLE was suggested to be derived from dysregulation of transcription or suppression of IL-2 production in SLE T cells [452]. The main consequences of the dysregulation of IL-2 secretion in SLE are the reduction in the number of Tregs that are involved in the inhibition of autoimmunity, the impairment of AICD, necessary for the down-regulation of expanded T cell clones [453, 454], and defective CD8 T cell cytotoxic functions [455]. Also consistent with the results observed here, *in vitro* studies in T cells isolated from SLE patients and activated with PHA, revealed impaired IL-2 secretion but normal expression of IL-2R [456].

Upon activation, T cells switch their metabolism from OXPHOS to aerobic glycolysis and glutaminolysis [84, 457]. The increased glycolytic flux during T cell activation leads to the concomitant production of lactate via aerobic glycolysis [458]. However, the results obtained here show a decrease in the extracellular levels of lactate in activated PBMC when compared with unactivated cells. In addition to being a by-product of highly proliferative cells, lactate, is also thought to be involved in the modulation of the immune response [459-462]. In T cells the accumulation of lactate in the inflammation site leads to a loss of T cell mobility and their consequent entrapment at the site, perpetuating the chronic inflammatory process. Sodium lactate was shown to inhibit the mobility of activated CD4 T cells upon engagement of the chemokine receptor CXCR3 with the chemokine CXCL10 due to interference with glycolysis. In CD8 T cells lactic acid is responsible for cell mobility inhibition, in a glucose-independent manner [463]. In accordance with this, the results obtained in the PBMC

citrullination study show that a higher lactate level was associated with hPAD2 activity, with lower IL-2 secretion and, consequently, a non-activated T cell profile.

Following these findings it was crucial to understand how PAD enzymes modifications, both at cell membrane level and intracellularly at gene expression level, were affecting the T cell response.

Alterations in gene expression were evaluated by microarray analysis and confirmed by RT-QPCR. In the microarray study, eight genes were identified as up-regulated by both PAD enzymes in activated PBMC, while thirty-five genes were identified as down-regulated in the same conditions. From these, genes involved in metabolism, redox signalling or membrane-associated processes were selected for further analysis. Up-regulated *ASS1* and *CTH* and down-regulated *HK3*, *CD163* and *SGMS2* were the genes analysed by RT-QPCR.

ASS1 encodes for ASS1 enzyme, which is involved in the conversion of citrulline into arginine in the urea cycle. ASS1 contributes to T cell differentiation and function. Deficiency in ASS1 enzyme (citrullinemia type I) affects *in vitro* Th1 and Th17 polarization negatively, and associates with primary immune dysfunction [464]. Moreover, it was previously shown that extracellular arginine depletion blocks proliferation of activated normal T cells [465-467] and aerobic glycolysis [468], but provided that citrulline is present extracellularly, T cells can overcome this impairment by *de novo* synthesis of arginine via ASS1 [464, 468, 469]. The results obtained here showed an up-regulation of *ASS1* in activated PBMC pre-treated with PAD enzymes, suggesting *de novo* synthesis of arginine possibly to overcome a decrease in the arginine supply that is related with impaired T cell proliferation. If this would be the case, aerobic glycolysis would also be impaired. To enforce this fact, *HK3* expression was found to be down-regulated in the microarray results. *HK3* encodes for HK3 enzyme that is responsible for the conversion of glucose into glucose 6-phosphate in the first step of glycolysis. Upon activation, T cells rely on glycolysis and glutamine oxidation, to produce biosynthetic precursors required for rapid cell growth and

proliferation [72]. Here, the treatment of PBMC with PAD enzymes, in particular with hPAD2 enzyme, revealed a decrease in the expression of *HK3*, consistent with an impairment of glycolysis.

CD163 and *SGMS2* both encode for cell surface proteins. CD163 is a monocyte/macrophage-specific scavenger receptor. As PBMC were used here as the studied population, it was not a surprise to detect genes expressed by other cell types than T cells. CD163 was previously shown to be up-regulated in RA [470] and spondylarthritis (SpA). The soluble form of CD163 was also associated with global inflammation and impairment of T cell activation in SpA synovium. [471]. On the contrary here, *CD163* was found to be down-regulated in activated PBMC pre-treated with PAD enzymes. The enzyme SGMS2 is encoded by *SGMS2* and is responsible for the biosynthesis of sphingomyelin, a key lipid component of the cell and Golgi membranes and lipid rafts. SGMS2 is also involved in the regulation of protein trafficking and secretion [472]. Furthermore, sphingomyelin is part of the specific microdomains of the plasma membrane that are associated with CD3-induced TCR activation [473, 474]. Several studies revealed that the sphingomyelin biosynthetic pathway is associated with TCR signalling in activated T cells. Asano and colleagues showed that SGMS1 and 2 deficiencies in mouse embryonic fibroblasts promote cell migration via CXCL12/CXCR4-dependent signalling pathway [475]. In another *in vivo* study, activated T cells from mice with impaired ceramide generation exhibited less secretion of IL-2 than wild type animals, due to a dysfunction of the secretory vesicle system [476]. *SGMS2* was one of the genes identified as down-regulated by PAD enzymes on the microarray results which is not in accordance with the studies discussed above. When the same experiment was assessed by RT-QPCR down-regulation of *SGMS2* in activated T cell pre-treated with PAD enzymes was not observed.

CTH gene encodes for CTH. This enzyme converts cystathionine into Cys, α-ketobutyrate and ammonia in one of the steps of the GSH biosynthesis pathway; it is

involved in redox signalling. Martin *et al.* have previously shown that physiological oxidative stress up-regulates the expression of this gene in rat hepatic cells [477]. Cys is essential for protein synthesis, cell proliferation and T cell activation [478]. However, in T cells CTH is not present. To overcome this, cystine can be imported from the extracellular environment via the plasma-membrane xc− cystine–glutamate exchanger. Once inside the cell, cystine is rapidly reduced to cysteine due to the reducing intracellular environment. Naïve T cells express no or very low levels of xc− transporter [479-481] and consequently depend on APC to export Cys that can then be imported by T cells via their alanine-serine-cysteine transporter and used for the synthesis of GSH [478]. In activated T cells, the xc− transporter was found strongly upregulated in human and mouse T cells, providing the necessary cystine/cysteine for cell proliferation [479, 482, 483]. *CTH* was detected as up-regulated on the microarray study and this was further confirmed by RT-QPCR. A possible reason for the detection of this gene and its up-regulation by PAD enzymes is the use of the entire PBMC population to study PAD enzyme effects instead of an individual T cell population. Despite the fact that *CTH* was quantified by RT-QPCR it is important to note that a raw C_T value less than forty was only obtained in one of the independent experiments performed, indicating low levels of expression of this gene.

A common fact between the different genes analysed was the high level of variation in the results between experiments. An explanation for this is the fact that the entire PBMC population was used for these studies instead of an individual cell population. To counteract this and to identify what T cell population is responsible for the gene expression, in subsequent studies, CD4 and CD8 T cells were isolated prior to RT-QPCR.

In combination with the identification of specific genes' expression affected by citrullination, the identification of modified MP that may mediate the effects of citrullination in T cells was also an objective of this chapter. In the previous chapter it was shown that 2D BN/SDS-PAGE, despite not ideal, could be a technique used for

the separation of T cells and that LC-CID-saETD-MS/MS could be used to the identification of arginine residues modified by citrullination. From the two analysed spots from PBMC citrullinated with PAD enzymes it was possible to identify proteins exclusively associated with PAD enzyme treatment: C1QBP, RhoGDI, synaptogyrin-2, ATP5B and CRT that associate with membranes. From the 2D BN/SDS-PAGE analysis these five proteins appeared to be down-regulated in PAD-treated PBMC.

C1QBP is a multicompartmental glycoprotein that is involved in inflammation, infection, ribosome biogenesis, apoptosis regulation, transcriptional regulation and pre-mRNA spicing. At the cell surface, this protein is involved in the inhibition of the classical pathway of the complement system, through the binding to component C1q [484]. In addition, C1QBP can bind to coagulation factor XII, promoting its auto-activation and the initiation of blood clotting via the intrinsic pathway of coagulation and inflammatory reactions [485].

RhoGDI is involved in the regulation of intracellular signalling through Rho GTPases. Rho GTPases are a family of signalling G proteins that are mainly involved in the regulation of the actin cytoskeleton but also influence cell polarity, microtubule dynamics, membrane transport pathways and transcription factor activity [486]. In T cells, the engagement of the TCR leads to the activation of Rac proteins, members of the Rho GTPase family, that are implicated in the regulation of MAPK, PI3K and calcium pathways [487]. Studies on Rac2 knockout animal models showed decrease activation of ERK1/2 and p38 and calcium mobilisation, defective TCR-mediated proliferation and lower levels of IL-2 and IFN-γ in CD4 T cells [488, 489]. RhoGDI inhibits the activation of Rho GTPases by preventing the dissociation of GDP and by blocking their recruitment to the plasma membrane [490]. RhoGDI is a substrate of gene related to anergy in lymphocytes (GRAIL), part of E3 ubiquitin ligase enzyme, suggesting that ubiquitination of RhoGDI is involved in the establishment of T cell anergy [491].

Synaptogyrin-2 is a membrane protein expressed with pre-synaptic vesicles in neuronal cells, being involved in synaptic plasticity. In view of its physiological localisation, synaptogyrin-2 will not be further considered.

ATP5B is part of the ATPase complex that is responsible for the synthesis and/or hydrolysis of ATP combined with the transport of protons across the mitochondrial membrane. ATP5B is localised mainly in the inner membrane of the mitochondria, but it can translocate from the mitochondria and be found on the outside of the cell membrane [492].

CRT is mainly localised in the endoplasmic reticulum where it acts as a calcium-binding (storage) protein. CRT is involved in the secretory pathway, where it main function is to prevent misfolded proteins from being exported from the endoplasmic reticulum to the Golgi apparatus. CRT deficiency was associated with a dysfunction of the T cell response in immunodeficient mice, suggesting that CRT-dependent calcium signalling modulates T cell immune response [493]. CRT can also be found on the surface of different cells, where it acts as a stimulatory molecule to B cells and macrophages via the TLR4/CD14 pathway, and CRT soluble form can be found in the sera of RA and SLE patients, suggesting its involvement in the pathogenesis of autoimmunity [494].

The analysis of MP from PBMC treated with hPAD2 or hPAD4 enzymes by 2D BN/SDS-PAGE followed by LC-CID-saETD-MS/MS revealed no PAD-specific citrullinated arginine residues associated with MP. The citrullinated peptide found in actin 1 protein was identified in both non PAD-, PAD2- and PAD4-treated PBMC. The citrullinated peptide found in complement component 1 Q subcomponent-binding protein from PAD4-treated PBMC was not identified in non-PAD treated PBMC. However, as this is a mitochondrial protein it is not one of the main targets of these study. Citrullination might not have been efficient as MP contain less arginine residues than intracellular proteins. Furthermore, this lower number of arginine residues in combination with potentially citrullinated arginine residues provide less possible sites

for trypsin cleavage and, consequently, bigger peptides less likely to be detected by mass spectrometry. Cell surface proteomic studies have found limitations on the identification of proteins due to the steric hindrance of proteases. Strategies to overcome this include the removal of N-linked glycans from proteins prior to proteolysis to prevent missed cleavages [495, 496], the use of alternative enzymes to trypsin for protein digestion or adaptations to the trypsin digestion protocol [497].

Taken together, the results obtained in this chapter showed that PAD enzymes induce a reduction in the T cell IL-2 response to activating stimuli. In addition, the analysis of gene expression suggested that the impairment in the IL-2 response is related to alterations in glucose and amino acid metabolism. Studies described in chapter 5 aim to validate whether metabolic differences are seen in T cells from PID patients compared to periodontally healthy controls. Furthermore, a down-regulation of the complement system is suggested by the data obtained by both MP identification by MS and the GO analysis of pathways on the microarray study. The activation of the complement system results in the opsonisation and lysis of pathogens and in the generation of pro-inflammatory molecules, having a crucial role in the innate immunity against pathogens. However, this system can also be linked to adaptive immunity through the modulation of T cell differentiation and effector functions [498]. T cells and APC have been shown to produce complement components and up-regulate the expression of complement receptors, promoting T cell differentiation, expansion and survival. Previous studies described that dysregulation of the complement system induces T cell-mediated autoimmunity [499]. In accordance with this, the data obtained here associates a down-regulation of the complement system, mediated by PAD enzymes, to an impaired IL-2 T cell response.

Chapter 5 Translating *ex vivo* studies of T cell modification by PAD to periodontitis clinical samples

5.1. Preface

PID is a chronic inflammatory disease in which citrullination has been implicated. In this chapter plasma and GCF samples from PID patients and periodontally HC were compared for levels of pro-inflammatory cytokines (IL-6 and IL-8), PAD activity and GSH levels. The expression of genes that were found to be up- or down-regulated in the *ex vivo* PBMC activation experiments, with and without PAD as described in Chapter 4, have been investigated in CD4 and CD8 T cells from PID patients.

5.2. Introduction

In 2012, the WHO reported that 15–20% of middle-aged (35–44 years) adults are affected by severe PID. PID is a chronic inflammatory disease characterised by localised infections and inflammatory conditions that affect one or more of the periodontal tissues (alveolar bone, periodontal ligament, cementum and gingiva) which support the teeth [500]. At the cellular level, PID involves accumulation of lymphocytes and monocytes, endothelial cell proliferation and matrix degradation [213]. PID can be categorised from gingivitis to aggressive periodontitis according to the composition of the subgingival microbial flora and also the factors that influence the host response to the microbial attack [161, 213]. Histologically, the lesion observed in gingivitis and PID can be divided into four stages: initial lesion, early lesion, established lesion and advanced lesion. Initial, early and established lesions are characteristic of gingivitis whereas an advanced lesion is a feature of periodontitis. In the initial lesion a response from resident leukocytes and endothelial cells to the bacterial biofilm can be observed. Furthermore, neurons are stimulated to produce neuropeptides responsible for triggering vasodilation of local blood vessels, which will allow the migration of neutrophils towards the periodontium in response to chemokines. In the early lesion, increased numbers of neutrophils are observed, complemented with the appearance of macrophages, lymphocytes, plasma and mast cells. The complement system is also activated, the epithelium proliferates and the gingival crevice fluid flow increases. The established lesion stage is when the immune response shifts from innate to adaptive, with a predominance of macrophages, plasma cells and T and B cells. Increased collagen degradation is also observed. The transition from gingivitis to PID is characterised by advanced lesions, where the inflammatory lesion extends to the alveolar bone and irreversible attachment and bone loss are observed [500, 501].

Amongst the bacterial species involved in PID, *P. gingivalis* appears to be the major infectious agent, being detected in higher abundance in patients with aggressive

forms of PID [227]. Furthermore, *P. gingivalis* was reported to produce a unique bacterial enzyme, PPAD, responsible for the conversion of peptidylarginine into peptidylcitrulline, a reaction known as citrullination [110, 228, 231]. Citrullination of host proteins by PPAD enzyme was described to induce production of ACPA, suggesting the triggering of an autoimmune response [254]. Furthermore, isoforms 2 and 4 of human PAD enzymes were also found in inflamed gingiva [443]. The autoimmune nature of PID suggests the involvement of T cells. Ivanyi and Lehner first suggested the contribution of T cells in PID in 1970 [232]. Since then, several studies have found evidence for the role of T cells in the homeostasis of periodontal tissues [233], modulation of the immune responses [234] and mediation of the bone loss characteristic from PID [235]. The association between different T cell subsets and PID progression has also been investigated. However, consensus on T cell subset involvement in PID has not been reached so far. Several studies reported decreased ratios of CD4/CD8 T cells in PID lesions compared with healthy controls [242, 244, 246], whereas others reported increased CD4/CD8 ratios [249, 250]. Furthermore, CD4 Th1 cells have been associated with stable PID lesions while CD4 Th2 have been linked to progressive lesions [502-507]. On the contrary, others have shown that up-regulation of Th1 and down-regulation of Th2 are associated with PID tissue destruction [508-510]. Several studies have also focused on Th17 subset. Gingival tissue and GCF from PID patients revealed high levels of IL-17 and other Th17-related cytokines when compared to healthy sites [511-518]. However, it is not clear if Th17 cells have a protective or destructive role in PID.

Here, the gene expression changes observed after the activation of T cells pre-treated with PAD enzymes in chapter 4 were studied in CD4 and CD8 T cell populations from PID patients and compared with HC, in order to explore the significance of previous *in vitro* findings to disease activity. Therefore, the aims of this chapter are as follows:

- To analyse the inflammatory status of plasma from PID patients, compared with HC;
- To assess the PAD activity of GCF from PID and HC individuals;
- To evaluate the redox status of plasma and GCF samples from PID and HC individuals;
- To compare the expression of metabolic and inflammatory genes, which are regulated by hPAD pretreatment and were identified in Chapter 4, in CD4 and CD8 T cell subsets from PID and HC.

5.3. Methods

5.3.1. Clinical samples

Plasma and GCF samples from PID patients and age-matched periodontally healthy controls (HC) were obtained from the periodontal clinic at Birmingham Dental Hospital, as detailed in section 2.5. Demographics of patients and controls are described in table 5.1.

5.3.2. Quantification of interleukin-6 and interleukin-8 levels in the plasma of periodontitis patients

IL-6 and IL-8 levels in the plasma of PID and HC individuals were quantified by sandwich ELISA, as described in section 2.16.

5.3.3. Quantification of reduced glutathione in the plasma and gingival crevicular fluid of periodontitis patients

The levels of GSH in the plasma and GCF of PID and HC individuals were assessed by the GSH recycling assay as outlined in section 2.18.

5.3.4. Quantification of peptidylarginine deiminase activity in the gingival crevicular fluid of periodontitis patients

ABAP kit assay was used to quantify the activity of PAD enzymes in the plasma and GCF of PID and HC individuals as detailed in section 2.19.

5.3.5. Quantification of gene expression in peripheral CD4 and CD8 T cells from periodontitis patients

Total RNA was isolated from CD4 and CD8 T cells extracted from the blood of PID and HC individuals, converted to cDNA and analysed by RT-QPCR as outlined in section 2.21. The mean of ΔC_T values relative to housekeeper from HC group was used as a

control condition for the comparison of gene expression between PID patients and HC individuals.

5.3.6. Statistical analysis

Data obtained was analysed according to section 2.23.

5.4. Results

Samples from PID patients attending the periodontal clinic at Birmingham Dental Hospital were collected and a summary of the demographics and main plasma and GCF findings are outlined in table 5.1.

Table 5.1 Demographics and results obtained for the two groups.

Parameter	HC group	PID group
N	6	6
Gender (M/F)	1/5	3/3
Age (years)	49.0 ± 10.1	49.5 ± 9.4
IL-6 (pg/mL)	3.96 ± 1.18	4.16 ± 0.86
IL-8 (pg/mL)	13.54 ± 2.46	15.82 ± 4.15
PAD activity (mU)	0.088 ± 0.030	0.337 ± 0.157
Plasma GSH (nmol/mg prot)	0.023 ± 0.005	0.029 ± 0.012
GCF GSH (nmol/mg prot)	62.47 ± 12.36	34.65 ± 5.70
Plasma GSH (μM)	1.51 ± 0.31	2.02 ± 0.92
GCF GSH (μM)	2.40 ± 0.11	2.39 ± 0.08

GCF – gingival crevicular fluid; GSH – reduced glutathione; HC – healthy controls; IL – interleukin; N – number of subjects in each group; PAD – peptidylarginine deiminase; PID – periodontitis patients. Age is expressed as mean ± SD and all the other variables are expressed in mean ± SEM.

5.4.1. Plasma inflammatory status of periodontitis patients

Pro-inflammatory plasma factors, such as cytokines, are elevated in PID patients [519], therefore, the first step of this chapter was to assess the inflammatory status of patients with PID in comparison with periodontally healthy individuals. No differences in the plasma levels of IL-6 and IL-8 were found when comparing PID and HC groups (Figure 5.1).

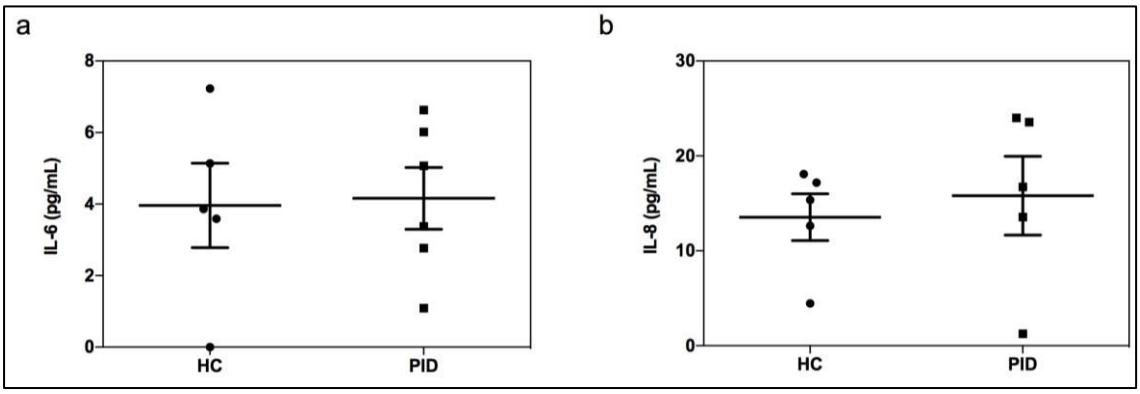

Figure 5.1 IL-6 and IL-8 plasma concentration in PID patients and age-matched periodontally healthy controls (HC). Plasma was collected from whole blood by centrifugation and the levels of IL-6 and IL-8 determined using an IL-6 Quantikine ELISA kit (R&D systems, Abington, UK) (a) and an IL-8 Quantikine ELISA kit (R&D systems, Abington, UK) (b), respectively. Data are presented as mean ± SEM. N = 5–6. Mann-Whitney test was performed using GraphPad Prism (v6.02) software and no statistical significance was found.

5.4.2. Citrullination status of the gingival crevicular fluid of periodontitis patients

The presence of PPAD enzyme, human PAD enzymes and citrullinated proteins in PID inflamed tissue constitutes a hallmark of this disease [443]. To evaluate the likelihood of citrullination in PID patients relative to HC individuals, PAD enzyme activity in the GCF was determined in both groups. The mean PAD activity was 0.337 mU (with a confidence interval of 75%) for PID patients and was 0.088 mU (with a confidence interval of 75%) for HC, i.e. PAD activity was more than three times higher in PID patients than in HC. The differences were not statistically significant but it is possible to observe that two out of the six PID patients had higher levels of PAD enzyme activity in GCF samples (Figure 5.2). This might indicate that with a larger number of PID samples, significant differences might be observed.

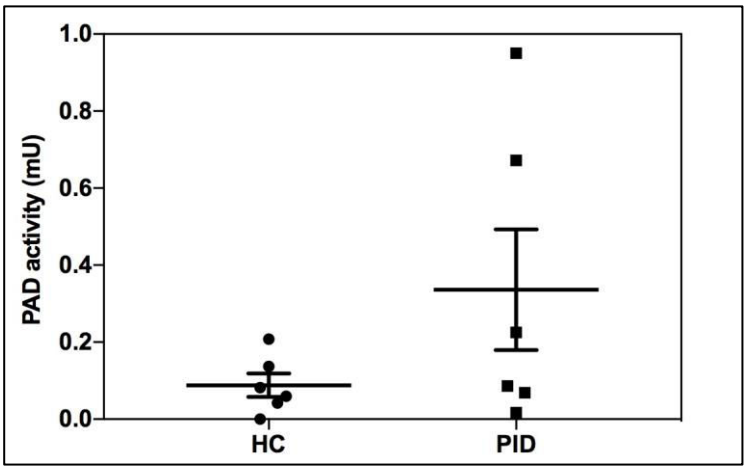

Figure 5.2 PAD enzyme activity in the GCF of PID patients and age-matched periodontally healthy controls (HC). GCF was collected on Periopaper™ strips (Oraflow Inc., Plainview, NY, USA) and extracted from the strips by centrifugation. PAD activity was determined using an ABAP kit (Modiquest Research B. V., Oss, Netherlands). Data are presented as mean ± SEM. N = 6. Mann-Whitney test was performed using GraphPad Prism (v6.02) software and no statistical significance was found.

5.4.3. Redox status of plasma and gingival crevicular fluid of periodontitis patients

The levels of antioxidants, like GSH, are known to be lower in PID patients [520, 521]. Here, GSH was quantified in the plasma and GCF of PID patients and HC. No differences were observed between the raw values of GSH in the plasma (Figure 5.3a) and in the GCF (Figure 5.3b) of PID and HC groups. The normalisation of the GSH levels for the amount of total protein present per sample showed a trend to lower levels of GSH in the GSF of PID patients, when compared with HC individuals (Figure 5.3d). No statistical significance was observed, possibly due to the small sample number. No differences were observed between the plasma levels of GSH in PID and HC individuals (Figure 5.3c).

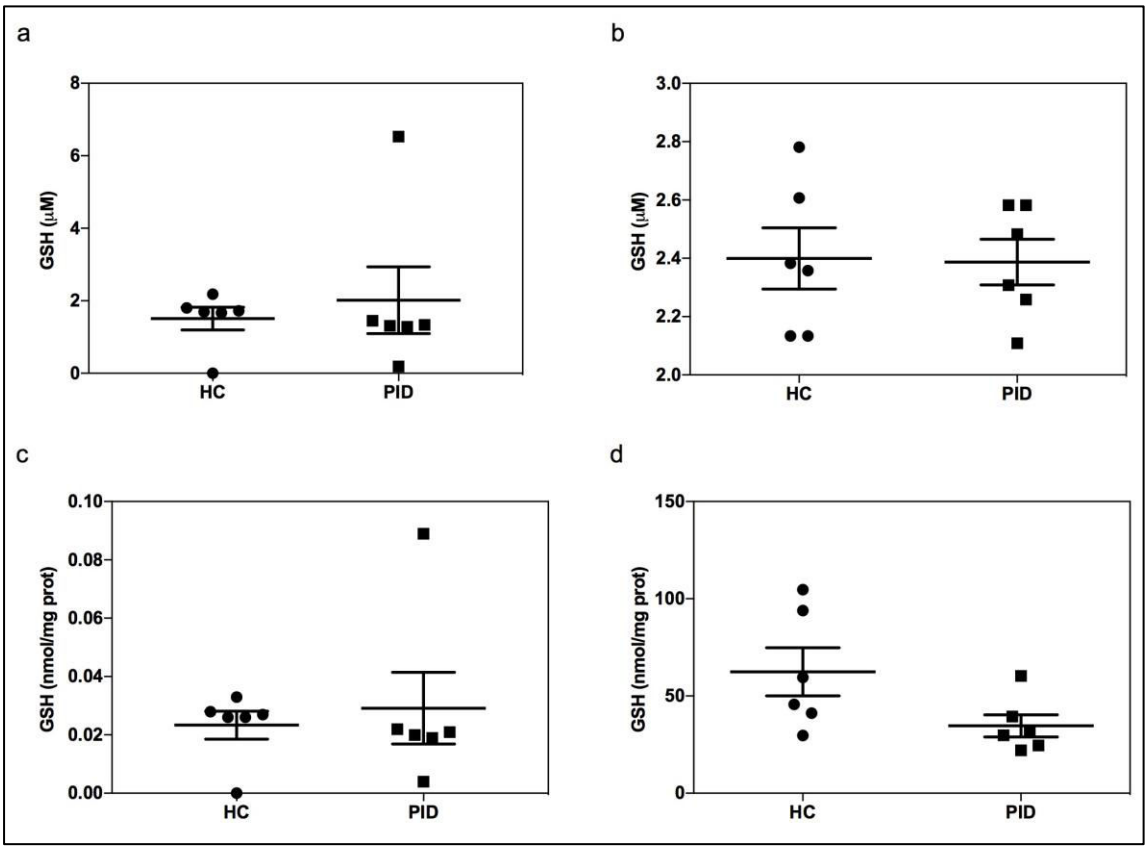

Figure 5.3 Reduced glutathione levels in the plasma (a, c) and GCF (b, d) of PID patients and age-matched periodontally healthy controls (HC). Plasma was collected from whole blood by centrifugation. GCF was collected on Periopaper™ strips (Oraflow Inc., Plainview, NY, USA) and extracted from the strips by centrifugation. GSH was determined by the recycling assay, as previously described (2.18). Data are presented as mean ± SEM, and was normalised to protein content on c and d. N = 6. Mann-Whitney test was performed using GraphPad Prism (v6.02) software and no statistical significance was found.

5.4.4. Validation of CD4 and CD8 T cell extraction for the study of gene expression in periodontitis patients

To evaluate the reproducibility of CD4 and CD8 T cells extraction and RT-QPCR analysis of selected genes, CD4 and CD8 T cells were extracted from whole blood of a healthy volunteer in triplicate. The purity of the CD4 and CD8 T cells obtained was assessed by flow cytometry as outlined in section 2.5.6.

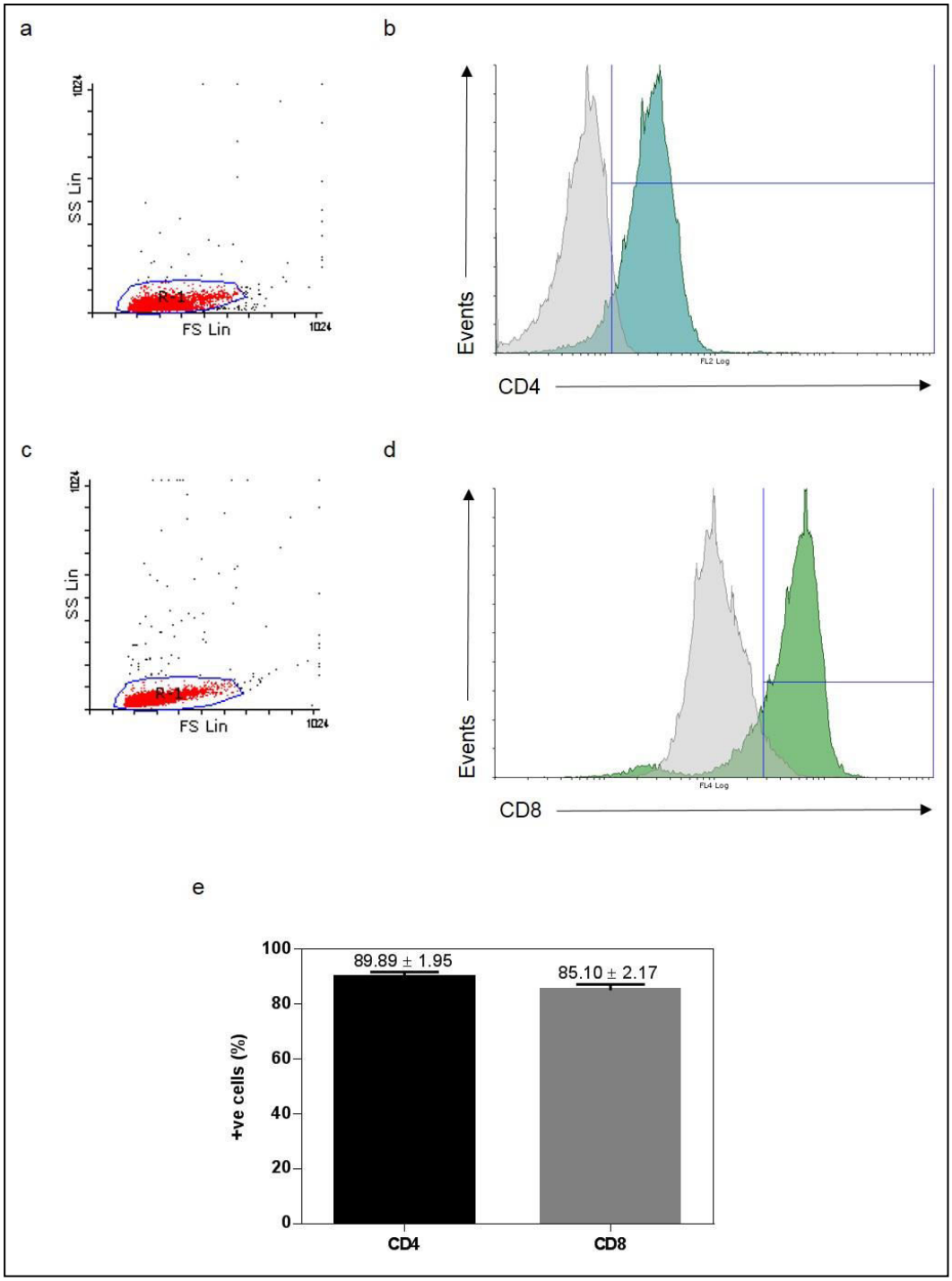

Figure 5.4 Purity of CD4 and CD8 T cells isolated from whole blood. CD4 and CD8 T cells were positively isolated as previously described and stained with anti-CD4-PE or PE isotype control and anti-CD8-PE-Cy5.5 or PE-Cy5.5 isotype control, respectively, and analysed by flow cytometry. Data acquisition was stopped when 25,000 events were obtained. a) FSC and SSC of the whole cell population stained for CD4. b) Overlay plot of isotype control (grey histogram) and anti-CD4-PE (blue histogram) stained T cell population. c) FSC and SSC of the whole cell population stained for CD8. d) Overlay plot of isotype control (grey histogram) and anti-CD8-PE-Cy5.5 (green histogram) stained T cell population. Positive cells were considered above 5% positive of isotype control staining. e) Percentage of CD4 and CD8 positive T cells calculated relative to 5% positive staining of the isotype control. Data are presented as mean ± SEM.

mRNA was extracted from CD4 and CD8 T cells, converted to cDNA and the expression of *ASS1* and *HK3* analysed by RT-QPCR. The amount of CD4 and CD8 T cells obtained from the same healthy donor in three replicate extractions showed high variability, however, the amount of mRNA obtained after lysis of the cells was similar. The analysis of *ASS1* and *HK3* genes and the housekeeper gene *YWHAZ* revealed C_T values very similar for CD4 and CD8 T cells. The gene expression, investigated by the comparative C_T method, also presented similar results of expression of *ASS1* and *HK3* in CD4 and CD8 T cells from one healthy donor analysed in triplicate (Table 5.2).

Table 5.2 Reproducibility of CD4 and CD8 T cell isolation. CD4 and CD8 T cells were positively isolated from one healthy donor in triplicate to assess reproducibility.

		10^5 cells/mL	mRNA (ng/µL)	raw C_T (*YWHAZ-ASS1*)	raw C_T (*YWHAZ-HK3*)	raw C_T (*ASS1*)	raw C_T (*HK3*)	2-ΔΔC_T (*ASS1*)	2-ΔΔC_T (*HK3*)
CD4	Replicate 1	3.9	15.8	19.54	19.99	25.32	31.90	0.72	0.40
	Replicate 2	11.2	13.7	19.74	20.18	25.03	31.80	1.01	0.49
	Replicate 3	1.0	13.2	20.33	20.85	25.34	31.67	1.23	0.86
CD8	Replicate 1	3.2	9.9	19.59	20.15	25.75	32.20	0.63	0.33
	Replicate 2	0.3	8.6	19.74	20.13	26.75	32.33	0.35	0.29
	Replicate 3	0.2	6.9	19.70	20.20	25.33	32.03	0.90	0.38

5.4.5. Gene expression in peripheral CD4 and CD8 T cells from periodontitis patients

In chapter 4, *ex vivo* studies on the effect of PAD enzymes on PBMC revealed expression alterations in some genes. Here, peripheral CD4 and CD8 T cells were isolated from blood of PID patients and HC individuals and analysed by RT-QPCR for the expression of the genes studied before (*ASS1*, *HK3*, *CD163*). Additionally, the expression of *IL-2* and *IFN-G* was also analysed to provide information regarding T cell activation status. *ENO* was also selected for study here; *ENO* encodes for α-enolase, an enzyme involved in glycolytic metabolism and that is also known to be citrullinated in RA [254]. The expression of *ULBP1* was also addressed. *ULBP1* was one of the genes found to be up-regulated by both PAD enzymes on the PBMC microarray study (Figure 4.10). *ULBP1* encodes for the cell surface UL16 binding protein 1, which is a ligand for the killer cell lectin-like receptor subfamily K, member 1 / natural killer group 2D receptor (KLRK1/NKG2D receptor) and, consequently, is involved in immune responses.

Initially, the peripheral CD4 and CD8 T cells positively isolated from whole blood of six PID patients and six HC individuals were lysed and mRNA extracted. The number of cells and the amount of mRNA obtained were variable between the two cell subsets (Table 5.3). Note that samples with less than 2 ng/μL of mRNA (highlighted in grey in table 5.3) were not further analysed by RT-QPCR since this amount of mRNA is not sufficient to be converted to cDNA and subsequent RT-QPCR.

Table 5.3 Number of cells and amount of mRNA obtained from peripheral CD4 and CD8 T cells from PID and HC groups. The samples highlighted represent samples where the amount of RNA extracted was not sufficient for the RT-QPCR experiment.

		10^6 cells/mL	mRNA (ng/µL)
CD4	PID	0.29	4.1
	PID	1.08	20.4
	PID	0.88	19.6
	PID	1.95	34
	PID	1.03	14.1
	PID	0.79	8.5
	HC	0.11	0.8
	HC	1.47	15.3
	HC	0.78	9
	HC	1.61	9.7
	HC	1.99	26.4
	HC	1.07	15.9
CD8	PID	0.27	1.5
	PID	1.03	8.3
	PID	0.68	9.8
	PID	1.12	20.9
	PID	0.8	11.7
	PID	0.9	11.6
	HC	0.05	0.7
	HC	0.61	6.4
	HC	0.33	4.1
	HC	1.62	5.1
	HC	0.89	11.1
	HC	5.37	8.2

ASS1 and *ULBP1* were found to be up-regulated in PBMC pre-treated with PAD enzymes and activated with anti-CD3/anti-CD28. This was found initially in the microarray studies and further confirmed by RT-QPCR for *ASS1* (Figures 4.10 and 4.14). However, the expression analysis for these genes by RT-QPCR on CD4 and CD8 T cells from PID and HC did not reveal statistically significant differences. *ASS1* and *ULBP1* expression showed a trend towards an increase in both peripheral CD4 and CD8 T cells from PID, when compared with HC (Figures 5.5a and 5.5c).

HK3 and *CD163* were two of the genes found to be down-regulated in PAD pre-treated and activated PBMC on the microarray studies (Figure 4.11). By RT-QPCR studies, the expression of *CD163* was shown to be down-regulated by both PAD enzymes on activated PBMC but the expression of *HK3* was only down-regulated by hPAD2 enzyme, while the hPAD4 enzyme induced an up-regulation of this gene after PBMC activation. In peripheral CD4 and CD8 T cells from PID and HC the expression

of *CD163* was not detected and the average expression of *HK3* was found to be down-regulated in PID when compared with HC (Figure 5.5b).

IL-2 and IFN-γ are markers of T cell activation. The expression of *IL-2* and *IFN-G* was also assessed here in order to provide information regarding the activation status of T cells. In HC individuals and PID patients and *IL-2* and *IFN-G* expression did not show statistical significant alterations in PID when compared with controls, however, both the average expression and paired expression pointed towards increased levels of *IL-2* and *IFN-G* expression in peripheral CD4 and CD8 T cells from PID, compared with HC (Figures 5.5d, 5.5e, 5.6d and 5.6e).

The expression of *ENO* in peripheral CD4 and CD8 T cells from PID patients revealed high inter-individual variability and no trend was seen (Figure 5.5f).

The paired analysis of the results corroborated the findings stated above (Figure 5.6); four out of five pairs showed higher expression of *ASS1*, *IFN-G* and *IL-2* in CD4 T cells from PID patients in comparison to HC individuals; four out of five pairs showed higher expression of *ASS1* and *IFN-G* in CD8 T cells from PID patients in comparison to HC individuals; four out of five pairs showed lower expression of *HK3* in CD4 and CD8 T cells from PID patients in comparison to HC individuals; *ULBP1* and *ENO* showed variable expression in both CD4 and CD8 T cells from PID patients in comparison to HC individuals.

Table 5.4 Raw C_T values of the housekeeper *YWHAZ* in the plate of each of the selected genes analysed by RT-QPCR. CD4 and CD8 T cells were positively isolated from six periodontitis patients (PID) and six periodontally healthy controls (HC) and the mRNA extracted, converted into cDNA and used to evaluate the levels of *ASS1*, *HK3*, *ULBP1*, *IL-2*, *IFN-G* and *ENO* transcripts by RT-QPCR in an Agilent Max3000P QPCR system (Agilent Technologies LDA UK Ltd, Stockport, UK). Raw C_T values are presented. N = number of independent experiments (donors) performed.

		YWHAZ C_T values for each primer plate																	
		ASS1 primer			*HK3* primer			*ULBP1* primer			*IL-2* primer			*IFN-G* primer			*ENO* primer		
		Mean	SEM	N	Mean	SEM	N	Mean	SEM	N	Mean	SEM	N	Mean	SEM	N	Mean	SEM	N
CD4	HC	20.58	0.15	5	21.10	0.16	5	20.60	0.09	5	20.26	0.13	5	20.63	0.07	5	20.60	0.23	5
	PID	20.36	0.14	6	20.92	0.15	6	20.53	0.09	6	20.23	0.09	6	20.48	0.06	6	20.56	0.38	6
CD8	HC	20.32	0.11	5	21.22	0.22	5	20.29	0.12	5	20.18	0.12	5	20.22	0.11	5	20.76	0.33	5
	PID	19.98	0.11	5	20.65	0.18	5	19.96	0.14	5	19.77	0.13	5	20.34	0.13	5	20.18	0.20	5

Table 5.5 Raw C_T values of selected genes analysed by RT-QPCR. CD4 and CD8 T cells were positively isolated from six periodontitis patients (PID) and six periodontally healthy controls (HC) and the mRNA extracted, converted into cDNA and used to evaluate the levels of *ASS1*, *HK3*, *ULBP1*, *IL-2*, *IFN-G* and *ENO* transcripts by RT-QPCR in an Agilent Max3000P QPCR system (Agilent Technologies LDA UK Ltd, Stockport, UK). Raw C_T values are presented. N = number of independent experiments (donors) performed.

		C_T values																	
		ASS1 primer			*HK3* primer			*ULBP1* primer			*IL-2* primer			*IFN-G* primer			*ENO* primer		
		Mean	SEM	N	Mean	SEM	N	Mean	SEM	N	Mean	SEM	N	Mean	SEM	N	Mean	SEM	N
CD4	HC	25.89	0.16	5	31.7	0.16	5	30.93	0.11	5	32.29	0.30	5	28.42	0.17	5	22.86	0.19	5
	PID	25.21	0.15	6	31.87	0.13	6	31.09	0.35	6	31.13	0.17	6	28.08	0.27	6	22.51	0.10	6
CD8	HC	25.81	0.18	5	31.65	0.09	5	29.34	0.18	5	33.12	0.23	5	26.25	0.33	5	22.29	0.09	5
	PID	25.13	0.20	5	31.66	0.11	5	28.83	0.36	5	31.95	0.55	5	25.22	0.12	5	22.10	0.10	5

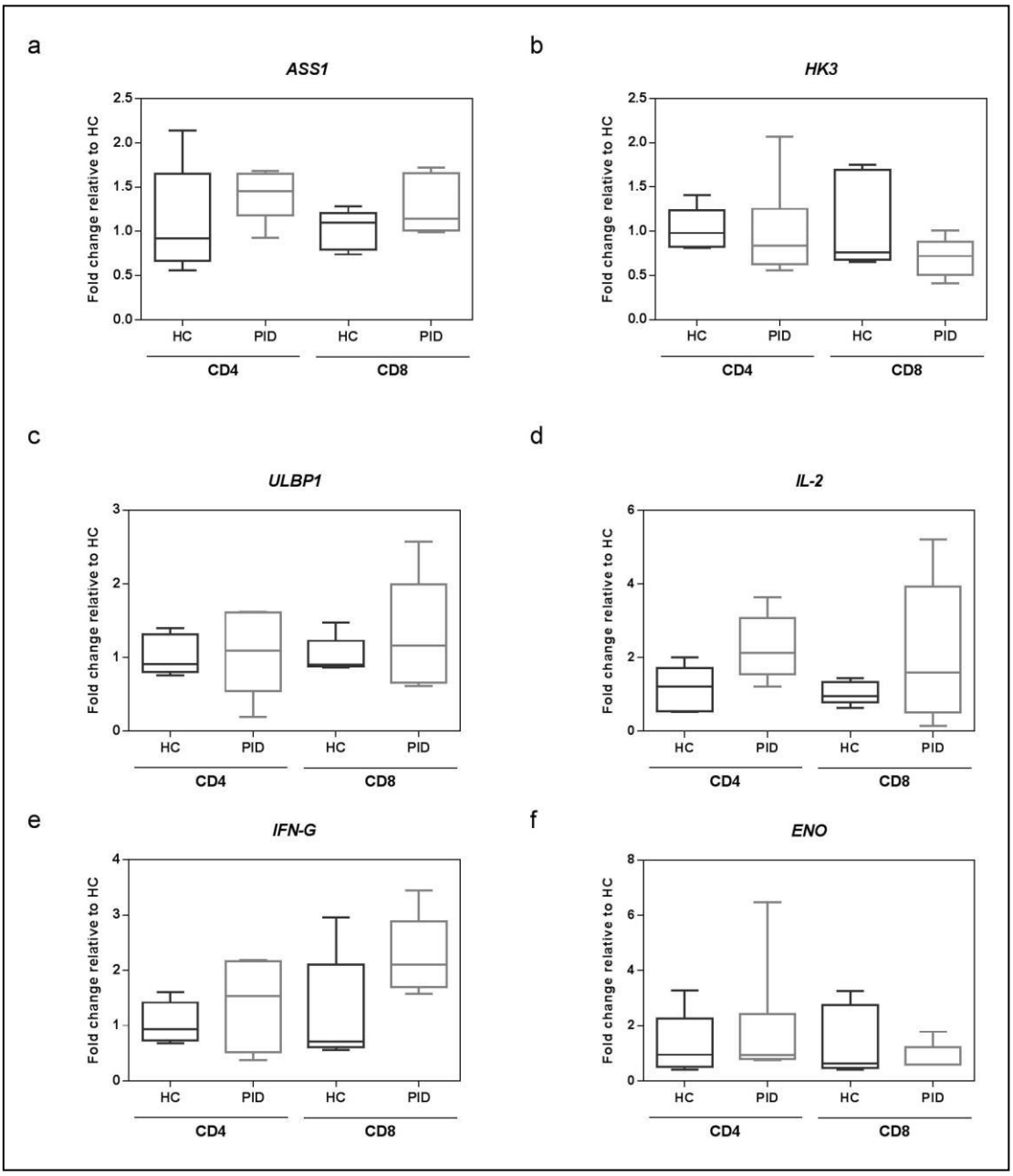

Figure 5.5 Fold changes in the expression of selected genes relative to HC. CD4 and CD8 T cells were positively isolated from five PID patients and five HC and the mRNA extracted, converted into cDNA and used to evaluate the levels of *ASS1* (a), *HK3* (b), *ULBP1* (c), *IL-2* (d), *IFN-G* (e) and *ENO* (f) transcripts by RT-QPCR. Results were obtained with the comparative C_T method and are expressed as fold change relative to HC. N = 5. Boxes represent 5–95 percentile range and the midline corresponds to the median. Mann-Whitney test was performed using GraphPad Prism (v6.02) software to compare PID and HC within CD4 and CD8 groups and no statistical significance was found.

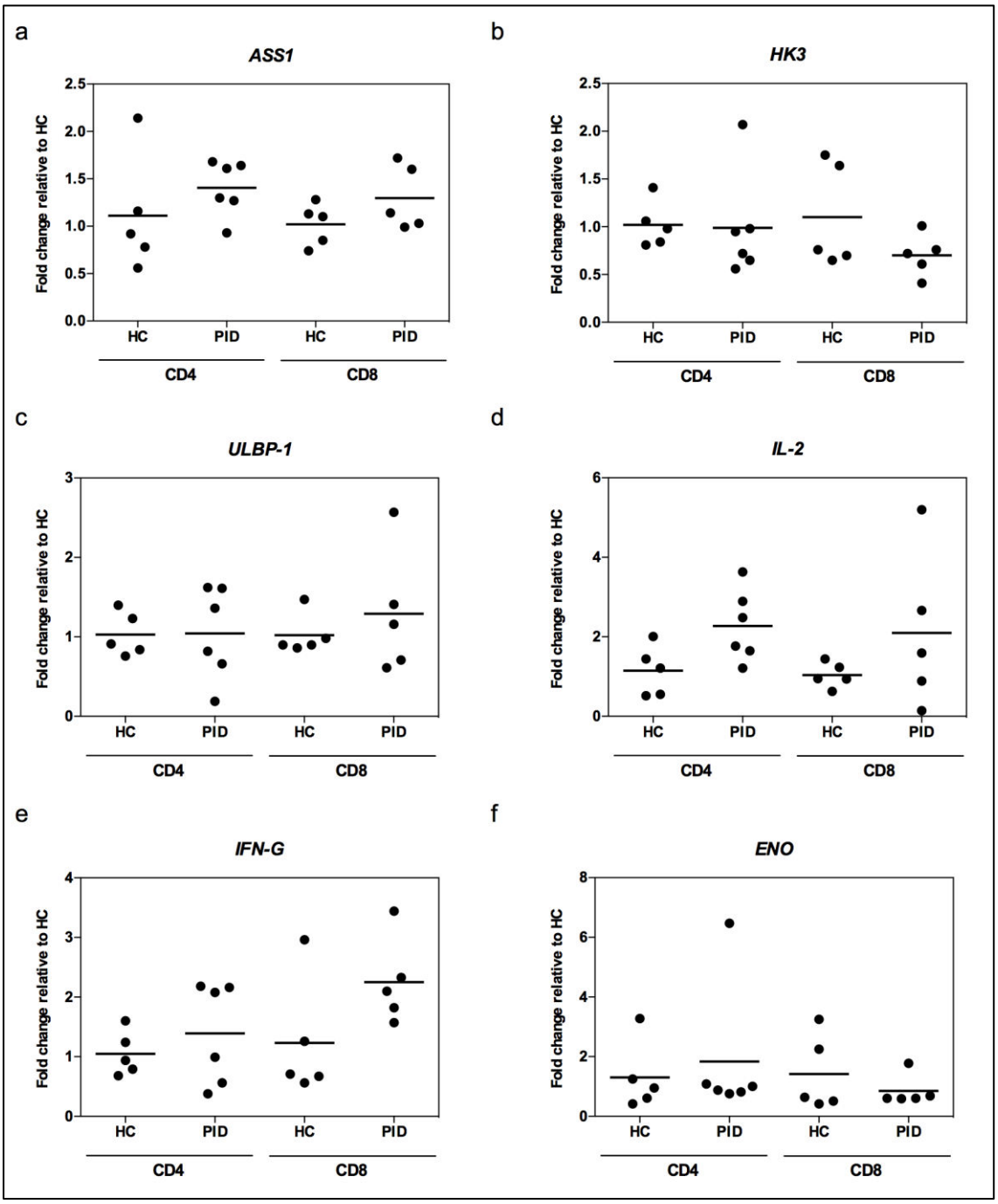

Figure 5.6 Individual fold changes in the expression of selected genes relative to HC. CD4 and CD8 T cells were positively isolated from six PID patients and six age-matched HC and the mRNA extracted, converted into cDNA and used to evaluate the levels of *ASS1* (a), *HK3* (b), *ULBP1* (c), *IL-2* (d), *IFN-G* (e) and *ENO* (f) transcripts by RT-QPCR. Results were obtained with the comparative C_T method and are expressed as fold change relative to age-matched HC. N = 5–6. Mann-Whitney test was performed using GraphPad Prism (v6.02) software to compare PID and HC within CD4 and CD8 groups and no statistical significance was found.

5.5. Discussion

PID is a chronic inflammatory disease that affects periodontal tissue. PID is characterised by the accumulation of lymphocytes [522, 523], the increase of pro-inflammatory plasma factors, such as cytokines [519], the decrease in antioxidant levels [520] and the occurrence of citrullination by PAD enzymes [443].

The parameters evaluated here in the plasma and GCF of PID patients and HC individuals did not show statistically significant differences. Only six individuals were included in each group which can be an explanation for the high individual variability on the results and the lack of statistical significance in the results. Gorska *et al.* have previously reported that cytokines profiles in serum samples from PID patients and healthy controls show high variability between individuals [524]. IL-6 and IL-8 were the selected cytokines to study since they were previously described as being involved in the activity of leukocytes, osteoblasts and osteoclasts in PID, both locally and systemically [525-527]. IL-6 is a multifunctional cytokine, involved in B cell differentiation, T cell proliferation and stimulation of Ig secretion by B cells [528]. IL-8 is particularly important in the mediation of chemotaxis and activation of neutrophils in the inflamed gingiva [529]. IL-6 and IL-8 levels were previously found to be increased in PID-associated tissues [527, 530-534].

PAD enzyme activity was found to be increased in some patients in the PID group relative to HC. This is in agreement with previous findings from Harvey *et al.*, who described that the expression of hPAD2 and hPAD4 enzymes and citrullinated proteins increased with the severity of inflammation observed in PID [443].

The control of redox balance is key for an efficient immune response. GSH is one of the most important regulators of this balance. Previous studies have shown that glutathione in its reduced form is decreased in GCF and plasma from PID patients [520, 521]. Here, we found no differences in the levels of GSH in the plasma of PID patients when compared with HC groups. Despite the fact that no statistical

significance was observed, the levels of GSH in the GCF of PID patients were lower when compared with HC individuals, in agreement with previous reported data [520, 521].

The results point towards an oxidation and citrullination-induced environment in PID patient plasma. The susceptibility for T cells to be modified by citrullination was shown with the experiments performed in chapter 4, where the effect of PAD enzymes on the activation of T cells within the PBMC population was studied.

Within PBMC, T cells are involved in immune regulation processes and are necessary for the specific antibody production and polyclonal B cell activation, observed in PID, being essential for the pathogenesis of periodontal inflammation [535-540]. Cytokine secretion profile can be used to subdivide CD4 (Th) and CD8 (Tc) T cells into Th1, Th2, Tc1 and Tc2, respectively [541-543]. Th1 cells produce IL-2, IFNγ and TNF-α and –β and are involved in cell-mediated responses in the elimination of intracellular pathogens. Th2 cells secrete IL-4 and IL-5 and promote B cell growth and differentiation [543]. Tc1 release IFNγ and TNF-α and are involved in cytotoxic events. Tc2 secrete IL-4 and provide help for Ig secretion by B cells [544]. An effective immune response is highly dependent on the balanced generation of the different subsets of T cells and secretion of the correspondent cytokines.

In advanced PID, a suppression of adaptive immunity response has been reported [236-240]. Lymphocyte suppression by bacteria involved in PID was demonstrated in several studies [236-240]. T cells isolated from tissue of PID patients were shown to have a reduced IL-2 response [243, 440] but no differences in intracellular IFNγ levels [545]. Additionally, T cells isolated from whole blood of PID patients revealed similar levels of T cells as healthy individuals but with reduced functional activities [545, 546]. Petit *et al.* showed that the proportion of peripheral CD4 and CD8 T cells committed to Th1/Th2 or Tc1/Tc2, respectively, from PID patients does not differ from periodontally healthy individuals. Moreover, these authors reported no differences in intracellular IFNγ and IL-4 levels on CD4 T cells from PID and HC but

they found an increase in the intracellular levels of IL-4 in CD8 T cells from PID when compared with controls, indicating a shift towards Tc2 functions in the CD8 T cell population.

Here, peripheral CD4 and CD8 T cells were isolated from PID and HC individuals, in order to assess gene expression patterns in the two T cell subsets. The number of CD4 and CD8 T cells between PID and HC showed no differences. The expression of *IL-2* and *IFN-G* was found to be increased in CD4 and CD8 T cells from PID patients when compared with HC individual, suggesting an increased T cell response. In this Chapter, gene expression levels of IL-2 and IFN-γ cytokine mRNA were evaluated, whereas in the previous studies reported by others, protein levels were measured. The difference in the analysed samples (mRNA versus protein) might explain the unconsistency of these results with previous ones since mRNA and protein have different processing times.

ASS1 and *HK3* expressions in CD4 and CD8 T cells from PID patients were found to be up- and down-regulated, respectively, consistent with what was previously found in chapter 4. The levels of ASS1 are related with T cell differentiation and function. An up-regulation of the gene responsible for this protein suggests *de novo* synthesis of arginine via ASS1 by T cells, possibly to counteract a decrease in the levels of arginine, resultant from impaired T cell proliferation [464, 468, 469]. Lower levels of arginine are also involved in impaired aerobic glycolysis [468], which corresponds to the down-regulation of *HK3* in T cells from PID patients that was identified in this Chapter.

CD163 is a monocyte/macrophage-specific scavenger receptor and consequently, it is not surprising that its expression was not detected on CD4 and CD8 T cells obtained here.

ULBP1 and *ENO* were two additional genes studied here that were not analysed in the previous chapter. ULBP1 is a NKG2D receptor that is present in both NK and T cells and is involved in the immune system activation, through the activation

of signal transduction pathways. ENO is responsible for the conversion of 2-phosphoglycerate to phosphoenolpyruvate in the final steps of glycolysis and is has also been identified as a citrullinated antigen in RA [254]. Additionally, ENO has been detected on the surface of vascular endothelium [547], monocytes, macrophages, B cells and T cells [548] and is recognised as a plasminogen receptor. In ageing studies, ENO was found to be lower on the surface of CD4 T cells in healthy older adults [549]. RT-QPCR data showed no differences in the expression of *ULBP1* and *ENO* in peripheral CD4 and CD8 T cells from PID patients relative to HC.

Taken together, the results from this chapter indicate that PID patients are characterised by lower levels of GSH and higher levels of citrullination activity by PAD enzymes in the GCF. Consistent with the previous chapter, which investigated the effect of citrullination on T cells, here PID patients presented T cell with metabolic changes that indicate decreased glycolysis and increased amino acid biosynthetic pathway. Since T cells rely on aerobic glycolysis and glutaminolysis to meet the energetic requirements of proliferation, an impairment of these metabolic pathways due to the effects of PAD enzymes can be associated with decreased T cell proliferation. Taking the data obtained in this chapter as a pilot and considering PAD activity as a critical readout for the observed effects of PAD enzymes it can be estimated that the inclusion of seven samples in each of the tested groups would lead to 80% probability of observing a significant difference (p-value < 0.05) in the levels of PAD activity between PID and HC individuals (G*power software calculation).

Chapter 6 Concluding remarks

6.1. General discussion

Citrullination is defined as the PTM resulting from the conversion of peptidylarginine to peptidylcitrulline catalysed by PAD enzymes [109]. Five human isoforms of PAD enzymes (PAD1–4 and PAD6) have been described in the human genome and are differentially expressed in specific tissues. Except for PAD4 enzyme, which translocate to the nucleus, PAD enzymes are typically located in the cytoplasm of different cell types [336]. Of particular interest, PAD enzymes expressed in white blood cells recruited to inflammation sites, can be released to the extracellular environment when apoptosis occurs and act on extracellular proteins. Physiologically, citrulline is a non-essential amino acid, but citrullination is a vital reaction, being involved in keratinization of epithelial cells [120-124], inflammation [133, 147-150] and apoptosis [133, 140]. However, this conversion or arginine residues into citrulline residues in the polypeptide chain of proteins results in the loss of positive charge, affecting the protein structure and can lead to the formation of new protein motifs [109, 335]. In susceptible individuals, this process can induce the formation of neoantigens and trigger an immune response through the production of ACPA. This mechanism of citrullination-induced autoimmunity has been described in diseases such as RA [421] and PID [286]. RA and PID share similar pathological processes, including gene- and environmentally-associated disease susceptibility, soft and hard tissue destruction triggered by an exaggerated inflammatory response and the involvement of bacteria in the aetiology of the disease [284, 422]. Other key factors linking these two inflammatory diseases include the local and systemic production of autoantibodies [282, 355, 422-425] and the production of citrullinated peptides recognised by autoreactive T cells [285, 426]. It is recognised that citrullination is involved in the loss of immunological tolerance of the immune system in diseases such as RA and PID. However, to date, no studies have investigated the effects of PAD enzymes on the cells that mediate the autoimmune response. T cells have been shown to have

important roles in the development of the immune response observed in RA and PID, so this study focused on the effects of citrullination in the modulation of T cell response to activation. Initially, conditions were optimised for the detection and identification of citrullination, using modified FNG as a model, and a functional T cell activation model was established in order to address this hypothesis. Next, the effects of PAD enzymes on the activation of T cells were studied in PBMC, focusing on genes with altered expression and cell surface proteins modified by PAD enzymes. Finally, samples from PID patients were used to corroborate the findings on metabolic alterations observed on PBMC pre-treated with PAD enzymes.

From the five isoforms of PAD enzyme, PAD2 and PAD4 enzymes were identified by others in the synovium of RA patients [187-189, 361] and in inflamed gingiva of PID patients [443]. Consequently, these isoforms were selected for this study. Isoforms 2 and 4 of PAD enzyme share sequence homology, but are expressed by different cells in the synovial tissue, their intracellular localisation is different and their expression and activation are separately regulated at transcription, translation and enzyme activation [133]. Furthermore, PAD2 and PAD4 enzyme stability, calcium dependency, optimal pH range and substrate specificity are significantly different [377, 378].

In chapter 4, a model to study T cell activation was established and citrullination studies were performed using this model. T cell activation responses in Jurkat E6.1 T cells, an immortalised cell line, were compared with the T cell response in primary T cells within the PBMC population, where T cell activation is closer to physiological conditions. To activate T cells, the lectin PHA-L and antibodies against CD3 and CD28 were compared. The levels of IL-2 secreted to the extracellular medium of the cells, measured by ELISA, and the expression of CD25 at the surface of the cells, analysed by flow cytometry, confirmed that PBMC stimulated with anti-CD3/anti-CD28 antibodies were the most suitable model to study T cell activation. After the establishment of the activation T cell model, PAD2 and PAD4 enzymes were incubated with the cells to

assess their effects on the stimulation of T cell responses with anti-CD3 and anti-CD28 antibodies. PBMC pre-treated with PAD2 and PAD4 enzymes prior to activation revealed a trend to lower levels of CD4 T cells expressing CD25 at the surface. The levels of IL-2 secreted by the cells showed a significant increase when the cells were activated via CD3/CD28, but PBMC pre-treated with PAD2 and PAD4 enzymes and activated via CD3/CD28 showed a significant decrease of more than 50% in the levels of secreted IL-2 when compared with activated cells, suggesting alterations in the IL-2 T cell response. IL-2 is essential for T cell activation and proliferation and homeostasis of the immune system [550]. Decreased IL-2 production was previously reported in patients with autoimmune disease SLE [449], in cultured lymphocytes from patients with SLE [450] and in murine SLE models [451]. The reduced IL-2 secretion in SLE was suggested to derive from dysregulation of transcription or suppression of IL-2 production in SLE T cells [452]. The main consequences of the dysregulation of IL-2 secretion in SLE are the reduction in the number of Tregs that are involved in the inhibition of autoimmunity, the impairment of AICD, necessary for the down-regulation of expanded T cell clones [453, 454], and defective CD8 T cell cytotoxic functions [455]. *In vitro* studies in T cells isolated from SLE patients and activated with PHA, revealed impaired IL-2 secretion but normal expression of IL-2R [456]. This suggests that the T cell dysfunction observed in PBMC treated with PAD enzymes, similar to what is reported in SLE, may be a driver for autoimmunity. Also, in PID models and T cells from PID patients impairments in T cell responses were also observed [232, 236-240, 243, 439, 440]. In PID, reports on the IL-2 T cell response are contradictory. *P. gingivalis*, *F. nucleatum* and *A. actinomycetemcomitans*, bacterial species involved in PID, have been shown to impair human lymphocyte responsiveness to both mitogens and antigens by targeting IL-2 expression at DNA, RNA and protein levels [237, 238, 439]. Andrukhov et al. reported decreased levels of IL-2 in the serum of PID patients [551]. On the other hand, T cells collected from PID inflamed tissue showed increased

production of IL-2 indicative of increased *in vivo* stimulation [440] and Gorska et al. reported increased levels of serum and tissue IL-2 from PID patients [524].

PAD enzymes used in this study were obtained through recombinant expression, according to the manufacturer and, consequently, endotoxin (lipopolysaccharide – LPS) was suspected to be present. To address the effects of contaminating LPS in the mediation of the effects observed on different cell functions after cells were pre-treated with PAD enzymes, a control with HI PAD enzymes was performed. The 1D SDS-PAGE separation profile of FNG incubated with HI PAD enzymes did not show any differences when compared with FNG citrullinated with PAD2 and PAD4 enzymes in the presence of EDTA (a calcium chelator), confirming that the PAD enzymes have been inactivated with heating and any effects observed in cells following HI-PAD exposure are not likely to be due to citrullination. In terms of cellular functions, no significant inhibition of IL-2 secretion by T cells pre-treated with HI PAD enzymes prior to activation was observed and therefore the effects of hPAD treatment could not be associated to a non-enzymatic contaminant, like endotoxin. Endotoxin activates cells of the immune system through TLR4 signalling. Despite the fact that TLR4 is present in T cells, previous studies have shown that no effect on T cell proliferation or cytokine secretion can be linked to this receptor [552-554].

One of the aims here was to understand how PAD enzymes may modify the T cell responses; to identify the proteins at the cell surface that have been modified by PAD enzymes and, additionally, to identify the arginine residues that were citrullinated in the identified MP. To address this, in chapter 3, FNG was used as a model protein to optimise conditions for the detection of citrullination. FNG is an example of an extracellular protein that was found to be citrullinated in RA [184, 197, 198]. ACPA against citrullinated FNG were also found in the serum and synovial fluid of RA patients [170, 201] and constitute a well-known marker for RA with excellent sensitivity and specificity [363, 427]. Citrullination is responsible for 1 Da increase in the MW of the protein for each arginine residue that is converted to citrulline [335]; this makes the

detection of this modification difficult. However, differences in the separation of citrullinated FNG when compared with non-citrullinated FNG were found by 1D SDS-PAGE, 2D IEF/SDS-PAGE and 2D BN/SDS-PAGE, possibly due to conformational changes induced by the loss of a positive charge. van Beers and colleagues have previously shown that *in vitro* FNG citrullinated sites could be mapped by combining high resolution tandem mass spectrometry with imaging surface plasmon resonance microarray using RA patient sera [379]. Creese and colleagues have also developed a method for the identification of citrullinated sites based on the occurrence of neutral loss of isocyanic acid (43 Da) from citrullinated peptides that enables differentiating citrullination from other 1 Da producing modifications. In this method, the occurrence of neutral loss of isocyanic acid in the CID mass spectrum, triggers saETD of the parent ion, improving the identification and localisation of the modification site [310]. The analysis of *in vitro* citrullinated FNG by this method allowed the identification of eighteen arginine residues citrullinated by hPAD2 or hPAD4 enzymes amongst the three polypeptide chains of FNG, constituting a total of 28% of all the arginine residues present in FNG. From these, seven arginine residues were only citrullinated by hPAD2, whereas five arginine residues were exclusively citrullinated by hPAD4, suggesting that hPAD2 has a broader range of action compared with hPAD4. In the results from chapter 4, no significant differences were found in the IL-2 response between the treatments with hPAD2 and hPAD4. However, in the gene expression study, the effects of citrullination on PBMC activation were more pronounced on PBMC treated with hPAD2 enzyme compared with hPAD4, which suggests that the number of citrullinated arginine residues might have an impact on the readout effects. The proteomics results suggest that PAD2 and PAD4 citrullinated FNG can be detected by 1D and 2D electrophoretic techniques and that citrullinated sites can be identified by LC-CID-saETD-MS/MS. Furthermore, the separation of citrullinated FNG by 2D BN/SDS-PAGE enabled detection of native FNG in the first dimension and the three chains of the protein in the second dimension, confirming the potential to obtain more

information about protein aggregates. The separation of MP by this technique also allows information about protein-protein associations, as previously described for human protein complexes, to be obtained [382-388]. The application of 2D BN/SDS-PAGE followed by LC-CID-saETD-MS/MS to PBMC citrullinated with PAD enzymes allowed the identification of MP that were only present in specific conditions, like after treatment with PAD2 or PAD4. Of particular interest, MS data and GO analysis of pathways on the microarray study revealed a down-regulation of the complement system, which is consistent with an induction of T cell-mediated autoimmunity [499]. Furthermore, CRT was one of the proteins identified exclusively associated with PAD enzymes in MP. Citrullinated-CRT was found in the synovial tissue of RA patients [555] and the binding of this modified protein to the SE was also found to potentiate the activation of the innate immune system, when compared with the non-modified form [555, 556]. However, it was not possible to identify citrullination sites on the protein sequence by this technique. Previous studies from van Beers et al. [379] and Creese et al. [310] successfully mapped citrullination sites, but these only focused on single proteins and synthetic peptides, respectively, and not in complex protein mixtures, like the MP used here. Limitations in cell surface proteomic studies are usually associated with the heterogeneity and the amphiphilic nature of MP, combined with overall low relative abundance [557-559]. Citrullination efficiency is also arguable since MP contain less arginine residues than intracellular proteins and modification of arginine residues result in a lower number of available trypsin-targeted sites. The use of combined proteolytic enzymes is a common approach to improve the sequence coverage and minimise the influence of citrullination on the proteolytic cleavage. In the FNG studies this approach revealed good results, however in the PBMC studies it was not possible to digest MP with different enzymes due to the low abundance of initial sample.

To investigate the intracellular effects of PAD enzymes in the activation of T cells, in chapter 4 microarray studies were performed on PBMC pre-treated with PAD

enzymes followed by activation. Eight genes were found to be up-regulated and thirty-five genes were found to be down-regulated simultaneously by PAD2 and PAD4 enzymes. From these, five genes (*ASS1, CTH, HK3*, *CD163* and *SGMS2*) were selected for validation by RT-QPCR. Further, in chapter 5, peripheral CD4 and CD8 T cells isolated from PID patient were used to study the expression levels of these genes and additional candidate genes that were selected because of their role in cytokine signalling and metabolism (*IL-2*, *IFN-G*, *ULBP1* and *ENO*).

The sphingomyelin biosynthetic pathway is associated with TCR signalling in activated T cells. Here, *SGMS2* was one of the genes identified to be down-regulated by PAD enzyme pre-incubation prior to PBMC activation on the microarray results which, according with Tafesse et al. [560] can be associated with an impairment in T cell activation. However, the analysis of this gene by RT-QPCR was not possible in the majority of the PBMC studies and, consequently, it was not assessed in T cells isolated from PID patients and HC.

The soluble form of CD163 has been shown to be up-regulated in the sera of RA patients [470] and was also associated with global inflammation and impairment of T cell activation in SpA patients' synovium [471]. CD163 is a monocyte/macrophage-specific scavenger receptor and, consequently, it is not surprising to have been detected in the PBMC studies on chapter 4. *CD163* was found to be down-regulated in activated PBMC pre-treated with PAD enzymes in microarray studies but this was not confirmed by RT-QPCR due to high variation in the results. In CD4 and CD8 T cells from PID patients, *CD163* expression was not detected, confirming that the presence of this gene in PBMC analysis was due to other immune cells.

CTH expression was found to be up-regulated by PAD enzymes in the studies described in chapter 4. However, the levels of this gene were low, only obtained for one of the independent experiments performed and were possibly due to the presence of a mixed population of cells (PBMC). As a consequence, the expression of this gene was not further explored.

ASS1 and HK3 are two enzymes involved in metabolic processes, urea cycle and glycolysis respectively. Upon activation, T cells rely on glycolysis and glutamine oxidation, to produce biosynthetic precursors required for rapid cell growth and proliferation [72, 82, 84]. The results obtained here showed an up-regulation of *ASS1* in activated PBMC pre-treated with PAD enzymes, suggesting *de novo* synthesis of arginine possibly to overcome a decrease in the arginine supply that is related with impaired T cell proliferation. This situation would also imply impairment of aerobic glycolysis, which can be correlated with a down-regulation of *HK3* expression, that was observed here when PBMC were pre-treated with PAD2 enzyme prior to activation. Consistent with these, in chapter 5, *ASS1* and *HK3* expression levels in peripheral CD4 and CD8 T cells from PID patients were found to be up- and down-regulated, respectively.

The metabolic switch from OXPHOS to aerobic glycolysis and glutaminolysis following activation of T cells, reduces the up-regulation of glycolytic enzymes and glucose transporters and induces an increased production of lactate [458, 561]. The results obtained in the PBMC citrullination study show that the higher lactate levels are associated with lower IL-2 secretion and, consequently, a non-activated T cell profile. However, an increase in the extracellular levels of lactate following T cell activation was not observed. An explanation for this might be the intracellular consumption of lactate to produce energy equivalents via OXPHOS. Lactate can be converted to pyruvate in the cytosol and this can then be transported to the mitochondria via the monocarboxylate transporter 1 and converted into pyruvate [562].

ENO was additionally selected for analysis in peripheral CD4 and CD8 T cells from PID patients since it is involved in glycolytic metabolism and it has also been identified as a citrullinated antigen in RA [254]. ENO was also detected on the surface of vascular endothelium [547], monocytes, macrophages, B cells and T cells [548] and is recognised as a plasminogen receptor. In ageing studies, ENO was found to be lower on the surface of CD4 T cells in healthy older adults [549]. However, RT-QPCR

data showed no differences in the expression of *ENO* in peripheral CD4 and CD8 T cells from PID patients relative to HC.

ULBP1 was one of the genes that was found to be up-regulated by PAD enzymes on the PBMC microarray study. The cell surface ULBP1, encoded by *ULBP1* gene, is a ligand for the KLRK1/ NKG2D receptor and is present on NK and T cells, being involved in the activation of several signalling pathways, resulting in the production of cytokines and chemokines. Although this gene was found to be up-regulated by PAD enzymes in PBMC, the analysis by RT-QPCR on peripheral CD4 and CD8 T cells revealed no differences between PID patients and HC individuals.

The cytokines IL-2 and IFNγ are established markers of T cell activation. In advanced PID, contradictory results have been obtained regarding the T cell response. For example, in the serum of PID patients, Andrukhov et al. reported a decrease in the levels of IL-2 but an increase in the levels of IFNγ [551], while Gorska et al. found higher concentrations of IL-2 and IFNγ in the serum and gingival tissue from PID patients [524]. Here, the expression of *IL-2* and *IFN-G* was found to be increased in peripheral CD4 and CD8 T cells from PID patients when compared with HC individuals, suggesting an increased T cell response. A possible explanation for the difference in the results obtained here is that expression of *IL-2* and *IFN-γ* genes were evaluated, whereas the studies reported in the literature protein levels were measured suggesting impairments in secretory pathways and not in the signalling via TCR.

In addition to peripheral CD4 and CD8 T cells, plasma and GCF from PID patients were assessed for inflammatory factors, like cytokines, antioxidants and occurrence of citrullination by PAD enzymes, all characteristic of PID [443, 519, 520, 522, 523]. IL-6 is a multifunctional cytokine, involved in B cell differentiation, T cell proliferation and stimulation of Ig secretion by B cells [528]. IL-8, a prototypic human chemokine, is particularly important in the mediation of chemotaxis and activation of neutrophils in the inflamed gingiva [529]. IL-6 and IL-8 were previously described as being involved in the activity of leukocytes, osteoblasts and osteoclasts in PID, both

locally and systemically [525-527]. IL-6 and IL-8 levels were previously found to be increased in PID-associated tissues [527, 530-534]. Here, no differences in the plasma levels of IL-6 and IL-8 were found in PID patients compared with age-matched periodontally healthy controls, probably due to the low number of samples.

The expression of hPAD2 and hPAD4 enzymes and citrullinated proteins were found to be increased with the severity of inflammation observed in PID [443]. Consistent with this, here, the PAD enzyme activity was found to be increased in the PID group relative to HC.

GSH is one of the most important regulators of the redox balance required for an efficient immune response. Previous studies have shown that glutathione in its reduced form is decreased in GCF and plasma from PID patients [520, 521]. Here, we found no differences in the levels of GSH in the plasma of PID patients when compared with HC groups. Despite the fact that no statistical significance was observed, the levels of GSH in the GCF of PID patients were lower when compared with HC individuals, in agreement with previous reported data [520, 521].

The parameters evaluated in the plasma and GCF of PID patients and HC individuals did not show statistically significant differences. Only six individuals were included in each group, which can be an explanation for the high individual variability on the results and the lack of statistical significance in the results. However, the use of G*Power software suggested that the inclusion of seven samples per group would result in 80% probability of observing a significant difference (p-value < 0.05) in the levels of PAD activity between the PID and HC groups.

Generally, one of the main limitations of this study is the low number of samples in the clinical studies and replicates in the PBMC *ex vivo* studies. This is an important point that can be overcome by the repetition of the *ex vivo* experiments and the recruitment of more PID and HC individuals. Such additional work has the potential to raise the relevance and impact of this study. Despite this, a major strength of this work is the translational research performed from *in vitro* single protein model to *ex*

vivo PBMC studies and from there to clinical samples. The simple *in vitro* model was important for the methodological optimisation, whereas the *ex vivo* studies were crucial to perform broad screening approaches that allowed to identify targets to be studied on clinical samples. Using such a translational approach is extremely advantageous as each method can provide different and complementary information that together can contribute to the general knowledge about the effects of citrullination on the breakdown of the immune system in PID.

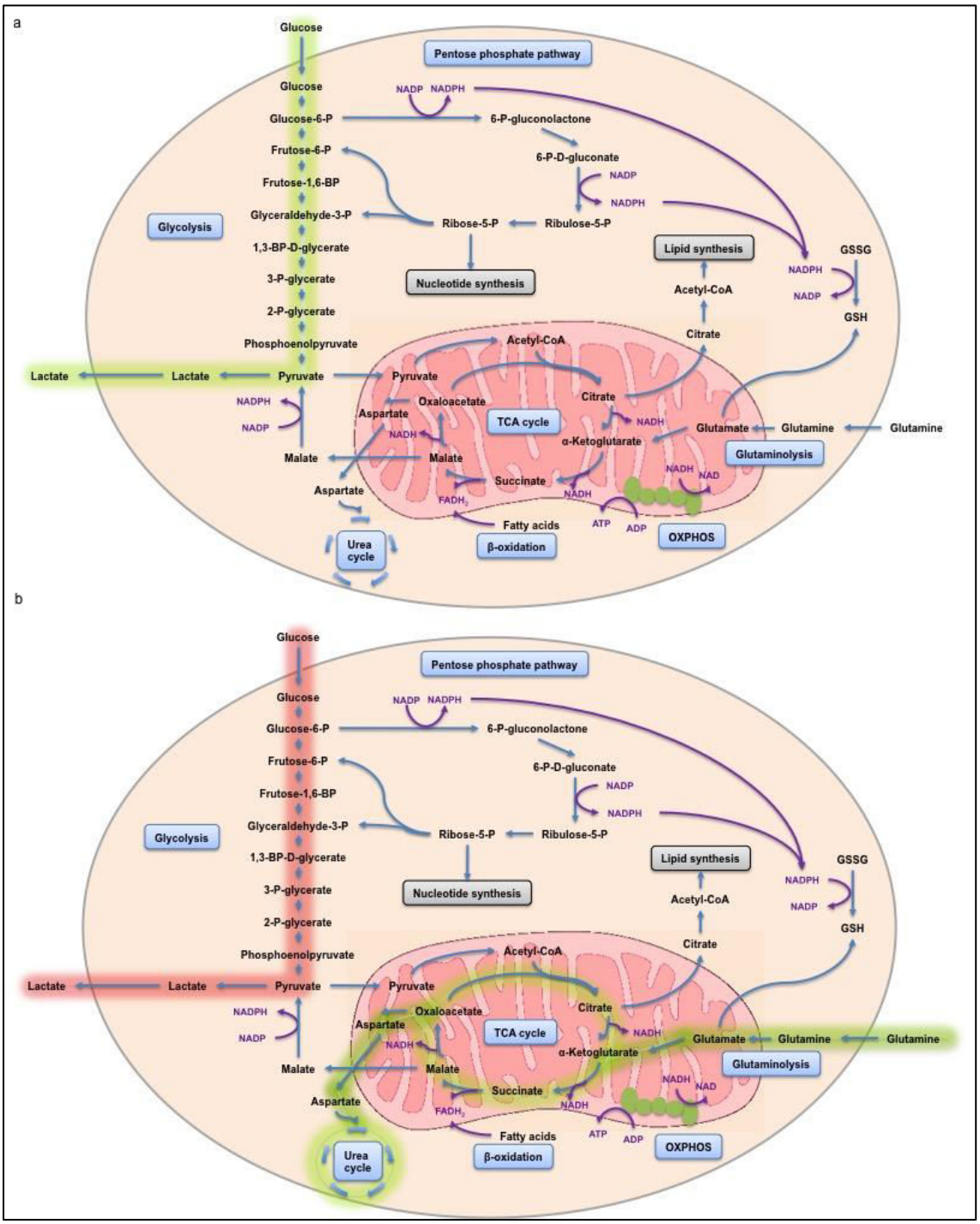

Figure 6.1 Schematic representation of glucose and glutamine metabolism in activated T cells (a) and activated T cells pre-treated with PAD enzymes (b). Green highlights up-regulated pathways and red highlights down-regulated pathways.

6.2. Future work

Several studies can be suggested to complement the translational approach used here. In the *in vitro* model, the combination of 1D SDS-PAGE and LC-CID-saETD-MS/MS showed to be valid for the detection of FNG chains and to identify the arginine residues modified by citrullination. The separation of MP from citrullinated PBMC by 2D BN/SDS-PAGE allowed identification of some proteins, however no specific PAD-mediated citrullination sites were identified. Due to their hydrophobic nature, MP are a particularly difficult class of proteins to analyse by common electrophoretic methods. The use of a 2D method here was adopted as a way of obtaining more information about the protein structure, in particular, protein-protein interaction, and also to maximise the separation of different proteins in order to identify differences between different treatments. Further optimisation of this approach is required, namely in terms of protein solubilisation. The use of different detergents and also different detergent/MP ratios are suggestions to improve the solubilisation of MP. Also, other methods of MP isolation could be approached, as biotinylated-based methods that use a cell impermeable biotinylated reagent to label exposed primary amines of proteins on the surface of intact cells and are then purified with avidin-based resins. Another proposed strategy to identify MP modified by citrullination is to use a targeted approach as opposed to a broad screening approach as the one used here. As the targeted cells of this study were T cells, the TCR complex is a potential target for citrullination, so, the immunoprecipitation of CD3 or CD28, for example, would allow the purification of the TCR complex and any associated proteins; LC-CID-saETD-MS/MS could be applied to detect and identify arginine residues in the proteins of the complex that are modified by PAD enzymes. This approach would only focused on the effects of PAD on the TCR complex, but as an impairment of the IL-2 response was observed, this would be a possible method to identify proteins at the cell surface modified by PAD enzymes and to localise the citrullinated arginine residues within the protein sequence. With a refined

method for the identification of MP and citrullinated residues it would be possible to apply the strategy to MP from PID and RA patients' peripheral CD4 and CD8 T cells or even other subsets, as Th17.

In order to understand the impairment of the IL-2 T cell response observed in chapter 4, some targeted studies could be performed. Obtaining information about the expression of *IL-2* gene would be a good first indicator if the effects of PAD to decrease T cell proliferation were due to up- or down-stream regulation of *IL-2* gene expression. According with the results of the *IL-2* gene expression, intracellular signalling studies could be performed in terms of TCR signalling or IL-2 translation and secretion. Another interesting way to investigate the impairment on T cell activation would be to target transcription factors like t-bet, since this is crucial for the differentiation of T cells. These experiments would elucidate about PAD-induced anomalies in the IL-2 signalling pathway that could be used for further therapeutic applications.

The results obtained in this study suggest that PAD enzymes induce an impairment of T cell response that is linked to alterations in glycolysis and amino acid metabolism. Further investigation of metabolic activity of the cells would be important to clarify this. The use of Seahorse XF technology (Agilent Technologies LDA UK Ltd., Stockport, UK) is a possible approach to obtain functional data from live cells, in real time, providing a greater understanding of cell metabolism. The Seahorse XF analyser combines an electro-optical instrument with plastic cartridges that provide real time measurement of the two major energy pathways of the cell (mitochondrial respiration and glycolysis) in a non-invasive, multi-well microplate format. Complementary to this information about the use of glycolysis of OXPHOS, it would also be interesting to target GLUT1 and MCT1, as this are vital transporters for the uptake of glucose and efflux of lactate, respectively, both outcomes of aerobic glycolysis. Another important complementary study to the RT-QPCR would be to match the results obtained with

protein and enzymatic activity data on ASS1 and HK3, since it is the protein form that is responsible for activity not the gene form.

The results obtained in chapter 5, regarding the pilot comparison of T cell gene expression in PID patients with age-matched periodontally HC were not powered to show significant differences so, as previously suggested, it would be important to increase the number of samples and also to assess parameters, such as the secretion of IL-2 and IFNγ to complement the results obtained from PBMC studies and RT-QPCR.

In general, it would also be interesting to compare the effects of human PAD enzymes, studied here, with the effects of PPAD enzyme on the activation of T cells. Khalaf and Bengtsson have previously suggested that arginine gingipain proteinases from *P. gingivalis* are involved in the suppression of IL-2 accumulation attenuating T cell proliferation and cellular communication, consequently being involved in the evasion of the host adaptive immune system [439]. Understanding the mechanism of action of human and bacterial PAD enzymes and blocking the generation of autoantigens that trigger the autoimmune response observe in RA and PID may lead to new knowledge that can be applied to develop powerful novel therapies for these diseases.

6.3. Conclusion

Taken together, the results obtained here suggest that PID patients are characterised by lower levels of GSH and higher levels of PAD enzymes in the GCF. Also, PAD enzyme modification of PBMC alters expression of genes involved with glucose and amino acid metabolism, which is associated with a reduction in the T cell IL-2 response. Consistent with this, PID patients presented with differences in T cell metabolism compared to HC that indicate decreased glycolysis and increased amino acid biosynthetic pathway and, consequently, impairment of T cell proliferation. Also, proteomic and genomic studies both revealed an involvement of the complement system in the impairment of the T cell response.

Chapter 7 References

1. Janeway, C.A., et al., *Immunobiology: The Immune System in Health and Disease*. 6th ed. 2004: New York: Garland Science.

2. Janeway CA Jr, T.P., Walport M, et al., *Immunobiology: The Immune System in Health and Disease*. 5th ed. 2001, New York: Garland Science.

3. Lindstrom, T.M. and W.H. Robinson, *Rheumatoid arthritis: a role for immunosenescence?* J Am Geriatr Soc, 2010. **58**(8): p. 1565-75.

4. Lacy, P. and J.L. Stow, *Cytokine release from innate immune cells: association with diverse membrane trafficking pathways.* Blood, 2011. **118**(1): p. 9-18.

5. Alberts B, J.A., Lewis J, et al. , *Molecular Biology of the Cell*. 4th ed. 2002, New York: Garland Science.

6. Dunkelberger, J.R. and W.C. Song, *Complement and its role in innate and adaptive immune responses.* Cell Res, 2010. **20**(1): p. 34-50.

7. Strainic, M.G., et al., *Locally produced complement fragments C5a and C3a provide both costimulatory and survival signals to naive CD4+ T cells.* Immunity, 2008. **28**(3): p. 425-35.

8. Lalli, P.N., et al., *Locally produced C5a binds to T cell-expressed C5aR to enhance effector T-cell expansion by limiting antigen-induced apoptosis.* Blood, 2008. **112**(5): p. 1759-66.

9. Heeger, P.S., et al., *Decay-accelerating factor modulates induction of T cell immunity.* J Exp Med, 2005. **201**(10): p. 1523-30.

10. Serhan, C.N., P.A. Ward, and D.W. Gilroy, *Fundamentals of inflammation. [electronic resource]*. 2010: Cambridge ; New York : Cambridge University Press, 2010.

11. Hitchon, C.A. and H.S. El-Gabalawy, *Oxidation in rheumatoid arthritis.* Arthritis Res Ther, 2004. **6**(6): p. 265-78.

12. Cooper, G.M., *The Cell: A Molecular Approach*. 2nd ed. 2000: Sunderland (MA): Sinauer Associates.

13. von Heijne, G., *Membrane-protein topology.* Nat Rev Mol Cell Biol, 2006. **7**(12): p. 909-18.

14. Tuteja, N., *Signaling through G protein coupled receptors.* Plant Signal Behav, 2009. **4**(10): p. 942-7.

15. Lemmon, M.A. and J. Schlessinger, *Cell signaling by receptor tyrosine kinases.* Cell, 2010. **141**(7): p. 1117-34.

16. Grotzinger, J., *Molecular mechanisms of cytokine receptor activation.* Biochim Biophys Acta, 2002. **1592**(3): p. 215-23.

17. Rojas, A.I. and A.R. Ahmed, *Adhesion receptors in health and disease.* Crit Rev Oral Biol Med, 1999. **10**(3): p. 337-58.

18. Hynes, R.O., *Cell adhesion: old and new questions.* Trends Cell Biol, 1999. **9**(12): p. M33-7.

19. Joseph-Silverstein, J. and R.L. Silverstein, *Cell adhesion molecules: an overview.* Cancer Invest, 1998. **16**(3): p. 176-82.

20. Sanchez-Madrid, F., et al., *Cell Adhesion Molecules: Selectins and Integrins.* 1999. **19**(5-6): p. 41.

21. Etzioni, A., C.M. Doerschuk, and J.M. Harlan, *Of man and mouse: leukocyte and endothelial adhesion molecule deficiencies.* Blood, 1999. **94**(10): p. 3281-8.

22. Gumbiner, B.M., *Regulation of cadherin adhesive activity.* J Cell Biol, 2000. **148**(3): p. 399-404.

23. Takeichi, M., *Cadherin cell adhesion receptors as a morphogenetic regulator.* Science, 1991. **251**(5000): p. 1451-5.

24. O'Connor, C.M. and J.U. Adams, *Essentials of Cell Biology*. 2010, Cambridge MA: NPG Education.

25. Ciofani, M., et al., *Stage-specific and differential notch dependency at the alphabeta and gammadelta T lineage bifurcation.* Immunity, 2006. **25**(1): p. 105-16.

26. Dudley, E.C., et al., *Alpha beta and gamma delta T cells can share a late common precursor.* Curr Biol, 1995. **5**(6): p. 659-69.

27. Petrie, H.T., R. Scollay, and K. Shortman, *Commitment to the T cell receptor-alpha beta or -gamma delta lineages can occur just prior to the onset of CD4 and CD8 expression among immature thymocytes.* Eur J Immunol, 1992. **22**(8): p. 2185-8.

28. Starr, T.K., S.C. Jameson, and K.A. Hogquist, *Positive and negative selection of T cells.* Annu Rev Immunol, 2003. **21**: p. 139-76.

29. Ken Murphy, P.T., Mark Walport, *Janeway's Immunobiology*. 7th ed. 2007: Garland Science.

30. Germain, R.N., *T-cell development and the CD4-CD8 lineage decision.* Nat Rev Immunol, 2002. **2**(5): p. 309-22.

31. Treiner, E. and O. Lantz, *CD1d- and MR1-restricted invariant T cells: of mice and men.* Curr Opin Immunol, 2006. **18**(5): p. 519-26.

32. Luckheeram, R.V., et al., *CD4(+)T cells: differentiation and functions.* Clin Dev Immunol, 2012. **2012**: p. 925135.

33. Joffre, O., et al., *Inflammatory signals in dendritic cell activation and the induction of adaptive immunity.* Immunol Rev, 2009. **227**(1): p. 234-47.

34. Cantrell, D.A., *T-cell antigen receptor signal transduction.* Immunology, 2002. **105**(4): p. 369-74.

35. Brownlie, R.J. and R. Zamoyska, *T cell receptor signalling networks: branched, diversified and bounded.* Nat Rev Immunol, 2013. **13**(4): p. 257-69.

36. Lin, J. and A. Weiss, *T cell receptor signalling.* J Cell Sci, 2001. **114**(Pt 2): p. 243-4.

37. Kuo, C.T. and J.M. Leiden, *Transcriptional regulation of T lymphocyte development and function.* Annu Rev Immunol, 1999. **17**: p. 149-87.

38. Rao, A. and O. Avni, *Molecular aspects of T-cell differentiation.* Br Med Bull, 2000. **56**(4): p. 969-84.

39. Malek, T.R. and I. Castro, *Interleukin-2 receptor signaling: at the interface between tolerance and immunity.* Immunity, 2010. **33**(2): p. 153-65.

40. Liao, W., J.X. Lin, and W.J. Leonard, *IL-2 family cytokines: new insights into the complex roles of IL-2 as a broad regulator of T helper cell differentiation.* Curr Opin Immunol, 2011. **23**(5): p. 598-604.

41. Wang, X., M. Rickert, and K.C. Garcia, *Structure of the quaternary complex of interleukin-2 with its alpha, beta, and gammac receptors.* Science, 2005. **310**(5751): p. 1159-63.

42. Stauber, D.J., et al., *Crystal structure of the IL-2 signaling complex: paradigm for a heterotrimeric cytokine receptor.* Proc Natl Acad Sci U S A, 2006. **103**(8): p. 2788-93.

43. Gaffen, S.L., *Signaling domains of the interleukin 2 receptor.* Cytokine, 2001. **14**(2): p. 63-77.

44. Boyman, O., et al., *Selective stimulation of T cell subsets with antibody-cytokine immune complexes.* Science, 2006. **311**(5769): p. 1924-7.

45. Cho, J.H., et al., *T cell receptor-dependent regulation of lipid rafts controls naive CD8+ T cell homeostasis.* Immunity, 2010. **32**(2): p. 214-26.

46. Vamosi, G., et al., *IL-2 and IL-15 receptor alpha-subunits are coexpressed in a supramolecular receptor cluster in lipid rafts of T cells.* Proc Natl Acad Sci U S A, 2004. **101**(30): p. 11082-7.

47. Le Bras, S., et al., *WIP is critical for T cell responsiveness to IL-2.* Proc Natl Acad Sci U S A, 2009. **106**(18): p. 7519-24.

48. Nelson, B.H. and D.M. Willerford, *Biology of the interleukin-2 receptor.* Adv Immunol, 1998. **70**: p. 1-81.

49. Yu, A., et al., *A low interleukin-2 receptor signaling threshold supports the development and homeostasis of T regulatory cells.* Immunity, 2009. **30**(2): p. 204-17.

50. Walsh, P.T., et al., *PTEN inhibits IL-2 receptor-mediated expansion of CD4+ CD25+ Tregs.* J Clin Invest, 2006. **116**(9): p. 2521-31.

51. Kim, H.P., J. Imbert, and W.J. Leonard, *Both integrated and differential regulation of components of the IL-2/IL-2 receptor system.* Cytokine Growth Factor Rev, 2006. **17**(5): p. 349-66.

52. Friedmann, M.C., et al., *Different interleukin 2 receptor beta-chain tyrosines couple to at least two signaling pathways and synergistically mediate interleukin 2-induced proliferation.* Proc Natl Acad Sci U S A, 1996. **93**(5): p. 2077-82.

53. Depper, J.M., et al., *Interleukin 2 (IL-2) augments transcription of the IL-2 receptor gene.* Proc Natl Acad Sci U S A, 1985. **82**(12): p. 4230-4.

54. Siegel, J.P., et al., *The IL-2 receptor beta chain (p70): role in mediating signals for LAK, NK, and proliferative activities.* Science, 1987. **238**(4823): p. 75-8.

55. Hemar, A., et al., *Endocytosis of interleukin 2 receptors in human T lymphocytes: distinct intracellular localization and fate of the receptor alpha, beta, and gamma chains.* J Cell Biol, 1995. **129**(1): p. 55-64.

56. Yu, A. and T.R. Malek, *The proteasome regulates receptor-mediated endocytosis of interleukin-2.* J Biol Chem, 2001. **276**(1): p. 381-5.

57. Chang, J.T., E.J. Wherry, and A.W. Goldrath, *Molecular regulation of effector and memory T cell differentiation.* Nat Immunol, 2014. **15**(12): p. 1104-15.

58. Kaech, S.M. and W. Cui, *Transcriptional control of effector and memory CD8+ T cell differentiation.* Nat Rev Immunol, 2012. **12**(11): p. 749-61.

59. Zhang, N. and M.J. Bevan, *CD8(+) T cells: foot soldiers of the immune system.* Immunity, 2011. **35**(2): p. 161-8.

60. Ashkar, S., et al., *Eta-1 (osteopontin): an early component of type-1 (cell-mediated) immunity.* Science, 2000. **287**(5454): p. 860-4.

61. Tao, X., et al., *Strength of TCR signal determines the costimulatory requirements for Th1 and Th2 CD4+ T cell differentiation.* J Immunol, 1997. **159**(12): p. 5956-63.

62. Feili-Hariri, M., D.H. Falkner, and P.A. Morel, *Polarization of naive T cells into Th1 or Th2 by distinct cytokine-driven murine dendritic cell populations: implications for immunotherapy.* J Leukoc Biol, 2005. **78**(3): p. 656-64.

63. Zhu, J. and W.E. Paul, *CD4 T cells: fates, functions, and faults.* Blood, 2008. **112**(5): p. 1557-69.

64. Tan, C. and I. Gery, *The unique features of Th9 cells and their products.* Crit Rev Immunol, 2012. **32**(1): p. 1-10.

65. Wambre, E., E.A. James, and W.W. Kwok, *Characterization of CD4+ T cell subsets in allergy.* Curr Opin Immunol, 2012. **24**(6): p. 700-6.

66. Marwaha, A.K., et al., *TH17 Cells in Autoimmunity and Immunodeficiency: Protective or Pathogenic?* Front Immunol, 2012. **3**: p. 129.

67. Jia, L. and C. Wu, *The biology and functions of Th22 cells.* Adv Exp Med Biol, 2014. **841**: p. 209-30.

68. Araki, K., et al., *mTOR regulates memory CD8 T-cell differentiation.* Nature, 2009. **460**(7251): p. 108-12.

69. Freemerman, A.J., et al., *Metabolic reprogramming of macrophages: glucose transporter 1 (GLUT1)-mediated glucose metabolism drives a proinflammatory phenotype.* J Biol Chem, 2014. **289**(11): p. 7884-96.

70. Jacobs, S.R., et al., *Glucose uptake is limiting in T cell activation and requires CD28-mediated Akt-dependent and independent pathways.* J Immunol, 2008. **180**(7): p. 4476-86.

71. Man, K., et al., *The transcription factor IRF4 is essential for TCR affinity-mediated metabolic programming and clonal expansion of T cells.* Nat Immunol, 2013. **14**(11): p. 1155-65.

72. MacIver, N.J., R.D. Michalek, and J.C. Rathmell, *Metabolic regulation of T lymphocytes.* Annu Rev Immunol, 2013. **31**: p. 259-83.

73. Palmer, C.S., et al., *Glucose metabolism regulates T cell activation, differentiation, and functions.* Front Immunol, 2015. **6**: p. 1.

74. Warburg, O., *On the origin of cancer cells.* Science, 1956. **123**(3191): p. 309-14.

75. Swainson, L., et al., *Glucose transporter 1 expression identifies a population of cycling CD4+ CD8+ human thymocytes with high CXCR4-induced chemotaxis.* Proc Natl Acad Sci U S A, 2005. **102**(36): p. 12867-72.

76. Yu, Q., et al., *In vitro evidence that cytokine receptor signals are required for differentiation of double positive thymocytes into functionally mature CD8+ T cells.* J Exp Med, 2003. **197**(4): p. 475-87.

77. Fox, C.J., P.S. Hammerman, and C.B. Thompson, *Fuel feeds function: energy metabolism and the T-cell response.* Nat Rev Immunol, 2005. **5**(11): p. 844-52.

78. Wang, R., et al., *The transcription factor Myc controls metabolic reprogramming upon T lymphocyte activation.* Immunity, 2011. **35**(6): p. 871-82.

79. van der Windt, G.J. and E.L. Pearce, *Metabolic switching and fuel choice during T-cell differentiation and memory development.* Immunol Rev, 2012. **249**(1): p. 27-42.

80. Pearce, E.L. and E.J. Pearce, *Metabolic pathways in immune cell activation and quiescence.* Immunity, 2013. **38**(4): p. 633-43.

81. Pearce, E.L., et al., *Fueling immunity: insights into metabolism and lymphocyte function.* Science, 2013. **342**(6155): p. 1242454.

82. Buck, M.D., D. O'Sullivan, and E.L. Pearce, *T cell metabolism drives immunity.* J Exp Med, 2015. **212**(9): p. 1345-60.

83. Ghesquiere, B., et al., *Metabolism of stromal and immune cells in health and disease.* Nature, 2014. **511**(7508): p. 167-76.

84. Finlay, D.K., *Regulation of glucose metabolism in T cells: new insight into the role of Phosphoinositide 3-kinases.* Front Immunol, 2012. **3**: p. 247.

85. Laplante, M. and D.M. Sabatini, *mTOR signaling at a glance.* J Cell Sci, 2009. **122**(Pt 20): p. 3589-94.

86. Laplante, M. and D.M. Sabatini, *mTOR signaling in growth control and disease.* Cell, 2012. **149**(2): p. 274-93.

87. Marko, A.J., et al., *Induction of glucose metabolism in stimulated T lymphocytes is regulated by mitogen-activated protein kinase signaling.* PLoS One, 2010. **5**(11): p. e15425.

88. Wofford, J.A., et al., *IL-7 promotes Glut1 trafficking and glucose uptake via STAT5-mediated activation of Akt to support T-cell survival.* Blood, 2008. **111**(4): p. 2101-11.

89. Tamas, P., et al., *Regulation of the energy sensor AMP-activated protein kinase by antigen receptor and Ca2+ in T lymphocytes.* J Exp Med, 2006. **203**(7): p. 1665-70.

90. Chehtane, M. and A.R. Khaled, *Interleukin-7 mediates glucose utilization in lymphocytes through transcriptional regulation of the hexokinase II gene.* Am J Physiol Cell Physiol, 2010. **298**(6): p. C1560-71.

91. Krauss, S., M.D. Brand, and F. Buttgereit, *Signaling takes a breath--new quantitative perspectives on bioenergetics and signal transduction.* Immunity, 2001. **15**(4): p. 497-502.

92. Marrack, P., J. Scott-Browne, and M.K. MacLeod, *Terminating the immune response.* Immunol Rev, 2010. **236**: p. 5-10.

93. Wing, K. and S. Sakaguchi, *Regulatory T cells exert checks and balances on self tolerance and autoimmunity.* Nat Immunol, 2010. **11**(1): p. 7-13.

94. Jiang, S. and R.I. Lechler, *Regulatory T cells in the control of transplantation tolerance and autoimmunity.* Am J Transplant, 2003. **3**(5): p. 516-24.

95. Mackay, I.R., *Tolerance and autoimmunity.* Western Journal of Medicine, 2001. **174**(2): p. 118-123.

96. Rosenblum, M.D., K.A. Remedios, and A.K. Abbas, *Mechanisms of human autoimmunity.* J Clin Invest, 2015. **125**(6): p. 2228-33.

97. Marson, A., W.J. Housley, and D.A. Hafler, *Genetic basis of autoimmunity.* J Clin Invest, 2015. **125**(6): p. 2234-41.

98. Zenewicz, L.A., et al., *Unraveling the genetics of autoimmunity.* Cell, 2010. **140**(6): p. 791-7.

99. Klein , J. and A. Sato *The HLA System.* New England Journal of Medicine, 2000. **343**(10): p. 702-709.

100. Doyle, H.A. and M.J. Mamula, *Post-translational protein modifications in antigen recognition and autoimmunity.* Trends Immunol, 2001. **22**(8): p. 443-9.

101. Anderton, S.M., *Post-translational modifications of self antigens: implications for autoimmunity.* Curr Opin Immunol, 2004. **16**(6): p. 753-8.

102. Kearney, P.L., et al., *Kinetic characterization of protein arginine deiminase 4: a transcriptional corepressor implicated in the onset and progression of rheumatoid arthritis.* Biochemistry, 2005. **44**(31): p. 10570-82.

103. Knuckley, B., M. Bhatia, and P.R. Thompson, *Protein arginine deiminase 4: evidence for a reverse protonation mechanism.* Biochemistry, 2007. **46**(22): p. 6578-87.

104. Knuckley, B., et al., *Substrate specificity and kinetic studies of PADs 1, 3, and 4 identify potent and selective inhibitors of protein arginine deiminase 3.* Biochemistry, 2010. **49**(23): p. 4852-63.

105. Knuckley, B., et al., *Haloacetamidine-based inactivators of protein arginine deiminase 4 (PAD4): evidence that general acid catalysis promotes efficient inactivation.* Chembiochem, 2010. **11**(2): p. 161-5.

106. Luo, Y., et al., *Inhibitors and inactivators of protein arginine deiminase 4: functional and structural characterization.* Biochemistry, 2006. **45**(39): p. 11727-36.

107. Luo, Y., et al., *Activity-based protein profiling reagents for protein arginine deiminase 4 (PAD4): synthesis and in vitro evaluation of a fluorescently labeled probe.* J Am Chem Soc, 2006. **128**(45): p. 14468-9.

108. Rogers, G.E., H.W. Harding, and I.J. Llewellyn-Smith, *The origin of citrulline-containing proteins in the hair follicle and the chemical nature of trichohyalin, an intracellular precursor.* Biochim Biophys Acta, 1977. **495**(1): p. 159-75.

109. Baka, Z., et al., *Citrullination under physiological and pathological conditions.* Joint Bone Spine, 2012. **79**(5): p. 431-6.

110. McGraw, W.T., et al., *Purification, characterization, and sequence analysis of a potential virulence factor from Porphyromonas gingivalis, peptidylarginine deiminase.* Infect Immun, 1999. **67**(7): p. 3248-56.

111. Arita, K., et al., *Structural basis for Ca(2+)-induced activation of human PAD4.* Nat Struct Mol Biol, 2004. **11**(8): p. 777-83.

112. Horikoshi, N., et al., *Structural and biochemical analyses of the human PAD4 variant encoded by a functional haplotype gene.* Acta Crystallogr D Biol Crystallogr, 2011. **67**(Pt 2): p. 112-8.

113. Slade, D.J., et al., *Protein arginine deiminase 2 binds calcium in an ordered fashion: implications for inhibitor design.* ACS Chem Biol, 2015. **10**(4): p. 1043-53.

114. Lewis, H.D., et al., *Inhibition of PAD4 activity is sufficient to disrupt mouse and human NET formation.* Nat Chem Biol, 2015. **11**(3): p. 189-91.

115. Nomura, K., *Specificity and mode of action of the muscle-type protein-arginine deiminase.* Arch Biochem Biophys, 1992. **293**(2): p. 362-9.

116. Kubilus, J., R.F. Waitkus, and H.P. Baden, *Partial purification and specificity of an arginine-converting enzyme from bovine epidermis.* Biochim Biophys Acta, 1980. **615**(1): p. 246-51.

117. Rus'd, A.A., et al., *Molecular cloning of cDNAs of mouse peptidylarginine deiminase type I, type III and type IV, and the expression pattern of type I in mouse.* Eur J Biochem, 1999. **259**(3): p. 660-9.

118. Terakawa, H., H. Takahara, and K. Sugawara, *Three types of mouse peptidylarginine deiminase: characterization and tissue distribution.* J Biochem, 1991. **110**(4): p. 661-6.

119. Tsuchida, M., et al., *cDNA nucleotide sequence and primary structure of mouse uterine peptidylarginine deiminase. Detection of a 3'-untranslated nucleotide sequence common to the mRNA of transiently expressed genes and rapid turnover of this enzyme's mRNA in the estrous cycle.* Eur J Biochem, 1993. **215**(3): p. 677-85.

120. Ishida-Yamamoto, A., et al., *Sequential reorganization of cornified cell keratin filaments involving filaggrin-mediated compaction and keratin 1 deimination.* J Invest Dermatol, 2002. **118**(2): p. 282-7.

121. Senshu, T., et al., *Detection of deiminated proteins in rat skin: probing with a monospecific antibody after modification of citrulline residues.* J Invest Dermatol, 1995. **105**(2): p. 163-9.

122. Senshu, T., K. Akiyama, and K. Nomura, *Identification of citrulline residues in the V subdomains of keratin K1 derived from the cornified layer of newborn mouse epidermis.* Exp Dermatol, 1999. **8**(5): p. 392-401.

123. Senshu, T., et al., *Preferential deimination of keratin K1 and filaggrin during the terminal differentiation of human epidermis.* Biochem Biophys Res Commun, 1996. **225**(3): p. 712-9.

124. Kan, S., H. Asaga, and T. Senshu, *Detection of Several Families of Deiminated Proteins Derived from Filaggrin and Keratins in Guinea Pig Skin.* Zoological Science, 1996. **13**(5): p. 673-678.

125. Senshu, T., et al., *Peptidylarginine deiminase in rat pituitary: sex difference, estrous cycle-related changes, and estrogen dependence.* Endocrinology, 1989. **124**(6): p. 2666-70.

126. Urano, Y., et al., *Immunohistochemical demonstration of peptidylarginine deiminase in human sweat glands.* Am J Dermatopathol, 1990. **12**(3): p. 249-55.

127. Watanabe, K., et al., *Combined biochemical and immunochemical comparison of peptidylarginine deiminases present in various tissues.* Biochim Biophys Acta, 1988. **966**(3): p. 375-83.

128. Watanabe, K. and T. Senshu, *Isolation and characterization of cDNA clones encoding rat skeletal muscle peptidylarginine deiminase.* J Biol Chem, 1989. **264**(26): p. 15255-60.

129. Nagata, S. and T. Senshu, *Peptidylarginine deiminase in rat and mouse hemopoietic cells.* Experientia, 1990. **46**(1): p. 72-4.

130. Yamakoshi, A., et al., *Cloning of cDNA encoding a novel isoform (type IV) of peptidylarginine deiminase from rat epidermis.* Biochim Biophys Acta, 1998. **1386**(1): p. 227-32.

131. Akiyama, K., K. Inoue, and T. Senshu, *Immunocytochemical demonstration of skeletal muscle type peptidylarginine deiminase in various rat tissues.* Cell Biol Int Rep, 1990. **14**(3): p. 267-73.

132. Vossenaar, E.R., et al., *Citrullination of synovial proteins in murine models of rheumatoid arthritis.* Arthritis Rheum, 2003. **48**(9): p. 2489-500.

133. Vossenaar, E.R., et al., *Expression and activity of citrullinating peptidylarginine deiminase enzymes in monocytes and macrophages.* Ann Rheum Dis, 2004. **63**(4): p. 373-81.

134. Takahara, H., et al., *Expression of peptidylarginine deiminase in the uterine epithelial cells of mouse is dependent on estrogen.* J Biol Chem, 1992. **267**(1): p. 520-5.

135. Takahara, H., et al., *Peptidylarginine deiminase of the mouse. Distribution, properties, and immunocytochemical localization.* J Biol Chem, 1989. **264**(22): p. 13361-8.

136. Watanabe, K., et al., *Estrous cycle dependent regulation of peptidylarginine deiminase transcripts in female rat pituitary.* Biochem Biophys Res Commun, 1990. **172**(1): p. 28-34.

137. Kubilus, J. and H.P. Baden, *Purification and properties of a brain enzyme which deiminates proteins.* Biochim Biophys Acta, 1983. **745**(3): p. 285-91.

138. Finch, P.R., D.D. Wood, and M.A. Moscarello, *The presence of citrulline in a myelin protein fraction.* FEBS Lett, 1971. **15**(2): p. 145-148.

139. Moscarello, M.A., et al., *Myelin in multiple sclerosis is developmentally immature.* J Clin Invest, 1994. **94**(1): p. 146-54.

140. Asaga, H., M. Yamada, and T. Senshu, *Selective deimination of vimentin in calcium ionophore-induced apoptosis of mouse peritoneal macrophages.* Biochem Biophys Res Commun, 1998. **243**(3): p. 641-6.

141. Inagaki, M., et al., *Ca2+-dependent deimination-induced disassembly of intermediate filaments involves specific modification of the amino-terminal head domain.* J Biol Chem, 1989. **264**(30): p. 18119-27.

142. Kanno, T., et al., *Human peptidylarginine deiminase type III: molecular cloning and nucleotide sequence of the cDNA, properties of the recombinant enzyme, and immunohistochemical localization in human skin.* J Invest Dermatol, 2000. **115**(5): p. 813-23.

143. Nishijyo, T., et al., *Isolation and molecular cloning of epidermal- and hair follicle-specific peptidylarginine deiminase (type III) from rat.* J Biochem, 1997. **121**(5): p. 868-75.

144. Rogers, G., et al., *Peptidylarginine deiminase of the hair follicle: characterization, localization, and function in keratinizing tissues.* J Invest Dermatol, 1997. **108**(5): p. 700-7.

145. Tarcsa, E., et al., *The fate of trichohyalin. Sequential post-translational modifications by peptidyl-arginine deiminase and transglutaminases.* J Biol Chem, 1997. **272**(44): p. 27893-901.

146. Tarcsa, E., et al., *Protein unfolding by peptidylarginine deiminase. Substrate specificity and structural relationships of the natural substrates trichohyalin and filaggrin.* J Biol Chem, 1996. **271**(48): p. 30709-16.

147. Asaga, H., et al., *Immunocytochemical localization of peptidylarginine deiminase in human eosinophils and neutrophils.* J Leukoc Biol, 2001. **70**(1): p. 46-51.

148. Hagiwara, T., et al., *Deimination of arginine residues in nucleophosmin/B23 and histones in HL-60 granulocytes.* Biochem Biophys Res Commun, 2002. **290**(3): p. 979-83.

149. Nakashima, K., T. Hagiwara, and M. Yamada, *Nuclear localization of peptidylarginine deiminase V and histone deimination in granulocytes.* J Biol Chem, 2002. **277**(51): p. 49562-8.

150. Nakashima, K., et al., *Molecular characterization of peptidylarginine deiminase in HL-60 cells induced by retinoic acid and 1alpha,25-dihydroxyvitamin D(3).* J Biol Chem, 1999. **274**(39): p. 27786-92.

151. Ishigami, A., et al., *Molecular cloning of two novel types of peptidylarginine deiminase cDNAs from retinoic acid-treated culture of a newborn rat keratinocyte cell line.* FEBS Lett, 1998. **433**(1-2): p. 113-8.

152. Wright, P.W., et al., *ePAD, an oocyte and early embryo-abundant peptidylarginine deiminase-like protein that localizes to egg cytoplasmic sheets.* Developmental Biology, 2003. **256**(1): p. 74-89.

153. van Winkelhoff, A.J., et al., *Porphyromonas gingivalis, Bacteroides forsythus and other putative periodontal pathogens in subjects with and without periodontal destruction.* J Clin Periodontol, 2002. **29**(11): p. 1023-8.

154. Shirai, H., T.L. Blundell, and K. Mizuguchi, *A novel superfamily of enzymes that catalyze the modification of guanidino groups.* Trends Biochem Sci, 2001. **26**(8): p. 465-8.

155. Bielecka, E., et al., *Peptidyl arginine deiminase from Porphyromonas gingivalis abolishes anaphylatoxin C5a activity.* J Biol Chem, 2014. **289**(47): p. 32481-7.

156. Pyrc, K., et al., *Inactivation of epidermal growth factor by Porphyromonas gingivalis as a potential mechanism for periodontal tissue damage.* Infect Immun, 2013. **81**(1): p. 55-64.

157. Gawron, K., et al., *Peptidylarginine deiminase from Porphyromonas gingivalis contributes to infection of gingival fibroblasts and induction of prostaglandin E2 -signaling pathway.* Mol Oral Microbiol, 2014. **29**(6): p. 321-32.

158. Abdullah, S.N., et al., *Porphyromonas gingivalis peptidylarginine deiminase substrate specificity.* Anaerobe, 2013. **23**: p. 102-8.

159. David L Scott, F.W., Tom W J Huizinga, *Rheumatoid arthritis.* Lancet, 2010. **376**: p. 1094–1108.

160. Choy, E.H., et al., *Therapeutic benefit of blocking interleukin-6 activity with an anti-interleukin-6 receptor monoclonal antibody in rheumatoid arthritis: a randomized, double-blind, placebo-controlled, dose-escalation trial.* Arthritis Rheum, 2002. **46**(12): p. 3143-50.

161. Bartold, P.M., et al., *Effect of Porphyromonas gingivalis-induced inflammation on the development of rheumatoid arthritis.* J Clin Periodontol, 2010. **37**(5): p. 405-11.

162. Kallberg, H., et al., *Gene-gene and gene-environment interactions involving HLA-DRB1, PTPN22, and smoking in two subsets of rheumatoid arthritis.* Am J Hum Genet, 2007. **80**(5): p. 867-75.

163. van der Woude, D., et al., *Quantitative heritability of anti-citrullinated protein antibody-positive and anti-citrullinated protein antibody-negative rheumatoid arthritis.* Arthritis Rheum, 2009. **60**(4): p. 916-23.

164. MacGregor AJ, S.H., Rigby AS, et al, *Characterizing the quantitative genetic contribution to rheumatoid arthritis using data from twins.* Arthritis Rheum 2000. **43**: p. 30-37.

165. Newton, J.L., et al., *A review of the MHC genetics of rheumatoid arthritis.* Genes Immun, 2004. **5**(3): p. 151-7.

166. Ágnes Gyetvai, et al., *New classification of the shared epitope in rheumatoid arthritis: impact on the production of various anti-citrullinated protein antibodies.* Rheumatology, 2010. **49**: p. 25-33.

167. Gregersen, P.K., J. Silver, and R.J. Winchester, *The shared epitope hypothesis. An approach to understanding the molecular genetics of susceptibility to rheumatoid arthritis.* Arthritis Rheum, 1987. **30**(11): p. 1205-13.

168. Meyer, J.M., et al., *HLA-DRB1 genotype influences risk for and severity of rheumatoid arthritis.* J Rheumatol, 1999. **26**(5): p. 1024-34.

169. Gorman, J.D., et al., *Impact of shared epitope genotype and ethnicity on erosive disease: a meta-analysis of 3,240 rheumatoid arthritis patients.* Arthritis Rheum, 2004. **50**(2): p. 400-12.

170. Hill, J.A., et al., *Arthritis induced by posttranslationally modified (citrullinated) fibrinogen in DR4-IE transgenic mice.* J Exp Med, 2008. **205**(4): p. 967-79.

171. Auger, I., et al., *Influence of HLA-DR genes on the production of rheumatoid arthritis-specific autoantibodies to citrullinated fibrinogen.* Arthritis Rheum, 2005. **52**(11): p. 3424-32.

172. Hammer, J., et al., *Peptide binding specificity of HLA-DR4 molecules: correlation with rheumatoid arthritis association.* J Exp Med, 1995. **181**(5): p. 1847-55.

173. Stolt, P., et al., *Quantification of the influence of cigarette smoking on rheumatoid arthritis: results from a population based case-control study, using incident cases.* Annals of the Rheumatic Diseases, 2003. **62**(9): p. 835-841.

174. Di Giuseppe, D., et al., *Cigarette smoking and smoking cessation in relation to risk of rheumatoid arthritis in women.* Arthritis Res Ther, 2013. **15**(2): p. R56.

175. Xuzhu, G., et al., *Resveratrol modulates murine collagen-induced arthritis by inhibiting Th17 and B-cell function.* Ann Rheum Dis, 2012. **71**(1): p. 129-35.

176. Carlens, C., et al., *Smoking, use of moist snuff, and risk of chronic inflammatory diseases.* Am J Respir Crit Care Med, 2010. **181**(11): p. 1217-22.

177. Liao, K.P., L. Alfredsson, and E.W. Karlson, *Environmental influences on risk for rheumatoid arthritis.* Curr Opin Rheumatol, 2009. **21**(3): p. 279-83.

178. Bos, W.H., et al., *Preferential decrease in IgG4 anti-citrullinated protein antibodies during treatment with tumour necrosis factor blocking agents in patients with rheumatoid arthritis.* Ann Rheum Dis, 2009. **68**(4): p. 558-63.

179. De Rycke, L., et al., *Rheumatoid factor and anticitrullinated protein antibodies in rheumatoid arthritis: diagnostic value, associations with radiological progression rate, and extra-articular manifestations.* Ann Rheum Dis, 2004. **63**(12): p. 1587-93.

180. Kudo-Tanaka, E., et al., *Autoantibodies to cyclic citrullinated peptide 2 (CCP2) are superior to other potential diagnostic biomarkers for predicting rheumatoid arthritis in early undifferentiated arthritis.* Clin Rheumatol, 2007. **26**(10): p. 1627-33.

181. Quinn, M.A., et al., *Anti-CCP antibodies measured at disease onset help identify seronegative rheumatoid arthritis and predict radiological and functional outcome.* Rheumatology (Oxford), 2006. **45**(4): p. 478-80.

182. Ronnelid, J., et al., *Longitudinal analysis of citrullinated protein/peptide antibodies (anti-CP) during 5 year follow up in early rheumatoid arthritis: anti-CP status predicts worse disease activity and greater radiological progression.* Ann Rheum Dis, 2005. **64**(12): p. 1744-9.

183. van der Linden, M.P., et al., *Value of anti-modified citrullinated vimentin and third-generation anti-cyclic citrullinated peptide compared with second-generation anti-cyclic citrullinated peptide and rheumatoid factor in predicting disease outcome in undifferentiated arthritis and rheumatoid arthritis.* Arthritis Rheum, 2009. **60**(8): p. 2232-41.

184. Cantaert, T., et al., *Citrullinated proteins in rheumatoid arthritis: crucial...but not sufficient!* Arthritis Rheum, 2006. **54**(11): p. 3381-9.

185. Soderlin, M.K., et al., *Antibodies against cyclic citrullinated peptide (CCP) and levels of cartilage oligomeric matrix protein (COMP) in very early arthritis: relation to diagnosis and disease activity.* Scand J Rheumatol, 2004. **33**(3): p. 185-8.

186. Rantapaa-Dahlqvist, S., et al., *Antibodies against cyclic citrullinated peptide and IgA rheumatoid factor predict the development of rheumatoid arthritis.* Arthritis Rheum, 2003. **48**(10): p. 2741-9.

187. Foulquier, C., et al., *Peptidyl arginine deiminase type 2 (PAD-2) and PAD-4 but not PAD-1, PAD-3, and PAD-6 are expressed in rheumatoid arthritis synovium in close association with tissue inflammation.* Arthritis Rheum, 2007. **56**(11): p. 3541-53.

188. De Rycke, L., et al., *Synovial intracellular citrullinated proteins colocalizing with peptidyl arginine deiminase as pathophysiologically relevant antigenic determinants of rheumatoid arthritis-specific humoral autoimmunity.* Arthritis Rheum, 2005. **52**(8): p. 2323-30.

189. Suzuki, A., et al., *Functional haplotypes of PADI4, encoding citrullinating enzyme peptidylarginine deiminase 4, are associated with rheumatoid arthritis.* Nat Genet, 2003. **34**(4): p. 395-402.

190. Brinkmann, V., et al., *Neutrophil extracellular traps kill bacteria.* Science, 2004. **303**(5663): p. 1532-5.

191. Segal, A.W., *How neutrophils kill microbes.* Annu Rev Immunol, 2005. **23**: p. 197-223.

192. Remijsen, Q., et al., *Dying for a cause: NETosis, mechanisms behind an antimicrobial cell death modality.* Cell Death Differ, 2011. **18**(4): p. 581-8.

193. Cuthbert, G.L., et al., *Histone deimination antagonizes arginine methylation.* Cell, 2004. **118**(5): p. 545-53.

194. Li, P., et al., *PAD4 is essential for antibacterial innate immunity mediated by neutrophil extracellular traps.* J Exp Med, 2010. **207**(9): p. 1853-62.

195. Spengler, J., et al., *Release of Active Peptidyl Arginine Deiminases by Neutrophils Can Explain Production of Extracellular Citrullinated Autoantigens in Rheumatoid Arthritis Synovial Fluid.* Arthritis Rheumatol, 2015. **67**(12): p. 3135-45.

196. Damgaard, D., et al., *Demonstration of extracellular peptidylarginine deiminase (PAD) activity in synovial fluid of patients with rheumatoid arthritis using a novel assay for citrullination of fibrinogen.* Arthritis Res Ther, 2014. **16**(6): p. 498.

197. Routsias, J.G., et al., *Autopathogenic correlation of periodontitis and rheumatoid arthritis.* Rheumatology (Oxford), 2011. **50**(7): p. 1189-93.

198. Uysal, H., et al., *Antibodies to citrullinated proteins: molecular interactions and arthritogenicity.* Immunol Rev, 2010. **233**(1): p. 9-33.

199. Vossenaar, E.R., et al., *Rheumatoid arthritis specific anti-Sa antibodies target citrullinated vimentin.* Arthritis Res Ther, 2004. **6**(2): p. R142-50.

200. Girbal-Neuhauser, E., et al., *The epitopes targeted by the rheumatoid arthritis-associated antifilaggrin autoantibodies are posttranslationally generated on various sites of (pro)filaggrin by deimination of arginine residues.* J Immunol, 1999. **162**(1): p. 585-94.

201. Masson-Bessiere, C., et al., *The major synovial targets of the rheumatoid arthritis-specific antifilaggrin autoantibodies are deiminated forms of the alpha- and beta-chains of fibrin.* J Immunol, 2001. **166**(6): p. 4177-84.

202. Chapuy-Regaud, S., et al., *Fibrin deimination in synovial tissue is not specific for rheumatoid arthritis but commonly occurs during synovitides.* J Immunol, 2005. **174**(8): p. 5057-64.

203. Hoet, R.M., et al., *Antiperinuclear factor, a marker autoantibody for rheumatoid arthritis: colocalisation of the perinuclear factor and profilaggrin.* Ann Rheum Dis, 1991. **50**(9): p. 611-8.

204. Nienhuis, R.L. and E. Mandema, *A New Serum Factor in Patients with Rheumatoid Arthritis; the Antiperinuclear Factor.* Ann Rheum Dis, 1964. **23**: p. 302-5.

205. Simon, M., et al., *The cytokeratin filament-aggregating protein filaggrin is the target of the so-called "antikeratin antibodies," autoantibodies specific for rheumatoid arthritis.* J Clin Invest, 1993. **92**(3): p. 1387-93.

206. Young, B.J., et al., *Anti-keratin antibodies in rheumatoid arthritis.* Br Med J, 1979. **2**(6182): p. 97-9.

207. Sebbag, M., et al., *The antiperinuclear factor and the so-called antikeratin antibodies are the same rheumatoid arthritis-specific autoantibodies.* J Clin Invest, 1995. **95**(6): p. 2672-9.

208. Despres, N., et al., *The Sa system: a novel antigen-antibody system specific for rheumatoid arthritis.* J Rheumatol, 1994. **21**(6): p. 1027-33.

209. Schellekens, G.A., et al., *The diagnostic properties of rheumatoid arthritis antibodies recognizing a cyclic citrullinated peptide.* Arthritis Rheum, 2000. **43**(1): p. 155-63.

210. van Venrooij, W.J., J.M. Hazes, and H. Visser, *Anticitrullinated protein/peptide antibody and its role in the diagnosis and prognosis of early rheumatoid arthritis.* Neth J Med, 2002. **60**(10): p. 383-8.

211. Masson-Bessiere, C., et al., *In the rheumatoid pannus, anti-filaggrin autoantibodies are produced by local plasma cells and constitute a higher proportion of IgG than in synovial fluid and serum.* Clin Exp Immunol, 2000. **119**(3): p. 544-52.

212. Kinloch, A., et al., *Synovial fluid is a site of citrullination of autoantigens in inflammatory arthritis.* Arthritis Rheum, 2008. **58**(8): p. 2287-95.

213. Mercado, F.B., R.I. Marshall, and P.M. Bartold, *Inter-relationships between rheumatoid arthritis and periodontal disease. A review.* J Clin Periodontol, 2003. **30**(9): p. 761-72.

214. Petersen, P.E. and H. Ogawa, *Strengthening the prevention of periodontal disease: the WHO approach.* J Periodontol, 2005. **76**(12): p. 2187-93.

215. Stabholz, A., W.A. Soskolne, and L. Shapira, *Genetic and environmental risk factors for chronic periodontitis and aggressive periodontitis.* Periodontol 2000, 2010. **53**: p. 138-53.

216. de Smit, M.J., et al., *Rheumatoid arthritis and periodontitis; a possible link via citrullination.* Anaerobe, 2011. **17**(4): p. 196-200.

217. Abusleme, L., et al., *The subgingival microbiome in health and periodontitis and its relationship with community biomass and inflammation.* ISME J, 2013. **7**(5): p. 1016-25.

218. Dewhirst, F.E., et al., *The human oral microbiome.* J Bacteriol, 2010. **192**(19): p. 5002-17.

219. Griffen, A.L., et al., *Distinct and complex bacterial profiles in human periodontitis and health revealed by 16S pyrosequencing.* ISME J, 2012. **6**(6): p. 1176-85.

220. Hajishengallis, G., R.P. Darveau, and M.A. Curtis, *The keystone-pathogen hypothesis.* Nat Rev Microbiol, 2012. **10**(10): p. 717-25.

221. Hajishengallis, G., et al., *Low-abundance biofilm species orchestrates inflammatory periodontal disease through the commensal microbiota and complement.* Cell Host Microbe, 2011. **10**(5): p. 497-506.

222. Jorth, P., et al., *Metatranscriptomics of the human oral microbiome during health and disease.* MBio, 2014. **5**(2): p. e01012-14.

223. Darveau, R.P., *Periodontitis: a polymicrobial disruption of host homeostasis.* Nat Rev Microbiol, 2010. **8**(7): p. 481-90.

224. Hajishengallis, G. and R.J. Lamont, *Beyond the red complex and into more complexity: the polymicrobial synergy and dysbiosis (PSD) model of periodontal disease etiology.* Mol Oral Microbiol, 2012. **27**(6): p. 409-19.

225. Rosier, B.T., et al., *Historical and contemporary hypotheses on the development of oral diseases: are we there yet?* Front Cell Infect Microbiol, 2014. **4**: p. 92.

226. Socransky, S.S., et al., *Microbial complexes in subgingival plaque.* J Clin Periodontol, 1998. **25**(2): p. 134-44.

227. Socransky, S.S. and A.D. Haffajee, *Effect of therapy on periodontal infections.* J Periodontol, 1993. **64**(8 Suppl): p. 754-9.

228. Farquharson, D., J.P. Butcher, and S. Culshaw, *Periodontitis, Porphyromonas, and the pathogenesis of rheumatoid arthritis.* Mucosal Immunol, 2012. **5**(2): p. 112-20.

229. Holt, S.C., et al., *Virulence factors of Porphyromonas gingivalis.* Periodontol 2000, 1999. **20**: p. 168-238.

230. Berglundh, T. and M. Donati, *Aspects of adaptive host response in periodontitis.* J Clin Periodontol, 2005. **32 Suppl 6**: p. 87-107.

231. Wegner, N., et al., *Peptidylarginine deiminase from Porphyromonas gingivalis citrullinates human fibrinogen and alpha-enolase: implications for autoimmunity in rheumatoid arthritis.* Arthritis Rheum, 2010. **62**(9): p. 2662-72.

232. Ivanyi, L. and T. Lehner, *Stimulation of lymphocyte transformation by bacterial antigens in patients with periodontal disease.* Arch Oral Biol, 1970. **15**(11): p. 1089-96.

233. Gemmell, E., K. Yamazaki, and G.J. Seymour, *The role of T cells in periodontal disease: homeostasis and autoimmunity.* Periodontol 2000, 2007. **43**: p. 14-40.

234. Azuma, M., *Fundamental mechanisms of host immune responses to infection.* J Periodontal Res, 2006. **41**(5): p. 361-73.

235. Teng, Y.T., et al., *Functional human T-cell immunity and osteoprotegerin ligand control alveolar bone destruction in periodontal infection.* J Clin Invest, 2000. **106**(6): p. R59-67.

236. Gemmell, E. and G.J. Seymour, *Interleukin 1, interleukin 6 and transforming growth factor-beta production by human gingival mononuclear cells following stimulation with Porphyromonas gingivalis and Fusobacterium nucleatum.* J Periodontal Res, 1993. **28**(2): p. 122-9.

237. Shenker, B.J. and S. Datar, *Fusobacterium nucleatum inhibits human T-cell activation by arresting cells in the mid-G1 phase of the cell cycle.* Infect Immun, 1995. **63**(12): p. 4830-6.

238. Shenker, B.J., W.P. McArthur, and C.C. Tsai, *Immune suppression induced by Actinobacillus actinomycetemcomitans. I. Effects on human peripheral blood lymphocyte responses to mitogens and antigens.* J Immunol, 1982. **128**(1): p. 148-54.

239. Shenker, B.J. and J. Slots, *Immunomodulatory effects of Bacteroides products on in vitro human lymphocyte functions.* Oral Microbiol Immunol, 1989. **4**(1): p. 24-9.

240. Stashenko, P., et al., *T cell responses of periodontal disease patients and healthy subjects to oral microorganisms.* J Periodontal Res, 1983. **18**(6): p. 587-600.

241. Gemmell, E., K.E. Drysdale, and G.J. Seymour, *Gene expression in splenic CD4 and CD8 cells from BALB/c mice immunized with Porphyromonas gingivalis.* J Periodontol, 2006. **77**(4): p. 622-33.

242. Cole, K.L., G.J. Seymour, and R.N. Powell, *Phenotypic and functional analysis of T cells extracted from chronically inflamed human periodontal tissues.* J Periodontol, 1987. **58**(8): p. 569-73.

243. Kimura, S., N. Fujimoto, and H. Okada, *Impaired autologous mixed-lymphocyte reaction of peripheral blood lymphocytes in adult periodontitis.* Infect Immun, 1991. **59**(12): p. 4418-24.

244. Stoufi, E.D., et al., *Phenotypic analyses of mononuclear cells recovered from healthy and diseased human periodontal tissues.* J Clin Immunol, 1987. **7**(3): p. 235-45.

245. Johannessen, A.C., et al., *Variation in the composition of gingival inflammatory cell infiltrates.* J Clin Periodontol, 1990. **17**(5): p. 298-305.

246. Jully, J.M., et al., *Immunohistological identification of cell subsets in human gingiva after local treatment for gingivitis or periodontitis.* J Clin Periodontol, 1986. **13**(3): p. 223-7.

247. Lappin, D.F., et al., *Relative proportions of mononuclear cell types in periodontal lesions analyzed by immunohistochemistry.* J Clin Periodontol, 1999. **26**(3): p. 183-9.

248. Reinhardt, R.A., et al., *In situ lymphocyte subpopulations from active versus stable periodontal sites.* J Periodontol, 1988. **59**(10): p. 656-70.

249. Modeer, T., et al., *Subpopulations of lymphocytes in connective tissue from adolescents with periodontal disease.* Acta Odontol Scand, 1990. **48**(3): p. 153-9.

250. Syrjanen, S., H. Markkanen, and K. Syrjanen, *Inflammatory cells and their subsets in lesions of juvenile periodontitis. A family study.* Acta Odontol Scand, 1984. **42**(5): p. 285-92.

251. Genco, R.J. and T.E. Van Dyke, *Prevention: Reducing the risk of CVD in patients with periodontitis.* Nat Rev Cardiol, 2010. **7**(9): p. 479-80.

252. Kebschull, M., R.T. Demmer, and P.N. Papapanou, *"Gum bug, leave my heart alone!"--epidemiologic and mechanistic evidence linking periodontal infections and atherosclerosis.* J Dent Res, 2010. **89**(9): p. 879-902.

253. Madianos, P.N., Y.A. Bobetsis, and S. Offenbacher, *Adverse pregnancy outcomes (APOs) and periodontal disease: pathogenic mechanisms.* J Clin Periodontol, 2013. **40 Suppl 14**: p. S170-80.

254. Lundberg, K., et al., *Antibodies to citrullinated alpha-enolase peptide 1 are specific for rheumatoid arthritis and cross-react with bacterial enolase.* Arthritis Rheum, 2008. **58**(10): p. 3009-19.

255. Whitmore, S.E. and R.J. Lamont, *Oral bacteria and cancer.* PLoS Pathog, 2014. **10**(3): p. e1003933.

256. Wilson, M., K. Reddi, and B. Henderson, *Cytokine-inducing components of periodontopathogenic bacteria.* J Periodontal Res, 1996. **31**(6): p. 393-407.

257. Han, Y.W. and X. Wang, *Mobile microbiome: oral bacteria in extra-oral infections and inflammation.* J Dent Res, 2013. **92**(6): p. 485-91.

258. Ott, S.J., et al., *Detection of diverse bacterial signatures in atherosclerotic lesions of patients with coronary heart disease.* Circulation, 2006. **113**(7): p. 929-37.

259. Totaro, M.C., et al., *Porphyromonas gingivalis and the pathogenesis of rheumatoid arthritis: analysis of various compartments including the synovial tissue.* Arthritis Res Ther, 2013. **15**(3): p. R66.

260. Michaud, D.S., et al., *Plasma antibodies to oral bacteria and risk of pancreatic cancer in a large European prospective cohort study.* Gut, 2013. **62**(12): p. 1764-70.

261. Silva-Boghossian, C.M., et al., *Microbiological changes after periodontal therapy in diabetic patients with inadequate metabolic control.* Braz Oral Res, 2014. **28**.

262. Chapple, I.L., et al., *Primary prevention of periodontitis: managing gingivitis.* J Clin Periodontol, 2015. **42 Suppl 16**: p. S71-6.

263. O'Reilly, P.G. and N.M. Claffey, *A history of oral sepsis as a cause of disease.* Periodontol 2000, 2000. **23**: p. 13-8.

264. Biyikoglu, B., et al., *Evaluation of t-PA, PAI-2, IL-1beta and PGE(2) in gingival crevicular fluid of rheumatoid arthritis patients with periodontal disease.* J Clin Periodontol, 2006. **33**(9): p. 605-11.

265. de Pablo, P., et al., *Periodontitis in systemic rheumatic diseases.* Nat Rev Rheumatol, 2009. **5**(4): p. 218-24.

266. Pischon, N., et al., *Association among rheumatoid arthritis, oral hygiene, and periodontitis.* J Periodontol, 2008. **79**(6): p. 979-86.

267. Abou-Raya, A., S. Abou-Raya, and H. Abu-Elkheir, *Periodontal disease and rheumatoid arthritis: is there a link?* Scand J Rheumatol, 2005. **34**(5): p. 408-10.

268. Abou-Raya, S., et al., *Rheumatoid arthritis, periodontal disease and coronary artery disease.* Clin Rheumatol, 2008. **27**(4): p. 421-7.

269. Deodhar, A.A. and R.M. Bennett, *Periodontal health in patients with rheumatoid arthritis: comment on the article by Kasser et al.* Arthritis Rheum, 1998. **41**(11): p. 2081-3.

270. Gleissner, C., et al., *Temporomandibular joint function in patients with longstanding rheumatoid arthritis - I. Role of periodontal status and prosthetic care - a clinical study.* Eur J Med Res, 2003. **8**(3): p. 98-108.

271. Gleissner, C., et al., *The role of risk factors for periodontal disease in patients with rheumatoid arthritis.* Eur J Med Res, 1998. **3**(8): p. 387-92.

272. Kasser, U.R., et al., *Risk for periodontal disease in patients with longstanding rheumatoid arthritis.* Arthritis Rheum, 1997. **40**(12): p. 2248-51.

273. Marotte, H., et al., *The association between periodontal disease and joint destruction in rheumatoid arthritis extends the link between the HLA-DR shared epitope and severity of bone destruction.* Ann Rheum Dis, 2006. **65**(7): p. 905-9.

274. Mercado, F.B., et al., *Relationship between rheumatoid arthritis and periodontitis.* J Periodontol, 2001. **72**(6): p. 779-87.

275. Nilsson, M. and S. Kopp, *Gingivitis and periodontitis are related to repeated high levels of circulating tumor necrosis factor-alpha in patients with rheumatoid arthritis.* J Periodontol, 2008. **79**(9): p. 1689-96.

276. Berthelot, J.M. and B. Le Goff, *Rheumatoid arthritis and periodontal disease.* Joint Bone Spine, 2010. **77**(6): p. 537-41.

277. Mangat, P., et al., *Bacterial and human peptidylarginine deiminases: targets for inhibiting the autoimmune response in rheumatoid arthritis?* Arthritis Res Ther, 2010. **12**(3): p. 209.

278. Ogrendik, M., *Rheumatoid arthritis is linked to oral bacteria: etiological association.* Mod Rheumatol, 2009. **19**(5): p. 453-6.

279. Moen, K., et al., *Synovial inflammation in active rheumatoid arthritis and psoriatic arthritis facilitates trapping of a variety of oral bacterial DNAs.* Clin Exp Rheumatol, 2006. **24**(6): p. 656-63.

280. Quirke, A.M., et al., Citrullination of autoantigens: upstream of TNFalpha in the pathogenesis of rheumatoid arthritis. FEBS Lett, 2011. **585**(23): p. 3681-8.

281. Lappin, D.F., et al., *Influence of periodontal disease, Porphyromonas gingivalis and cigarette smoking on systemic anti-citrullinated peptide antibody titres.* J Clin Periodontol, 2013. **40**(10): p. 907-15.

282. Dissick, A., et al., *Association of periodontitis with rheumatoid arthritis: a pilot study.* J Periodontol, 2010. **81**(2): p. 223-30.

283. Maresz, K.J., et al., *Porphyromonas gingivalis facilitates the development and progression of destructive arthritis through its unique bacterial peptidylarginine deiminase (PAD).* PLoS Pathog, 2013. **9**(9): p. e1003627.

284. Rosenstein, E.D., et al., *Hypothesis: the humoral immune response to oral bacteria provides a stimulus for the development of rheumatoid arthritis.* Inflammation, 2004. **28**(6): p. 311-8.

285. Lundberg, K., et al., *Periodontitis in RA-the citrullinated enolase connection.* Nat Rev Rheumatol, 2010. **6**(12): p. 727-30.

286. Nair, S., M. Faizuddin, and J. Dharmapalan, *Role of autoimmune responses in periodontal disease.* Autoimmune Dis, 2014. **2014**: p. 596824.

287. Bartelt, R.R., et al., *Comparison of T cell receptor-induced proximal signaling and downstream functions in immortalized and primary T cells.* PLoS One, 2009. **4**(5): p. e5430.

288. Harford, J.B., *Preparation and Isolation of Cells*, in *Current Protocols in Cell Biology*. 2004, John Wiley & Sons, Inc. p. 2.0.1-2.6.6.

289. Brock, G.R., et al., *Local and systemic total antioxidant capacity in periodontitis and health.* J Clin Periodontol, 2004. **31**(7): p. 515-21.

290. Thavasu, P.W., et al., *Measuring cytokine levels in blood. Importance of anticoagulants, processing, and storage conditions.* J Immunol Methods, 1992. **153**(1-2): p. 115-24.

291. Subrahmanyam, M.V. and M. Sangeetha, *Gingival crevicular fluid a marker of the periodontal disease activity.* Indian J Clin Biochem, 2003. **18**(1): p. 5-7.

292. Smith, P.K., et al., *Measurement of protein using bicinchoninic acid.* Anal Biochem, 1985. **150**(1): p. 76-85.

293. Bradford, M.M., *A rapid and sensitive method for the quantitation of microgram quantities of protein utilizing the principle of protein-dye binding.* Anal Biochem, 1976. **72**: p. 248-54.

294. Davis, D.R. and R.E. Budd, *Continuous electrophoresis; quantitative fractionation of serum proteins.* J Lab Clin Med, 1959. **53**(6): p. 958-65.

295. Raymond, S. and L. Weintraub, *Acrylamide gel as a supporting medium for zone electrophoresis.* Science, 1959. **130**(3377): p. 711.

296. Bonifacino, J.S., *Chapter 6: Electrophoresis and Immunoblotting*, in *Current Protocols in Cell Biology*. 2002, John Wiley & Sons, Inc. p. 6.0.1-6.9.14.

297. Garfin, D. and S. Ahuja, *Handbook of isoelectric focusing and proteomics*. 2005: Elsevier Inc.

298. Garfin, D.E., *Two-dimensional gel electrophoresis: an overview.* TrAC Trends in Analytical Chemistry, 2003. **22**(5): p. 263-272.

299. Schagger, H. and G. von Jagow, *Blue native electrophoresis for isolation of membrane protein complexes in enzymatically active form.* Anal Biochem, 1991. **199**(2): p. 223-31.

300. Schagger, H., W.A. Cramer, and G. von Jagow, *Analysis of molecular masses and oligomeric states of protein complexes by blue native electrophoresis and isolation of membrane protein complexes by two-dimensional native electrophoresis.* Anal Biochem, 1994. **217**(2): p. 220-30.

301. Fiala, G.J., W.W. Schamel, and B. Blumenthal, *Blue native polyacrylamide gel electrophoresis (BN-PAGE) for analysis of multiprotein complexes from cellular lysates.* J Vis Exp, 2011(48).

302. Wittig, I., H.P. Braun, and H. Schagger, *Blue native PAGE.* Nat Protoc, 2006. **1**(1): p. 418-28.

303. Swamy, M., et al., *Blue Native Polyacrylamide Gel Electrophoresis (BN-PAGE) for the Identification and Analysis of Multiprotein Complexes.* Science Signaling, 2006. **2006**(345): p. pl4-pl4.

304. Reisinger, V. and L.A. Eichacker, *Analysis of membrane protein complexes by blue native PAGE.* Proteomics, 2006. **6 Suppl 2**: p. 6-15.

305. Ho, C.S., et al., *Electrospray ionisation mass spectrometry: principles and clinical applications.* Clin Biochem Rev, 2003. **24**(1): p. 3-12.

306. Rosenfeld, J., et al., *In-gel digestion of proteins for internal sequence analysis after one- or two-dimensional gel electrophoresis.* Anal Biochem, 1992. **203**(1): p. 173-9.

307. Shevchenko, A., et al., *In-gel digestion for mass spectrometric characterization of proteins and proteomes.* Nat. Protocols, 2007. **1**(6): p. 2856-2860.

308. Yates, J.R., C.I. Ruse, and A. Nakorchevsky, *Proteomics by mass spectrometry: approaches, advances, and applications.* Annu Rev Biomed Eng, 2009. **11**: p. 49-79.

309. Canas, B., et al., *Mass spectrometry technologies for proteomics.* Brief Funct Genomic Proteomic, 2006. **4**(4): p. 295-320.

310. Creese, A.J., et al., *On-line liquid chromatography neutral loss-triggered electron transfer dissociation mass spectrometry for the targeted analysis of citrullinated peptides.* Analytical Methods, 2011. **3**(2): p. 259-266.

311. Swaney, D.L., et al., *Supplemental activation method for high-efficiency electron-transfer dissociation of doubly protonated peptide precursors.* Anal Chem, 2007. **79**(2): p. 477-85.

312. Hensen, S.M.M. and G.J.M. Pruijn, *Methods for the Detection of Peptidylarginine Deiminase (PAD) Activity and Protein Citrullination.* Molecular & Cellular Proteomics, 2014. **13**(2): p. 388-396.

313. Strober, W., *Trypan blue exclusion test of cell viability.* Curr Protoc Immunol, 2001. **Appendix 3**: p. Appendix 3B.

314. Biosciences, B., *Introduction to flow cytometry: a learning guide*. 2002, San Jose, CA, USA: Becton, Dickinson & Company.

315. Zendman, A.J.W., et al., *ABAP: Antibody-based assay for peptidylarginine deiminase activity.* Analytical Biochemistry, 2007. **369**(2): p. 232-240.

316. Lindsay, G.K., P.F. Roslansky, and T.J. Novitsky, *Single-step, chromogenic Limulus amebocyte lysate assay for endotoxin.* Journal of Clinical Microbiology, 1989. **27**(5): p. 947-951.

317. Kingston, R.E., *Chapter 4: Preparation and Analysis of RNA*, in *Current Protocols in Molecular Biology*. 2002, John Wiley & Sons, Inc.

318. Wilfinger, W.W., K. Mackey, and P. Chomczynski, *Effect of pH and ionic strength on the spectrophotometric assessment of nucleic acid purity.* Biotechniques, 1997. **22**(3): p. 474-6, 478-81.

319. Coen, D.M., *Chapter 15: The Polymerase Chain Reaction*, in *Current Protocols in Molecular Biology*. 2001, John Wiley & Sons, Inc. p. 15.0.1-15.8.21.

320. Livak, K.J. and T.D. Schmittgen, *Analysis of relative gene expression data using real-time quantitative PCR and the 2(-Delta Delta C(T)) Method.* Methods, 2001. **25**(4): p. 402-8.

321. Schmittgen, T.D. and K.J. Livak, *Analyzing real-time PCR data by the comparative C(T) method.* Nat Protoc, 2008. **3**(6): p. 1101-8.

322. Doolittle, R.F., G. Spraggon, and S.J. Everse, *Three-dimensional structural studies on fragments of fibrinogen and fibrin.* Curr Opin Struct Biol, 1998. **8**(6): p. 792-8.

323. Herrick, S., et al., *Fibrinogen.* Int J Biochem Cell Biol, 1999. **31**(7): p. 741-6.

324. Fish, R.J. and M. Neerman-Arbez, *Fibrinogen gene regulation.* Thromb Haemost, 2012. **108**(3): p. 419-26.

325. Kollman, J.M., et al., *Crystal structure of human fibrinogen.* Biochemistry, 2009. **48**(18): p. 3877-86.

326. Hoppe, B., *Fibrinogen and factor XIII at the intersection of coagulation, fibrinolysis and inflammation.* Thromb Haemost, 2014. **112**(4): p. 649-58.

327. Davalos, D. and K. Akassoglou, *Fibrinogen as a key regulator of inflammation in disease.* Semin Immunopathol, 2012. **34**(1): p. 43-62.

328. Mosesson, M.W., *Fibrinogen and fibrin structure and functions.* J Thromb Haemost, 2005. **3**(8): p. 1894-904.

329. Ugarova, T.P. and V.P. Yakubenko, *Recognition of fibrinogen by leukocyte integrins.* Ann N Y Acad Sci, 2001. **936**: p. 368-85.

330. Gardiner, E.E. and S.E. D'Souza, *A mitogenic action for fibrinogen mediated through intercellular adhesion molecule-1.* J Biol Chem, 1997. **272**(24): p. 15474-80.

331. Forsyth, C.B., et al., *Integrin alpha(M)beta(2)-mediated cell migration to fibrinogen and its recognition peptides.* J Exp Med, 2001. **193**(10): p. 1123-33.

332. Richardson, D.L., D.S. Pepper, and A.B. Kay, *Chemotaxis for human monocytes by fibrinogen-derived peptides.* Br J Haematol, 1976. **32**(4): p. 507-13.

333. Senior, R.M., et al., *Effects of fibrinogen derivatives upon the inflammatory response. Studies with human fibrinopeptide B.* J Clin Invest, 1986. **77**(3): p. 1014-9.

334. Solovjov, D.A., E. Pluskota, and E.F. Plow, *Distinct roles for the alpha and beta subunits in the functions of integrin alphaMbeta2.* J Biol Chem, 2005. **280**(2): p. 1336-45.

335. De Ceuleneer, M., et al., *Quantification of citrullination by means of skewed isotope distribution pattern.* J Proteome Res, 2012. **11**(11): p. 5245-51.

336. Vossenaar, E.R., et al., *PAD, a growing family of citrullinating enzymes: genes, features and involvement in disease.* Bioessays, 2003. **25**(11): p. 1106-18.

337. Gyorgy, B., et al., *Citrullination: a posttranslational modification in health and disease.* Int J Biochem Cell Biol, 2006. **38**(10): p. 1662-77.

338. Lee, D.M. and M.E. Weinblatt, *Rheumatoid arthritis.* Lancet, 2001. **358**(9285): p. 903-11.

339. Ingegnoli, F., et al., *Inflammatory and prothrombotic biomarkers in patients with rheumatoid arthritis: effects of tumor necrosis factor-alpha blockade.* J Autoimmun, 2008. **31**(2): p. 175-9.

340. So, A.K., et al., *Arthritis is linked to local and systemic activation of coagulation and fibrinolysis pathways.* J Thromb Haemost, 2003. **1**(12): p. 2510-5.

341. Weinberg, J.B., A.M. Pippen, and C.S. Greenberg, *Extravascular fibrin formation and dissolution in synovial tissue of patients with osteoarthritis and rheumatoid arthritis.* Arthritis Rheum, 1991. **34**(8): p. 996-1005.

342. Adams, R.A., et al., *The fibrin-derived gamma377-395 peptide inhibits microglia activation and suppresses relapsing paralysis in central nervous system autoimmune disease.* J Exp Med, 2007. **204**(3): p. 571-82.

343. Petzelbauer, P., et al., *The fibrin-derived peptide Bbeta15-42 protects the myocardium against ischemia-reperfusion injury.* Nat Med, 2005. **11**(3): p. 298-304.

344. Zacharowski, K., et al., *The effects of the fibrin-derived peptide Bbeta(15-42) in acute and chronic rodent models of myocardial ischemia-reperfusion.* Shock, 2007. **27**(6): p. 631-7.

345. Roesner, J.P., et al., *The fibrin-derived peptide Bbeta15-42 is cardioprotective in a pig model of myocardial ischemia-reperfusion injury.* Crit Care Med, 2007. **35**(7): p. 1730-5.

346. Roesner, J.P., et al., *Bbeta15-42 (FX06) reduces pulmonary, myocardial, liver, and small intestine damage in a pig model of hemorrhagic shock and reperfusion.* Crit Care Med, 2009. **37**(2): p. 598-605.

347. Wiedemann, D., et al., *The fibrin-derived peptide Bbeta(15-42) significantly attenuates ischemia-reperfusion injury in a cardiac transplant model.* Transplantation, 2010. **89**(7): p. 824-9.

348. Varisco, P.A., et al., *Effect of thrombin inhibition on synovial inflammation in antigen induced arthritis.* Ann Rheum Dis, 2000. **59**(10): p. 781-7.

349. Marty, I., et al., *Amelioration of collagen-induced arthritis by thrombin inhibition.* J Clin Invest, 2001. **107**(5): p. 631-40.

350. Han, M.H., et al., *Proteomic analysis of active multiple sclerosis lesions reveals therapeutic targets.* Nature, 2008. **451**(7182): p. 1076-81.

351. Akassoglou, K., et al., *Fibrin depletion decreases inflammation and delays the onset of demyelination in a tumor necrosis factor transgenic mouse model for multiple sclerosis.* Proc Natl Acad Sci U S A, 2004. **101**(17): p. 6698-703.

352. Paul, J., S. Strickland, and J.P. Melchor, *Fibrin deposition accelerates neurovascular damage and neuroinflammation in mouse models of Alzheimer's disease.* J Exp Med, 2007. **204**(8): p. 1999-2008.

353. Ryu, J.K. and J.G. McLarnon, *A leaky blood-brain barrier, fibrinogen infiltration and microglial reactivity in inflamed Alzheimer's disease brain.* J Cell Mol Med, 2009. **13**(9A): p. 2911-25.

354. Vidal, B., et al., *Fibrinogen drives dystrophic muscle fibrosis via a TGFbeta/alternative macrophage activation pathway.* Genes Dev, 2008. **22**(13): p. 1747-52.

355. Schellekens, G.A., et al., *Citrulline is an essential constituent of antigenic determinants recognized by rheumatoid arthritis-specific autoantibodies.* J Clin Invest, 1998. **101**(1): p. 273-81.

356. Zendman, A.J., E.R. Vossenaar, and W.J. van Venrooij, *Autoantibodies to citrullinated (poly)peptides: a key diagnostic and prognostic marker for rheumatoid arthritis.* Autoimmunity, 2004. **37**(4): p. 295-9.

357. Nielen, M.M., et al., *Specific autoantibodies precede the symptoms of rheumatoid arthritis: a study of serial measurements in blood donors.* Arthritis Rheum, 2004. **50**(2): p. 380-6.

358. Robinson, W.H. and J. Sokolove, *Citrullination of fibrinogen: generation of neoepitopes and enhancement of immunostimulatory properties.* Arthritis Research & Therapy, 2012. **14**(Suppl 1): p. O30-O30.

359. van der Helm-van Mil, A.H., et al., *Antibodies to citrullinated proteins and differences in clinical progression of rheumatoid arthritis.* Arthritis Res Ther, 2005. **7**(5): p. R949-58.

360. van Gaalen, F.A., et al., *Autoantibodies to cyclic citrullinated peptides predict progression to rheumatoid arthritis in patients with undifferentiated arthritis: a prospective cohort study.* Arthritis Rheum, 2004. **50**(3): p. 709-15.

361. Chang, X., et al., *Localization of peptidylarginine deiminase 4 (PADI4) and citrullinated protein in synovial tissue of rheumatoid arthritis.* Rheumatology (Oxford), 2005. **44**(1): p. 40-50.

362. Takizawa, Y., et al., *Citrullinated fibrinogen detected as a soluble citrullinated autoantigen in rheumatoid arthritis synovial fluids.* Ann Rheum Dis, 2006. **65**(8): p. 1013-20.

363. Nogueira, L., et al., *Autoantibodies to deiminated fibrinogen are the most efficient serological criterion for early rheumatoid arthritis diagnosis.* Arthritis Research & Therapy, 2003. **5**(Suppl 1): p. 18-18.

364. Vossenaar, E.R., et al., *The presence of citrullinated proteins is not specific for rheumatoid synovial tissue.* Arthritis Rheum, 2004. **50**(11): p. 3485-94.

365. Bausch-Fluck, D., et al., *A mass spectrometric-derived cell surface protein atlas.* PLoS One, 2015. **10**(3): p. e0121314.

366. Salmond, R.J., et al., *T-cell receptor proximal signaling via the Src-family kinases, Lck and Fyn, influences T-cell activation, differentiation, and tolerance.* Immunol Rev, 2009. **228**(1): p. 9-22.

367. Daniels, M.A., K.A. Hogquist, and S.C. Jameson, *Sweet 'n' sour: the impact of differential glycosylation on T cell responses.* Nat Immunol, 2002. **3**(10): p. 903-10.

368. Earl, L.A. and L.G. Baum, *CD45 glycosylation controls T-cell life and death.* Immunol Cell Biol, 2008. **86**(7): p. 608-15.

369. Redegeld, F.A., et al., *Phosphorylation of T-lymphocyte plasma membrane-associated proteins by ectoprotein kinases: implications for a possible role for ectophosphorylation in T-cell effector functions.* Biochim Biophys Acta, 1997. **1328**(2): p. 151-65.

370. Jury, E.C., et al., *Increased ubiquitination and reduced expression of LCK in T lymphocytes from patients with systemic lupus erythematosus.* Arthritis Rheum, 2003. **48**(5): p. 1343-54.

371. Braun, R.J., et al., *Two-dimensional electrophoresis of membrane proteins.* Anal Bioanal Chem, 2007. **389**(4): p. 1033-45.

372. Kügler, M., et al., *Analysis of the chloroplast protein complexes by blue-native polyacrylamide gel electrophoresis (BN-PAGE).* Photosynthesis Research, 1997. **53**(1): p. 35-44.

373. Ludwig, J., et al., *Identification and characterization of a novel 9.2-kDa membrane sector-associated protein of vacuolar proton-ATPase from chromaffin granules.* J Biol Chem, 1998. **273**(18): p. 10939-47.

374. Schagger, H., *Blue-native gels to isolate protein complexes from mitochondria.* Methods Cell Biol, 2001. **65**: p. 231-44.

375. Pfeiffer, K., et al., *Cardiolipin stabilizes respiratory chain supercomplexes.* J Biol Chem, 2003. **278**(52): p. 52873-80.

376. Schagger, H., *Native electrophoresis for isolation of mitochondrial oxidative phosphorylation protein complexes.* Methods Enzymol, 1995. **260**: p. 190-202.

377. Nakayama-Hamada, M., et al., *Comparison of enzymatic properties between hPADI2 and hPADI4.* Biochemical and Biophysical Research Communications, 2005. **327**(1): p. 192-200.

378. Stensland, M.E., et al., *Primary sequence, together with other factors, influence peptide deimination by peptidylarginine deiminase-4.* Biol Chem, 2009. **390**(2): p. 99-107.

379. van Beers, J.J., et al., *Mapping of citrullinated fibrinogen B-cell epitopes in rheumatoid arthritis by imaging surface plasmon resonance.* Arthritis Res Ther, 2010. **12**(6): p. R219.

380. Saveliev, S., et al., *Trypsin/Lys-C protease mix for enhanced protein mass spectrometry analysis.* Nat Meth, 2013. **10**(11).

381. Li, L., C.L. Wilbur, and K.L. Mintz, *Kinetics of Hydrothermal Inactivation of Endotoxins.* Applied and Environmental Microbiology, 2011. **77**(8): p. 2640-2647.

382. Camacho-Carvajal, M.M., et al., *Two-dimensional Blue native/SDS gel electrophoresis of multi-protein complexes from whole cellular lysates: a proteomics approach.* Mol Cell Proteomics, 2004. **3**(2): p. 176-82.

383. Culvenor, J.G., et al., *Characterization of presenilin complexes from mouse and human brain using Blue Native gel electrophoresis reveals high expression in embryonic brain and minimal change in complex mobility with pathogenic presenilin mutations.* Eur J Biochem, 2004. **271**(2): p. 375-85.

384. Evin, G., et al., *Transition-state analogue gamma-secretase inhibitors stabilize a 900 kDa presenilin/nicastrin complex.* Biochemistry, 2005. **44**(11): p. 4332-41.

385. Ilaya, N.T., et al., *Nicastrin expression in mouse peripheral tissues is not co-ordinated with presenilin and is high in muscle.* J Neurochem, 2004. **91**(1): p. 230-7.

386. Nyabi, O., et al., *Presenilins mutated at Asp-257 or Asp-385 restore Pen-2 expression and Nicastrin glycosylation but remain catalytically inactive in the absence of wild type Presenilin.* J Biol Chem, 2003. **278**(44): p. 43430-6.

387. Rodriguez, P., et al., *NAP-2 is part of multi-protein complexes in HeLa cells.* J Cell Biochem, 2004. **93**(2): p. 398-408.

388. Shibatani, T., et al., *Proteomic analysis of mammalian oligosaccharyltransferase reveals multiple subcomplexes that contain Sec61, TRAP, and two potential new subunits.* Biochemistry, 2005. **44**(16): p. 5982-92.

389. Richter, J., et al., *CD161 receptor participates in both impairing NK cell cytotoxicity and the response to glycans and vimentin in patients with rheumatoid arthritis.* Clin Immunol, 2010. **136**(1): p. 139-47.

390. Bartold, P.M., R.I. Marshall, and D.R. Haynes, *Periodontitis and rheumatoid arthritis: A review.* Journal of Periodontology, 2005. **76**(11): p. 2066-2074.

391. Sahaf, B., et al., *The extracellular microenvironment plays a key role in regulating the redox status of cell surface proteins in HIV-infected subjects.* Arch Biochem Biophys, 2005. **434**(1): p. 26-32.

392. Carilho Torrao, R.B., et al., *Healthy ageing and depletion of intracellular glutathione influences T cell membrane thioredoxin-1 levels and cytokine secretion.* Chem Cent J, 2013. **7**(1): p. 150.

393. Wild, A.C., H.R. Moinova, and R.T. Mulcahy, *Regulation of gamma-glutamylcysteine synthetase subunit gene expression by the transcription factor Nrf2.* J Biol Chem, 1999. **274**(47): p. 33627-36.

394. Holmgren, A., *Thioredoxin.* Annu Rev Biochem, 1985. **54**: p. 237-71.

395. Holmgren, A. and M. Bjornstedt, *Thioredoxin and thioredoxin reductase.* Methods Enzymol, 1995. **252**: p. 199-208.

396. Holmgren, A., *Thioredoxin and glutaredoxin systems.* J Biol Chem, 1989. **264**(24): p. 13963-6.

397. Holmgren, A., *Thioredoxin structure and mechanism: conformational changes on oxidation of the active-site sulfhydryls to a disulfide.* Structure, 1995. **3**(3): p. 239-43.

398. Landino, L.M., T.E. Skreslet, and J.A. Alston, *Cysteine oxidation of tau and microtubule-associated protein-2 by peroxynitrite: modulation of microtubule assembly kinetics by the thioredoxin reductase system.* J Biol Chem, 2004. **279**(33): p. 35101-5.

399. Ravi, D., H. Muniyappa, and K.C. Das, *Endogenous thioredoxin is required for redox cycling of anthracyclines and p53-dependent apoptosis in cancer cells.* J Biol Chem, 2005. **280**(48): p. 40084-96.

400. Benhar, M., et al., *Regulated protein denitrosylation by cytosolic and mitochondrial thioredoxins.* Science, 2008. **320**(5879): p. 1050-4.

401. Nakamura, T., et al., *Redox regulation of lung inflammation by thioredoxin.* Antioxid Redox Signal, 2005. **7**(1-2): p. 60-71.

402. Nakamura, H., K. Nakamura, and J. Yodoi, *Redox regulation of cellular activation.* Annu Rev Immunol, 1997. **15**: p. 351-69.

403. Bertini, R., et al., *Thioredoxin, a redox enzyme released in infection and inflammation, is a unique chemoattractant for neutrophils, monocytes, and T cells.* J Exp Med, 1999. **189**(11): p. 1783-9.

404. Kern, R., et al., *Chaperone properties of Escherichia coli thioredoxin and thioredoxin reductase.* Biochem J, 2003. **371**(Pt 3): p. 965-72.

405. Lahav, J., et al., *Sustained integrin ligation involves extracellular free sulfhydryls and enzymatically catalyzed disulfide exchange.* Blood, 2002. **100**(7): p. 2472-8.

406. Manickam, N., et al., *Protein disulphide isomerase in platelet function.* Br J Haematol, 2008. **140**(2): p. 223-9.

407. Fenouillet, E., et al., *The catalytic activity of protein disulfide isomerase is involved in human immunodeficiency virus envelope-mediated membrane fusion after CD4 cell binding.* J Infect Dis, 2001. **183**(5): p. 744-52.

408. Fenouillet, E., R. Barbouche, and I.M. Jones, *Cell entry by enveloped viruses: redox considerations for HIV and SARS-coronavirus.* Antioxid Redox Signal, 2007. **9**(8): p. 1009-34.

409. Gallina, A., et al., *Inhibitors of protein-disulfide isomerase prevent cleavage of disulfide bonds in receptor-bound glycoprotein 120 and prevent HIV-1 entry.* J Biol Chem, 2002. **277**(52): p. 50579-88.

410. Markovic, I., et al., *Thiol/disulfide exchange is a prerequisite for CXCR4-tropic HIV-1 envelope-mediated T-cell fusion during viral entry.* Blood, 2004. **103**(5): p. 1586-94.

411. Papandreou, M.J., et al., *Mapping of domains on HIV envelope protein mediating association with calnexin and protein-disulfide isomerase.* J Biol Chem, 2010. **285**(18): p. 13788-96.

412. Reyes, B.M., et al., *Redox equilibrium in mucosal T cells tunes the intestinal TCR signaling threshold.* J Immunol, 2005. **175**(4): p. 2158-66.

413. Aon, M.A., S. Cortassa, and B. O'Rourke, *Redox-optimized ROS balance: a unifying hypothesis.* Biochim Biophys Acta, 2010. **1797**(6-7): p. 865-77.

414. Torrao, R.C., et al., *Does metabolic reprogramming underpin age-associated changes in T cell phenotype and function?* Free Radic Biol Med, 2014. **71**: p. 26-35.

415. Rodriguez, S.B., B.L. Stitt, and D.E. Ash, *Cysteine 351 is an essential nucleophile in catalysis by Porphyromonas gingivalis peptidylarginine deiminase.* Arch Biochem Biophys, 2010. **504**(2): p. 190-6.

416. Vander Heiden, M.G., L.C. Cantley, and C.B. Thompson, *Understanding the Warburg effect: the metabolic requirements of cell proliferation.* Science, 2009. **324**(5930): p. 1029-33.

417. Anastasiou, D., et al., *Inhibition of pyruvate kinase M2 by reactive oxygen species contributes to cellular antioxidant responses.* Science, 2011. **334**(6060): p. 1278-83.

418. Macintyre, A.N. and J.C. Rathmell, *Activated lymphocytes as a metabolic model for carcinogenesis.* Cancer Metab, 2013. **1**(1): p. 5.

419. Nelson, B.H., *IL-2, Regulatory T Cells, and Tolerance.* The Journal of Immunology, 2004. **172**: p. 3983.

420. Kmieciak, M., et al., *Human T cells express CD25 and Foxp3 upon activation and exhibit effector/memory phenotypes without any regulatory/suppressor function.* J Transl Med, 2009. **7**: p. 89.

421. Jones, J.E., et al., *Protein arginine deiminase 4 (PAD4): Current understanding and future therapeutic potential.* Curr Opin Drug Discov Devel, 2009. **12**(5): p. 616-27.

422. The, J. and J.L. Ebersole, *Rheumatoid factor from periodontitis patients cross-reacts with epitopes on oral bacteria.* Oral Dis, 1996. **2**(4): p. 253-62.

423. Havemose-Poulsen, A., et al., *Periodontal and hematological characteristics associated with aggressive periodontitis, juvenile idiopathic arthritis, and rheumatoid arthritis.* J Periodontol, 2006. **77**(2): p. 280-8.

424. Hendler, A., et al., *Involvement of autoimmunity in the pathogenesis of aggressive periodontitis.* J Dent Res, 2010. **89**(12): p. 1389-94.

425. The, J. and J.L. Ebersole, *Rheumatoid factor (RF) distribution in periodontal disease.* J Clin Immunol, 1991. **11**(3): p. 132-42.

426. Feitsma, A.L., et al., *Identification of citrullinated vimentin peptides as T cell epitopes in HLA-DR4-positive patients with rheumatoid arthritis.* Arthritis Rheum, 2010. **62**(1): p. 117-25.

427. Nielen, M.M., et al., *Antibodies to citrullinated human fibrinogen (ACF) have diagnostic and prognostic value in early arthritis.* Ann Rheum Dis, 2005. **64**(8): p. 1199-204.

428. Nurieva, R., et al., *T-cell tolerance or function is determined by combinatorial costimulatory signals.* EMBO J, 2006. **25**(11): p. 2623-33.

429. Harada, Y., et al., *A single amino acid alteration in cytoplasmic domain determines IL-2 promoter activation by ligation of CD28 but not inducible costimulator (ICOS).* J Exp Med, 2003. **197**(2): p. 257-62.

430. Pei, Y., et al., *Nuclear export of NF90 to stabilize IL-2 mRNA is mediated by AKT-dependent phosphorylation at Ser647 in response to CD28 costimulation.* J Immunol, 2008. **180**(1): p. 222-9.

431. Thomas, R.M., L. Gao, and A.D. Wells, *Signals from CD28 induce stable epigenetic modification of the IL-2 promoter.* J Immunol, 2005. **174**(8): p. 4639-46.

432. Beadling, C. and K.A. Smith, *DNA array analysis of interleukin-2-regulated immediate/early genes.* Med Immunol, 2002. **1**(1): p. 2.

433. Ceuppens, J.L., et al., *Human T cell activation with phytohemagglutinin. The function of IL-6 as an accessory signal.* J Immunol, 1988. **141**(11): p. 3868-74.

434. Larsson, E.L. and A. Coutinho, *The role of mitogenic lectins in T-cell triggering.* Nature, 1979. **280**(5719): p. 239-41.

435. Ada M. Kruisbeek, Ethan Shevach, and A.M. Thornton, *Proliferative Assays for T Cell Function* in *Current Protocols in Immunology*. 2004.

436. Ozato, K., J. Cebra, and J.D. Ebert, *Cell-mediated mitogenic response induced by leukoagglutinin and Lens culinaris lectin in mouse lymphocytes.* J Exp Med, 1977. **146**(3): p. 779-91.

437. Duarte, R.F., et al., *Functional impairment of human T-lymphocytes following PHA-induced expansion and retroviral transduction: implications for gene therapy.* Gene Ther, 2002. **9**(20): p. 1359-68.

438. Bolen, C.R., M. Uduman, and S.H. Kleinstein, *Cell subset prediction for blood genomic studies.* BMC Bioinformatics, 2011. **12**: p. 258.

439. Khalaf, H. and T. Bengtsson, *Altered T-cell responses by the periodontal pathogen Porphyromonas gingivalis.* PLoS One, 2012. **7**(9): p. e45192.

440. Seymour, G.J., et al., *Interleukin-2 production and bone-resorption activity in vitro by unstimulated lymphocytes extracted from chronically-inflamed human periodontal tissues.* Arch Oral Biol, 1985. **30**(6): p. 481-4.

441. Mastronardi, F.G., et al., *Increased citrullination of histone H3 in multiple sclerosis brain and animal models of demyelination: a role for tumor necrosis factor-induced peptidylarginine deiminase 4 translocation.* J Neurosci, 2006. **26**(44): p. 11387-96.

442. Darrah, E., et al., *Peptidylarginine deiminase 2, 3 and 4 have distinct specificities against cellular substrates: novel insights into autoantigen selection in rheumatoid arthritis.* Ann Rheum Dis, 2012. **71**(1): p. 92-8.

443. Harvey, G.P., et al., *Expression of peptidylarginine deiminase-2 and -4, citrullinated proteins and anti-citrullinated protein antibodies in human gingiva.* J Periodontal Res, 2013. **48**(2): p. 252-61.

444. Crosley, L.K., et al., *Variation in protein levels obtained from human blood cells and biofluids for platelet, peripheral blood mononuclear cell, plasma, urine and saliva proteomics.* Genes Nutr, 2009. **4**(2): p. 95-102.

445. Uhlen, P., et al., *Calcium signaling in neocortical development.* Dev Neurobiol, 2015. **75**(4): p. 360-8.

446. Takahara, H., H. Okamoto, and K. Sugawara, *Calcium-dependent Properties of Peptidylarginine Deiminase from Rabbit Skeletal Muscle.* Agricultural and Biological Chemistry, 1986. **50**(11): p. 2899-2904.

447. Darrah, E., et al., *Erosive rheumatoid arthritis is associated with antibodies that activate PAD4 by increasing calcium sensitivity.* Sci Transl Med, 2013. **5**(186): p. 186ra65.

448. Arandjelovic, S., et al., *ATP induces protein arginine deiminase 2-dependent citrullination in mast cells through the P2X7 purinergic receptor.* J Immunol, 2012. **189**(8): p. 4112-22.

449. Linker-Israeli, M., et al., *Defective production of interleukin 1 and interleukin 2 in patients with systemic lupus erythematosus (SLE).* J Immunol, 1983. **130**(6): p. 2651-5.

450. Alcocer-Varela, J. and D. Alarcon-Segovia, *Decreased production of and response to interleukin-2 by cultured lymphocytes from patients with systemic lupus erythematosus.* J Clin Invest, 1982. **69**(6): p. 1388-92.

451. Wofsy, D., et al., *Deficient interleukin 2 activity in MRL/Mp and C57BL/6J mice bearing the lpr gene.* J Exp Med, 1981. **154**(5): p. 1671-80.

452. Solomou, E.E., et al., *Molecular basis of deficient IL-2 production in T cells from patients with systemic lupus erythematosus.* J Immunol, 2001. **166**(6): p. 4216-22.

453. Kovacs, B., et al., *Defective CD3-mediated cell death in activated T cells from patients with systemic lupus erythematosus: role of decreased intracellular TNF-alpha.* Clin Immunol Immunopathol, 1996. **81**(3): p. 293-302.

454. Xu, L., et al., *Human lupus T cells resist inactivation and escape death by upregulating COX-2.* Nat Med, 2004. **10**(4): p. 411-5.

455. Williams, M.A., A.J. Tyznik, and M.J. Bevan, *Interleukin-2 signals during priming are required for secondary expansion of CD8+ memory T cells.* Nature, 2006. **441**(7095): p. 890-3.

456. de Faucal, P., et al., *Impaired IL2 production by lymphocytes of patients with systemic lupus erythematosus.* Ann Immunol (Paris), 1984. **135D**(2): p. 161-72.

457. Gerriets, V.A. and J.C. Rathmell, *Metabolic pathways in T cell fate and function.* Trends Immunol, 2012. **33**(4): p. 168-73.

458. Mauro, C. and F.M. Marelli-Berg, *T cell immunity and cardiovascular metabolic disorders: does metabolism fuel inflammation?* Front Immunol, 2012. **3**: p. 173.

459. Colegio, O.R., et al., *Functional polarization of tumour-associated macrophages by tumour-derived lactic acid.* Nature, 2014. **513**(7519): p. 559-63.

460. Fischer, K., et al., *Inhibitory effect of tumor cell-derived lactic acid on human T cells.* Blood, 2007. **109**(9): p. 3812-9.

461. Leite, T.C., et al., *Lactate downregulates the glycolytic enzymes hexokinase and phosphofructokinase in diverse tissues from mice.* FEBS Lett, 2011. **585**(1): p. 92-8.

462. Hashimoto, T., et al., *Lactate sensitive transcription factor network in L6 cells: activation of MCT1 and mitochondrial biogenesis.* FASEB J, 2007. **21**(10): p. 2602-12.

463. Haas, R., et al., *Lactate Regulates Metabolic and Pro-inflammatory Circuits in Control of T Cell Migration and Effector Functions.* PLoS Biol, 2015. **13**(7): p. e1002202.

464. Tarasenko, T.N., J. Gomez-Rodriguez, and P.J. McGuire, *Impaired T cell function in argininosuccinate synthetase deficiency.* J Leukoc Biol, 2015. **97**(2): p. 273-8.

465. Zea, A.H., et al., *L-Arginine modulates CD3zeta expression and T cell function in activated human T lymphocytes.* Cell Immunol, 2004. **232**(1-2): p. 21-31.

466. Rodriguez, P.C., et al., *L-arginine deprivation regulates cyclin D3 mRNA stability in human T cells by controlling HuR expression.* J Immunol, 2010. **185**(9): p. 5198-204.

467. Rodriguez, P.C., D.G. Quiceno, and A.C. Ochoa, *L-arginine availability regulates T-lymphocyte cell-cycle progression.* Blood, 2007. **109**(4): p. 1568-73.

468. Fletcher, M., et al., *l-Arginine depletion blunts antitumor T-cell responses by inducing myeloid-derived suppressor cells.* Cancer Res, 2015. **75**(2): p. 275-83.

469. Qualls, J.E., et al., *Sustained generation of nitric oxide and control of mycobacterial infection requires argininosuccinate synthase 1.* Cell Host Microbe, 2012. **12**(3): p. 313-23.

470. Matsushita, N., et al., *Elevated levels of soluble CD163 in sera and fluids from rheumatoid arthritis patients and inhibition of the shedding of CD163 by TIMP-3.* Clin Exp Immunol, 2002. **130**(1): p. 156-61.

471. Baeten, D., et al., *Association of CD163+ macrophages and local production of soluble CD163 with decreased lymphocyte activation in spondylarthropathy synovitis.* Arthritis Rheum, 2004. **50**(5): p. 1611-23.

472. Subathra, M., A. Qureshi, and C. Luberto, *Sphingomyelin synthases regulate protein trafficking and secretion.* PLoS One, 2011. **6**(9): p. e23644.

473. Zech, T., et al., *Accumulation of raft lipids in T-cell plasma membrane domains engaged in TCR signalling.* EMBO J, 2009. **28**(5): p. 466-76.

474. Molano, A., et al., *Age-dependent changes in the sphingolipid composition of mouse CD4+ T cell membranes and immune synapses implicate glucosylceramides in age-related T cell dysfunction.* PLoS One, 2012. **7**(10): p. e47650.

475. Asano, S., et al., *Regulation of cell migration by sphingomyelin synthases: sphingomyelin in lipid rafts decreases responsiveness to signaling by the CXCL12/CXCR4 pathway.* Mol Cell Biol, 2012. **32**(16): p. 3242-52.

476. Stoffel, B., et al., *Ceramide-independent CD28 and TCR signaling but reduced IL-2 secretion in T cells of acid sphingomyelinase-deficient mice.* Eur J Immunol, 1998. **28**(3): p. 874-80.

477. Martin, J.A., et al., *Oxidative stress as a signal to up-regulate gamma-cystathionase in the fetal-to-neonatal transition in rats.* Cell Mol Biol (Noisy-le-grand), 2007. **53 Suppl**: p. OL1010-7.

478. Srivastava, M.K., et al., *Myeloid-derived suppressor cells inhibit T-cell activation by depleting cystine and cysteine.* Cancer Res, 2010. **70**(1): p. 68-77.

479. Garg, S.K., et al., *Differential dependence on cysteine from transsulfuration versus transport during T cell activation.* Antioxid Redox Signal, 2011. **15**(1): p. 39-47.

480. Ishii, T., Y. Sugita, and S. Bannai, *Regulation of glutathione levels in mouse spleen lymphocytes by transport of cysteine.* J Cell Physiol, 1987. **133**(2): p. 330-6.

481. Messina, J.P. and D.A. Lawrence, *Effects of 2-mercaptoethanol and buthionine sulfoximine on cystine metabolism by and proliferation of mitogen-stimulated human and mouse lymphocytes.* Int J Immunopharmacol, 1992. **14**(7): p. 1221-34.

482. Castellani, P., et al., *The thiol redox state of lymphoid organs is modified by immunization: role of different immune cell populations.* Eur J Immunol, 2008. **38**(9): p. 2419-25.

483. Levring, T.B., et al., *Activated human CD4+ T cells express transporters for both cysteine and cystine.* Sci Rep, 2012. **2**: p. 266.

484. Ghebrehiwet, B., et al., *Isolation, cDNA cloning, and overexpression of a 33-kD cell surface glycoprotein that binds to the globular "heads" of C1q.* J Exp Med, 1994. **179**(6): p. 1809-21.

485. Johne, J., et al., *Platelets promote coagulation factor XII-mediated proteolytic cascade systems in plasma.* Biol Chem, 2006. **387**(2): p. 173-8.

486. Etienne-Manneville, S. and A. Hall, *Rho GTPases in cell biology.* Nature, 2002. **420**(6916): p. 629-35.

487. Pernis, A.B., *Rho GTPase-mediated pathways in mature CD4+ T cells.* Autoimmun Rev, 2009. **8**(3): p. 199-203.

488. Li, B., et al., *Role of the guanosine triphosphatase Rac2 in T helper 1 cell differentiation.* Science, 2000. **288**(5474): p. 2219-22.

489. Yu, H., et al., *Deficiency of small GTPase Rac2 affects T cell activation.* J Exp Med, 2001. **194**(7): p. 915-26.

490. DerMardirossian, C. and G.M. Bokoch, *GDIs: central regulatory molecules in Rho GTPase activation.* Trends Cell Biol, 2005. **15**(7): p. 356-63.

491. Su, L., et al., *A novel E3 ubiquitin ligase substrate screen identifies Rho guanine dissociation inhibitor as a substrate of gene related to anergy in lymphocytes.* J Immunol, 2006. **177**(11): p. 7559-66.

492. Ma, Z., et al., *Mitochondrial F1Fo-ATP synthase translocates to cell surface in hepatocytes and has high activity in tumor-like acidic and hypoxic environment.* Acta Biochim Biophys Sin (Shanghai), 2010. **42**(8): p. 530-7.

493. Porcellini, S., et al., *Regulation of peripheral T cell activation by calreticulin.* J Exp Med, 2006. **203**(2): p. 461-71.

494. Hong, C., et al., *Functional analysis of recombinant calreticulin fragment 39-272: implications for immunobiological activities of calreticulin in health and disease.* J Immunol, 2010. **185**(8): p. 4561-9.

495. Liu, Y.C., et al., *Sialylation and fucosylation of epidermal growth factor receptor suppress its dimerization and activation in lung cancer cells.* Proc Natl Acad Sci U S A, 2011. **108**(28): p. 11332-7.

496. Chandler, K.B. and C.E. Costello, *Glycomics and glycoproteomics of membrane proteins and cell-surface receptors: Present trends and future opportunities.* Electrophoresis, 2016. **37**(11): p. 1407-1419.

497. Griffin, N.M. and J.E. Schnitzer, *Overcoming key technological challenges in using mass spectrometry for mapping cell surfaces in tissues.* Mol Cell Proteomics, 2011. **10**(2): p. R110 000935.

498. Kemper, C. and J.P. Atkinson, *T-cell regulation: with complements from innate immunity.* Nat Rev Immunol, 2007. **7**(1): p. 9-18.

499. Kwan, W.H., W. van der Touw, and P.S. Heeger, *Complement regulation of T cell immunity.* Immunol Res, 2012. **54**(1-3): p. 247-53.

500. Newman, M.G., et al., *Carranza's Clinical Periodontology*. 10th ed. 2006: Elsevier.

501. Hasan, A. and R.M. Palmer, *A clinical guide to periodontology: pathology of periodontal disease.* Br Dent J, 2014. **216**(8): p. 457-61.

502. Aoyagi, T., et al., *Interleukin 4 (IL-4) and IL-6-producing memory T-cells in peripheral blood and gingival tissue in periodontitis patients with high serum antibody titers to Porphyromonas gingivalis.* Oral Microbiol Immunol, 1995. **10**(5): p. 304-10.

503. Gemmell, E. and G.J. Seymour, *Cytokines and T cell switching.* Crit Rev Oral Biol Med, 1994. **5**(3-4): p. 249-79.

504. Manhart, S.S., et al., *Gingival cell IL-2 and IL-4 in early-onset periodontitis.* J Periodontol, 1994. **65**(9): p. 807-13.

505. Sigusch, B., et al., *Early-onset and adult periodontitis associated with abnormal cytokine production by activated T lymphocytes.* J Periodontol, 1998. **69**(10): p. 1098-104.

506. Tokoro, Y., et al., *Relevance of local Th2-type cytokine mRNA expression in immunocompetent infiltrates in inflamed gingival tissue to periodontal diseases.* Clin Exp Immunol, 1997. **107**(1): p. 166-74.

507. Reinhardt, R.A., et al., *IgG subclasses in gingival crevicular fluid from active versus stable periodontal sites.* J Periodontol, 1989. **60**(1): p. 44-50.

508. Ebersole, J.L. and M.A. Taubman, *The protective nature of host responses in periodontal diseases.* Periodontol 2000, 1994. **5**: p. 112-41.

509. Takeichi, O., et al., *Cytokine profiles of T-lymphocytes from gingival tissues with pathological pocketing.* J Dent Res, 2000. **79**(8): p. 1548-55.

510. Ukai, T., et al., *Immunohistological study of interferon-gamma- and interleukin-4-bearing cells in human periodontitis gingiva.* Arch Oral Biol, 2001. **46**(10): p. 901-8.

511. Cardoso, C.R., et al., *Evidence of the presence of T helper type 17 cells in chronic lesions of human periodontal disease.* Oral Microbiol Immunol, 2009. **24**(1): p. 1-6.

512. Dutzan, N., et al., *Interleukin-21 expression and its association with proinflammatory cytokines in untreated chronic periodontitis patients.* J Periodontol, 2012. **83**(7): p. 948-54.

513. Honda, T., et al., *Elevated expression of IL-17 and IL-12 genes in chronic inflammatory periodontal disease.* Clin Chim Acta, 2008. **395**(1-2): p. 137-41.

514. Lester, S.R., et al., *Gingival concentrations of interleukin-23 and -17 at healthy sites and at sites of clinical attachment loss.* J Periodontol, 2007. **78**(8): p. 1545-50.

515. Moutsopoulos, N.M., et al., *Porphyromonas gingivalis promotes Th17 inducing pathways in chronic periodontitis.* J Autoimmun, 2012. **39**(4): p. 294-303.

516. Ohyama, H., et al., *The involvement of IL-23 and the Th17 pathway in periodontitis.* J Dent Res, 2009. **88**(7): p. 633-8.

517. Szkaradkiewicz, A.K., et al., *Protective effect of oral Lactobacilli in pathogenesis of chronic periodontitis.* J Physiol Pharmacol, 2011. **62**(6): p. 685-9.

518. Vernal, R., et al., *Levels of interleukin-17 in gingival crevicular fluid and in supernatants of cellular cultures of gingival tissue from patients with chronic periodontitis.* J Clin Periodontol, 2005. **32**(4): p. 383-9.

519. Gainet, J., et al., *Neutrophil dysfunctions, IL-8, and soluble L-selectin plasma levels in rapidly progressive versus adult and localized juvenile periodontitis: variations according to disease severity and microbial flora.* J Immunol, 1999. **163**(9): p. 5013-9.

520. Chapple, I.L., et al., *Glutathione in gingival crevicular fluid and its relation to local antioxidant capacity in periodontal health and disease.* Mol Pathol, 2002. **55**(6): p. 367-73.

521. Savita, A.M., et al., *Evaluation of glutathione level in gingival crevicular fluid in periodontal health, in chronic periodontitis and after nonsurgical periodontal therapy: A clinicobiochemical study.* Contemp Clin Dent, 2015. **6**(2): p. 206-10.

522. Taubman, M.A., et al., *Phenotypic studies of cells from periodontal disease tissues.* J Periodontal Res, 1984. **19**(6): p. 587-90.

523. McGhee, M.L., et al., *Cellular analysis of functional mononuclear cells from chronically inflamed gingival tissue.* Reg Immunol, 1989. **2**(2): p. 103-10.

524. Gorska, R., et al., *Relationship between clinical parameters and cytokine profiles in inflamed gingival tissue and serum samples from patients with chronic periodontitis.* J Clin Periodontol, 2003. **30**(12): p. 1046-52.

525. Fentoglu, O., et al., *Pro-inflammatory cytokine levels in association between periodontal disease and hyperlipidaemia.* J Clin Periodontol, 2011. **38**(1): p. 8-16.

526. Cazalis, J., et al., *Tetracyclines and chemically modified tetracycline-3 (CMT-3) modulate cytokine secretion by lipopolysaccharide-stimulated whole blood.* Inflammation, 2009. **32**(2): p. 130-7.

527. Birkedal-Hansen, H., *Role of cytokines and inflammatory mediators in tissue destruction.* J Periodontal Res, 1993. **28**(6 Pt 2): p. 500-10.

528. Hirano, T., et al., *Biological and clinical aspects of interleukin 6.* Immunol Today, 1990. **11**(12): p. 443-9.

529. Bastos, M.F., et al., *TNF-alpha and IL-4 levels in generalized aggressive periodontitis subjects.* Oral Dis, 2009. **15**(1): p. 82-7.

530. Okada, H. and S. Murakami, *Cytokine expression in periodontal health and disease.* Crit Rev Oral Biol Med, 1998. **9**(3): p. 248-66.

531. Dongari-Bagtzoglou, A.I. and J.L. Ebersole, *Increased presence of interleukin-6 (IL-6) and IL-8 secreting fibroblast subpopulations in adult periodontitis.* J Periodontol, 1998. **69**(8): p. 899-910.

532. Cesar-Neto, J.B., et al., *Smoking modulates interleukin-6:interleukin-10 and RANKL:osteoprotegerin ratios in the periodontal tissues.* J Periodontal Res, 2007. **42**(2): p. 184-91.

533. Javed, F., M. Al-Askar, and K. Al-Hezaimi, *Cytokine profile in the gingival crevicular fluid of periodontitis patients with and without type 2 diabetes: a literature review.* J Periodontol, 2012. **83**(2): p. 156-61.

534. Ribeiro, F.V., et al., *Cytokines and bone-related factors in systemically healthy patients with chronic periodontitis and patients with type 2 diabetes and chronic periodontitis.* J Periodontol, 2011. **82**(8): p. 1187-96.

535. Bick, P.H., et al., *Polyclonal B-cell activation induced by extracts of Gram-negative bacteria isolated from periodontally diseased sites.* Infect Immun, 1981. **34**(1): p. 43-9.

536. Carpenter, A.B., et al., *T-cell regulation of polyclonal B-cell activation induced by extracts of oral bacteria associated with periodontal diseases.* Infect Immun, 1984. **43**(1): p. 326-36.

537. Donaldson, S.L., et al., *Blastogenic responses by lymphocytes from periodontally healthy populations induced by periodontitis-associated bacteria.* J Periodontol, 1982. **53**(12): p. 743-51.

538. Ito, H., et al., *Possible role of T cells in the establishment of IgG plasma cell-rich periodontal lesion--augmentation of IgG synthesis in the polyclonal B cell activation response by autoreactive T cells.* J Periodontal Res, 1988. **23**(1): p. 39-45.

539. Mangan, D.F. and D.E. Lopatin, *Polyclonal activation of human peripheral blood B lymphocytes by Fusobacterium nucleatum.* Infect Immun, 1983. **40**(3): p. 1104-11.

540. Okada, H., H. Ito, and Y. Harada, *T-cell requirement for establishment of the IgG-dominant B-cell lesion in periodontitis.* J Periodontal Res, 1987. **22**(3): p. 187-9.

541. Mosmann, T.R. and R.L. Coffman, *TH1 and TH2 cells: different patterns of lymphokine secretion lead to different functional properties.* Annu Rev Immunol, 1989. **7**: p. 145-73.

542. Mosmann, T.R. and S. Sad, *The expanding universe of T-cell subsets: Th1, Th2 and more.* Immunol Today, 1996. **17**(3): p. 138-46.

543. Sad, S., R. Marcotte, and T.R. Mosmann, *Cytokine-induced differentiation of precursor mouse CD8+ T cells into cytotoxic CD8+ T cells secreting Th1 or Th2 cytokines.* Immunity, 1995. **2**(3): p. 271-9.

544. Hamann, D., et al., *Phenotypic and functional separation of memory and effector human CD8+ T cells.* J Exp Med, 1997. **186**(9): p. 1407-18.

545. Petit, M.D., et al., *Phenotypical and functional analysis of T cells in periodontitis.* J Periodontal Res, 2001. **36**(4): p. 214-20.

546. Emingil, G., et al., *Phenotypic and functional analysis of peripheral blood mononuclear cells in generalised aggressive and chronic periodontitis patients.* J Int Acad Periodontol, 2001. **3**(4): p. 87-94.

547. Dudani, A.K., et al., *Isolation of a novel 45 kDa plasminogen receptor from human endothelial cells.* Thromb Res, 1993. **69**(2): p. 185-96.

548. Miles, L.A., et al., *Role of cell-surface lysines in plasminogen binding to cells: identification of alpha-enolase as a candidate plasminogen receptor.* Biochemistry, 1991. **30**(6): p. 1682-91.

549. Bennett, S.J., et al., *CD4(+) T cell surface alpha enolase is lower in older adults.* Mech Ageing Dev, 2015. **152**: p. 56-62.

550. Boyman, O. and J. Sprent, *The role of interleukin-2 during homeostasis and activation of the immune system.* Nat Rev Immunol, 2012. **12**(3): p. 180-90.

551. Andrukhov, O., et al., *Serum cytokine levels in periodontitis patients in relation to the bacterial load.* J Periodontol, 2011. **82**(6): p. 885-92.

552. Sutmuller, R.P., et al., *Toll-like receptor 2 controls expansion and function of regulatory T cells.* J Clin Invest, 2006. **116**(2): p. 485-94.

553. Xu, D., M. Komai-Koma, and F.Y. Liew, *Expression and function of Toll-like receptor on T cells.* Cell Immunol, 2005. **233**(2): p. 85-9.

554. Zanin-Zhorov, A., et al., *Heat shock protein 60 inhibits Th1-mediated hepatitis model via innate regulation of Th1/Th2 transcription factors and cytokines.* J Immunol, 2005. **174**(6): p. 3227-36.

555. Ling, S., et al., *Citrullinated calreticulin potentiates rheumatoid arthritis shared epitope signaling.* Arthritis Rheum, 2013. **65**(3): p. 618-26.

556. Ling, S., et al., *Activation of nitric oxide signaling by the rheumatoid arthritis shared epitope.* Arthritis Rheum, 2006. **54**(11): p. 3423-32.

557. Elschenbroich, S., et al., *Isolation of cell surface proteins for mass spectrometry-based proteomics.* Expert Rev Proteomics, 2010. **7**(1): p. 141-54.

558. Macher, B.A. and T.Y. Yen, *Proteins at membrane surfaces-a review of approaches.* Mol Biosyst, 2007. **3**(10): p. 705-13.

559. Tan, S., H.T. Tan, and M.C. Chung, *Membrane proteins and membrane proteomics.* Proteomics, 2008. **8**(19): p. 3924-32.

560. Tafesse, F.G., et al., *Both sphingomyelin synthases SMS1 and SMS2 are required for sphingomyelin homeostasis and growth in human HeLa cells.* J Biol Chem, 2007. **282**(24): p. 17537-47.

561. Droge, W., et al., *Regulation of T-cell functions by L-lactate.* Cell Immunol, 1987. **108**(2): p. 405-16.

562. Murray, C.M., et al., *Monocarboxylate transporter MCT1 is a target for immunosuppression.* Nat Chem Biol, 2005. **1**(7): p. 371-6.

563. Thompson, J.D., D.G. Higgins, and T.J. Gibson, *CLUSTAL W: improving the sensitivity of progressive multiple sequence alignment through sequence weighting, position-specific gap penalties and weight matrix choice.* Nucleic Acids Res, 1994. **22**(22): p. 4673-80.

Chapter 8 Appendices

Appendix 1: LC-CID-saETD-MS/MS identification of citrullination sites in fibrinogen

Table 8.1 Description of peptides where citrullinated sites were detected. Data from the MS experiment was analysed with Proteome Discoverer software (Thermo Fisher Scientific Inc., Loughborough, UK) and the protein identification determined by comparison with the IPI human database. Citrullination sites were identified using the neutral loss method and the data was validated by sequence analysis. High confidence interval corresponds to 1% false discovery rate.

Band	Sample	Identification	Peptide	Citrullinated site(s) (high confidence)
1	FNG	α-chain	KPGSSGPGSTGSWNSGSSGTGSTGNQNPGSPrPGSTGTWNPGSSERGSAGHW	R353
			rPDSPGSGNARPNNPDWGTF	R394
			EVVTSEDGSDCPEAMDLGTLSGIGTLDGFr	R510
			TNTKESSSHHPGIAEFPSrGKSSSY	R573
2	FNG	β-chain	KAPDAGGCLHADPDLGVLCPTGCQLQEALLQQERPIr	R121
4	FNG+hPAD2	α-chain	GDFSSANNrDNTYNR	R123
			ERPGGNEITrGGSTSY	R263
			MELERPGGNEITrGGSTSYGTGSETESPR	R271
			GTGSETESPrNPSSAGSW	R287
			NSGSSGTGSTGNQNPGSPRPGSTGTWNPGSSErGSAGHW	R367
			HSESGSFrPDSPGSGNARPNNPDWGTF	R394
			HSESGSFrPDSPGSGNArPNNPDWGTF	R394, R404
			EEVSGNVSPGTrREY	R425
			EEVSGNVSPGTrrEY	R425, R426
			EVVTSEDGSDCPEAMDLGTLSGIGTLDGFr	R510
			EVVTSEDGSDCPEAMDLGTLSGIGTLDGFrHR	R510
			rHRHPDEAAFF	R510
			HrHPDEAAFFDTASTGK	R512
			SPMLGEFVSETESrGSESGIF	R547
			TNTKESSSHHPGIAEFPSrGKSSSY	R573
			ESSSHHPGIAEFPSrGK	R573

Table 8.1 Continuation.

Band	Sample	Identification	Peptide	Citrullinated site(s) (high confidence)
5	FNG+hPAD2	β-chain	KREEAPSLrPAPPPISGGGYR	R60
			DKKREEAPSLrPAPPPISGGGY	R60
			QQErPIRNSVDELNNNVEAVSQTSSSSF	R121
			DNENVVNEYSSELEKHQLYIDETVNSNIPTNLr	R196
			TMTIHNGMFFSTYDrDNDGWLTSDPRK	R410
7	FNG+hPAD4	α-chain	TDMPQMRMELERPGGNEITrGGSTSY	R271
			KPGSSGPGSTGSWNSGSSGTGSTGNQNPGSPRPGSTGTWNPGSSErGSAGHW	R367
			EEVSGNVSPGTrREY	R425
			EEVSGNVSPGTrrEY	R425, R426
			EEVSGNVSPGTrrEYHTEKL	R425, R426
			SPMLGEFVSETESrGSESGIF	R547
			TNTKESSSHHPGIAEFPSrGKSSSY	R573
			ESSSHHPGIAEFPSrGK	R573
			NrGDSTFESKSY	R591
			TSSTSYNrGDSTFESKSY	R591
			SKQFTSSTSYNrGDSTF	
8	FNG+hPAD4	β-chain	DKKREEAPSLrPAPPPISGGGY	R53, R60
			DKKREEAPSLrPAPPPISGGGY	R60
			AHYGGFTVQNEANKYQISVNKYr	R376
9	FNG+hPAD4	γ-chain	VATrDNCCILDERF	R31
			VELEDWNGr	R282
			NGrTSTADYAMF	R282
			IHLISTQSAIPYALRVELEDWNGr	R282

Appendix 2: Sequence homology between hPAD2 and hPAD4

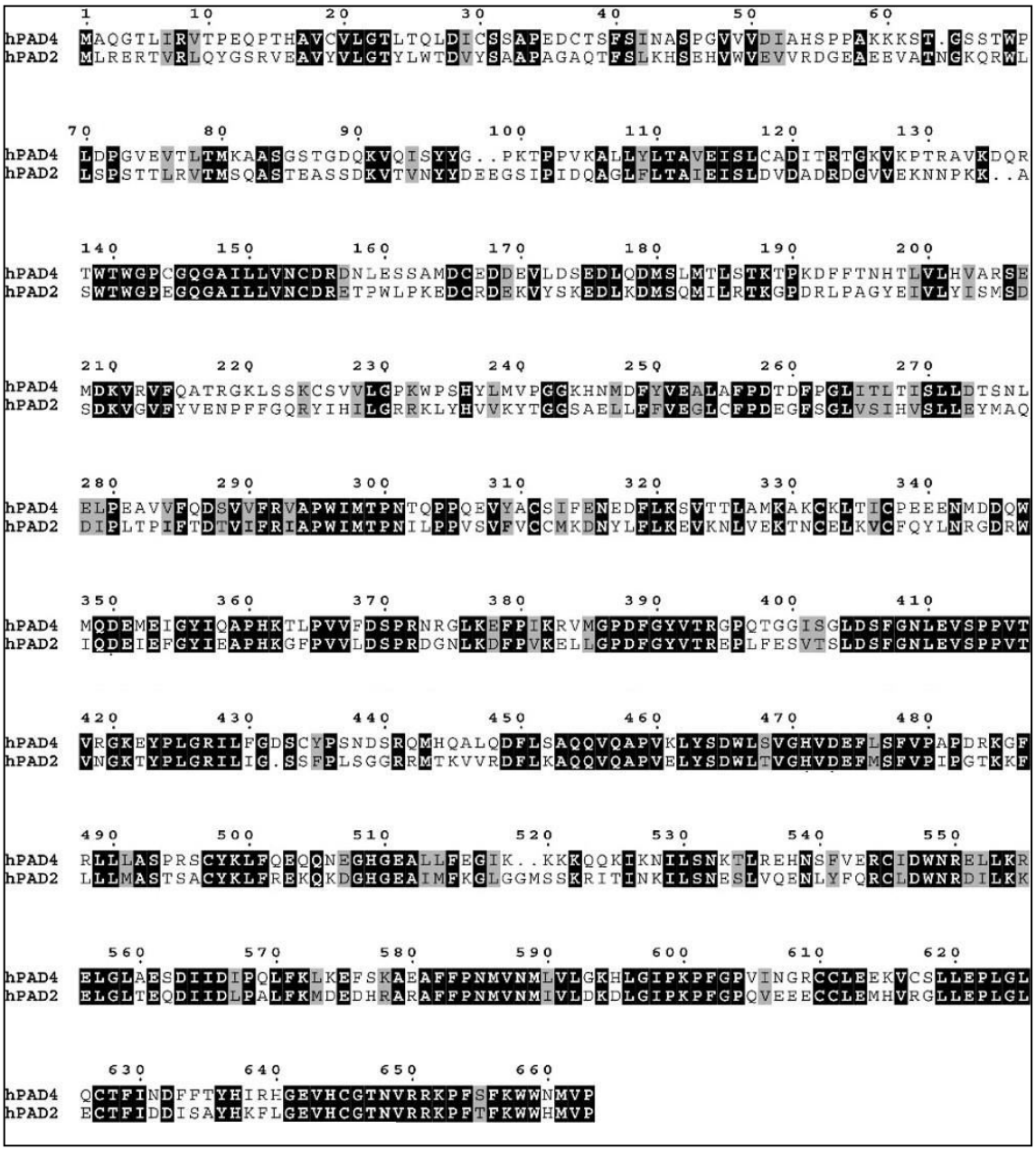

Figure 8.1 A CLUSTALW 2.0.5 alignment of hPAD2 and hPAD4 enzymes [563]. Black shading denotes identical residues and grey shading denotes physicochemical similar residues.

.

Appendix 3: Microarray expression profile of selected genes

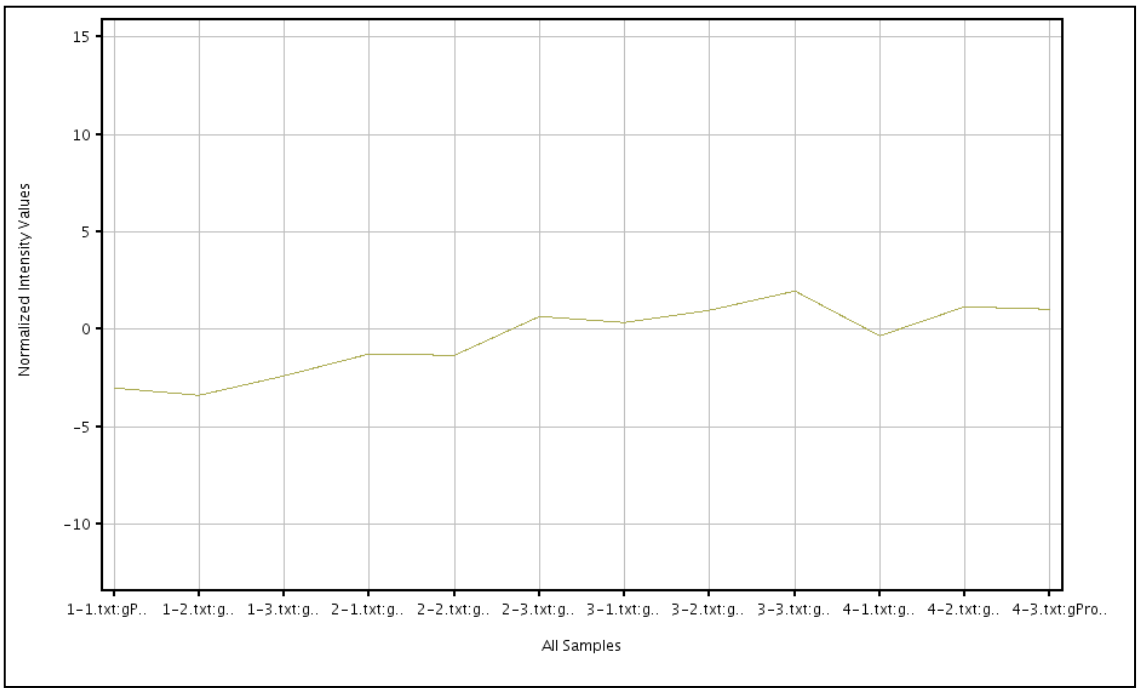

Figure 8.2 Expression profile of *ASS1* gene. 1 – unactivated PBMC; 2 – Activated PBMC; 3 – PBMC + hPAD2 prior to activation; 4 – PBMC + hPAD4 prior to activation.

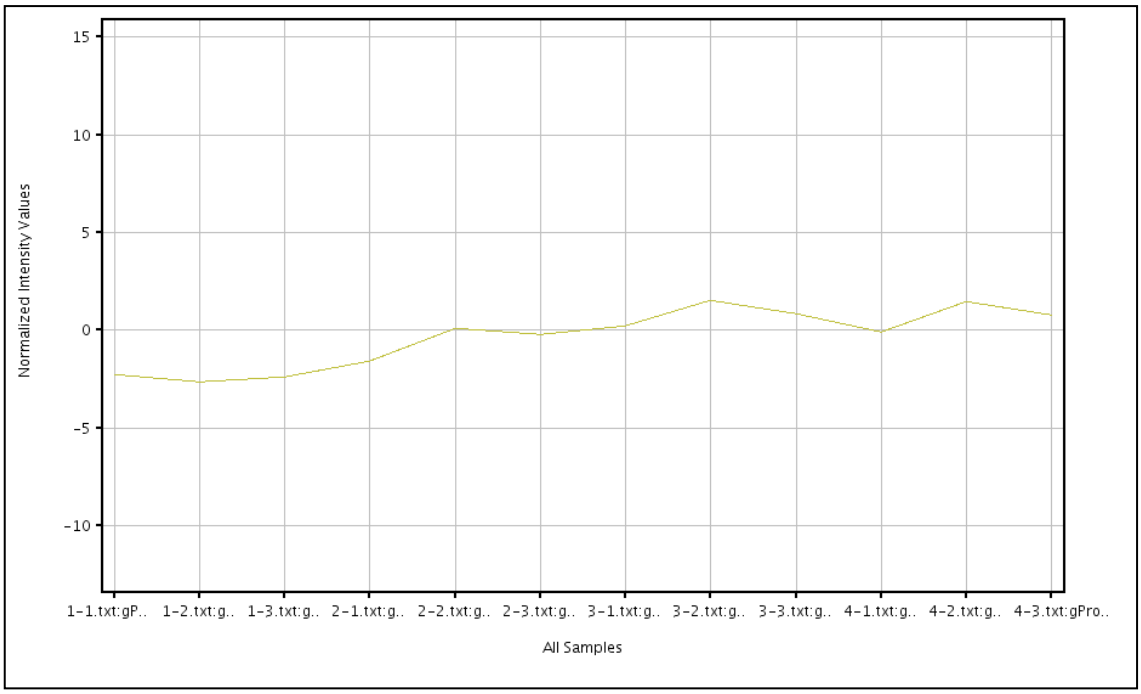

Figure 8.3 Expression profile of *CTH* gene. 1 – unactivated PBMC; 2 – Activated PBMC; 3 – PBMC + hPAD2 prior to activation; 4 – PBMC + hPAD4 prior to activation.

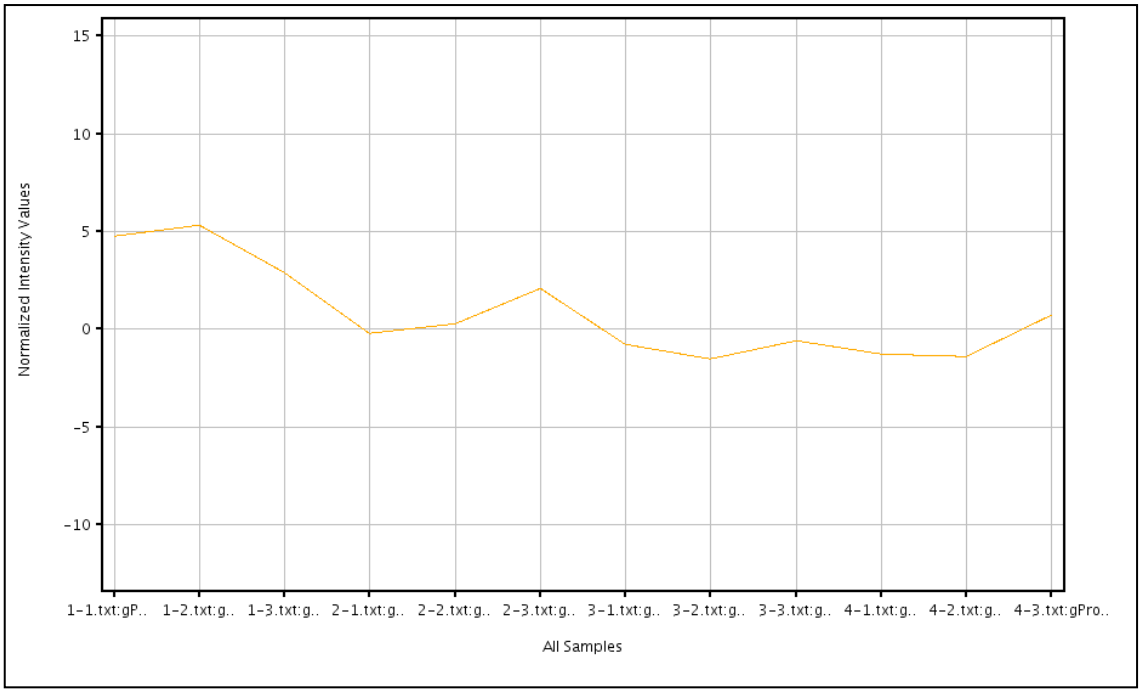

Figure 8.4 Expression profile of *HK3* gene. 1 – unactivated PBMC; 2 – Activated PBMC; 3 – PBMC + hPAD2 prior to activation; 4 – PBMC + hPAD4 prior to activation.

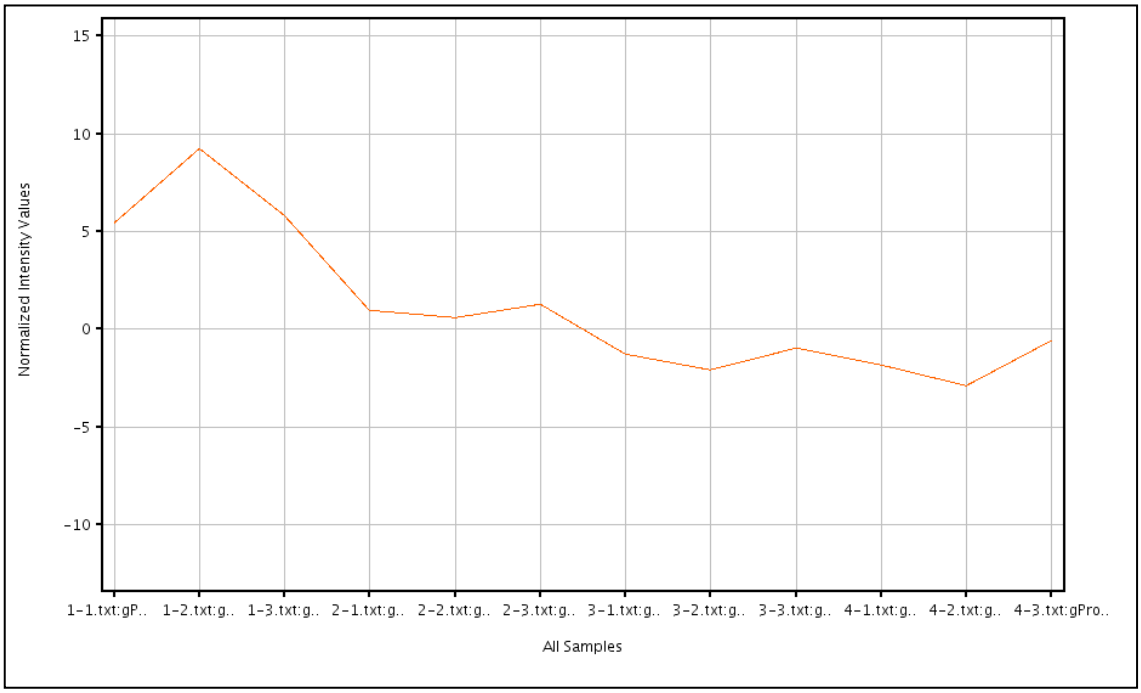

Figure 8.5 Expression profile of *CD163* gene. 1 – unactivated PBMC; 2 – Activated PBMC; 3 – PBMC + hPAD2 prior to activation; 4 – PBMC + hPAD4 prior to activation.

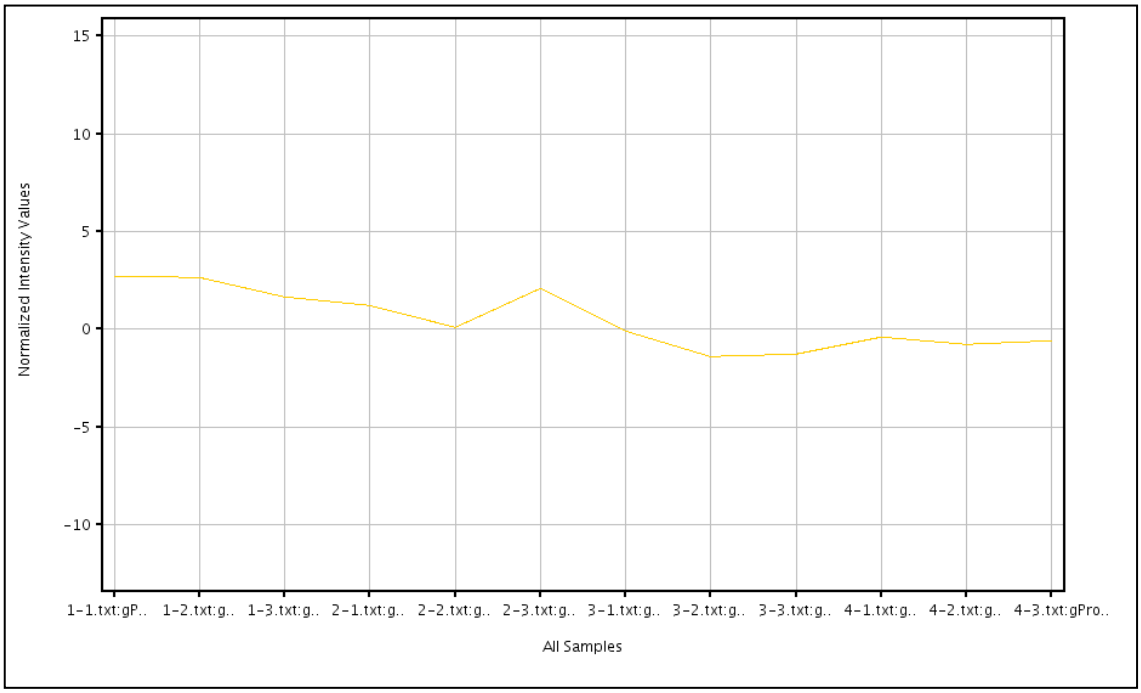

Figure 8.6 Expression profile of *SGMS2* gene. 1 – unactivated PBMC; 2 – Activated PBMC; 3 – PBMC + hPAD2 prior to activation; 4 – PBMC + hPAD4 prior to activation.

Appendix 4: LC-CID-saETD-MS/MS protein identification of spots 244 and 245

Table 8.2 Results of protein identification for spot number 244 in non-PAD enzyme treated PBMC. The accession number is the unique identifier used for the protein sequence. The number of unique peptides represents the number of peptides matching the protein identified. The coverage indicates the percentage of the protein sequence that has been covered by the identified protein. Citrullination displays the peptides where citrullination was detected in the highlighted arginine residues.

Accession number	Protein	Unique Peptides	MW (kDa)	Coverage (%)	Citrullination
Q5T7C4	High mobility group protein B1	7	18.3	48.1	
Q06323	Proteasome activator complex subunit 1	8	28.7	41.77	
P38117	Electron transfer flavoprotein subunit beta	7	27.8	33.73	
F5H6Q2	Polyubiquitin-C (Fragment)	2	13.7	33.61	
H0YGX7	Rho GDP-dissociation inhibitor 2 (Fragment)	4	22.4	33.33	
P31946-2	Isoform Short of 14-3-3 protein beta/alpha	3	27.8	31.56	
P60709	Actin, cytoplasmic 1	6	41.7	25.87	TTGIVmDSGDGVTH TVPIYEGYALPHAILr
O15144	Actin-related protein 2/3 complex subunit 2	6	34.3	25,00	
P13804	Electron transfer flavoprotein subunit alpha, mitochondrial	6	35.1	23.12	
P81605	Dermcidin	3	11.3	22.73	
P02647	Apolipoprotein A-I	4	30.8	19.1	
P26583	High mobility group protein B2	2	24.0	18.18	
P63104	14-3-3 protein zeta/delta	3	27.7	17.14	
Q96C19	EF-hand domain-containing protein D2	3	26.7	15.83	
P07339	Cathepsin D	5	44.5	15.78	
O15173	Membrane-associated progesterone receptor component 2	3	23.8	15.25	
H0YM70	Proteasome activator complex subunit 2	2	26.0	14.91	
P07355	Annexin A2	4	38.6	14.75	
P62258-2	Isoform SV of 14-3-3 protein epsilon	2	26.5	14.16	
F5H018	GTP-binding nuclear protein Ran (Fragment)	2	22.4	14.14	
P30084	Enoyl-CoA hydratase, mitochondrial	4	31.4	13.79	
P16403	Histone H1.2	4	21.4	13.62	
Q9H3N1	Thioredoxin-related transmembrane protein 1	3	31.8	12.86	
M0R208	ATP-dependent Clp protease proteolytic subunit	2	20.6	12.11	
P30040	Endoplasmic reticulum resident protein 29	3	29.0	11.88	
K7ELS8	Synaptogyrin-2 (Fragment)	2	14.7	11.85	
P50897	Palmitoyl-protein thioesterase 1	2	34.2	10.78	
P05090	Apolipoprotein D	2	21.3	10.58	
Q15691	Microtubule-associated protein RP/EB family member 1	2	30.0	10.45	

Table 8.3 Results of protein identification for spot number 244 in hPAD2 enzyme treated PBMC. The accession number is the unique identifier used for the protein sequence. The number of unique peptides represents the number of peptides matching the protein identified. The coverage indicates the percentage of the protein sequence that has been covered by the identified protein. Citrullination displays the peptides where citrullination was detected.

Accession number	Protein	Unique Peptides	MW (kDa)	Coverage (%)	Citrullination
Q5T7C4	High mobility group protein B1	9	18.3	48.73	
B4DJF2	14-3-3 protein epsilon	2	10.9	31.91	
Q06323	Proteasome activator complex subunit 1	6	28.7	31.73	
H0YKF0	Electron transfer flavoprotein subunit alpha, mitochondrial (Fragment)	6	30.2	25.26	
P81605	Dermcidin	2	11.3	22.73	
O15144	Actin-related protein 2/3 complex subunit 2	5	34.3	21.33	
I3L3Q7	Complement component 1 Q subcomponent-binding protein, mitochondrial (Fragment)	2	20.0	19.77	
P26583	High mobility group protein B2	2	24.0	18.18	
A8MW50	L-lactate dehydrogenase (Fragment)	2	25.2	18.1	
P31946-2	Isoform Short of 14-3-3 protein beta/alpha	2	27.8	16.8	
J3KTF8	Rho GDP-dissociation inhibitor 1 (Fragment)	2	21.5	16.06	
O15173	Membrane-associated progesterone receptor component 2	3	23.8	15.25	
P38117	Electron transfer flavoprotein subunit beta	3	27.8	14.12	
P63104	14-3-3 protein zeta/delta	3	27.7	13.88	
B7Z6B8	2,4-dienoyl-CoA reductase, mitochondrial	3	35.0	13.8	
Q96C19	EF-hand domain-containing protein D2	3	26.7	13.75	
P16403	Histone H1.2	3	21.4	13.62	
P60709	Actin, cytoplasmic 1	4	41.7	13.6	
O43760	Synaptogyrin-2	3	24.8	12.5	
Q15691	Microtubule-associated protein RP/EB family member 1	2	30.0	10.45	

Table 8.4 Results of protein identification for spot number 244 in hPAD4 enzyme treated PBMC. The accession number is the unique identifier used for the protein sequence. The number of unique peptides represents the number of peptides matching the protein identified. The coverage indicates the percentage of the protein sequence that has been covered by the identified protein. Citrullination displays the peptides where citrullination was detected in the highlighted arginine residues.

Accession number	Protein	Unique Peptides	MW (kDa)	Coverage (%)	Citrullination
P63104	14-3-3 protein zeta/delta	8	27.7	54.29	
P52566	Rho GDP-dissociation inhibitor 2	7	23.0	49.25	
Q5T7C4	High mobility group protein B1	8	18.3	48.1	
P31946-2	Isoform Short of 14-3-3 protein beta/alpha	4	27.8	47.95	
H0YL12	Electron transfer flavoprotein subunit alpha, mitochondrial (Fragment)	8	24.9	46.86	
Q06323	Proteasome activator complex subunit 1	9	28.7	45.78	
P81605	Dermcidin	3	11.3	32.73	
P22626-2	Isoform A2 of Heterogeneous nuclear ribonucleoproteins A2/B1	5	36.0	31.96	
Q9UL46	Proteasome activator complex subunit 2	5	27.4	30.13	
H3BMH2	Ras-related protein Rab-11A (Fragment)	5	17.7	29.68	
O15144	Actin-related protein 2/3 complex subunit 2	8	34.3	29.33	
P09651-3	Isoform 2 of Heterogeneous nuclear ribonucleoprotein A1	4	29.4	27.72	
I3L3Q7	Complement component 1 Q subcomponent-binding protein, mitochondrial (Fragment)	3	20.0	27.12	ATFmVGSYGPrPE EYEFLTPVEEAPK
P60709	Actin, cytoplasmic 1	7	41.7	26.93	
P18669	Phosphoglycerate mutase 1	5	28.8	25.59	
P38117	Electron transfer flavoprotein subunit beta	5	27.8	24.31	
J3KTF8	Rho GDP-dissociation inhibitor 1 (Fragment)	4	21.5	23.83	
P62873	Guanine nucleotide-binding protein G(I)/G(S)/G(T) subunit beta-1	2	37.4	23.53	
P61981	14-3-3 protein gamma	3	28.3	23.08	
P27348	14-3-3 protein theta	3	27.7	20.82	
Q04917	14-3-3 protein eta	2	28.2	20.33	
D6R9A6	High mobility group protein B2 (Fragment)	2	15.4	20.15	
O15143	Actin-related protein 2/3 complex subunit 1B	5	40.9	19.89	
F8VV32	Lysozyme C	2	11.5	19.23	
P07195	L-lactate dehydrogenase B chain	4	36.6	19.16	
P07355	Annexin A2	5	38.6	18.88	
P16403	Histone H1.2	5	21.4	17.84	
Q9NUQ9	Protein FAM49B	4	36.7	16.05	
Q9HC38	Glyoxalase domain-containing protein 4	4	32.0	15.57	

Table 8.4 Continuation.

Accession number	Protein	Unique Peptides	MW (kDa)	Coverage (%)	Citrullination
P30084	Enoyl-CoA hydratase, mitochondrial	5	31.4	15.52	
P30040	Endoplasmic reticulum resident protein 29	3	29.0	14.18	
P62258-2	Isoform SV of 14-3-3 protein epsilon	2	36.0	14.16	
M0R0Y2	Alpha-soluble NSF attachment protein	3	29.1	12.89	
J3KPE3	Guanine nucleotide-binding protein subunit beta-2-like 1	3	30.1	12.82	
O43760	Synaptogyrin-2	3	24.8	12.5	
P53597	Succinyl-CoA ligase [ADP/GDP-forming] subunit alpha, mitochondrial	3	36.2	12.14	
M0R208	ATP-dependent Clp protease proteolytic subunit	2	20.6	12.11	
Q9NUJ1	Mycophenolic acid acyl-glucuronide esterase, mitochondrial	3	33.9	11.44	
Q9H3N1	Thioredoxin-related transmembrane protein 1	3	31.8	11.07	
Q07955-3	Isoform ASF-3 of Serine/arginine-rich splicing factor 1	2	22.4	10.95	
P00387-2	Isoform 2 of NADH-cytochrome b5 reductase 3	2	31.7	10.75	
Q15691	Microtubule-associated protein RP/EB family member 1	2	30.0	10.45	

Table 8.5 Results of protein identification for spot number 245 in non-PAD enzyme treated PBMC. The accession number is the unique identifier used for the protein sequence. The number of unique peptides represents the number of peptides matching the protein identified. The coverage indicates the percentage of the protein sequence that has been covered by the identified protein. Citrullination displays the peptides where citrullination was detected in the highlighted arginine residues.

Accession number	Protein	Unique Peptides	MW (kDa)	Coverage (%)	Citrullination
P60709	Actin, cytoplasmic 1	7	41.7	44,00	
P13796	Plastin-2	13	70.2	28.07	
F5H8J2	Uncharacterized protein	7	51.1	19.73	
F8VPV9	ATP synthase subunit beta	5	55.3	14.48	
P81605	Dermcidin	2	11.3	12.73	

Table 8.6 Results of protein identification for spot number 245 in hPAD2 enzyme treated PBMC. The accession number is the unique identifier used for the protein sequence. The number of unique peptides represents the number of peptides matching the protein identified. The coverage indicates the percentage of the protein sequence that has been covered by the identified protein. Citrullination displays the peptides where citrullination was detected in the highlighted arginine residues.

Accession number	Protein	Unique Peptides	MW (kDa)	Coverage (%)	Citrullination
P60709	Actin, cytoplasmic 1	3	41.7	28.53	TTGIVmDSGDGVTH TVPIYEGYALPHAILr
P81605	Dermcidin	3	11.3	22.73	
P13796	Plastin-2	6	70.2	14.83	

Table 8.7 Results of protein identification for spot number 245 in hPAD4 enzyme treated PBMC. The accession number is the unique identifier used for the protein sequence. The number of unique peptides represents the number of peptides matching the protein identified. The coverage indicates the percentage of the protein sequence that has been covered by the identified protein. Citrullination displays the peptides where citrullination was detected.

Accession number	Protein	Unique Peptides	MW (kDa)	Coverage (%)	Citrullination
P60709	Actin, cytoplasmic 1	7	41.7	46.93	TTGIVmDSGDGVTH TVPIYEGYALPHAILr
P81605	Dermcidin	2	11.3	20,00	
P06576	ATP synthase subunit beta, mitochondrial	7	56.5	19.66	
P13796	Plastin-2	7	70.2	14.19	
P27797	Calreticulin	3	48.1	11.03	